



---

# Development of Thickness Design Tables Based on the M-E PDG

Technical Report BDH10-1

---

TEXAS TRANSPORTATION INSTITUTE  
THE TEXAS A&M UNIVERSITY SYSTEM  
COLLEGE STATION, TEXAS

FLORIDA DEPARTMENT OF TRANSPORTATION

in cooperation with the  
Federal Highway Administration and the  
Florida Department of Transportation

*Final Report*

**DEVELOPMENT OF THICKNESS DESIGN TABLES BASED  
ON THE M-E PDG**

Research Project Title: M-E PDG Program Implementation in Florida  
Contract No. BDH10

*Submitted to:*

Florida Department of Transportation  
605 Suwannee Street  
Tallahassee, FL 32399

**TEXAS TRANSPORTATION INSTITUTE**

Jeongho Oh  
Emmanuel G. Fernando  
Material and Pavements Division  
3135 TAMU  
College Station, TX 77343-3135

June 2008



## **DISCLAIMER**

The opinions, findings, and conclusions expressed in this publication are those of the authors and not necessarily those of the State of Florida Department of Transportation. This report does not constitute a standard, specification, or regulation, nor is it intended for construction, bidding, or permit purposes. The United States Government and the State of Florida do not endorse products or manufacturers. Trade or manufacturers' names appear herein solely because they are considered essential to the object of this report. The engineer in charge of the project was Dr. Emmanuel G. Fernando.



**SI\* (MODERN METRIC) CONVERSION FACTORS**

**APPROXIMATE CONVERSIONS TO SI UNITS**

SYMBOL	WHEN YOU KNOW	MULTIPLY BY	TO FIND	SYMBOL
<b>LENGTH</b>				
in	inches	25.4	millimeters	mm
ft	feet	0.305	meters	m
yd	yards	0.914	meters	m
mi	miles	1.61	kilometers	km
<b>AREA</b>				
in <sup>2</sup>	square inches	645.2	square millimeters	mm <sup>2</sup>
ft <sup>2</sup>	square feet	0.093	square meters	m <sup>2</sup>
yd <sup>2</sup>	square yard	0.836	square meters	m <sup>2</sup>
ac	acres	0.405	hectares	ha
mi <sup>2</sup>	square miles	2.59	square kilometers	km <sup>2</sup>
<b>VOLUME</b>				
fl oz	fluid ounces	29.57	milliliters	mL
gal	gallons	3.785	liters	L
ft <sup>3</sup>	cubic feet	0.028	cubic meters	m <sup>3</sup>
yd <sup>3</sup>	cubic yards	0.765	cubic meters	m <sup>3</sup>

NOTE: volumes greater than 1000 L shall be shown in m<sup>3</sup>

<b>MASS</b>				
oz	ounces	28.35	grams	g
lb	pounds	0.454	kilograms	kg
T	short tons (2000 lb)	0.907	megagrams (or "metric ton")	Mg (or "t")
<b>TEMPERATURE (exact degrees)</b>				
°F	Fahrenheit	5 (F-32)/9 or (F-32)/1.8	Celsius	°C
<b>ILLUMINATION</b>				
fc	foot-candles	10.76	lux	lx
fl	foot-Lamberts	3.426	candela/m <sup>2</sup>	cd/m <sup>2</sup>
<b>FORCE and PRESSURE or STRESS</b>				
lbf	poundforce	4.45	newtons	N
lbf/in <sup>2</sup>	poundforce per square inch	6.89	kilopascals	kPa

\*SI is the symbol for the International System of Units. Appropriate rounding should be made to comply with Section 4 of ASTM E380. (Revised March 2003)

**APPROXIMATE CONVERSIONS FROM SI UNITS**

SYMBOL	WHEN YOU KNOW	MULTIPLY BY	TO FIND	SYMBOL
<b>LENGTH</b>				
mm	millimeters	0.039	inches	in
m	meters	3.28	feet	ft
m	meters	1.09	yards	yd
km	kilometers	0.621	miles	mi
<b>AREA</b>				
mm <sup>2</sup>	square millimeters	0.0016	square inches	in <sup>2</sup>
m <sup>2</sup>	square meters	10.764	square feet	ft <sup>2</sup>
m <sup>2</sup>	square meters	1.195	square yards	yd <sup>2</sup>
ha	hectares	2.47	acres	ac
km <sup>2</sup>	square kilometers	0.386	square miles	mi <sup>2</sup>
<b>VOLUME</b>				
mL	milliliters	0.034	fluid ounces	fl oz
L	liters	0.264	gallons	gal
m <sup>3</sup>	cubic meters	35.314	cubic feet	ft <sup>3</sup>
m <sup>3</sup>	cubic meters	1.307	cubic yards	yd <sup>3</sup>

<b>MASS</b>				
g	grams	0.035	ounces	oz
kg	kilograms	2.202	pounds	lb
Mg (or "t")	megagrams (or "metric ton")	1.103	short tons (2000 lb)	T
<b>TEMPERATURE (exact degrees)</b>				
°C	Celsius	1.8C+32	Fahrenheit	°F
<b>ILLUMINATION</b>				
lx	lux	0.0929	foot-candles	fc
cd/m <sup>2</sup>	candela/m <sup>2</sup>	0.2919	foot-Lamberts	fl
<b>FORCE and PRESSURE or STRESS</b>				
N	newtons	0.225	poundforce	lbf
kPa	kilopascals	0.145	poundforce per square inch	lbf/in <sup>2</sup>



**Technical Report Documentation Page**

1. Report No. BDH10-1		2. Government Accession No.		3. Recipient's Catalog No.	
4. Title and Subtitle DEVELOPMENT OF THICKNESS DESIGN TABLES BASED ON THE M-E PDG				5. Report Date June 2008 Published:	
				6. Performing Organization Code	
7. Author(s) Jeongho Oh and Emmanuel G. Fernando				8. Performing Organization Report No. BDH10-1	
9. Performing Organization Name and Address Texas Transportation Institute The Texas A&M University System College Station, Texas 77843-3135				10. Work Unit No. (TRAIS)	
				11. Contract or Grant No. BDH10	
12. Sponsoring Agency Name and Address Florida Department of Transportation Research and Development Office 605 Suwannee Street, MS 30 Tallahassee, Florida 32399-0450				13. Type of Report and Period Covered Technical Report March 2007 – June 2008	
				14. Sponsoring Agency Code	
15. Supplementary Notes Research performed in cooperation with the Florida Department of Transportation. Research Project Title: M-E PDG Program Implementation in Florida					
16. Abstract <p>In this project, Texas Transportation Institute (TTI) researchers and engineers with the Florida Department of Transportation (FDOT) conducted a cooperative effort to establish and characterize field test sections for the purpose of compiling a database of materials, geometric, and traffic-related design variables to verify the predictions from the Mechanistic-Empirical Pavement Design Guide (M-E PDG) program and perform local model calibrations as warranted. Researchers conducted sensitivity analyses to investigate the impact of a broad range of M-E PDG input variables on the performance predictions and identify critical variables for developing design tables based on the M-E PDG. From these efforts, researchers and FDOT engineers established thickness design tables for hot-mix asphalt and jointed plain concrete pavements. This report documents the development work carried out to implement the mechanistic-empirical pavement design guide in Florida.</p>					
17. Key Word Mechanistic-empirical pavement design, M-E PDG program, Pavement performance prediction, Model calibration, Sensitivity analysis, Thickness design				18. Distribution Statement	
19. Security Classif. (of this report) Unclassified		20. Security Classif. (of this page) Unclassified		21. No. of Pages 308	22. Price

## ACKNOWLEDGMENTS

The work reported herein was conducted as part of a project sponsored by the Florida Department of Transportation to support its implementation of a pavement design method based on the mechanistic-empirical pavement design guide that came out of NCHRP Project 1-37A. The authors gratefully acknowledge the steadfast support and technical guidance of the project manager, Mr. Bruce Dietrich, Florida State Pavement Design Engineer. Mr. Dietrich played a major role in planning the test program conducted in this project to characterize pavement sections for the purpose of developing a database for M-E PDG performance model calibration. He also provided valuable technical guidance in developing the thickness design tables from this project.

This project was truly a cooperative effort between researchers and the Florida Department of Transportation. Without the steadfast cooperation of FDOT engineers, it would not have been possible to execute the test program established in this project. The researchers are extremely grateful to the FDOT engineers who participated in this effort, and would like to acknowledge and give them credit in this report:

- Mike Bergin
- Michael Bienvenu
- Conrad Campbell
- Ron Chin
- Claudia Coll
- Richard M. DeLorenzo
- Charles Dunn
- Joey Gordon
- Henry Haggerty
- Charles Holzschuher
- David Horhota
- Charles Ishee
- Shanna Johnson
- Wiley Cunagin
- Timothy Keefe
- Frank Kreis
- Howard Moseley
- Jonathan Moxley
- Jim Musselman
- Dan Pitocchi
- Jeffrey Rescigno
- Stephen Sedwick
- Greg Sholar
- Deborah Snyder
- Michael Suggs
- Emmanuel Uwaibi
- Sam Weede
- Gregory Schiess

## EXECUTIVE SUMMARY

Version 1.0 of the *Mechanistic-Empirical Pavement Design Guide* (M-E PDG) program was released in May 2007. For an engineer to design a specific pavement using this program, he or she needs to assume a trial design, and run the program repetitively until a pavement design is identified that satisfies the performance criteria for the given problem. The performance models in the new program were developed and calibrated based on a national database of field pavement performance data. For states seeking to implement the M-E PDG, the developers of the design guide have recommended that the models be calibrated to local conditions. Given these considerations, Texas Transportation Institute (TTI) researchers and engineers with the Florida Department of Transportation (FDOT) conducted a cooperative effort to establish and characterize field test sections for the purpose of compiling a database of materials, geometric and traffic-related design variables to verify the predictions from the M-E PDG program, and perform local model calibrations as warranted. Researchers conducted sensitivity analyses to investigate the impact of a broad range of M-E PDG input variables on the performance predictions and identify critical variables for developing design tables based on the M-E PDG. From these efforts, researchers and FDOT engineers established thickness design tables for hot-mix asphalt and jointed plain concrete pavements. This summary provides a brief description of accomplishments, key findings, and recommendations resulting from this study. The primary accomplishments and findings are summarized as follows:

- For jointed plain concrete pavements, the sensitivity analyses identified the concrete coefficient of thermal expansion (CTE), and compressive strength as significant predictors of PCC pavement performance. In addition, joint spacing, dowel diameter, and slab width were found to significantly affect the performance predictions from the M-E PDG program. The moduli of the underlying unbound materials as well as the modulus of subgrade reaction were found to have minimal effect on the PCC performance predictions. Since the PCC performance predictions are highly influenced by the concrete coefficient of thermal expansion, researchers made a careful selection of the CTE values for generating the PCC thickness design tables based on the M-E PDG. This decision considered CTE measurements obtained from tests on molded specimens and cores from FDOT construction projects; the standard

deviations of repeat CTE measurements reported in the literature; and work conducted in other M-E PDG implementation projects.

- For flexible pavements, researchers found that the base modulus significantly influences the predicted amounts of alligator (bottom-up) cracking from the M-E PDG program. The sensitivity analyses also revealed a moderate benefit to placing a mechanically stabilized subgrade over the embankment, particularly for embankment moduli of 10 ksi or less. In view of on-going national studies to develop models for predicting top-down cracking, reflective cracking, and rutting, the thickness design tables from this project were developed based on alligator cracking.
- The sensitivity analyses indicated that predicted pavement performance is highly tied to the cumulative ESALs, which depend on the heavy vehicle distribution and axle load spectra. Researchers found that the predicted pavement performance from the M-E PDG program varies with the cumulated ESALs, with pavements subjected to different heavy vehicle distributions exhibiting similar performance when the average annual daily truck traffic is varied to produce the same number of ESALs. Since ESAL was determined to be a useful index for quantifying the joint effects of truck traffic distribution and axle load spectra, the decision was made in this project to generate the design tables as a function of cumulative 18-kip ESALs. It was also recognized that considerable research by the Department's Transportation Statistics Office would be required to develop appropriate axle load distributions for pavement design. As a transition to the new guide, the design tables were established to permit input of the ESAL forecasts currently produced by Planning, and which engineers presently use with the Department's current pavement design methods.
- To account for climatic effects, researchers used the weather data embedded in the M-E PDG program to investigate the effects of climatic factors on predicted pavement performance. The sensitivity analyses showed that climatic factors have a more pronounced effect on the performance predictions for rigid pavements under Florida conditions. From the investigations of climatic effects, researchers established five climatic regions for developing the thickness design tables for rigid pavements based on the M-E PDG.
- The required AC thicknesses from the design tables based on the M-E PDG range from 2 to 9 inches for new pavement designs and 1.5 to 7.5 inches for asphalt

concrete overlays. These requirements were determined over a range of ESALs from  $1 \times 10^6$  to  $70 \times 10^6$  for a 20-year design period. The comparison of the required AC thickness based on the design tables derived from the M-E PDG and the thickness determined using the current FDOT design method showed differences ranging from -2 to +2 inches for new pavement designs. For these cases, the required AC thicknesses based on the M-E PDG tables were slightly conservative when using a limerock base modulus of 30 ksi. The change of base modulus from 30 ksi to 45 ksi shifted the distribution of the differences with the highest frequency shifting from 1 to 0.5 inch. For overlay design, the thickness difference was slightly lower compared to new design with differences of 0 and 0.5 inch showing the highest frequency of occurrence. These results are for an assumed base modulus of 45 ksi and 2 inches of existing AC thickness. With respect to existing pavement condition, there was a 0.5-inch shift in the highest frequency when the existing AC structure was varied from poor to good condition.

- Two sets of PCC tables, *Design I* and *Design II*, were developed based on the levels of CTE and compressive strength used in running the M-E PDG program. The slab thicknesses in these tables vary from 8 to 14.5 inches for the range of variables used in their development. Researchers note that a minimum slab thickness of 8 inches was adopted in developing the design tables. The required slab thicknesses for *Design II* generally showed 1- to 1.5-inch reductions from corresponding thicknesses in the *Design I* tables due to the lower CTE and higher compressive strength values assumed for *Design II*. Researchers also compared the new thickness design tables with the current FDOT design tables. For this comparison, the required slab thicknesses at 90 percent reliability level for regions 1 and 5 were examined. The differences in the required slab thickness between the two methods ranged from -4.0 to 1.0 inches, with the M-E PDG-based design thicknesses generally being thinner than the corresponding slab thicknesses from the current FDOT PCC design tables. The required slab thicknesses based on the *Design I* table for region 1 were observed to be the most comparable with the existing design method. Among the five regions, Region 1 also required the greatest design slab thickness. The required PCC slab thicknesses for region 5 were found to be generally thinner than the corresponding thicknesses based on the current method for both the *Design I* and *Design II* tables.

- The concrete coefficient of thermal expansion was found to be a critical factor controlling the predicted performance of jointed plain concrete pavements. Researchers recommend that a CTE materials specification be established as part of quality assurance tests to be conducted on PCC pavement construction projects. Implementation of this specification will require training of inspectors and contractor personnel on the test method adopted to verify CTE values achieved from construction.
- The PCC design tables developed from this project are based on a 13-ft slab width, which was found to be optimal from sensitivity analyses of predicted PCC pavement performance. Thus, researchers recommend building 13-ft wide slabs (with tied shoulders) unless right-of-way restrictions dictate a narrower slab width. For such cases, the current PCC design method may be used or a slab 1.5-inch thicker than the corresponding required thickness based on a 13-ft wide slab may be placed for cumulative ESALs of 50 million or less. Alternatively, the engineer may decide to run the M-E PDG program to establish the PCC design thickness for a 12-ft slab width.
- Researchers recommend that a follow-up project be undertaken to review and revise the flexible pavement thickness design tables from this study to incorporate other performance criteria based on the improved top-down cracking, reflection cracking, and rutting models that are being developed in on-going national studies. Until then, FDOT flexible pavement designs can be achieved using the current design method with the M-E PDG-based design tables used for comparative checks.
- In line with the above recommendation, the Department needs to consider establishing a data base of verification/calibration sections on selected FDOT resurfacing or new construction projects. This recommendation would entail assembling materials and construction information within a selected section of each project that, with the performance data collected over time, can be used to verify the predictions from the M-E PDG program, and perform calibrations in the future, as necessary. These sections might possibly require performance monitoring separate from the PCS surveys that are done annually by the Department to measure the pavement condition and track the performance of each specific verification/calibration section.

# TABLE OF CONTENTS

	Page
LIST OF FIGURES .....	xv
LIST OF TABLES .....	xxiii
CHAPTER	
I INTRODUCTION .....	1
Background.....	1
Research Objectives .....	2
Scope of Research Report .....	3
II REVIEW OF M-E PDG INPUT REQUIREMENTS .....	5
Multi-Level Input Approach .....	6
Characterization of Asphalt Concrete Materials.....	7
Characterization of Portland Cement Concrete Materials .....	12
Characterization of Unbound Granular and Subgrade Materials .....	14
Characterization of Chemically Stabilized Materials .....	15
Recycled Concrete Materials .....	16
Recycled Hot-Mix Asphalt Materials .....	16
Bedrock Materials .....	16
Required Tests to Determine M-E PDG Inputs for Model Calibrations .....	16
III DETERMINATION OF CANDIDATE SECTIONS FOR MODEL CALIBRATION .....	21
Initial Selection Stage .....	21
Final Selection Stage .....	34
IV FIELD AND LABORATORY TESTING .....	37
Determination of Coring and Trench Locations .....	37
Field Testing .....	44
Laboratory Testing .....	47
Characterization of Asphalt Concrete Properties .....	47
Characterization of Portland Cement Concrete .....	51
Characterization of Underlying Materials .....	53
V SUPPLEMENTARY FLEXIBLE PAVEMENT THICKNESS DESIGN TABLES BASED ON M-E PDG .....	65
Sensitivity Analysis .....	65
Development of Flexible Pavement Design Tables .....	74

CHAPTER	Page
Characterization of Asphalt Concrete Layer .....	75
Characterization of Underlying Layers .....	76
Consideration of Overlay Projects .....	77
Final Selection of Variables for Design Tables .....	78
M-E PDG Runs for Generating Design Tables .....	79
Comparison of M-E PDG Based Design Tables with Current FDOT Design Tables.....	79
 VI SUPPLEMENTARY RIGID PAVEMENT THICKNESS DESIGN TABLES BASED ON M-E PDG .....	 85
Verification and Calibration of M-E PDG Performance Models .....	85
Establishing Rigid Pavement Design Tables .....	94
Selection of Performance Criteria .....	95
Investigation of Rigid Pavement Cross-Sections .....	96
Consideration of Environmental Effects .....	96
Selection of Design Variables .....	98
Comparison of M-E PDG Based Design Tables with Current FDOT Design Tables .....	106
 VII PROJECT SUMMARY AND RECOMMENDATIONS .....	 109
REFERENCES .....	119
 APPENDIX	
A CANDIDATE PCS SEGMENTS FOR MODEL CALIBRATIONS .....	121
B SUMMARY OF FWD AND PCS DATA .....	135
C SUMMARY OF CORE DATA .....	167
D SUMMARY OF EXTRACTION AND DSR DATA ON AC CORES .....	195
E BACKCALCULATING ORIGINAL AIR VOIDS .....	221
F SUMMARY OF RESILIENT MODULUS DATA ON UNDERLYING MATERIALS .....	233
G M-E PDG BASED FLEXIBLE PAVEMENT DESIGN TABLES .....	253
H M-E PDG BASED RIGID PAVEMENT DESIGN TABLES .....	271

## LIST OF FIGURES

FIGURE	Page
3.1 WIM Stations and Candidate PCC Segments (dots indicate WIM stations while stars denote mid-points of each candidate PCC segment) .....	23
3.2 Candidate AC Segments in the Arterial Subsystems Considering Proximity of PCS Segments to WIM Stations (dots indicate WIM stations while stars denote candidate segments) .....	27
3.3 Candidate AC Segments in the Interstate Subsystem Considering Proximity of PCS Segments to WIM Stations (dots indicate WIM stations while stars denote candidate segments) .....	28
3.4 Candidate AC Segments in the Turnpike Subsystem Considering Proximity of PCS Segments to WIM Stations (dots indicate WIM stations while stars denote candidate segments) .....	29
3.5 Candidate Segments with Service Lives > 20 Years (WIM stations identified by dots and corresponding WIM site numbers while stars denote long-life segments) .....	31
4.1 Sensitivity of Top-Down Cracking Performance Predictions to Base Modulus for HMAC Pavement Section .....	39
4.2 Sensitivity of Top-Down Cracking Performance Predictions to Subgrade Modulus for HMAC Pavement Section .....	39
4.3 Sensitivity of PCC Crack Predictions to Base Modulus .....	40
4.4 Sensitivity of PCC Crack Predictions to Subgrade Modulus .....	40
4.5 Sensitivity of PCC Crack Predictions to Subgrade Modulus of Reaction .....	41
4.6 Illustration of Field Work on HMAC Calibration Sections .....	45
4.7 Measurement of Joint Spacing and Dowel Diameter .....	46
4.8 Top-Down Cracking Observed on AC Core .....	46
4.9 Illustration of Extractions Done on Asphalt Cores .....	49
4.10 Test Set Up for (a) Compressive Strength and (b) Concrete Coefficient of Thermal Expansion .....	52
4.11 Resilient Modulus for Base (Section 93310).....	54

FIGURE	Page
4.12 Resilient Modulus for Subgrade (Section 93310) .....	55
4.13 Resilient Modulus for Embankment Material (Section 93310) .....	55
4.14 Soil-Water Characteristic Curve of Embankment Soil from Section 26005 .....	60
4.15 Soil-Water Characteristic Curve of Embankment Soil from Section 28040 .....	60
4.16 Soil-Water Characteristic Curve of Embankment Soil from Section 58060 .....	61
4.17 Soil-Water Characteristic Curve of Embankment Soil from Section 86190 .....	61
4.18 Soil-Water Characteristic Curve of Embankment Soil from Section 10060 .....	62
4.19 Soil-Water Characteristic Curve of Limerock Base .....	64
4.20 Soil-Water Characteristic Curve of Stabilized Subgrade .....	64
5.1 Sensitivity of Alligator Cracking to Base Modulus .....	66
5.2 Sensitivity of Alligator Cracking to Embankment Modulus .....	67
5.3 Sensitivity of Alligator Cracking to AC Air Voids Content.....	67
5.4 Sensitivity of Alligator Cracking to Regional Environmental Differences.....	68
5.5 Sensitivity of Alligator Cracking to Truck Traffic Classification (TTC) .....	68
5.6 Sensitivity of Alligator Cracking to Stabilized Subgrade Modulus .....	69
5.7 Sensitivity of Alligator Cracking to Base Thickness.....	69
5.8 Sensitivity of Alligator Cracking to PG Binder Grade .....	70
5.9 Sensitivity of Predicted Tensile Strains and Number of Load Repetitions to Base Modulus.....	72
5.10 Sensitivity of Predicted Tensile Strains and Number of Load Repetitions to Base Thickness .....	73
5.11 Sensitivity of Predicted Tensile Strains and Number of Load Repetitions to Embankment Modulus.....	73
5.12 M-E PDG General Information Screen.....	74

FIGURE	Page
5.13 Distribution of Underlying Layer Resilient Modulus .....	76
5.14 Distribution of Thickness Differences for New Design Assuming 45 ksi Base Modulus .....	82
5.15 Distribution of Thickness Differences for New Design Assuming 30 ksi Base Modulus .....	83
5.16 Distribution of Thickness Differences for Overlay Design Assuming 45 ksi Base Modulus and Poor Condition of Existing AC Material .....	83
5.17 Distribution of Thickness Differences for Overlay Design Assuming 45 ksi Base Modulus and Good Condition of Existing AC Material .....	84
6.1 Comparison of Predicted and Measured Transverse Cracking.....	90
6.2 Comparison of Predicted and Measured IRI.....	90
6.3 Comparison of Predicted and Measured Faulting.....	91
6.4 M-E PDG Screen of Faulting Model Calibration Settings .....	92
6.5 M-E PDG Screen of IRI Model Calibration Settings .....	92
6.6 Comparison of Measured and Predicted IRIs after Calibration.....	94
6.7 Comparison of Measured and Predicted Faulting after Calibration .....	95
6.8 Rigid Pavement Cross-Sections Analyzed for Developing Design Tables .....	97
6.9 Map of Required PCC Slab Thickness at 90% reliability and $50 \times 10^6$ Cumulative ESALs .....	99
6.10 Sensitivity of Transverse Cracking Predictions to CTE .....	102
6.11 Sensitivity of Transverse Cracking Predictions to Compressive Strength .....	102
6.12 Sensitivity of Transverse Cracking Predictions to the TTC .....	103
6.13 Sensitivity of Transverse Cracking Predictions to Slab Width.....	103
6.14 Sensitivity of Transverse Cracking Predictions to Subgrade Modulus of Reaction .....	104
6.15 Distributions of Differences in Required Slab Thicknesses .....	107

FIGURE	Page
B1 Illustration of FWD Data of 260050000 at Alachua County .....	137
B2 PCS Data of 26005000 at Alachua County .....	137
B3 Illustration of FWD Data of 28040000 at Bradford County .....	138
B4 PCS Data of 28040000 at Bradford County .....	138
B5 Illustration of FWD Data of 86190000 at Broward County .....	139
B6 PCS Data of 86190000 at Broward County .....	139
B7 Illustration of FWD Data of 01010000 at Charlotte County .....	140
B8 PCS Data of 01010000 at Charlotte County .....	140
B9 Illustration of FWD Data of 87060000 at Dade County .....	141
B10 PCS Data of 87060000 at Dade County .....	141
B11 Illustration of FWD Data of 87270000 at Dade County .....	142
B12 PCS Data of 87270000 at Dade County .....	142
B13 Illustration of FWD Data of 87061000 at Dade County .....	143
B14 PCS Data of 87061000 at Dade County .....	143
B15 Illustration of FWD Data of 87030000R at Dade County .....	144
B16 PCS Data of 87030000R at Dade County .....	144
B17 Illustration of FWD Data of 87030000L at Dade County .....	145
B18 PCS Data of 87030000L at Dade County .....	145
B19 Illustration of FWD Data of 50010000 at Gadsden County .....	146
B20 PCS Data of 50010000 at Gadsden County .....	146
B21 Illustration of FWD Data of 10060000 at Hillsborough County .....	147
B22 PCS Data of 10060000 at Hillsborough County .....	147
B23 Illustration of FWD Data of 10160000 at Hillsborough County .....	148

FIGURE	Page
B24 PCS Data of 10160000 at Hillsborough County .....	148
B25 Illustration of FWD Data of 10075000A at Hillsborough County .....	149
B26 PCS Data of 10075000A at Hillsborough County .....	149
B27 PCS Data of 10075000B at Hillsborough County .....	150
B28 Illustration of FWD Data of 10250001 at Hillsborough County .....	151
B29 PCS Data of 10250001 at Hillsborough County .....	151
B30 Illustration of FWD Data of 11020000 at Lake County .....	152
B31 PCS Data of 11020000 at Lake County .....	152
B32 Illustration of FWD Data of 90060000 at Monroe County .....	153
B33 PCS Data of 90060000 at Monroe County .....	153
B34 Illustration of FWD Data of 93310000 at Palm Beach County .....	154
B35 PCS Data of 93310000 at Palm Beach County .....	154
B36 Illustration of FWD Data of 93100000 at Palm Beach County .....	155
B37 PCS Data of 93100000 at Palm Beach County.....	155
B38 Illustration of FWD Data of 15190000R at Pinellas County .....	156
B39 PCS Data of 15190000R at Pinellas County .....	156
B40 Illustration of FWD Data of 15190000L at Pinellas County .....	157
B41 PCS Data of 15190000L at Pinellas County .....	157
B42 Illustration of FWD Data of 15003000R at Pinellas County .....	158
B43 PCS Data of 15003000R at Pinellas County .....	158
B44 Illustration of FWD Data of 15003000L at Pinellas County .....	159
B45 PCS Data of 15003000L at Pinellas County .....	159
B46 Illustration of FWD Data of 16250000 at Polk County .....	160

FIGURE	Page
B47 PCS Data of 16250000 at Polk County .....	160
B48 Illustration of FWD Data of 16003001 at Polk County .....	161
B49 PCS Data of 16003001 at Polk County .....	161
B50 Illustration of FWD Data of 16100000 at Polk County .....	162
B51 PCS Data of 16100000 at Polk County .....	162
B52 Illustration of FWD Data of 58060000 at Santa Rosa County .....	163
B53 PCS Data of 58060000 at Santa Rosa County .....	163
B54 Illustration of FWD Data of 77040000 at Seminole County .....	164
B55 PCS Data of 77040000 at Seminole County .....	164
B56 Illustration of FWD Data of 78020000 at St. Johns County .....	165
B57 PCS Data of 78020000 at St. Johns County .....	165
B58 Illustration of FWD Data of 79270000 at Volusia County .....	166
B59 PCS Data of 79270000 at Volusia County .....	166
E1 Comparison of Backcalculated Original Air Voids based on Penetration Data with Corresponding Values from LTPP Inventory Data .....	223
E2 Comparison of Backcalculated Original Air Voids based on Computed Original Binder Viscosities with Corresponding Values from LTPP Inventory Data.....	225
E3 Top-Down Cracking Sensitivity to the Change of Air Voids .....	227
E4 Bottom-Up Cracking Sensitivity to the Change of Air Voids .....	227
E5 IRI Sensitivity to the Change of Air Voids .....	228
E6 Rutting Sensitivity to the Change of Air Voids .....	228
F1 Resilient Modulus for Base (Section 86190).....	235
F2 Resilient Modulus for Subgrade (Section 86190) .....	235
F3 Resilient Modulus for Embankment (Section 86190) .....	236

FIGURE	Page
F4 Resilient Modulus for Base (Section 93100) .....	236
F5 Resilient Modulus for Subgrade (Section 93100).....	237
F6 Resilient Modulus for Embankment (Section 93100) .....	237
F7 Resilient Modulus for Base (Section 10060).....	238
F8 Resilient Modulus for Subgrade (Section 10060).....	238
F9 Resilient Modulus for Embankment (Section 10060) .....	239
F10 Resilient Modulus for Base (Section 16003).....	239
F11 Resilient Modulus for Subgrade (Section 16003).....	240
F12 Resilient Modulus for Embankment (Section 16003) .....	240
F13 Resilient Modulus for Base (Section 10160) .....	241
F14 Resilient Modulus for Subgrade (Section 10160).....	241
F15 Resilient Modulus for Embankment (Section 10160).....	242
F16 Resilient Modulus for Embankment (Section 16250).....	242
F17 Resilient Modulus for Base (Section 79270) .....	243
F18 Resilient Modulus for Subgrade (Section 79270).....	243
F19 Resilient Modulus for Embankment (Section 79270).....	244
F20 Resilient Modulus for Subgrade (Section 77040).....	244
F21 Resilient Modulus for Embankment (Section 77040).....	245
F22 Resilient Modulus for Base (Section 26005) .....	245
F23 Resilient Modulus for Subgrade (Section 26005).....	246
F24 Resilient Modulus for Embankment (Section 26005).....	246
F25 Resilient Modulus for Subgrade (Section 28040).....	247
F26 Resilient Modulus for Embankment (Section 28040).....	247

FIGURE	Page
F27 Resilient Modulus for Subgrade (Section 50010) .....	248
F28 Resilient Modulus for Embankment (Section 50010).....	248
F29 Resilient Modulus for Base (Section 58060) .....	249
F30 Resilient Modulus for Subgrade (Section 58060) .....	249
F31 Resilient Modulus for Embankment (Section 58060).....	250
F32 Resilient Modulus for Base (Section 90060) .....	250
F33 Resilient Modulus for Base (Section 87060) .....	251
F34 Resilient Modulus for Subgrade (Section 87060).....	251

## LIST OF TABLES

TABLE	Page
2.1	Material Input Requirements by Material Group (Olidis and Hein, 2004).....6
2.2	Proposed Test Plan for Characterizing Material Properties on Model Calibration Sections.....19
3.1	Summary of Candidate Sections from the Initial Stage .....22
3.2	Summary of Candidate AC Segments Considering Proximity to WIM Sites .....26
3.3	Summary of PCC Candidate Segments Considering Proximity to WIM Sites .....26
3.4	Summary of Candidate PCS Segments with Service Lives > 20 Years .....31
3.5	Candidate Test Sections for Model Calibration after the Initial Stage .....32
3.6	Final List of Calibration Sections .....35
4.1	Proposed Core and Trench Locations .....42
4.2	Tests on Asphalt Concrete Cores .....48
4.3	Tests on Portland Cement Concrete Cores .....48
4.4	Tests on Base, Stabilized Subgrade, and Embankment Materials .....49
4.5	Properties Determined from Extractions and DSR Testing on Core Samples from Section 16003001 in Polk County .....50
4.6	Properties Determined from PCC Core Samples .....52
4.7	Summary of Soil Index Properties from Laboratory Tests on Underlying Materials .....58
4.8	Soil Suction Coefficients for Embankment Soils .....62
5.1	Variables and Factor Levels Used for Sensitivity Analyses.....66
5.2	Input Data and Levels for BISAR Runs .....71
5.3	Asphalt Concrete Material Properties Used in M-E PDG Runs.....75
5.4	Predictions of Alligator Cracking (%) for Different AC Layer Combinations .....75

TABLE	Page
5.5 Required AC Thickness for New Design Based on Current FDOT Procedure.....	80
5.6 Required AC Thickness for Overlay Design Based on Current FDOT Procedure (poor condition with 2 inch existing AC).....	80
6.1 Compiled Pavement Performance Data on Calibration Sections .....	87
6.2 Compiled Traffic Data on Calibration Sections .....	88
6.3 Compiled Material and Structural Data on Calibration Sections .....	89
6.4 Sensitivity of Calibration Factors in Faulting Model .....	93
6.5 List of Counties for the Different Thickness Regions.....	100
6.6 Cumulative ESALs vs. Number of Heavy Trucks .....	105
7.1 Comparison of Thickness Requirements between 12- and 13-foot Wide Slabs for <i>Design I</i> .....	117
7.2 Comparison of Thickness Requirements between 12- and 13-foot Wide Slabs for <i>Design II</i> .....	118
A1 Candidate AC Segments .....	123
A2 Candidate PCC Segments .....	129
A3 Candidate AC Segments with Long Service Lives .....	130
A4 Candidate PCC Segments with Long Service Lives .....	133
C1 Core Data of 58060000 at SR 89 in Santa Rosa County .....	169
C2 Core Data of 50010000 at US90 and SR10 in Gadsden County .....	170
C3 Core Data of 123811 at I-10 in Gadsden County .....	171
C4 Core Data of 26005000 at SR 222 in Alachua County .....	171
C5 Core Data of 28040000 at SR 18 in Bradford County.....	173
C6 Core Data of 78020000 at US 1 in St. Johns County.....	175
C7 Core Data of 77040000 at SR46 in Seminole County .....	175

TABLE	Page
C8 Core Data of 11020000 at SR50 in Lake County .....	177
C9 Core Data of 79270000 at SR483 in Volusia County .....	177
C10 Core Data of 16250000 at SR37 in Polk County .....	178
C11 Core Data of 16003000 at SR563 in Polk County .....	179
C12 Core Data of 16100000 at US 92 in Polk County .....	180
C13 Core Data of 01010000 at US 41 in Charlotte County .....	180
C14 Core Data of 10075000A at I-75 in Hillsborough County .....	181
C15 Core Data of 10075000B at I-75 in Hillsborough County .....	181
C16 Core Data of 10250001 at 22 <sup>nd</sup> St. at SR 60 in Hillsborough County .....	182
C17 Core Data of 10060000 at US 41 in Hillsborough County .....	182
C18 Core Data of 10160000 at SR 60 in Hillsborough County .....	184
C19 Core Data of 15003000 at I-175 in Pinellas County .....	185
C20 Core Data of 15190000 at I-275 in Pinellas County .....	186
C21 Core Data of 86190000 at SR 823 in Broward County .....	187
C22 Core Data of 93310000 at SR 710 in Palm Beach County .....	188
C23 Core Data of 93100000 at SR 710 in Palm Beach County .....	189
C24 Core Data of 87061000 at SR 886 in Dade County .....	190
C25 Core Data of 87270000 at SR 9/9A in Dade County .....	190
C26 Core Data of 87030000 at SR 5 in Dade County .....	191
C27 Core Data of 87060000 at SR A1A in Dade County .....	192
C28 Core Data of 90060000 at US1 in Monroe County .....	193
D1 Properties Determined from Extractions and DSR Tests on Core Samples from Section 16250000 in Polk County .....	197

TABLE	Page
D2 Properties Determined from Extractions and DSR Tests on Core Samples from Section 26005000 in Alachua County .....	199
D3 Properties Determined from Extractions and DSR Tests on Core Samples from Section 28040000 in Bradford County .....	201
D4 Properties Determined from Extractions and DSR Tests on Core Samples from Section 50100000 in Gadsden County .....	203
D5 Properties Determined from Extractions and DSR Tests on Core Samples from Section 58060000 in Santa Rosa County .....	205
D6 Properties Determined from Extractions and DSR Tests on Core Samples from Section 86190000 in Broward County .....	207
D7 Properties Determined from Extractions and DSR Tests on Core Samples from Section 93100000 in Palm Beach County .....	208
D8 Properties Determined from Extractions and DSR Tests on Core Samples from Section 93310000 in Palm Beach County .....	209
D9 Properties Determined from Extractions and DSR Tests on Core Samples from Section 77040000 in Seminole County.....	210
D10 Properties Determined from Extractions and DSR Tests on Core Samples from Section 79270000 in Volusia County .....	212
D11 Properties Determined from Extractions and DSR Tests on Core Samples from Section 90060000 in Monroe County .....	213
D12 Properties Determined from Extractions and DSR Tests on Core Samples from Section 87060000 in Dade County .....	215
D13 Properties Determined from Extractions and DSR Tests on Core Samples from Section 10060000 in Hillsborough County .....	217
D14 Properties Determined from Extractions and DSR Tests on Core Samples from Section 10160000 in Hillsborough County.....	218
E1 Data for Backcalculating Initial Air Voids Content on US27 LTPP Sections .....	222
E2 Cases Considered in Sensitivity Analysis of Initial Air Voids Content .....	226
E3 Recommended Original Air Voids for Calibration of M-E PDG Models .....	230

TABLE

Page

G1 Required AC Layer Thickness for New Design with 45 ksi Base Modulus .....255

G2 Required AC Layer Thickness for New Design with 30 ksi Base Modulus .....255

G3 Required AC Overlay Thickness (poor condition, 2-inch existing AC thickness after milling with 30 ksi base modulus).....256

G4 Required AC Overlay Thickness (fair condition, 2-inch existing AC thickness after milling with 30 ksi base modulus).....256

G5 Required AC Overlay Thickness (good condition, 2-inch existing AC thickness after milling with 30 ksi base modulus).....257

G6 Required AC Overlay Thickness (poor condition, 3-inch existing AC thickness after milling with 30 ksi base modulus).....257

G7 Required AC Overlay Thickness (fair condition, 3-inch existing AC thickness after milling with 30 ksi base modulus).....258

G8 Required AC Overlay Thickness (good condition, 3-inch existing AC thickness after milling with 30 ksi base modulus).....258

G9 Required AC Overlay Thickness (poor condition, 4-inch existing AC thickness after milling with 30 ksi base modulus).....259

G10 Required AC Overlay Thickness (fair condition, 4-inch existing AC thickness after milling with 30 ksi base modulus).....259

G11 Required AC Overlay Thickness (good condition, 4-inch existing AC thickness after milling with 30 ksi base modulus).....260

G12 Required AC Overlay Thickness (poor condition, 5-inch existing AC thickness after milling with 30 ksi base modulus).....260

G13 Required AC Overlay Thickness (fair condition, 5-inch existing AC thickness after milling with 30 ksi base modulus).....261

G14 Required AC Overlay Thickness (good condition, 5-inch existing AC thickness after milling with 30 ksi base modulus).....261

G15 Required AC Overlay Thickness (poor condition, 6-inch existing AC thickness after milling with 30 ksi base modulus).....262

G16 Required AC Overlay Thickness (fair condition, 6-inch existing AC thickness after milling with 30 ksi base modulus).....262

TABLE

Page

G17 Required AC Overlay Thickness (good condition, 6-inch existing AC thickness after milling with 30 ksi base modulus).....263

G18 Required AC Overlay Thickness (poor condition, 2-inch existing AC thickness after milling with 45 ksi base modulus).....263

G19 Required AC Overlay Thickness (fair condition, 2-inch existing AC thickness after milling with 45 ksi base modulus).....264

G20 Required AC Overlay Thickness (good condition, 2-inch existing AC thickness after milling with 45 ksi base modulus).....264

G21 Required AC Overlay Thickness (poor condition, 3-inch existing AC thickness after milling with 45 ksi base modulus).....265

G22 Required AC Overlay Thickness (fair condition, 3-inch existing AC thickness after milling with 45 ksi base modulus).....265

G23 Required AC Overlay Thickness (good condition, 3-inch existing AC thickness after milling with 45 ksi base modulus).....266

G24 Required AC Overlay Thickness (poor condition, 4-inch existing AC thickness after milling with 45 ksi base modulus).....266

G25 Required AC Overlay Thickness (fair condition, 4-inch existing AC thickness after milling with 45 ksi base modulus).....267

G26 Required AC Overlay Thickness (good condition, 4-inch existing AC thickness after milling with 45 ksi base modulus).....267

G27 Required AC Overlay Thickness (poor condition, 5-inch existing AC thickness after milling with 45 ksi base modulus).....268

G28 Required AC Overlay Thickness (fair condition, 5-inch existing AC thickness after milling with 45 ksi base modulus).....268

G29 Required AC Overlay Thickness (good condition, 5-inch existing AC thickness after milling with 45 ksi base modulus).....269

G30 Required AC Overlay Thickness (poor condition, 6-inch existing AC thickness after milling with 45 ksi base modulus).....269

G31 Required AC Overlay Thickness (fair condition, 6-inch existing AC thickness after milling with 45 ksi base modulus).....270

TABLE

Page

G32	Required AC Overlay Thickness (good condition, 6-inch existing AC thickness after milling with 45 ksi base modulus).....	270
H1	Required PCC Slab Thicknesses (Region 1) .....	273
H2	Required PCC Slab Thicknesses (Region 2) .....	274
H3	Required PCC Slab Thicknesses (Region 3) .....	275
H4	Required PCC Slab Thicknesses (Region 4) .....	276
H5	Required PCC Slab Thicknesses (Region 5) .....	277
H6	Required PCC Slab Thicknesses (90% reliability) .....	278



# CHAPTER I. INTRODUCTION

## BACKGROUND

The National Cooperative Highway Research Program (NCHRP) Project 1-37A delivered the *Mechanistic-Empirical Pavement Design Guide* (M-E PDG) and its companion software (Version 0.7) in 2004. The M-E PDG represents a major change in the way pavement design is performed. The design method considers site conditions (traffic, climate, subgrade, existing pavement condition for rehabilitation) and construction conditions in proposing a trial design for new pavement construction or rehabilitation. The trial design is then evaluated for adequacy through the prediction of key pavement performance indicators and comparisons of these predictions with performance criteria set by the engineer. Since its initial release, state departments of transportation (DOTs) have embarked on efforts to implement the M-E PDG program. Research projects have also been initiated to evaluate the original program and develop performance models for top-down cracking, reflection cracking, and rutting. Through reviews conducted on research projects, implementation efforts within state DOTs, and from pavement practitioners, the design program has seen a number of updates since its initial release. At the time of completing this project, the M-E PDG development team released software Version 1.0 in May 2007.

The Florida Department of Transportation (FDOT) sponsored a research project with the Texas Transportation Institute (TTI) to implement the M-E PDG program in the state. The Department presently uses a design method based on the 1993 pavement design guide approved by the American Association of State Highway and Transportation Officials (AASHTO). Pavement design with the M-E PDG program will entail a significant change in current design practice within the Florida DOT. Since the new program requires comprehensive input data for a given analysis, considerable efforts are needed to characterize traffic and material inputs with field and laboratory testing. For an engineer to design a specific pavement, it is necessary to assume an initial structure and run the program repetitively until a pavement design is identified that satisfies the performance criteria for the given problem. From this perspective, many practitioners have remarked that the program is not a pavement design program per se but an analytical tool for predicting pavement performance given the design parameters. In this respect, it is unlike the current Florida pavement design method. Implementing the M-E PDG program as is will mean a significant

change in current practice within state DOTs that are presently using the AASHTO design method.

The performance models in the new program were also developed and calibrated based on a national database of field pavement performance data. For states seeking to implement the M-E PDG, the developers of the design guide have recommended that the models be calibrated to local conditions. For this purpose, the authors of the new guide included an option in the program that permits users to input calibration factors to tailor the performance models to local conditions.

Given the above considerations, and recognizing that further changes to the design guide will come about from on-going national research projects, a staged implementation of the M-E PDG in Florida was conducted. In the current project, this implementation established and tested in-service pavement sections across Florida to develop a database for calibrating the existing M-E PDG performance models. Researchers also established thickness design tables for flexible and rigid pavements on the basis of sensitivity analyses and local calibrations of performance models for rigid pavements. This report documents the initial steps taken to implement an M-E PDG-based design procedure within the Florida DOT.

## **RESEARCH OBJECTIVES**

The primary objectives of this project are to:

- provide a database for verifying and calibrating, as necessary, the performance models in the existing M-E PDG program; and
- establish thickness design tables for flexible and rigid pavements based on the M-E PDG.

To accomplish these objectives, the following tasks were conducted:

- examination of Florida's pavement condition survey (PCS) database to identify in-service pavement sections for model calibrations;
- sensitivity analyses to identify critical factors affecting predicted pavement performance from the M-E PDG program;
- field and laboratory tests to characterize material properties of in-service pavement sections for model calibration and for developing thickness design tables;
- compilation of database for model calibration;

- local calibrations of performance models for rigid pavements; and
- development of M-E PDG-based supplemental thickness design tables for flexible and rigid pavements.

## **SCOPE OF RESEARCH REPORT**

This report documents the initial steps taken to implement an M-E PDG-based design procedure in Florida. The report is organized into the following chapters:

- Chapter I provides the impetus for this project and states its objectives.
- Chapter II describes the material characterizations required for the mechanistic-empirical design approach used in the new guide. This background material is provided for the purpose of establishing the test plan to characterize in-service pavement sections for model calibration.
- Chapter III presents the determination of candidate sections for model calibration.
- Chapter IV describes the field and laboratory tests conducted in this project to characterize in-service pavement sections established for model calibration.
- Chapter V presents the M-E PDG based supplemental thickness design tables for flexible pavements.
- Chapter VI presents the M-E PDG based supplemental thickness design tables for rigid pavements.
- Chapter VII summarizes the findings from this project and presents recommendations for future efforts to implement the M-E PDG in Florida.

The appendices provide supporting material for the tasks conducted in this project that are documented in the different chapters of this report.



## CHAPTER II. REVIEW OF M-E PDG INPUT REQUIREMENTS

This chapter describes the material characterizations required for the mechanistic-empirical design approach used in the guide. It provides background material on the input requirements of the M-E design guide system for the purpose of establishing a test plan to characterize the pavement sections proposed for model calibration. To provide a common basis for understanding the material requirements, the following M-E-based sub-categories have been developed (NCHRP 1-37A, 2004):

- In the first category are material properties required to predict the states of stress, strain, and displacement within pavement structures when subjected to wheel loads. These properties include elastic modulus and Poisson's ratio of each pavement material.
- In the second category are the materials-related inputs that are used directly in the distress and smoothness models incorporated into the M-E PDG. For each of these distresses, the critical structural response under a given wheel and climatic loading condition is affected by modulus and Poisson's ratio. In addition, parameters such as strength, expansion-contraction characteristics, friction between slab and base, erodibility of underlying layers, layer drainage characteristics, plasticity, gradation, and other materials-related parameters are needed in predicting the development of pavement distresses.
- Finally, in the third category are materials-related inputs that are used with the climatic module in the design guide program to determine the temperature and moisture profiles through the pavement cross section. These include engineering index properties, gradation parameters, and thermal properties.

Table 2.1 is a tabular summary of the material inputs required for mechanistic-empirical design arranged by the major material categories. Researchers used the information from this review to identify the laboratory and field tests needed to characterize material properties for calibrating the performance models in the design guide program.

**Table 2.1. Material Input Requirements by Material Group (Olidis and Hein, 2004).**

Material	Required Information
Hot Mix Asphalt	Dynamic modulus Poisson's ratio Tensile strength Coefficient of thermal expansion Thermal Conductivity Asphalt binder stiffness Aggregate properties
Portland Cement Concrete	Modulus of elasticity Poisson's ratio Unit weight Coefficient of thermal expansion Mix properties Aggregate type Thermal Conductivity Heat capacity
Chemically Stabilized Material	Elastic modulus Poisson's ratio Unit weight Modulus of rupture Thermal Conductivity Heat capacity
Unbound Material	Resilient modulus Poisson's ratio Unit weight Gradation Optimum moisture content Plasticity index
Recycled Asphalt Pavement	Resilient modulus Poisson's ratio Unit weight Gradation Hydraulic conductivity Optimum moisture content Plasticity index
Bedrock	Elastic modulus Poisson's ratio Unit weight

### **MULTI-LEVEL INPUT APPROACH**

The M-E PDG program provides three levels for selecting or determining traffic, material, and environment-related inputs for pavement performance predictions. Since users may employ combinations of these three main levels for a particular design problem, the new

guide provides flexibility in characterizing program inputs for analysis. Level 1 involves comprehensive laboratory and field testing to characterize design inputs. Cases in which a Level 1 design would be appropriate are on projects where a high confidence level is required, such as a principal arterial with high traffic volumes or test sections used for pavement research. In contrast, Level 3 requires the designer to estimate the most appropriate design input value of a material property based on experience with little or no testing. This level has the least accuracy and would typically be used for lower volume roadways. Inputs at Level 2 are estimated through correlations with other material properties that are measured from laboratory or field tests.

As indicated previously, it is possible for a designer to mix and match the levels of input for a specific project or region. For example, a user may select Level 2 to specify subgrade properties because the subgrade in a particular region is well characterized by other tests such as CBR, and Level 1 to specify traffic inputs determined from weigh-in-motion data collected at a comparable facility.

## CHARACTERIZATION OF ASPHALT CONCRETE MATERIALS

The primary stiffness property for asphalt materials in the M-E PDG program is the time-temperature dependent dynamic modulus ( $E^*$ ). Dynamic modulus testing (as proposed by NCHRP 1-28, “Harmonized Test Methods for Laboratory Determination of Resilient Modulus for Flexible Pavement Design”), and asphalt binder complex shear modulus and phase angle testing (AASHTO T315) are used to develop a master curve that represents the time-temperature behavior of the asphalt concrete (AC) mix based on the following equation:

$$\log E^* = \delta + \frac{\alpha}{1 + e^{\beta + \gamma \log t_r}} \quad (2.1)$$

where  $t_r$  is the time of loading at the reference temperature, and the model coefficients  $\delta$ ,  $\alpha$ ,  $\beta$ , and  $\gamma$  are defined as follows:

$$\delta = 3.750 + 0.029 p_{200} - 0.002 (p_{200})^2 - 0.003 p_4 - 0.058 V_a - 0.802 \left( \frac{V_{beff}}{V_{beff} + V_a} \right) \quad (2.2)$$

$$\alpha = 3.872 - 0.002 p_4 + 0.004 p_{38} - 0.000017 p_{38}^2 + 0.005 p_{34} \quad (2.3)$$

$$\beta = -0.603 - 0.394 \log \eta_r \quad (2.4)$$

$$\gamma = 0.313 \quad (2.5)$$

It is observed that  $\delta$  and  $\alpha$  are functions of volumetric mixture properties, specifically:

- air voids content  $V_a$  (%)
- effective bitumen content by volume  $V_{beff}$  (%),
- cumulative percent retained on 3/4-inch sieve,  $p_{34}$ ,
- cumulative percent retained on 3/8-inch sieve,  $p_{38}$ ,
- cumulative percent retained on No. 4 sieve,  $p_4$ , and
- cumulative percent retained on No. 200 sieve.

The loading time  $t_r$  in Eq. (2.1) is related to the loading time  $t$  at the temperature of interest through the equation:

$$\log \frac{t_r}{t} = -1.256 \log \frac{\eta}{\eta_T} \quad (2.6)$$

where  $\eta$  and  $\eta_T$  are the bitumen viscosities at the corresponding temperatures.

The asphalt concrete materials characterization procedure used in the design guide accounts for short term binder aging during asphalt mixing and placement at initial construction, and age hardening on the basis of the global aging system. For a Level 1 rehabilitation project, the master curve for the asphalt concrete is developed using test data collected from the falling weight deflectometer (FWD) and from laboratory testing of extracted cores. To obtain the relationship between the backcalculated modulus and temperature, the test temperature needs to be recorded during the FWD data collection. Cores extracted from the pavement are subjected to standard asphalt concrete testing (air voids, asphalt cement content and gradation) to develop an undamaged master curve for the aged asphalt concrete. A damage transfer function then combines the results of the backcalculation and laboratory testing to develop a field master curve. The Level 2 design uses some additional resilient modulus testing while the Level 3 analysis employs a typical asphalt concrete master curve and the visual survey data to determine the field master curve.

The asphalt concrete master curves are used as inputs to the distress prediction equations to determine the amount of cracking and rutting. The following additional tests are conducted (as applicable for the given local conditions) to predict thermal cracking:

- Tensile strength and creep compliance (AASHTO T322); and
- Thermal conductivity and heat capacity (ASTM E1592 and ASTM D2766).

For the first set of properties, the indirect tensile test (AASHTO T322) is performed on hot-mix asphaltic concrete (HMAC) specimens. Tensile strength and creep compliance are significant predictors of thermal cracking in the M-E PDG program. In addition, if the NCHRP 1-28 test protocol is employed to determine HMAC resilient modulus, the tensile strength of the material needs to be known to establish loading levels in accordance with the SHRP P07 protocol.

Based on the review of the design guide, researchers suggested that FWD testing and coring be performed to characterize material properties of pavement sections proposed for model calibrations. In addition, the individual AC lifts need to be identified from the cores to establish the requirements for characterizing the asphalt-bound material for predicting the performance of the calibration sections using the M-E PDG program. Researchers also recommended that pavement test temperatures be recorded during FWD testing, with infrared surface temperatures taken as a minimum to predict pavement temperatures at the time of testing using an existing method like the BELLS equation (Stubstad et al., 1998).

With respect to the asphalt concrete modulus, extracted cores may be tested in accordance with NCHRP 1-28 or AASHTO T315. If a core specimen has more than one layer, the layers should be separated at the layer interfaces by sawing. Layers containing more than one lift of the same material as placed under contract specification may be tested as a single specimen. If the NCHRP 1-28 protocol is selected, the resilient modulus is measured using the repeated load indirect tensile test. This allows characterization of the moduli of different asphalt lifts instead of a composite modulus that is estimated from the backcalculation. Alternatively, cores can be tested to establish mix volumetric parameters (air voids, asphalt volume, gradation, and asphalt viscosity) to estimate dynamic modulus using the equation by Witczak and Fonseca (1996) that is incorporated into the M-E pavement design guide.

To consider aging of materials, the binder viscosity can be estimated using conventional asphalt test data such as ring and ball softening point, absolute and kinematic viscosities, or through the Brookfield viscometer. If the binder viscosity-temperature relationship cannot be determined from binder testing, consideration may be given to using typical A-VTS coefficients provided in the design guide software based on performance grade, viscosity, or penetration grade of the binder.

Finally, the indirect tensile test (AASHTO T322) may be performed to measure tensile strength and creep compliance properties needed to predict crack propagation for low-temperature cracking. For a Level 2 analysis, this test may be conducted only for the intermediate temperature of 14 °F. Alternatively, the following regression equations may be used in the absence of indirect tensile test data:

$$TS(\text{psi}) = 7417 - 114V_a - 0.304V_a^2 - 123VFA + 0.704VFA^2 + 406\text{Log}(Pen_{77}) - 2039\text{Log}(A) \quad (2.7)$$

$$D(t) = D_1 t^m \quad (2.8)$$

$$\log D_1 = -8.524 + 0.013\text{Temp} + 0.796\log V_a + 2.010\log VFA - 1.923\log A \quad (2.9)$$

$$m = 1.163 - 0.002\text{Temp} - 0.046V_a - 0.011VFA + 0.002Pen_{77} + 0.002\text{Temp} \times Pen_{77}^{0.4905} \quad (2.10)$$

where,

- $TS$  = indirect tensile strength (psi) at 14 °F,
- $V_a$  = as-constructed air voids (percent),
- $VFA$  = voids filled with asphalt (percent),
- $Pen_{77}$  = binder penetration (mm/10) at 77 °F,
- $A$  = intercept of binder viscosity- temperature relationship,
- $D(t)$  = creep compliance as a function of loading time  $t$ , and
- $\text{Temp}$  = temperature (°F) at which creep compliance is measured.

Dynamic modulus curves in the form of a sigmoidal function can be developed by shifting laboratory test data. The resulting shift factors can be expressed as a function of binder viscosity. This step allows the consideration of binder aging using the global aging system (Mirza and Witczak, 1995), which includes four models:

- original to mix laydown model,
- surface aging model,
- air void adjustment, and
- viscosity-depth model.

To consider the effect of aging in the performance prediction, it is necessary to estimate the initial properties, i.e., viscosity and air void content. The M-E design guide program goes step by step through each of the above aging models beginning with the known initial properties to establish the undamaged master curve for the mix. However, for the

model calibrations, tests would be run on existing pavements and samples taken from the calibration sections. Thus, the test data would represent aged conditions. For calibration, it would be necessary to backcalculate the initial properties using the M-E design guide aging models in reversed order, i.e., from the viscosity-depth model to the original mix/lay-down model. Since the current M-E PDG program does not support this reversed application of the aging models, the backcalculation of initial properties from measured aged properties would have to be implemented in a separate procedure external to the design program. The results from this backcalculation would then be input to the M-E PDG program for model calibrations. The steps in the backcalculation procedure are given in the following:

- Determine aged volumetric and bitumen properties from cored samples.
- Estimate the mix laydown viscosity  $\eta_{t=0}$  given the aged mix properties from tests on cores using the viscosity-depth model and the surface aging model. From the former model:

$$\eta_{t,z} = \frac{\eta_t (4 + E) - E (\eta_{t=0})(1 - 4z)}{4(1 + E z)} \quad (2.11)$$

$$E = 23.83e^{-0.0308 Maat} \quad (2.12)$$

where,

$\eta_{t,z}$  = known aged viscosity at a specific time  $t$  (months) and depth  $z$  (inches),

$\eta_t$  = aged surface viscosity,

$\eta_{t=0}$  = mix laydown viscosity, and

$Maat$  = mean annual air temperature, °F.

From the surface aging model:

$$\log \log(\eta_t) = \alpha = \frac{\log \log(\eta_{t=0}) + A t}{1 + B t} \quad (2.13)$$

$$\eta_t = 10^{10^\alpha} \quad (2.14)$$

In Eq. (2.13),  $A$  is a function of the binder temperature  $T_R$  in °R, mean annual air temperature, and mix laydown viscosity, while  $B$  is a function of  $T_R$ . By substituting Equation 2.13 into Equation 2.11, the mix laydown viscosity  $\eta_{t=0}$  can be determined.

- Estimate the original bitumen viscosity  $\eta_{orig}$  using the calculated value of  $\eta_{t=0}$  in the original to mix laydown model:

$$\log \log(\eta_{t=0}) = a_0 + a_1 \log \log(\eta_{orig}) \quad (2.15)$$

$$a_0 = 0.054 + 0.004 \text{ code} \quad (2.16)$$

$$a_1 = 0.972 + 0.011 \text{ code} \quad (2.17)$$

where code is the hardening ratio with a recommended value of zero for average hardening resistance.

- Estimate the original air voids  $VA_{orig}$  using the air void adjustment model with the measured air voids content  $VA$  from core samples and the other known parameters. The air void adjustment model is given by:

$$VA = \frac{VA_{orig} + 0.011(t) - 2}{1 + 4.24 \times 10^{-4}(t)(Maat) + 1.169 \times 10^{-3} \left( \frac{t}{\eta_{orig}} \right)} + 2 \quad (2.18)$$

Once the initial bitumen viscosity and air voids content are determined, the M-E design guide program is executed using these as inputs to the aging model to predict the pavement performance for a given calibration section.

## CHARACTERIZATION OF PORTLAND CEMENT CONCRETE MATERIALS

The Portland cement concrete (PCC) modulus of elasticity is used as an input to characterize the performance of PCC pavements. For Level 1, the PCC modulus of elasticity and Poisson's ratio are determined through laboratory testing using ASTM C469, "Static Modulus of Elasticity and Poisson's Ratio of Concrete in Compression." PCC elastic modulus values for the proposed mixture are required at 7, 14, 28, and 90 days. However, in practice, it might be difficult to perform these tests due to time constraints. For these cases, the modulus can also be backcalculated from FWD data. In this regard, the modulus values obtained from laboratory tests have been reported to be less than the corresponding moduli determined from nondestructive tests conducted with the FWD or with seismic methods. The ratio is approximately 0.8.

For Level 2, AASHTO T22, "Compressive Strength of Cylindrical Concrete Specimens," is performed at 7, 14, 28, and 90 days. Once the compressive strength data are input to the design program, PCC elastic modulus is internally determined using the following equation:

$$E_c = 33\rho^{3/2}(f'_c)^{1/2} \quad (2.19)$$

where,

$$E_c = \text{PCC elastic modulus (psi),}$$

$\rho$  = unit weight of concrete (lb/ft<sup>3</sup>), and  
 $f'_c$  = compressive strength (psi).

Level 3 uses a correlation equation and the specified 28-day strength of the concrete mix to estimate the elastic modulus.

The flexural strength (MR) is defined as the maximum tensile stress at rupture at the bottom of a simply supported concrete beam during a flexural test with third point loading. For Level 1 design, the flexural strength is determined in the laboratory by testing beams under three point loading (AASHTO T97, “Flexural Strength of Concrete”) for specimens aged at 7, 14, 28 and 90 days. Level 2 uses the compressive strength measured on cores taken at various ages (7, 14, 28 and 90 days) and a correlation equation to estimate MR. Level 3 uses a correlation equation and the specified 28-day strength of the concrete mix.

Poisson’s ratio is a required input to the structural response computation models, although its effect on computed pavement response is not great. As a result, this parameter is rarely measured and is often assumed. Poisson’s ratio for normal concrete typically ranges between 0.11 and 0.21, and values between 0.15 and 0.18 are typically assumed for PCC pavement design.

For Level 1 analysis, the unit weight of PCC materials may be determined by testing in accordance with AASHTO T121 “Mass per Cubic Meter, Yield, and Air Content of Concrete” and AASHTO T271 “Density of Plastic and Hardened Concrete in-Place by Nuclear Method” for new and rehabilitation projects, respectively. There is no specific correlation with other parameters that may be used for a Level 2 analysis. Typical values for normal weight concrete range from 140 to 160 lb/ft<sup>3</sup>. A unit weight within this range may be assumed for a Level 3 design.

Other important parameters of PCC materials considered by the M-E design guide include:

- coefficient of thermal expansion (AASHTO TP60, “Coefficient of Thermal Expansion of Hydraulic Cement Concrete”),
- PCC shrinkage (AASHTO T160, “Length Change of Hardened Hydraulic Cement Mortar and Concrete”),
- thermal conductivity (ASTM E1592), and
- heat capacity (ASTM D2766, “Standard Test Method for Specific Heat of Liquids and Solids”).

These properties are important in modeling the effects of temperature and moisture variations on the properties of the PCC slabs. Shrinkage and thermal expansion can cause significant curling and warping in PCC slabs, resulting in pavement cracking. In particular, determining the thermal expansion coefficient through direct testing under Level 1 is recommended since this parameter is extremely significant.

## **CHARACTERIZATION OF UNBOUND GRANULAR AND SUBGRADE MATERIALS**

The material parameters required for unbound granular materials, subgrade, and bedrock may be classified in one of three major groups:

1. pavement response model material inputs (resilient modulus and Poisson's ratio),
2. enhance integrated climatic model (EICM) material inputs (gradation, Atterberg limits, and hydraulic conductivity), and
3. other material properties (for example, the coefficient of lateral pressure).

For Level 1 analysis, resilient modulus ( $M_r$ ) values for unbound granular materials, subgrade, and bedrock are determined from cyclic triaxial tests on prepared representative samples. The recommended standard methods for modulus testing are:

1. NCHRP 1-28A, "Harmonized Test Methods for Laboratory Determination of Resilient Modulus for Flexible Pavement Design," and
2. AASHTO T307, "Determining the Resilient Modulus of Soil and Aggregate Materials."

The Level 1 procedure is applicable to new design, reconstruction, and rehabilitation projects. For reconstruction and rehabilitation purposes, material samples can be obtained through destructive testing (i.e., coring, trenching). Furthermore, for rehabilitation and reconstruction of the existing pavement layer, the FWD may be used to backcalculate layer moduli.

At Level 2, relationships between soil index properties, strength properties, and resilient modulus may be used to estimate  $M_r$ . For Level 3 designs, the resilient modulus of unbound granular materials is selected based on the unbound material classification (AASHTO or Unified Soil Classification system). The design guide provides a general range of typical modulus values based on averages from data collected on long term pavement performance (LTPP) sections. These typical values are provided for each unbound granular material classification at their optimum moisture contents.

Other important parameters of unbound materials considered by the design guide include:

- Atterberg limits (AASHTO T89-90),
- grain size distribution (AASHTO T27), and
- moisture-density relationship (AASHTO T99).

It is highly recommended that samples be taken to identify properties mentioned above because these properties are critical in the assessment of moisture variation and seasonal modulus values that significantly affect predicted pavement performance.

## **CHARACTERIZATION OF CHEMICALLY STABILIZED MATERIALS**

Chemically stabilized materials covered in the design guide include lean concrete, cement-stabilized, cement-treated open-graded drainage layers, soil-cement, lime, cement and fly ash-treated materials. The elastic modulus of the layer is the primary input parameter for chemically stabilized materials. For lean concrete and cement-treated materials in new pavements, the elastic modulus is determined using ASTM C469. For lime-stabilized materials, AASHTO T307 protocols apply. For each of the stabilized materials, relationships between the elastic modulus and compressive strength have been developed. For rehabilitation projects, the elastic modulus of the stabilized layer is determined through FWD backcalculation, or through dynamic cone penetrometer (DCP) testing in conjunction with a correlation equation.

The flexural strength of a stabilized layer is an important input parameter for flexible pavements only. Level 1 test procedures for chemically stabilized materials include:

- AASHTO T97 for testing lean concrete, cement-treated aggregate layers, and lime, cement and fly ash-treated layers, and
- ASTM D1635 for testing soil cement.

Level 2 test procedures use correlations to estimate the flexural strength for stabilized materials. Alternatively, the DCP can be used to obtain estimates of stiffness. The DCP provides a log of resistance to penetration under an impact load and has been correlated to CBR which is correlated with in situ modulus. Other important parameters of stabilized materials considered by the design guide include:

- thermal conductivity (ASTM E1952), and
- heat capacity (ASTM D2766).

## **RECYCLED CONCRETE MATERIALS**

Recycled concrete materials are treated similarly as unbound materials. The recycled concrete is tested to determine its resilient modulus by laboratory testing (if broken to aggregate-sized pieces) or through FWD testing if broken in the field into fractured slabs.

## **RECYCLED HOT-MIX ASPHALT MATERIALS**

Recycled hot mix asphalt is treated similarly as new asphalt concrete materials with inputs required to determine the modulus for each temperature, and shift factors obtained by data shifting from the master curve.

## **BEDROCK MATERIALS**

The M-E design guide also requires input of the bedrock modulus for predicting the performance of a given pavement section. As actual resilient modulus testing of bedrock for pavement design is rare, the design guide provides the following default resilient modulus values for bedrock:

1. uniform, solid bedrock – 1000 ksi, and
2. highly fractured, weathered bedrock – 500 ksi.

The Poisson's ratio for bedrock is selected as 0.15 for uniform, solid bedrock and 0.30 for highly fractured and weathered bedrock.

## **REQUIRED TESTS TO DETERMINE M-E PDG INPUTS FOR MODEL CALIBRATIONS**

Based on the review of M-E design guide inputs, researchers summarized the required tests to characterize the materials found on PCS pavement sections to calibrate the M-E design guide performance models to Florida conditions. To establish the scope of tests, researchers reviewed published reports on the sensitivity of the performance predictions to the design guide inputs and conducted sensitivity analyses to evaluate the effects of design guide input parameters, assuming pavement sections and environmental conditions representative of those found in Florida. For this purpose, researchers used conventional flexible and rigid pavement cross-sections in the runs made of the M-E PDG program (Version 0.8). Researchers note that this version was the one available at the time the plans for the field and laboratory tests were being developed. The flexible pavement structure comprised a four-layer pavement system with an asphalt concrete layer (4 inches thick), a

limerock base (10 inches thick), stabilized subgrade (12 inches thick), and sand subgrade. The rigid pavement structure consisted of six-layers with an 8-inch jointed plain concrete pavement (JPCP) slab, existing AC layers consisting of 4 inches of asphalt permeable base over a 2-inch dense graded mix, a 10-inch limerock base, 12-inch stabilized subgrade, and sand subgrade. Both pavements were assumed to receive an average annual daily truck traffic (AADTT) of 7000, which translates to approximately 40 million cumulative heavy trucks during the assumed 20-year design period. Climatic conditions representative of Orlando were input into the EICM module of the M-E pavement design guide system.

Table 2.2 identifies those variables that are deemed important on the basis of the sensitivity of the IRI and cracking predictions to changes in these input parameters and presents proposed tests to characterize these variables on the basis of these results. The sensitivity of the predicted pavement performance to the different input variables is indicated by the arrow in the second column of Table 2.2. An upward arrow indicates high sensitivity of the predicted performance to the given variable, and vice versa.

The sensitivity of AC modulus on the performance predictions based on cracking and IRI was performed at two different levels. For Level 1, researchers varied dynamic modulus values at different temperatures and frequencies by  $\pm 30$  percent. For Level 2, researchers specified different levels of gradation, air voids, and effective binder content to determine low, medium, and high AC modulus values considered representative of properties found in practice. The low AC modulus mixture contains a larger amount of percent passing the No. 200 sieve, and smaller amounts of percent retained on the  $\frac{3}{4}$ -inch,  $\frac{3}{8}$ -inch, and No. 4 sieve sizes. Researchers varied the effective binder content from 10 to 12 percent by volume, and the air voids contents from 9 to 7 percent to determine, respectively, the low and high levels of AC modulus. Researchers observed that the pavement with higher AC modulus performed well with respect to both longitudinal cracking and IRI.

For PCC pavements, the variation of AC modulus under the slab did not show a significant influence on the predicted PCC pavement performance. For these pavements, the dominant factors are the concrete thermal coefficient of expansion and compressive strength. Also, variations of the dowel bar diameter and joint spacing affected the predicted pavement performance considerably.

The resilient moduli of base and subgrade materials were found to have a significant effect on the predicted performance of flexible pavements. For this reason, researchers recommend resilient modulus tests to characterize the base, subgrade, and embankment materials on the selected HMAC calibration sections. In addition, FWD tests should be performed to verify the correlation between laboratory resilient modulus and the corresponding modulus based on FWD backcalculations. Table 2.2 gives the recommendations for FWD testing on this project.

Researchers also found that the parameters of the soil-water characteristic curve significantly influenced the predicted pavement performance, especially for flexible pavements. For the Level 1 analysis, researchers varied the soil suction parameters to represent soils with high moisture content (low suction), and low moisture content (high suction). At this level, the optimum moisture content, maximum dry unit weight, percent passing the No. 200 sieve, and the plasticity index (PI) are required to compute the specific gravity and saturated volumetric water content. For the Level 2 analysis, researchers varied the soil physical properties (optimum moisture content, maximum dry unit weight, percent passing the No. 200 sieve, and PI) to determine soil suction parameters using correlation equations between soil properties and suction parameters. Researchers found that the change of suction parameters was significantly related to the development of predicted distresses. In practice, the soil-water characteristic curve for a given material can be characterized using filter paper or the psychrometer. Based on current test practice, researchers provided estimates of the sample quantities required to obtain suction parameters and soil properties. Table 2.2 shows these estimates.

**Table 2.2. Proposed Test Plan for Characterizing Material Properties on Model Calibration Sections.**

Parameter	Sensitivity	Level	Applicable Test(s)	Recommendation
AC modulus	↑	1	NCHRP (1-28A) : 4"×6"	A Level 2 approach is recommended. Since most AC layers are composed of several lifts, test each layer property. Most lift thicknesses are expected to be thin and not appropriate for testing dynamic modulus. In addition, air voids, gradation, and asphalt content are general input parameters to the M-E design guide program and must be input even for a Level I analysis.
		2	AASHTO T315	
Layer thickness	↑	1	GPR, DCP and/or coring	GPR and coring are recommended.
Tensile strength & creep compliance	↑	1	AASHTO T322	A Level 1 approach is recommended. (4~6" diameter and 2~3" height) (Test temperature : -4, 14, and 32 °F for creep compliance and 14 °F for tensile strength)
		2	AASHTO T322 (Test only at 14 °F for tensile strength and creep compliance)	
Base modulus	↑	1	FWD (ASTM D4694)	The minimum recommended number of test points is 30 or at 0.1-mile intervals, whichever is less. Three drops should be performed at each test point, with the first two drops applied to seat the load. A target load of 9 kips is recommended for the third drop (usually achieved under drop height two of the FWD). Pavement temperature measurements are required.
Subgrade modulus	↑	1	FWD (ASTM D4694)	
Soil suction	↑	1	Suction test, AASHTO T27, AASHTO T90, FM 1-T 180	A Level 1 approach is recommended. In addition, soil properties (PI, gradation, optimum moisture content, and maximum dry unit weight) need to be measured. Estimates of the required material quantities are: Suction test (50 lbs), FM 1-T180 (50 lbs), and AASHTO T27 (35 lbs).
		2	AASHTO T27, AASHTO T90, FM 1-T 180	
Bedrock modulus	↓	N/A	Not typically tested.	Assume typical value for analysis.
Thermal coefficient of expansion	↑	1	AASHTO TP60	If a catalog of thermal coefficients from tests done on typical concrete mixtures is available, then use this catalog to get appropriate value. Otherwise, run test.
Joint spacing	↑	N/A	Field survey or historical data	Measure joint spacing.
Dowel bar spacing	↓	N/A	Historical data or plan sheets	No recommendation. Assume typical value for analysis.
Dowel bar diameter	↑	N/A	Coring or plan sheets	Check plan sheets or ask pavement design engineer. If not available, take a core at the joint.
PCC compressive strength	↑	2	AASHTO T22 (7,14,28, and 90 days)	A Level 3 approach is recommended. Run test to get compressive strength at 28 days on 4-inch diameter, 8-inch high concrete samples.
		3	AASHTO T22	
Vehicle speed	↓	N/A	Traffic data collection	Use posted highway speed.



## **CHAPTER III. DETERMINATION OF CANDIDATE SECTIONS FOR MODEL CALIBRATION**

This chapter describes how researchers identified candidate in-service pavement sections for verifying and calibrating the performance models in the existing M-E PDG program. The factors considered in selecting candidate sections were established based on consultation with the Department's project manager. These factors are the observed performance history and the availability of traffic data from existing weigh-in-motion (WIM) sites located on highways with the same functional classification as a given candidate section. Researchers used FDOT's PCS database to identify candidate calibration sections so that the performance history reported in the database can be used for the planned calibration.

### **INITIAL SELECTION STAGE**

From the PCS data, researchers initially identified segments where the pavement condition ratings (PCRs) have reached the critical value or have become deficient within the recent three years (2001 ~ 2004) at the time this task was completed. Specifically, asphalt concrete pavements with PCRs of 6.6 or less and Portland cement concrete pavements with PCRs of 7.0 or less were first considered. Because the number of PCC segments is much less than the number of AC pavements, researchers used a higher critical PCR for PCC pavements to identify more candidate segments for this pavement type. In addition, researchers identified segments with no indications of unreported maintenance or rehabilitation treatments and/or erroneous rating values by examining the trends in the ratings provided in the PCS data base for a given segment. Since the M-E PDG program has different models for predicting the progression of cracking, rutting, and ride quality through a pavement's life cycle, a list of candidate segments was prepared for each of the three pavement condition indicators of cracking, rutting, and ride that FDOT reports in its PCS data base. The following criteria were used in identifying candidate segments for a given distress type:

- The distress rating has reached the critical value (6.6 for AC and 7.0 for PCC pavements).
- The length of the current cycle corresponding to the last rating reported in the data base is greater than 5 years.
- The minimum rating value for the current cycle is greater than 5 for observations

before the current year.

- The range of the rating values for each distress type is greater than or equal to 2 for the current cycle.
- The rating values within the current cycle show a decreasing trend. Specifically, if the following nonlinear curve is fitted to the current cycle data, the estimates of  $\beta_1$  should be greater than 0.01:

$$Distress\ rating = 20 \left( 1 - \frac{1}{1 + e^{-(\beta_0 + \beta_1 Age)}} \right) + error \quad (3.1)$$

- The average residual sum of squares from fitting Eq. (3.1) to the condition survey data for a given PCS segment is less than 0.15.

Since each distress type has a different list of candidate segments, a summary of the candidate segments identified for each distress is given in Table 3.1. The two right most columns in the table indicate the cumulative length of candidate segments (in centerline miles) and the total number of segments without duplication for each subsystem and pavement type (note that a PCS segment can be used for calibrating more than one distress model).

**Table 3.1. Summary of Candidate Sections from the Initial Stage.**

Type	Subsystem	PCR		Cracks		Ride		Rutting		Unique Total	
		Length	#seg.	Length	#seg.	Length	#seg.	Length	#seg.	Length	#seg.
AC	Arterial 1	39.56	12	4.02	4	6.60	4	22.85	6	60.33	21
	Arterial 2	76.00	20	3.20	3	11.82	6	1.20	2	77.49	23
	Arterial 3	13.47	10	8.99	6	7.70	6	3.06	3	25.84	18
	Arterial 4	25.21	8	5.73	4	10.37	6	7.76	3	35.52	15
	Arterial 5	72.69	19	24.94	8	6.60	4	41.09	9	80.71	24
	Arterial 6	12.85	9	1.99	1	9.32	6	4.38	3	20.54	13
	Arterial 7	15.83	8	8.52	1	4.89	4	12.68	5	27.63	12
	Interstate	12.26	5	40.09	5	0.00	0	17.51	3	55.11	10
	Turnpike	16.06	6	0.00	0	0.00	0	6.40	2	22.47	8
	Subtotal	283.92	97	97.47	32	57.30	36	116.92	36	405.64	144
PCC	Arterial 2	4.17	2	0.00	0	5.13	3	0.00	0	5.13	3
	Arterial 5	1.86	1	0.00	0	1.86	1	0.00	0	1.86	1
	Arterial 6	1.28	1	2.55	2	0.00	0	0.00	0	2.55	2
	Arterial 7	0.00	0	0.25	1	0.00	0	0.00	0	0.25	1
	Interstate	2.14	1	2.06	3	8.01	3	0.00	0	12.22	7
	Turnpike	0	0	0	0	0	0	0	0	0	0
		Subtotal	9.44	5	4.86	6	15.00	7	0.00	0	22.01
	Total	293.36	102	102.33	38	72.30	43	116.92	36	427.65	158

Since the M-E PDG program requires the axle load distribution for performance predictions, the proximity of a PCS segment to a WIM station was one criterion used by researchers to establish candidate segments for model calibration. The weigh-in-motion data can be used to determine the axle load distribution required by the program. Hence, researchers further screened the candidate segments to identify those that are close to a WIM station. Figure 3.1 shows the locations of WIM stations and candidate PCC segments. In this figure, the WIM station is identified by the WIM site number assigned by FDOT while the candidate PCC segment is identified by its roadway ID from the PCS database. The large printed numbers (1 to 7) denote the Florida Districts.

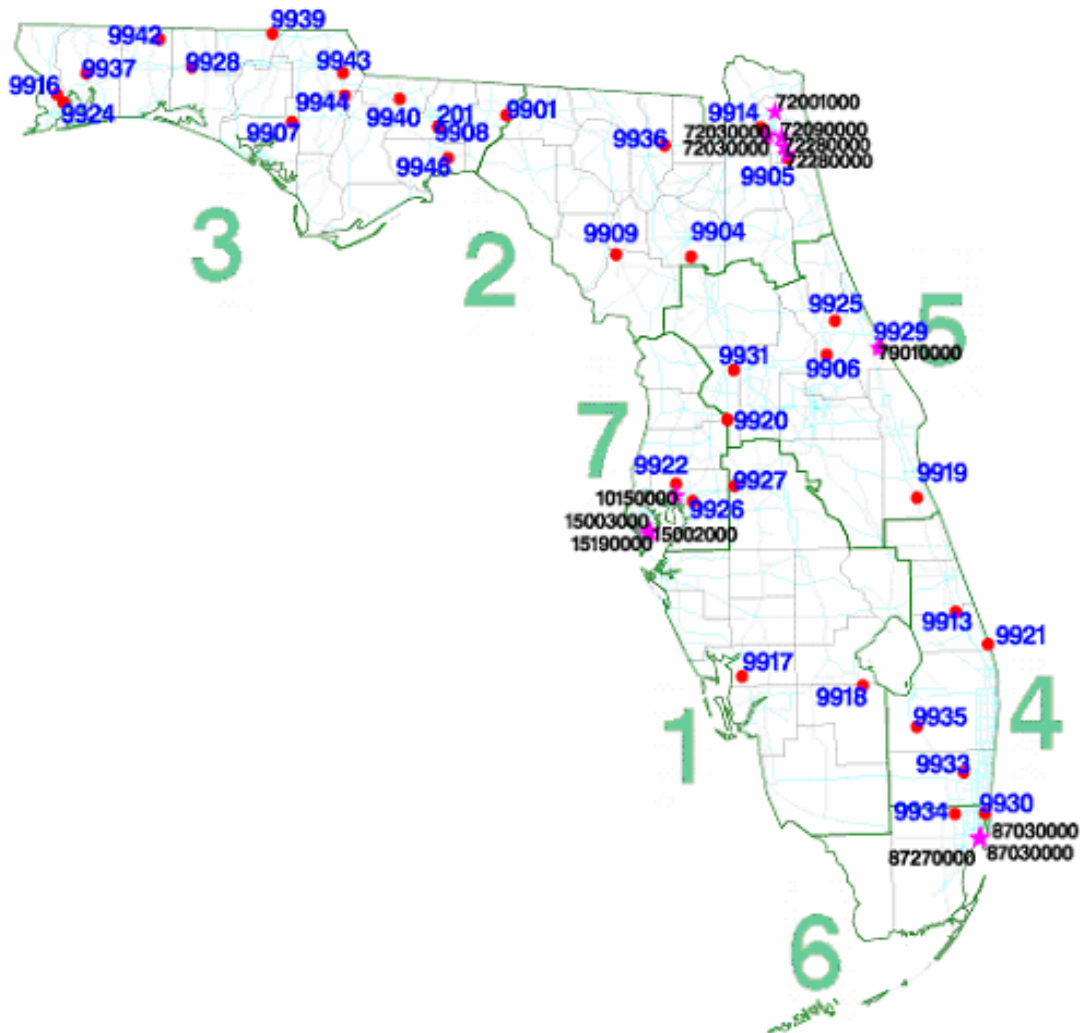


**Figure 3.1. WIM Stations and Candidate PCC Segments (dots indicate WIM stations while stars denote mid-points of each candidate PCC segment).**

For mapping purposes, researchers established the latitude-longitude (lat-long) coordinates utilizing the SAS road map data file (Roadnet2.SD2) provided by the FDOT project manager. Initially, the mid-mile post limits (MMP) of PCS segments were defined as follows:

$$\text{mid-mile post limit} = \frac{1}{2}(\text{ending mile post limit} + \text{beginning mile post limit}) \quad (3.2)$$

For each roadway ID, the lat-long coordinates of PCS segments were estimated to be proportional to those of the road map data. Because the road map data file has lat-long coordinates by mile post limits (MPs), the latitude and longitude coordinates of PCS segments can be interpolated. Consider a segment with MMP between  $MP_1$  and  $MP_2$ , where  $MP_1$  and  $MP_2$  are MPs in the road map data file. Let  $Lat_1$  and  $Lat_2$  be the latitudes of  $MP_1$  and  $MP_2$ , respectively. Then, the latitude and longitude coordinates of the mid-point of a PCS segment can be estimated as follows:

$$\begin{aligned} \text{Latitude}(\circ) &= Lat_1 + \frac{Lat_2 - Lat_1}{MP_2 - MP_1} (MMP - MP_1) \\ \text{Longitude}(\circ) &= Long_1 + \frac{Long_2 - Long_1}{MP_2 - MP_1} (MMP - MP_1) \end{aligned} \quad (3.3)$$

For the segment after the last MP in each roadway ID, researchers estimated the coordinates of the mid-mile post limit of the given PCS segment by extending the trend of the last two MPs.

To calculate the straight line distance between two locations based on lat-long coordinates, the coordinates were first converted from degrees to radians using the following equations:

$$\begin{aligned} \text{Latitude}(\text{rad}) &= \frac{\tan^{-1}(1)}{45} \text{Latitude}(\circ) \\ \text{Longitude}(\text{rad}) &= \frac{\tan^{-1}(1)}{45} \text{Longitude}(\circ) \end{aligned} \quad (3.4)$$

Then, if  $X_1$  and  $Y_1$  are the longitude and latitude, respectively, of a PCS segment in radians, and  $X_2$  and  $Y_2$  are the corresponding coordinates for a given WIM station, the *Great Circle Distance Formula* given by Eq. (3.5) can be used to calculate the distance in miles between two pairs of latitude/longitude values specified in radians:

$$D = 3949.99 \cos^{-1} \left\{ \sin Y_1 \sin Y_2 + \cos Y_1 \cos Y_2 \cos (X_1 - X_2) \right\} \quad (3.5)$$

Researchers obtained the above formula from the following web site: *SAS technical support*. For a candidate segment, researchers calculated all possible distances to the 36 WIM stations set up in Florida. For each candidate PCS segment, researchers then identified the WIM station closest to that segment based on the distances calculated from the lat-long coordinates.

Tables A1 and A2 in the appendix list all candidate segments for AC and PCC pavements, respectively. In these tables, the *SITE* and the *Distance of WIM* columns give the identification number and the distance of the nearest WIM station to the given candidate segment. The column *Road Condition* indicates the values of the pavement condition rating, cracks, ride, and rut (PCR, CR, RI, and RU) at the end of the life-cycle of a given segment. The mean residual sum of squares from fitting the non-linear model given by Eq. (3.1) to the PCS data for each candidate segment is given under the *Mean RSS* column. The column *Application* indicates the distress model(s) on which the given candidate segment can be used for model calibration. Note that a segment can be used for calibrating more than one distress model. The applicable distress models are identified by an *x* in the corresponding cells.

When the roadway ID of a candidate segment cannot be found in the road map data, the nearest WIM station and the distance to that station cannot be calculated. In this instance, the corresponding cells are filled in with *NAs* (not available). Researchers excluded these segments in the selection of PCS segments for model calibration. In addition, candidate segments that are more than 40 miles away from the nearest WIM station are screened out from this selection. These segments are highlighted in Tables A1 and A2.

Tables 3.2 and 3.3 summarize the candidate segments that remained after filtering out PCS segments (in the second round) where the WIM distance cannot be calculated, or where the nearest WIM station is more than 40 miles away from the given segment. Because few candidate PCC segments were found (relative to the number of AC segments), all candidate PCC pavements were selected in the pared down list of candidate segments established after considering the proximity to a WIM location. These PCC segments are also within 40 miles of a WIM station. In addition, candidate segments in the Interstate and Turnpike subsystems are within 40 miles of the corresponding WIM sites. Hence, all of these segments were selected. Figures 3.2, 3.3 and 3.4 identify the selected AC candidate segments in the Arterial, Interstate, and Turnpike subsystems, respectively. Since no PCC segments were screened out, the selected PCC candidate segments after the second round are as shown in Figure 3.1.

**Table 3.2. Summary of Candidate AC Segments Considering Proximity to WIM Sites.**

Subsystem	PCR		Cracks		Ride		Rutting		Overall	
	Length	#seg	Length	#seg	Length	#seg	Length	#seg	Length	#seg
Arterial 1	33.97	9	1.56	2	5.48	3	19.28	4	50.95	16
Arterial 2	75.56	19	3.2	3	11.39	5	1.2	2	77.05	22
Arterial 3	13.47	10	8.99	6	7.7	6	3.06	3	25.84	18
Arterial 4	25.21	8	5.73	4	10.37	6	7.76	3	35.52	15
Arterial 5	72.08	18	24.94	8	6.6	4	40.48	8	80.1	23
Arterial 6	8.52	7	1.99	1	9.32	6	4.38	3	16.22	11
Arterial 7	15.83	8	8.52	1	4.89	4	12.2	4	27.15	11
Interstate	12.26	5	40.09	5	0	0	17.51	3	55.11	10
Turnpike	16.06	6	0	0	0	0	6.4	2	22.47	8
Total	272.96	90	95.01	30	55.74	34	112.26	32	390.38	134

**Table 3.3. Summary of PCC Candidate Segments Considering Proximity to WIM Sites.**

Subsystem	PCR		Cracks		Ride		Overall	
	Length	#seg	Length	#seg	Length	#seg	Length	#seg
Arterial 2	4.17	2			5.13	3	5.13	3
Arterial 5	1.86	1			1.86	1	1.86	1
Arterial 6	1.28	1	2.55	2			2.55	2
Arterial 7			0.25	1			0.25	1
Interstate	2.14	1	2.06	3	8.01	3	12.22	7
Total	9.444	5	4.863	6	14.997	7	22.002	14

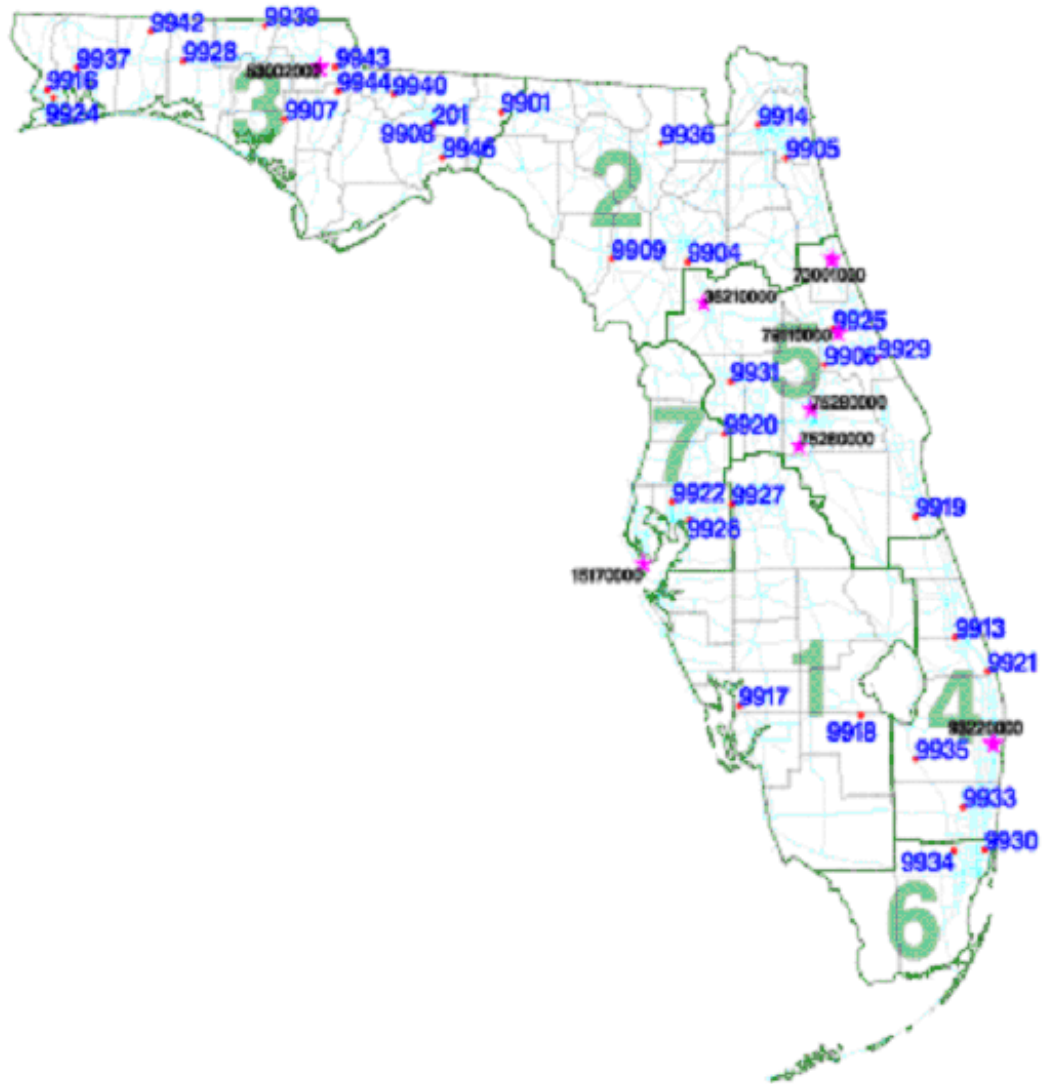


**Figure 3.2. Candidate AC Segments in the Arterial Subsystems Considering Proximity of PCS Segments to WIM Stations (dots indicate WIM stations while stars denote candidate segments).**

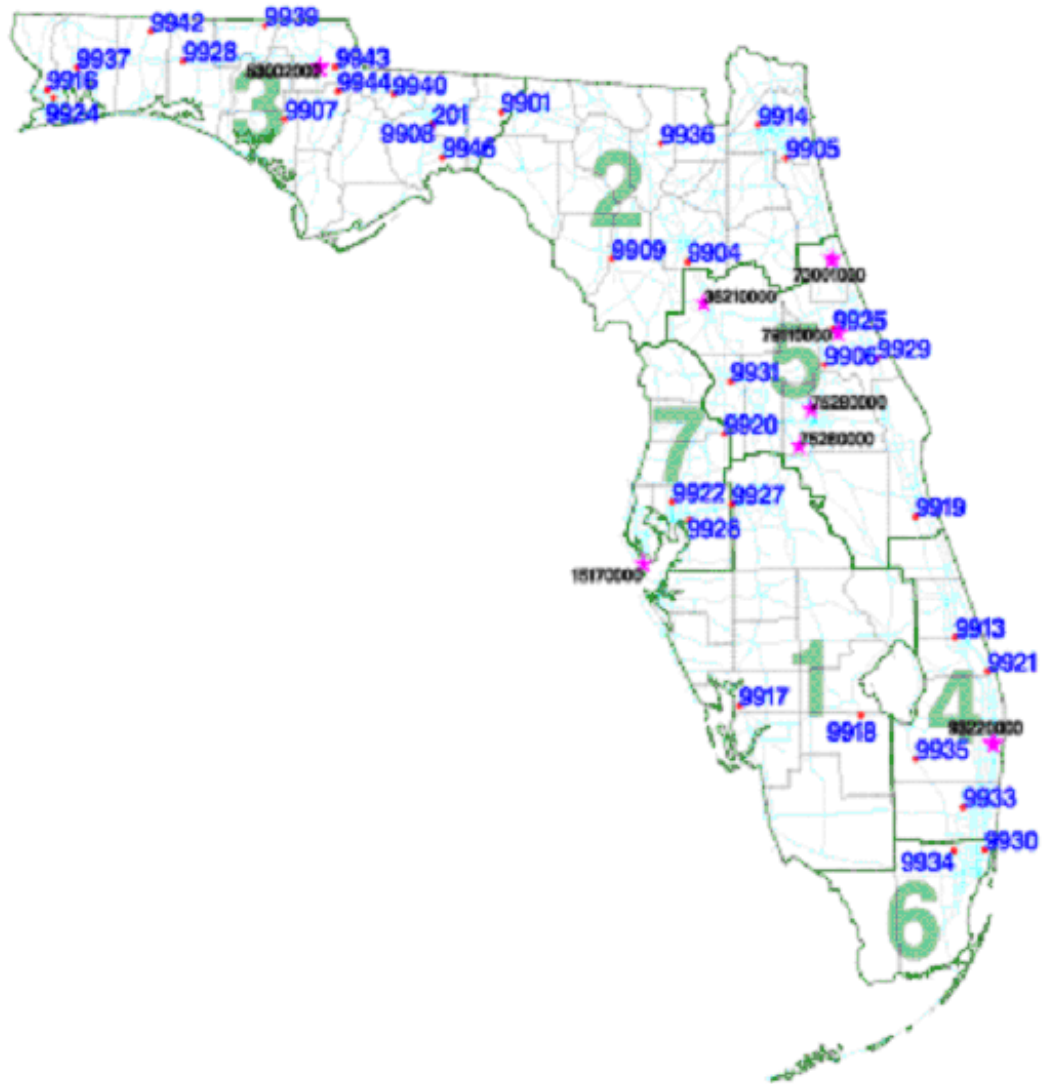


**Figure 3.3. Candidate AC Segments in the Interstate Subsystem Considering Proximity of PCS Segments to WIM Stations (dots indicate WIM stations while stars denote candidate segments).**

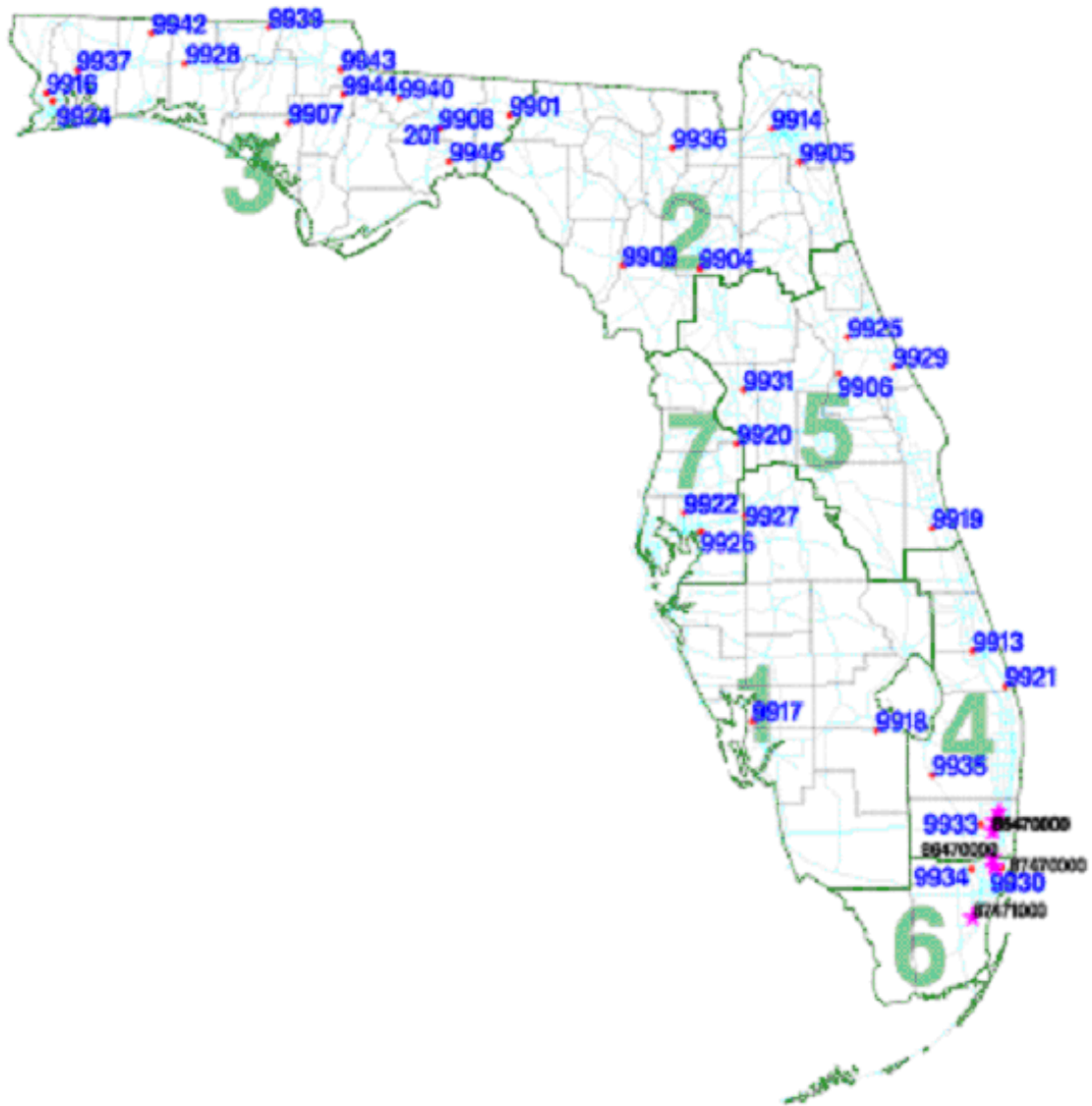


**Figure 3.4. Candidate AC Segments in the Turnpike Subsystem Considering Proximity of PCS Segments to WIM Stations (dots indicate WIM stations while stars denote candidate segments).**

For model calibrations, it is also important to consider PCS segments that exhibit long service lives. Calibrations that include these pavements can identify factors that are important in terms of designing longer-lasting pavements or generating cost-effective pavement designs. In addition, the presence of outliers in the condition survey ratings can influence any model calibration in the short term, because of the small number of observations. However, in the long term, the effects of outliers can be offset by many other normal observations. Thus, researchers identified PCS segments that showed service lives of more than 20 years before reaching the critical PCR values of 6.6 for AC and 7.0 for PCC pavements in the recent 3 years. Table 3.4 and Figure 3.5 summarize the PCS segments identified based on this criterion. In addition, Tables A3 and A4 in the appendix list AC and PCC segments, respectively, that exhibited service lives of more than 20 years.

Discussions with the project manager raised an additional criterion that researchers considered. Specifically, using data from a WIM site located along a roadway with the same functional classification as a given calibration section would be an appropriate approach for estimating the axle load distribution on the section. Thus, researchers applied this criterion to the list of candidate PCS segments previously identified. Table 3.5 shows the revised list of candidate segments that resulted from this screening. Three of the candidate sections (with roadway IDs 26060000, 89010000, and 71020000) overlap with test sections used in a previous FDOT project conducted by Ping, Wang and Yang (2000) of Florida State University (FSU). For each segment, Table 3.5 identifies the closest WIM station located along a roadway having the same functional class as the candidate segment. The straight line distance between the segment and the WIM site is also given in Table 3.5.

Table 3.5 identifies the specific distress for which a given segment may be used for calibration. In establishing this preliminary list of candidate segments, researchers gave higher consideration to PCS segments that became deficient by cracking inasmuch as this is the predominant distress observed on Florida pavements. From this list, 21 test sections (15 for AC and 6 for PCC) were selected as shown in the last column.

**Table 3.4. Summary of Candidate PCS Segments with Service Lives > 20 Years.**

Subsystem	AC		PCC		Total	
	length	#seg	length	#seg	length	#seg
Arterial 1	53.56	14	8.1	5	61.64	19
Arterial 2	50.05	20	11.1	6	61.12	26
Arterial 3	3.44	4	1.8	1	5.27	5
Arterial 4	24.66	17			24.66	17
Arterial 5	46.72	17	8.7	5	55.45	22
Arterial 6	12.60	8	0.5	1	13.09	9
Arterial 7	2.60	4	0.3	1	2.85	5
Interstate			9.0	13	9.02	13
Turnpike	0.32	1			0.32	1
Total	193.94	85	39.5	32	233.41	117

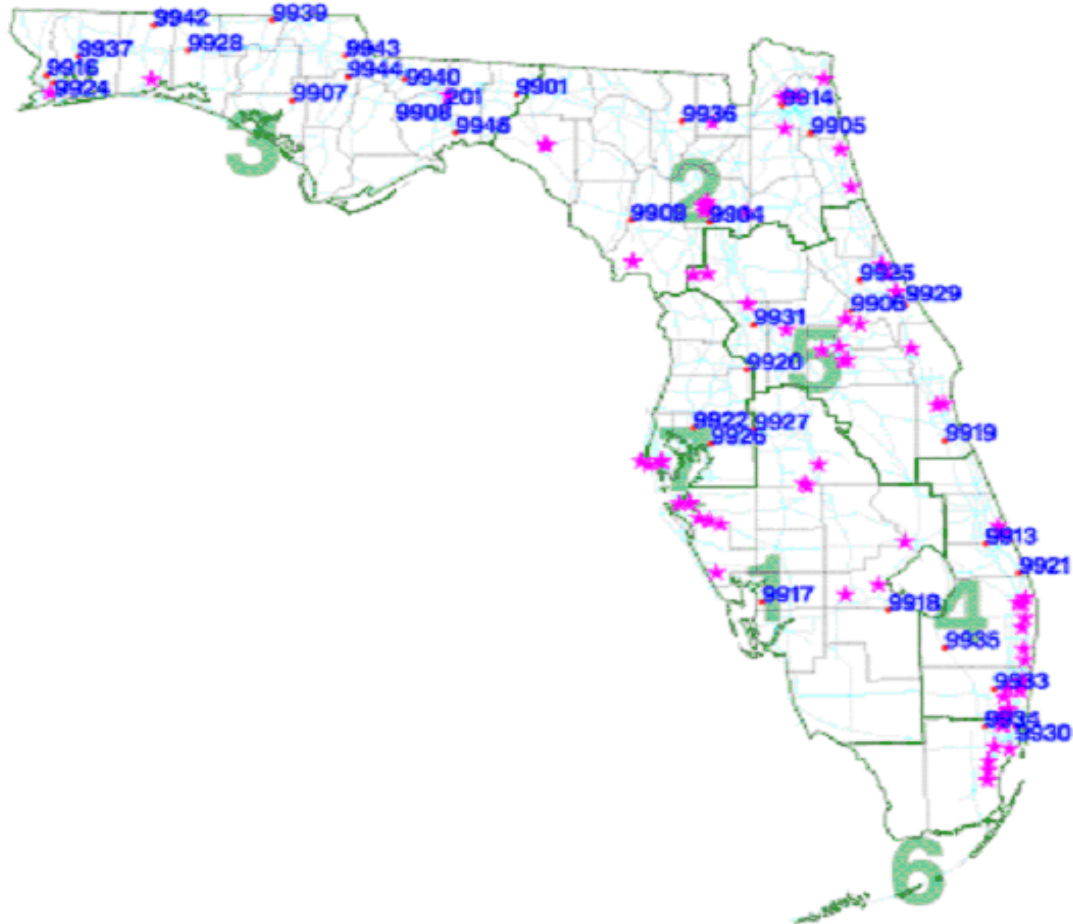


**Figure 3.5. Candidate Segments with Service Lives > 20 Years (WIM stations identified by dots and corresponding WIM site numbers while stars denote long-life segments).**

**Table 3.5. Candidate Test Sections for Model Calibration after the Initial Stage.**

RDWYID	Beginning Milepost	Ending Milepost	RDWYSIDE	System	District	New Year	Year	Age	Functional Class	Average Daily Traffic	ESALS per day	WIM Site	Straight Line Distance from WIM site	Pavement Type	Calibration for				Selected Calib. Sections
															PCR	Cracks	Ride	Rutting	
87060000	14.05	14.87	L	1	6	1997	2004	8	NON-FREEWAY URBAN	33500	535	9930	2.37	AC	x		x		
87090000	0.79	3.69	R	1	6	1986	2004	19	NON-FREEWAY RURAL	17100	408	9934	2.74	AC			x		
50010000	16.48	18.57	R	1	3	1996	2004	9	NON-FREEWAY RURAL	10933	297	9940	3.34	AC	x	x			✓
87080000	0.69	2.68	R	1	6	1992	2004	13	NON-FREEWAY URBAN	37500	611	9930	4.44	AC		x	x		✓
87080001	2.29	3.08	C	1	6	1997	2004	8	NON-FREEWAY URBAN	16500	622	9930	5.66	AC	x		x		
48003000	6.12	6.75	R	1	3	1987	2004	18	NON-FREEWAY URBAN	23500	546	9916	6.46	AC	x		x		
86100000	1.53	2.73	R	1	4	1981	2004	24	NON-FREEWAY URBAN	48000	983	9930	7.02	AC	x		x		
86190000	2.33	3.67	R	1	4	1999	2004	6	NON-FREEWAY URBAN	30750	238	9930	10.01	AC		x			✓
61010000	13.33	16.33	C	1	3	1986	2001	16	NON-FREEWAY RURAL	6200	300	9939	12.96	AC		x			✓
58010000	9.32	10.75	L	1	3	1989	2004	16	NON-FREEWAY URBAN	33000		9916	13.54	AC	x	x			✓
58010000	11.05	11.68	L	1	3	1989	2004	16	NON-FREEWAY URBAN	21500	509	9916	14.72	AC	x	x	x		✓
58060000	20.72	21.80	C	1	3	1997	2004	8	NON-FREEWAY RURAL	2400	81	9937	18.96	AC	x	x			✓
79270000	1.62	2.39	L	1	5	1997	2004	8	NON-FREEWAY URBAN	23500	367	9929	21.67	AC		x			✓
86020000	7.91	9.00	R	1	4	1983	2004	22	NON-FREEWAY URBAN	45250	257	9930	21.93	AC		x		x	✓
48010000	2.15	2.90	R	1	3	1987	2002	16	NON-FREEWAY RURAL	3621	190	9937	23.45	AC	x	x	x		✓
26060000	20.53	25.34	R	1	2	1995	2004	10	NON-FREEWAY RURAL	8600	1059	9909	47.55	AC		x			4
89010000	18.04	19.58	R	1	4	1987	2004	18	NON-FREEWAY URBAN	48750	222	9930	88.30	AC			x		2A
71020000	1.78	6.56	R	1	2	1996	2004	9	NON-FREEWAY URBAN	20968	454	9929	92.04	AC		x			5
87170000	3.70	5.23	L	1	6	1987	2004	18	NON-FREEWAY URBAN	39250	471	9930	1.34	AC	x				
18010000	19.48	21.60	C	1	5	1986	2002	17	NON-FREEWAY RURAL	7600	295	9931	3.07	AC	x			x	
87030000	24.96	25.38	R	1	6	1989	2004	16	NON-FREEWAY URBAN	37000		9930	4.10	AC	x				
48020000	7.87	9.65	L	1	3	1987	2004	18	NON-FREEWAY URBAN	27750	766	9916	5.88	AC			x		
86470000	8.51	15.16	L	5	4	1988	2001	14	FREEWAY	67207	1557	9933	6.10	AC	x				
86470000	8.51	15.16	R	5	4	1988	2001	14	FREEWAY	67207	1557	9933	6.10	AC	x				
86470000	15.16	16.95	L	5	4	1990	2001	12	FREEWAY	58199	1140	9933	6.26	AC	x				
48003000	6.12	6.75	L	1	3	1988	2004	17	NON-FREEWAY URBAN	23500	546	9916	6.46	AC	x				
79070000	26.97	29.29	R	1	5	1981	2004	24	NON-FREEWAY URBAN	18200	730	9929	7.54	AC	x		x		
93200000	0.00	1.37	C	1	4	1994	2004	11	NON-FREEWAY RURAL	20700	712	9935	28.36	AC		x			
77030000	5.09	6.04	R	1	5	1994	2004	11	NON-FREEWAY URBAN	14750	1223	9929	28.56	AC	x	x			✓
10060000	8.91	17.43	R	1	7	1994	2004	11	NON-FREEWAY URBAN	104838	3816	9927	30.11	AC	x	x			✓

**Table 3.5. Candidate Test Sections for Model Calibration after the Initial Stage (continued).**

RDWYID	Beginning Milepost	Ending Milepost	RDWYSIDE	System	District	New Year	Year	Age	Functional Class	Average Daily Traffic	ESALS per day	WIM Site	Straight Line Distance from WIM site	Pavement Type	Calibration for				Selected Calib. Sections
															PCR	Cracks	Ride	Rutting	
75280000	1.00	8.84	L	4	5	1992	2001	10	FREEWAY	52000	584	9920	35.02	AC	x	x			✓
75003000	2.05	5.00	R	1	5	1995	2004	10	NON-FREEWAY URBAN	52000	584	9929	39.24	AC	x	x			✓
75003000	2.05	4.92	L	1	5	1995	2004	10	NON-FREEWAY URBAN	82333	1334	9929	39.27	AC	x	x			✓
72280000	6.08	7.48	L	4	2	1988	2004	17	FREEWAY	80167	2852	9905	2.24	PCC			x		
72280000	7.48	13.10	L	4	2	1988	2004	17	FREEWAY	28250	1957	9905	5.62	PCC			x		
72001000	34.52	35.51	R	4	2	1983	2004	22	FREEWAY	33000	1622	9914	9.65	PCC			x		
72090000	8.23	11.14	R	1	2	1983	2004	22	FREEWAY	19100	719	9905	10.19	PCC	x		x		
87030000	8.83	10.10	L	1	6	1996	2004	9	NON-FREEWAY URBAN	19100	719	9930	11.01	PCC	x	x			✓
87030000	8.83	10.10	R	1	6	1996	2004	9	NON-FREEWAY URBAN	10501	95	9930	11.01	PCC		x			✓
79010000	9.60	11.46	L	1	5	1990	2004	15	NON-FREEWAY RURAL	20900		9925	23.76	PCC	x		x		
15002000	0.00	0.16	R	4	7	1983	2001	19	FREEWAY	19967	105	9926	23.93	PCC		x			✓
15003000	0.37	1.29	R	4	7	1983	2004	22	FREEWAY	61400	689	9926	24.03	PCC		x			✓
15190000	2.29	4.43	R	4	7	1983	2004	22	FREEWAY	39250	435	9926	25.37	PCC	x				
10150000	12.59	12.84	L	1	7	1983	2004	22	NON-FREEWAY URBAN	65500	2915	9927	27.56	PCC		x			✓
87270000	0.00	0.98	R	4	6	1983	2001	19	FREEWAY	50000	294	9933	30.13	PCC		x			✓
72030000	7.46	8.71	R	1	2	1983	2004	22	NON-FREEWAY URBAN	49000	662	9929	107.54	PCC	x		x		
72030000	9.43	10.39	R	1	2	1983	2004	22	NON-FREEWAY URBAN			9929	108.22	PCC			x		

## **FINAL SELECTION STAGE**

After identifying candidate test sections, researchers selected calibration sections from the list generated during the initial selection stage based on discussions with FDOT engineers and considering the available funds on this project. Table 3.6 shows the list of calibration sections on which field tests to characterize material properties were conducted during the project. Researchers note that as the field tests progressed, some sections were added and others replaced due to the timing of resurfacing projects. A total of 31 calibration sections, consisting of 15 flexible and 16 rigid pavement sections were established.

**Table 3.6. Final List of Calibration Sections.**

County	District	Roadway ID	Location	Type	Section Limits (mile)	Age (years)
Charlotte	1	10100000	US 41	PCC	4.98 ~ 0.49	29
Polk	1	16250000	SR 37	HMAC	4.616 ~ 7.38	19
Polk	1	16003001	SR 563	HMAC	8.484 ~ 10.0	14
Polk	1	16100000	US 92	PCC	0.46~1.74	37
Alachua	2	26005000	SR 222	HMAC	10.691 ~ 7.954	16
Bradford	2	28040000	SR 18	HMAC	0.0 ~ 5.509	14
St. Johns	2	78020000	US 1	PCC	0.7 ~ 0.02	52
Gadsden	3	50010000	US 90	HMAC	16.48 ~ 18.57	10
Gadsden	3	123811	I 10	PCC	500 ft	31
Santa Rosa	3	58060000	SR 89	HMAC	21.80 ~ 20.72	17
Broward	4	86190000	SR 823	HMAC	2.33 ~ 3.67	7
Palm Beach	4	93100000	SR25/US27	HMAC	11.904 ~ 12.617	11
Palm Beach	4	93310000	SR 710	HMAC	17.796 ~ 12.215	18
Lake	5	11020000	SR 50	PCC	14.03 ~ 14.12	29
Seminole	5	77040000	SR 46	HMAC	5.808 ~ 11.046	13
Volusia	5	79270000	SR 483	HMAC	2.39 ~ 1.62	9
Monroe	6	90060000	US 1	HMAC	13.032 ~ 16.384	17
Dade	6	87060000	A1A	HMAC	2.715 ~ 0.872	12
Dade	6	87030000	SR 5	PCC	8.83 ~ 10.0	48
Dade	6	87030000	SR 5	PCC	10.0 ~ 8.83	48
Dade	6	87270000	9/9A	PCC	0.0 ~ 0.98	44
Dade	6	87061000	SR 886	PCC	0.21 ~ 0.0	16
Hillsborough	7	10060000	US 41	HMAC	8.91 ~ 17.43	12
Hillsborough	7	10160000	SR 60	HMAC	0.0 ~ 6.773	16
Hillsborough	7	10250001	SR 60	PCC	0.0 ~ 1.102	1
Hillsborough	7	10075000	I 75	PCC	19.0 ~ 20.4	20
Hillsborough	7	10075000	I 75	PCC	23.4 ~ 24.69	20
Pinellas	7	15003000	I 175	PCC	0.37 ~ 1.29	21
Pinellas	7	15003000	I 175	PCC	1.29 ~ 0.37	21
Pinellas	7	15190000	I 275	PCC	2.287 ~ 4.44	20
Pinellas	7	15190000	I 275	PCC	4.44 ~ 2.287	20



## **CHAPTER IV. FIELD AND LABORATORY TESTING**

Researchers discussed the proposed test plan presented in Chapter II in several meetings with Florida DOT engineers to identify testing needs, request the Department's assistance in conducting the proposed field and laboratory tests, and coordinate the field activities at the different calibration sites. To determine the scope of coring and trenching activities, researchers analyzed the FWD data collected on the test sections, reviewed available data in FDOT's coring database, conducted additional sensitivity analyses of the M-E PDG program, and viewed video logs of the calibration sections maintained by the Department. This chapter describes how researchers established the coring and trenching locations, and the field tests conducted on the calibration sections. Data from tests completed in this project are also presented in the appendices to this report.

### **DETERMINATION OF CORING AND TRENCH LOCATIONS**

With FDOT's assistance, material samples were collected from each calibration section by coring and trenching, for the purpose of running tests in the laboratory to characterize material properties needed for calibrating the performance models in the M-E PDG program. Researchers reviewed PCS and coring data, and viewed video logs of the calibration sections found on FDOT's intranet (<http://webapp01.dot.state.fl.us/videolog/default.asp>) to determine appropriate coring and trench locations. In addition, researchers examined the deflection profile along each section as determined from FWD testing to establish the uniformity of the section on the basis of the measured deflections and identify areas that show relatively high deflections. Appendix B shows FWD data and PCS data collected on the different calibration sites.

From examination of the FWD deflection data and review of available coring data and video logs, researchers selected locations where material samples would be taken by coring and trenching. Locations close to intersections and within residential areas were avoided to the extent possible. Compared to coring, trenching requires more time and personnel resources due to the associated operational requirements. Therefore, researchers tried to minimize the number of trench locations based on results from additional sensitivity analyses conducted to establish the scope of coring and trenching operations. These sensitivity analyses were conducted using a later version (0.90) of the M-E PDG program to

verify the results from the earlier analyses conducted with version 0.8. Researchers note that a number of versions of the M-E PDG program were released during this project that required verification of findings from previous analyses.

To verify the sensitivity of the performance predictions to base and subgrade resilient moduli, researchers considered two pavement sections. One section is the HMAC pavement located in Santa Rosa County with roadway ID 58010000. According to information obtained from FDOT's coring data base, this section consists of 4.5 inches of asphalt mix, overlying a 20-inch sand/clay base, on top of a silty sand subgrade. The other section is a typical Portland cement concrete (PCC) pavement consisting of a 10-inch concrete slab, 2-inch asphalt permeable base, 10-inch limerock base, and 12-inch stabilized subgrade on top of sandy soil subgrade.

For the sensitivity analyses of the HMAC and PCC sections using a version of 0.9 M-E PDG program, the base modulus was varied from 40 to 60 ksi in 10 ksi increments, while the subgrade modulus was varied from 15 to 35 ksi, also in 10 ksi increments. In addition, researchers examined the sensitivity of the PCC performance predictions to the modulus of subgrade reaction (k-value) by varying this variable from 100 to 400 pci in the analysis. Climatic, soils and traffic data considered representative of the conditions at the sites selected were input to the M-E PDG program. The results from the sensitivity analyses are shown in Figures 4.1 to 4.5. Figures 4.1 and 4.2 indicate that the predictions from the flexible pavement top-down cracking model in the MEPDG program are sensitive to the base and subgrade resilient moduli. It is interesting to note that higher subgrade modulus results in larger amounts of top-down cracks predicted for the HMAC section, as shown in Figure 4.2. A similar trend is also reported in Appendix II-2 of the MEPDG program supplemental documentation (ARA, 2004). In view of this finding, and recognizing that further changes in the M-E PDG performance models will come about from on-going national studies on top-down cracking, reflective cracking, and rutting, researchers developed the flexible pavement design tables from this project based on alligator (bottom-up) cracking.

In contrast to the sensitivity results on the HMAC section, the base and subgrade moduli did not appear to significantly influence the predicted level of cracking on the PCC pavement section, as indicated in Figures 4.3 and 4.4. The change of k-value affected cracking in a somewhat different manner as shown in Figure 4.5. Researchers note that most

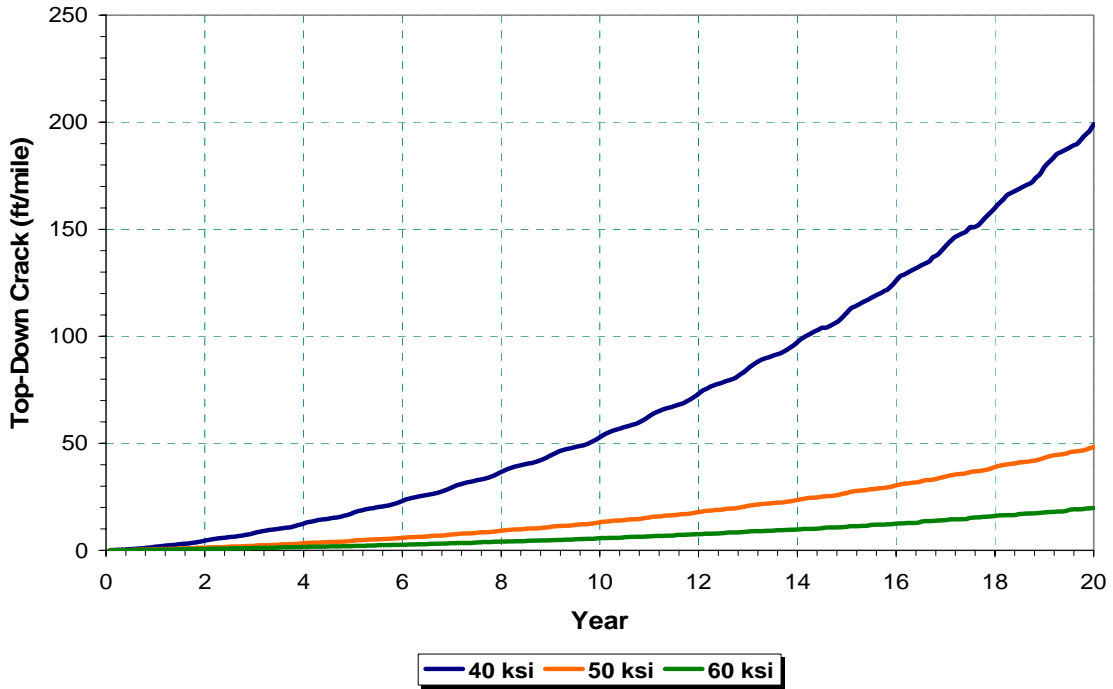


**Figure 4.1. Sensitivity of Top-Down Cracking Performance Predictions to Base Modulus for HMAC Pavement Section.**

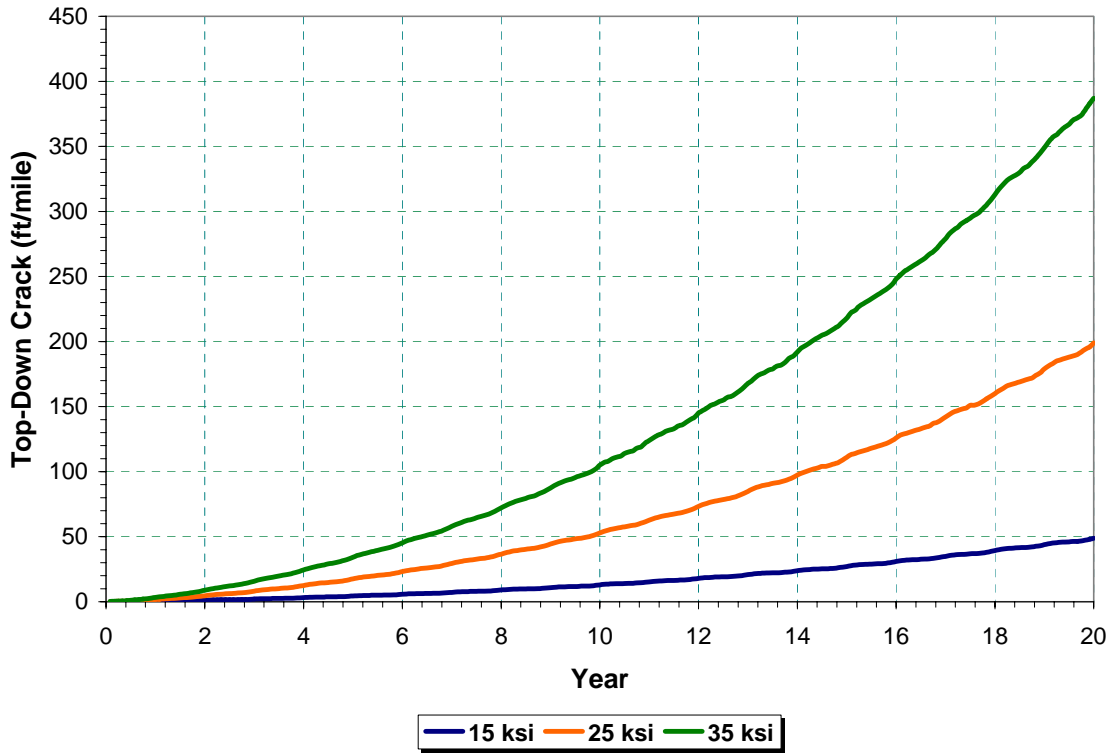


**Figure 4.2. Sensitivity of Top-Down Cracking Performance Predictions to Subgrade Modulus for HMAC Pavement Section.**

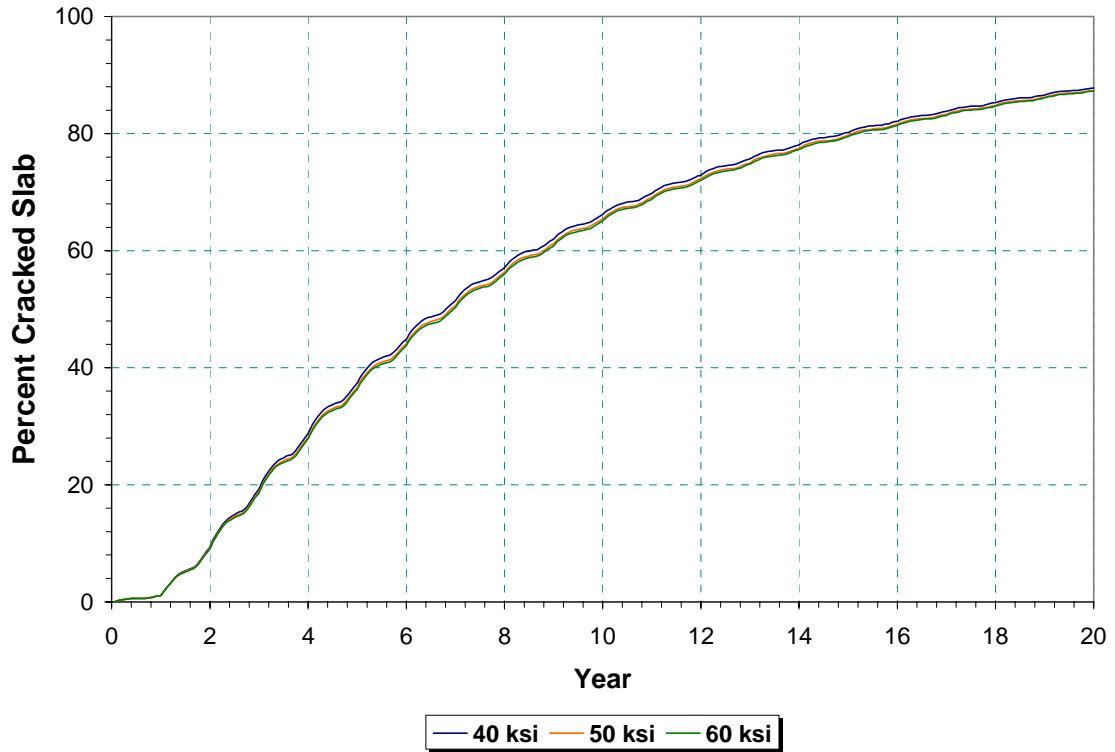


**Figure 4.3. Sensitivity of PCC Crack Predictions to Base Modulus.**

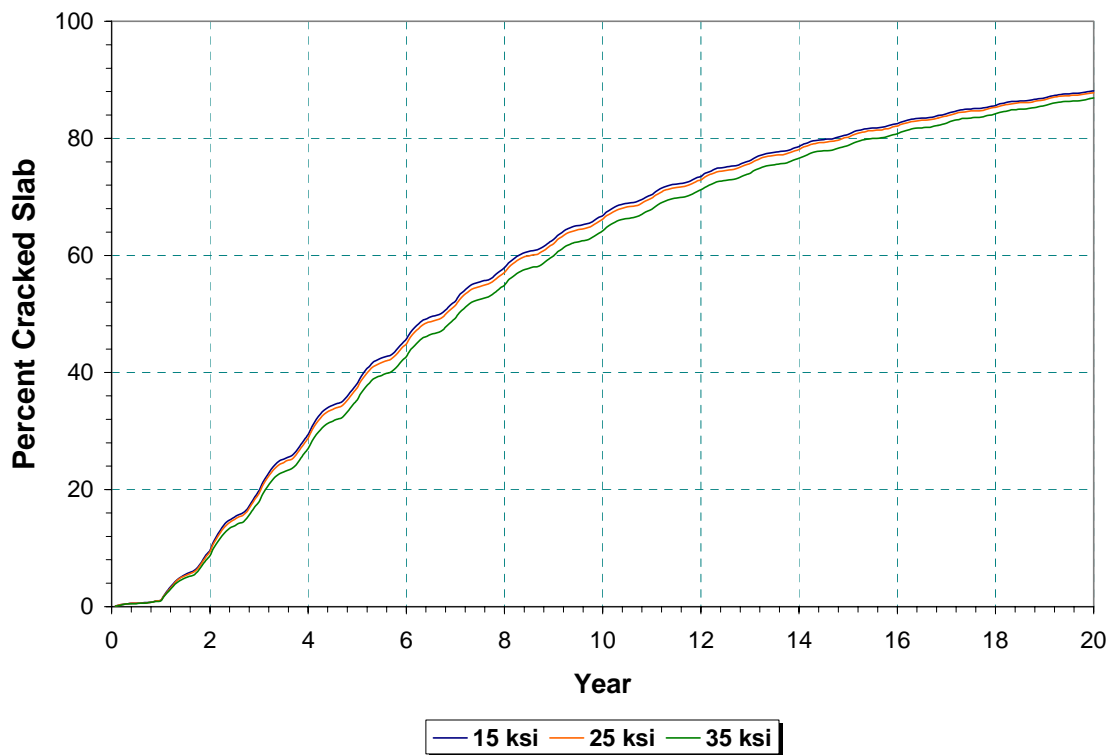


**Figure 4.4. Sensitivity of PCC Crack Predictions to Subgrade Modulus.**

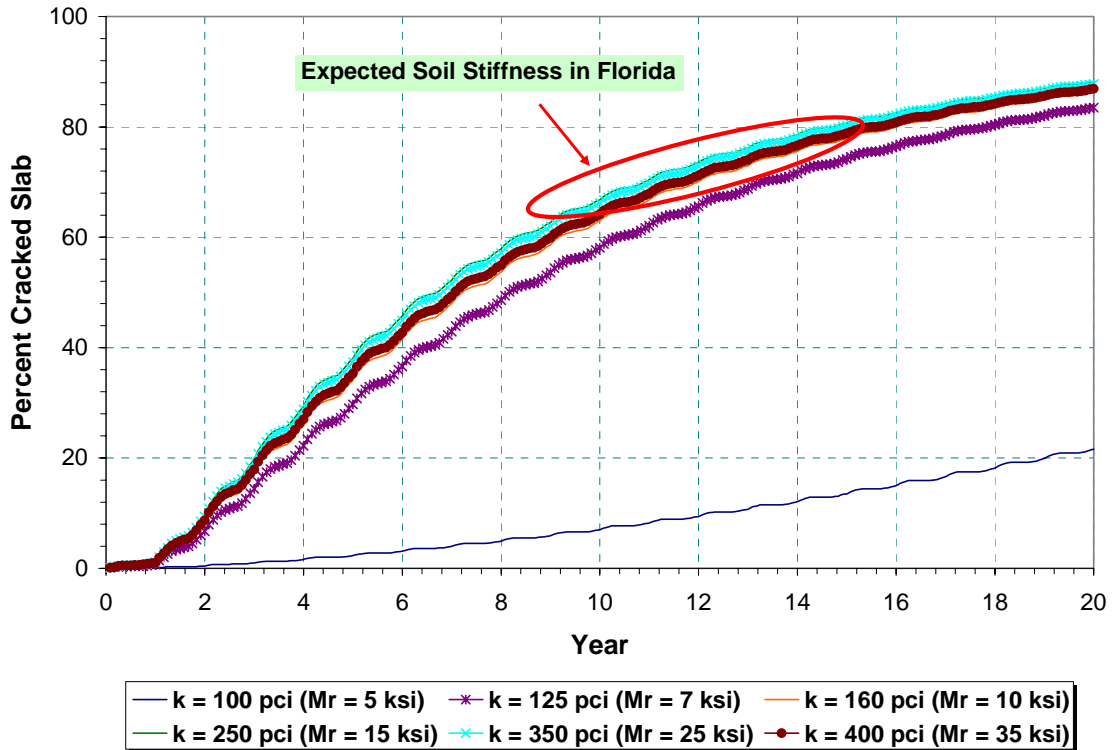


**Figure 4.5. Sensitivity of PCC Crack Predictions to Subgrade Modulus of Reaction.**

of the predicted performance curves are close together except for the case where the k-value is 100 pci, which is equivalent to a subgrade modulus of 5 ksi based on the M-E PDG program output for the pavement section analyzed.

In view of the results obtained from the sensitivity analyses, one trench location was established for each flexible pavement calibration section. This location was generally within an area where the FWD deflections are high (relative to the range of deflections measured within the section) or where visual distresses were observed from the video logs. In the case of rigid pavements, the results from the sensitivity analyses suggested that trenching was not as important for the PCC calibration sections as it was for the HMAC sections. In view of these results and after consulting with the project manager, the decision was made to forego trenching in rigid pavement sections. For these sections, FWD test data were used to characterize the underlying materials for the PCC model calibrations.

Table 4.1 identifies the specific coring and trench stations established by researchers. In this table, the mileposts printed in red identify locations where researchers proposed to core through cracks to verify the type of cracking (top-down or bottom-up) observed on the sections from the photo logs viewed from FDOT's intranet site.

**Table 4.1. Proposed Core and Trench Locations.**

District	County	Roadway ID	Type	Section Limits	Core Stations (milepost)	Trench Station (milepost)
1	Charlotte	10100000	PCC	4.98 ~ 0.49	4.517, 3.092, 2.327, 0.687	-
	Polk	16250000	AC	4.616 ~ 7.38	4.652, 4.881, 5.109, <b>5.432, 5.789</b> , 5.895, <b>6.143</b> , 6.287, 6.536, 6.859, 7.143	6.143
	Polk	16003001	AC	8.484 ~ 10.0	8.606, <b>8.736</b> , 8.80, <b>8.996</b> , 9.20, <b>9.6</b> , 9.866	8.736
	Polk	16100000	PCC	0.46~1.74	0.59, 0.75, 0.95, 0.967, 1.074, 1.538, 1.59	-
2	Alachua	26005000	AC	10.691 ~ 7.954	10.637, 10.40, 10.10, 9.925, <b>9.60, 9.30, 9.10, 8.642</b> , 8.426, <b>8.142</b> , 8.071	9.60
	Bradford	28040000	AC	0.0 ~ 5.509	0.1, 0.288, 0.7, 0.967, <b>1.40</b> , 1.7, 1.967, 2.357, <b>2.536</b> , 2.7, 3.288, 3.754, 4.4, 4.7, <b>5.1, 5.323</b>	2.536
	St. Johns	78020000	PCC	0.7 ~ 0.02	0.5, 0.323, 0.14	-
3	Gadsden	50010000	AC	16.48 ~ 18.57	<b>16.699, 16.977, 17.196</b> , 17.275, <b>17.412</b> , 17.765, 18.04, 18.393	17.412
	Gadsden	123811	PCC			-
	Santa Rosa	58060000	AC	21.80 ~ 20.72	21.78,21.693, 21.617, 21.53, <b>21.4, 21.336, 21.227</b> , 20.971, 20.798	21.227
4	Broward	86190000	AC	2.33 ~ 3.67	2.401, 2.686, <b>2.837, 3.07</b> , 3.20, 3.53	3.07
	Palm Beach	93100000	AC	11.904 ~ 12.617	<b>12.047, 12.157, 12.305, 12.40</b> , 12.547	12.305
	Palm Beach	93310000	AC	17.796 ~ 12.215	<b>17.52</b> , 17.2, 17.02, 16.444, <b>15.195</b> , 14.666, <b>13.695</b> , 13.196, <b>12.675</b>	17.52
5	Lake	11020000	PCC	14.03 ~ 14.12	14.06, 14.12	-
	Seminole	77040000	AC	5.808 ~ 11.046	<b>6.073, 6.222</b> , 6.352, 6.682, 7.143, <b>7.462, 7.643</b> , 8.214 <b>8.643</b> , 9.323, 9.672, 10.282, 10.69, <b>10.922</b>	7.462
	Volusia	79270000	AC	2.39 ~ 1.62	2.34, 2.327, 2.134, 2.0, 1.927, <b>1.713, 1.642</b>	1.713
6	Monroe	90060000	AC	13.032 ~ 16.384	13.3, 13.534, <b>13.76, 14.08, 14.155, 14.328</b> , 14.73, 15.067, <b>15.337, 15.528</b> , 15.917, 16.2	15.528
	Dade	87060000	AC	2.715 ~ 0.872	2.595, 2.266, <b>2.149</b> , 2.009, <b>1.792</b> , 1.629, <b>1.493, 1.429</b> , <b>1.289</b> , 0.996	2.595
	Dade	87030000A	PCC	8.83 ~ 10.0	8.96, 9.13, 9.69, 9.50	-
	Dade	87030000B	PCC	10.0 ~ 8.83	9.888, 9.517, 9.288, 8.962	-
	Dade	87270000	PCC	0.0 ~ 0.98	0.229, 0.56	-
	Dade	87061000	PCC	0.21 ~ 0.0	0.195, 0.126	-

**Table 4.1. Proposed Core and Trench Locations (continued).**

District	County	Roadway ID	Type	Section Limits	Core Stations (milepost)	Trench Station (milepost)
7	Hillsborough	10060000	AC	8.91 ~ 17.43	9.37, 9.84, 10.281, 10.5, 10.642, 11.377, 11.785, 12.40, 13.085, 13.661, 14.05, 14.238, 15.079, 15.491, 16.634, 17.222	10.50
	Hillsborough	10160000	AC	0.0 ~ 6.773	0.11, 0.282, 0.84, 1.436, 2.17, 2.51, 2.98, 3.45, 3.843, 4.214, 4.851, 5.157, 6.0, 6.296, 6.588	2.17
	Hillsborough	10250001	PCC	0.0 ~ 1.102		-
	Hillsborough	10075000A	PCC	19.0 ~ 20.4	19.071, 19.57, 20.003	-
	Hillsborough	10075000B	PCC	23.4 ~ 24.69	23.56, 23.74, 23.99, 24.5	-
	Pinellas	15003000A	PCC	0.37 ~ 1.29	0.63, 0.80, 1.0	-
	Pinellas	15003000B	PCC	1.29 ~ 0.37	1.17, 0.889, 0.859	-
	Pinellas	15190000A	PCC	2.287 ~ 4.44	2.65, 2.92, 3.60, 4.10	-
Pinellas	15190000B	PCC	4.44 ~ 2.287	4.285, 3.555, 3.165, 2.445, 2.395	-	

## **FIELD TESTING**

With the assistance of the District Material Offices, researchers obtained samples of hot mix asphalt concrete, Portland cement concrete, base, subgrade and embankment materials from the calibration sections. For hot-mix asphalt concrete sections, 6-inch diameter cores were sampled for the proposed laboratory tests to get asphalt volumetric properties and viscosity (AASHTO T 315). For PCC sections, cores at least 4 inches in diameter and 8 inches high were obtained for the thermal coefficient of expansion test (AASHTO TP60) and the compressive strength test (AASHTO T22). Two cores per station were extracted for the AASHTO TP60 test to permit comparative testing between FDOT and TTI laboratories as discussed in a project meeting with FDOT engineers.

With respect to trenching, base, stabilized subgrade, and embankment materials were sampled for resilient modulus testing, sieve analysis, plastic limit, moisture-density, and soil suction tests. Three hundred fifty pounds of each material were collected. Prior to coring and trenching, District engineers marked test locations based on the mileposts presented in Table 4.1. Field sampling was conducted under traffic control at the outside lane. All cores were taken between the wheel paths except cracked cores, which were taken at selected crack locations. The ground water table depth at each site was determined by boring adjacent to the trench location. In addition, field densities and moisture contents were measured using the nuclear density gage. The automated dynamic cone penetrometer (ADCP) test was performed from the top of the base layer to obtain correlations between test results and resilient modulus in an in-house study by the Florida DOT. ADCP tests were not conducted on test sections located within Districts 4 and 6 due to machine down time.

Sampled materials were marked, then packed cautiously to protect from damage during shipping. Figure 4.6 illustrates the activities performed during the field tests. In PCC sections, joint spacing and dowel diameter were measured when it was feasible to core at the joint as shown in Figure 4.7. Whenever cores were taken, the layer composition and thickness of each lift were determined and recorded on the data sheets as presented in Appendix C. In addition, the depths to the ground water table were recorded on the same sheets at locations where borings were made. Additionally, comments were made whenever any notable findings were detected during field sampling.



*a. Core at trench location*



*b. Record core data and wrap samples*



*c. Trench*



*d. Nuclear density testing*



*e. ADCP testing at trench location*



*f. Boring close to trench location*

**Figure 4.6. Illustration of Field Work on HMAC Calibration Sections.**



**Figure 4.7. Measurement of Joint Spacing and Dowel Diameter.**



**Figure 4.8. Top-Down Cracking Observed on AC Core.**

During coring, researchers also made an attempt to characterize the crack type by coring through selected cracks. The predominant distress on Florida pavements is top-down cracking. Figure 4.8 shows an example of this type of cracking observed on a core taken from the calibration section located in Seminole County.

## **LABORATORY TESTING**

Tables 4.2 to 4.4 present the proposed laboratory tests to characterize material properties of cores and underlying materials taken from the calibration sections. The State Materials Office of the Florida DOT conducted resilient modulus tests on base, subgrade, and embankment materials, extractions on AC cores, and tests on PCC cores to obtain compressive strength and thermal expansion coefficients. TTI conducted laboratory tests to obtain soil suction properties, and thermal expansion coefficients of PCC cores for comparing with the FDOT measurements. Detailed test data are presented in the appendices.

### **Characterization of Asphalt Concrete Properties**

Extractions and dynamic shear rheometer (DSR) tests were conducted on selected AC lifts of cores sampled from the calibration sections. Extractions (Figure 4.9) provided mix volumetric and gradation properties that were needed to predict dynamic modulus of asphalt mixtures in the M-E PDG program. DSR tests were also performed on the extracted binder to characterize the viscosity-temperature relationship for dynamic modulus prediction.

Table 4.5 presents data from extractions and DSR tests conducted on AC samples taken on section 16003001 in Polk County. The volumetric properties shown were determined using the equations given in Table 4.2. The viscosity values are obtained from the FDOT DSR test programs. Data for other sections are tabulated in Appendix D. The test results indicated that cored samples appeared to be fairly aged, exhibiting a relatively high air voids (over 10 percent) and high PG grade at the top most layer. Because of this aging, it is necessary to backcalculate initial air voids for calibrating performance models. As proposed in the Chapter II, initial air voids were estimated using aging model incorporated in the M-E PDG program based on several recommendations. Details on this task are presented in Appendix E.

**Table 4.2. Tests on Asphalt Concrete Cores.**

Property	Test Protocol	
	AASHTO / ASTM	Florida Standard Test Method (FSTM)
Binder content, % by weight	ASTM D 2172-01	FM 5-544
Gradation in terms of cumulative % retained on 3/4", 3/8", and #4 sieves, and % passing #200	AASHTO T30	FM 1-T 030
Effective bitumen content, % by volume ( $V_{be}$ )*	Following tests are needed to be done to calculate $V_{beff}$ . (a) Measure the bulk specific gravity ( $G_{sb}$ ) of the coarse aggregate (AASHTO T 85 or ASTM C 127) and of the fine aggregate (AASHTO T 84 or ASTM C128). (b) Measure the specific gravity ( $G_b$ ) of the asphalt cement (AASHTO T 228 or ASTM D 70). (c) Measure the bulk specific gravity ( $G_{mb}$ ) of compacted paving mixture sample (FM 1-T 166 or AASHTO T 166-00 or ASTM D 2726). Measure the maximum specific gravity ( $G_{mm}$ ) of paving mixture (FM 1-T 209 or AASHTO T 209-99 or ASTM D 2041).	
Air void (%)**	AASHTO T269	-
Temperature-viscosity relationship	AASHTO T315	-

\*Effective bitumen content by volume is calculated using below equations;

$$V_{be} = G_{mb} \left[ \frac{P_b}{G_b} - (100 - P_b) \frac{(G_{se} - G_{sb})}{G_{se} * G_{sb}} \right] \quad \text{and} \quad G_{se} = \frac{100 - P_b}{\frac{100}{G_{mm}} - \frac{P_b}{G_b}} \quad \text{where } P_b \text{ is binder}$$

content by weight which is obtained from extraction and  $G_{se}$  is effective specific gravity of the aggregate.

\*\*Air void is calculated using the following equation:

$$V_a = 100 * \frac{G_{mm} - G_{mb}}{G_{mm}}$$

**Table 4.3. Tests on Portland Cement Concrete Cores.**

Property	Test Protocol	
	AASHTO / ASTM	Florida Standard Test Method (FSTM)
Coefficient of thermal expansion	AASHTO TP 60	-
Compressive strength	AASHTO T22	FM 1-T 022

**Table 4.4. Tests on Base, Stabilized Subgrade, and Embankment Materials.**

Property	Test Protocol	
	AASHTO / ASTM	Florida Standard Test Method (FSTM)
Gradation	AASHTO T27	FM 1-T 027
Atterberg limits	AASHTO T90	FM 1-T 090
Moisture-density curve	AASHTO T99 or AASHTO T180	FM 1-T 180
Resilient modulus*	AASHTO T307	
Soil water characteristic or soil suction curve**	Filter paper method	

\*Resilient modulus performed at optimum moisture content. The output data set needs to include the confining pressure, deviatoric stress, and resilient modulus.

\*\*Soil suction tests conducted by TTI using 50 lbs of each material type sampled from the trenches.



**Figure 4.9. Illustration of Extractions Done on Asphalt Cores.**

**Table 4.5. Properties Determined from Extractions and DSR Testing on Core Samples from Section 16003001 in Polk County.**

Project No. 16003001 EXTRACTION DATA							
Sample No.	G <sub>mb</sub>	G <sub>mm</sub>	P <sub>b</sub> (%)	G <sub>se</sub>	G <sub>sb</sub>	V <sub>bc</sub> (%)	% AV
1-1	2.07	2.39	6.45	2.63	2.57	11.20	13.35
1-2	2.21	2.37	5.30	2.56	2.48	8.92	6.86
1-3	2.19	2.39	5.13	2.57	2.48	7.79	8.26
2-1	2.05	2.39	6.45	2.63	2.57	11.09	14.19
2-2	2.23	2.37	5.30	2.56	2.48	8.99	6.18
2-3	2.22	2.39	5.13	2.57	2.48	7.89	7.17
3-1	2.11	2.39	6.45	2.63	2.57	11.39	11.86
3-2	2.27	2.37	5.30	2.56	2.48	9.16	4.40
3-3	2.16	2.39	5.13	2.57	2.48	7.70	9.35
4-1	2.12	2.39	6.45	2.63	2.57	11.45	11.43
4-2	2.29	2.37	5.30	2.56	2.48	9.23	3.58
4-3	2.16	2.39	5.13	2.57	2.48	7.69	9.52
5-1	2.09	2.39	6.45	2.63	2.57	11.27	12.82
5-2	2.24	2.37	5.30	2.56	2.48	9.05	5.46
5-3	2.17	2.39	5.13	2.57	2.48	7.71	9.21
6-1	2.03	2.39	6.45	2.63	2.57	10.98	15.06
6-2	2.20	2.37	5.30	2.56	2.48	8.89	7.20
6-3	2.16	2.39	5.13	2.57	2.48	7.69	9.50
7-1	2.07	2.39	6.45	2.63	2.57	11.20	13.35
7-2	2.25	2.37	5.30	2.56	2.48	9.07	5.27
7-3	2.17	2.39	5.13	2.57	2.48	7.71	9.25

**Gradation**

Property	Layer 1	Layer 2	Layer 3
Retained 3/4	0	0	0
Retained 3/8	0	11.51	8.18
Retained #4	0.81	20.66	23.06
% #200	6.05	8.74	7.85
Ave. V <sub>bc</sub> (%)	11.22	9.04	7.74
Ave. AV (%)	13.1	5.6	8.9

**DSR**

Temp.(°C)	Layer 1			Layer 2			Layer 3		
	Vis.(cP)	G* (Pa)	δ°	Vis.(cP)	G* (Pa)	δ°	Vis.(cP)	G* (Pa)	δ°
52	28,400,000	284,000	53.93	2,422,816	184,667	71.03	11,433,300	114,333	61.59
58	13,533,300	135,333	58.08	1,133,498	76,667	67.33	5,043,300	50,467	65.55
64	6,223,300	62,267	62.42	481,894	34,600	69.09	2,280,000	22,800	69.64
70	2,920,000	29,233	66.79	206,871	16,100	71.76	1,100,000	11,000	73.51
76	1,366,700	13,667	71.26	90,789	7,693	75.13	518,000	5,183	77.44
82	626,300	6,267	75.62	42,385	3,817	78.15	233,000	2,330	80.67
88	326,700	3,290	78.47	19,015	1,800	81.41	117,000	1,170	83.28
A-VTS	8.89	-2.89		9.32	-3.05		9.57	-3.15	

Researchers note that the indirect tensile test method currently implemented by the Florida DOT to obtain resilient modulus, creep compliance, and tensile strength properties of HMAC samples does not provide properties directly compatible with the low-temperature cracking prediction model in the M-E PDG program. In a project meeting held at the State Materials Office, FDOT engineers also noted that low-temperature cracking is not a problem in Florida. Thus, low-temperature cracking was not considered in this project.

### **Characterization of Portland Cement Concrete**

Cored PCC samples were tested to obtain the concrete thermal expansion coefficient and compressive strength as shown in Figure 4.10. For the coefficient of thermal expansion tests, samples were submerged in a water tank for about a month prior to testing, following standard SMO practice. Table 4.6 shows the properties determined from tests on the core samples. Note that these properties represent aged conditions since the concrete cores were taken from highways that have been in service over a period ranging from about a year to 50 years. Except for three cases, the test data in Table 4.6 show that the thermal coefficients of expansion of the aged concrete cores are typically below  $6 \mu\epsilon/^\circ\text{F}$ . However, results of other tests done by SMO on molded specimens and on cores taken from new construction projects showed CTE values above  $6 \mu\epsilon/^\circ\text{F}$ . These results as well as the variability in the measured CTEs, and the high sensitivity of the performance predictions to this design variable were considered in establishing the CTE values that were used to generate the PCC thickness design tables. In addition, researchers note that reliability in the M-E PDG program is determined based on the prediction error of each performance model, and not on the variability of the input parameters. The current program does not provide for input of material variability.

The CTE values measured from FDOT and TTI tests appear to agree quite well in terms of the average and coefficient of variation of the test results. Researchers note that the compressive strength of section 10100000 in Charlotte County is quite lower compared to the values obtained on the other sections. The cores from this section consist of 4 inches of concrete with 8.0 inches of econcrete base. The two lifts could

not be cut for testing due to height limitations. Researchers plan to model the first layer of this section as a composite layer for the model calibrations.

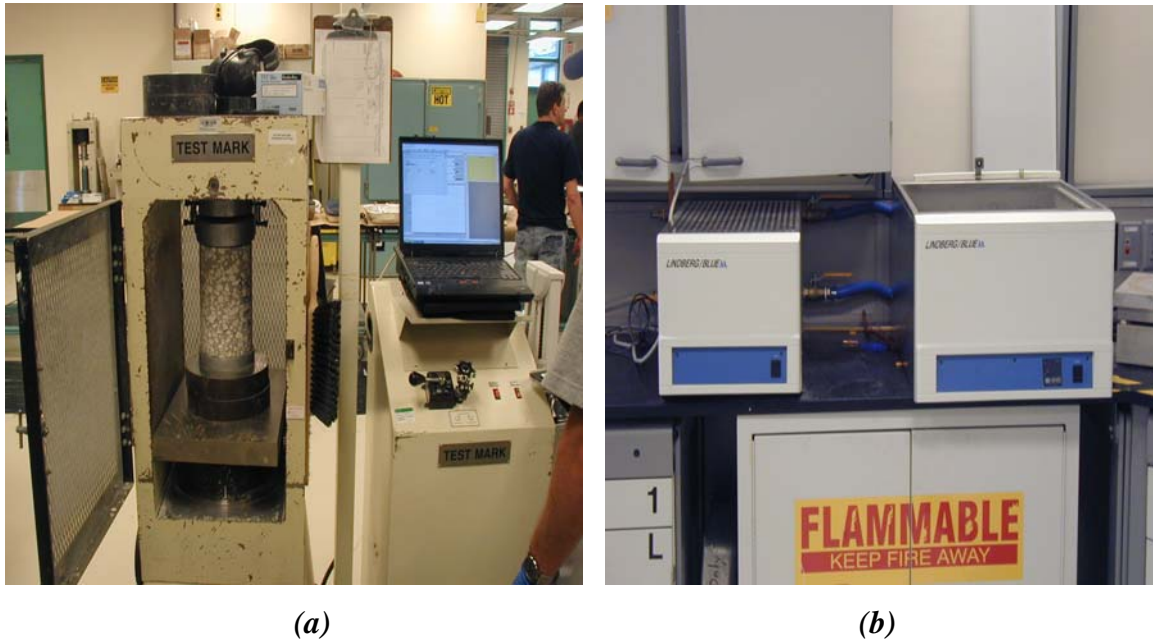


**Figure 4.10. Test Set Up for (a) Compressive Strength and (b) Concrete Coefficient of Thermal Expansion.**

**Table 4.6. Properties Determined from PCC Core Samples.**

Core	CTE_FDOT (microstrain/°F)	CTE_TTI (microstrain/°F)	Comp. Strength (psi)
123811-1	5.20	5.00	5106
123811-2	5.02	5.03	5492
78020-1	4.81	5.03	8386
78020-2	3.94	4.05	5988
78020-3	4.39	4.67	6521
11020-1	4.81	4.47	4601
11020-2	4.31	4.65	4414
16100-1	4.99	5.31	5076
16100-2	4.71	4.71	6969
16100-3	4.62	4.48	7066
16100-4	5.29	5.42	6272
16100-5	4.32	4.32	5452
16100-6	4.50	4.17	5458
01010-1	5.74	6.06	2882
01010-2	5.46	5.32	2326
10750A-1	5.61	5.23	5299
10750A-2	4.89	4.89	5304
10750A-3	4.61	4.24	6241
10750B-1	5.52	5.85	5553

**Table 4.6. Properties Determined from PCC Core Samples (continued).**

Core	CTE_FDOT (microstrain/°F)	CTE_TTI (microstrain/°F)	Comp. Strength (psi)
10750B-2	5.31	5.27	4892
10750B-3	4.85	4.56	4579
10750B-4	4.83	5.23	4886
10250-1	5.06	4.73	6332
10250-2	4.57	4.99	4433
10250-3	4.52	4.47	5690
15003E-1	4.88	4.78	4886
15003E-2	5.07	4.70	5262
15003E-3	4.74	5.15	5384
15003W-1	5.34	4.85	5000
15003W-2	5.05	5.01	4770
15003W-3	4.75	4.92	5085
15190N-1	5.26	4.98	4255
15190N-2	4.79	4.57	6789
15190N-3	4.52	4.45	3760
15190N-4	5.11	4.82	4109
15190S-1	4.59	5.06	8165
15190S-2	4.17	4.18	4084
15190S-3	5.21	4.74	6954
15190S-4	4.47	4.89	4149
15190S-5	4.51	4.58	5364
87061-1	4.46	4.63	5041
87061-2	4.86	4.93	5412
87270-1	5.67	5.31	5808
87270-2	4.84	5.10	5648
87030N-1	6.18	6.35	5311
87030N-2	5.35	5.64	5560
87030N-3	5.05	4.85	6136
87030S-1	6.61	6.28	5496
87030S-2	4.33	4.72	6292
87030S-3	5.08	5.52	6254
<b>Average</b>	4.93	4.94	5400
<b>Std. dev.</b>	0.50	0.50	1128
<b>COV (%)</b>	10.19	10.18	21

### Characterization of Underlying Materials

Underlying materials sampled from trenching were tested to obtain physical soil properties, gradation, moisture-density relationship, resilient modulus, and soil suction parameters. Resilient modulus was tested at optimum moisture content and field moisture content based on nuclear density gage measurements. Figure 4.11 to 4.13 illustrate the results of resilient modulus tests on samples of base, stabilized subgrade,

and embankment taken from Section 93310. These figures also show the fitted bulk stress model for each material as determined by the State Materials Office. This model is used by FDOT to characterize resilient modulus as a function of the bulk stress ( $\theta$ ) according to the equation:

$$M_R = k_1 \theta^{k_2} \quad (4.1)$$

Appendix E presents the resilient modulus test results from the State Materials Office.

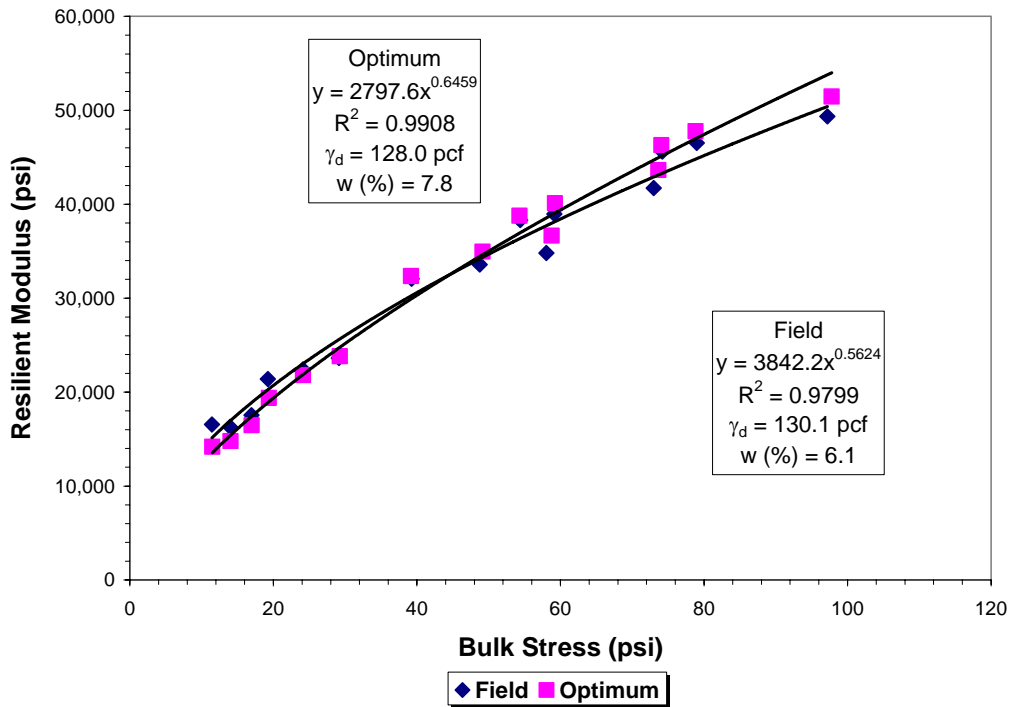


**Figure 4.11. Resilient Modulus for Base (Section 93310).**

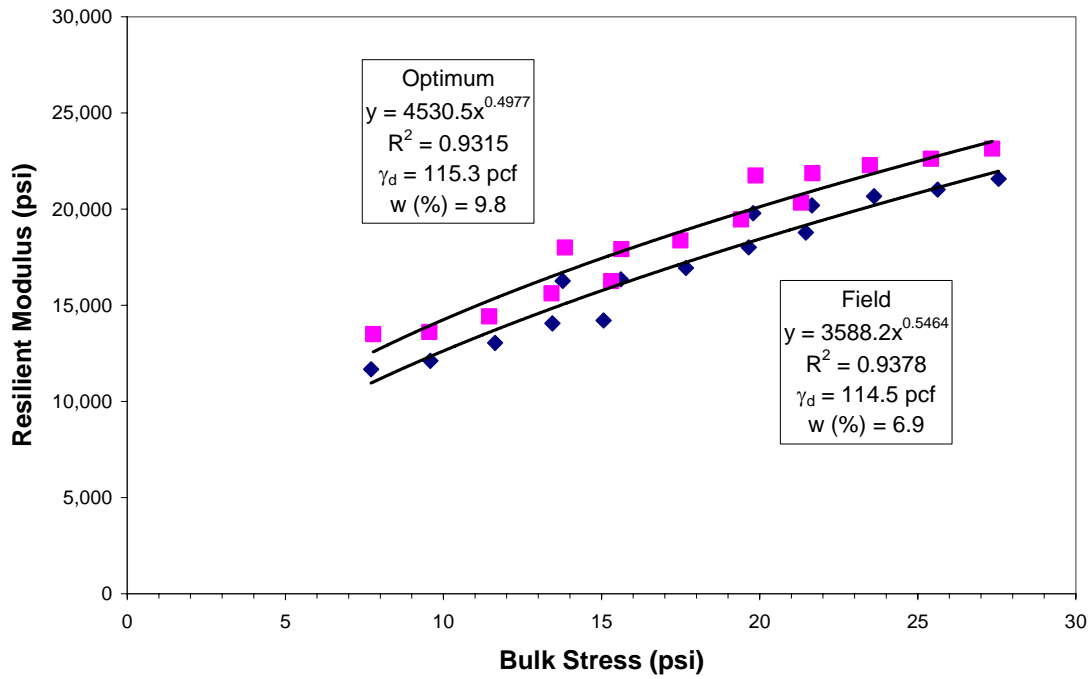


**Figure 4.12. Resilient Modulus for Subgrade (Section 93310).**

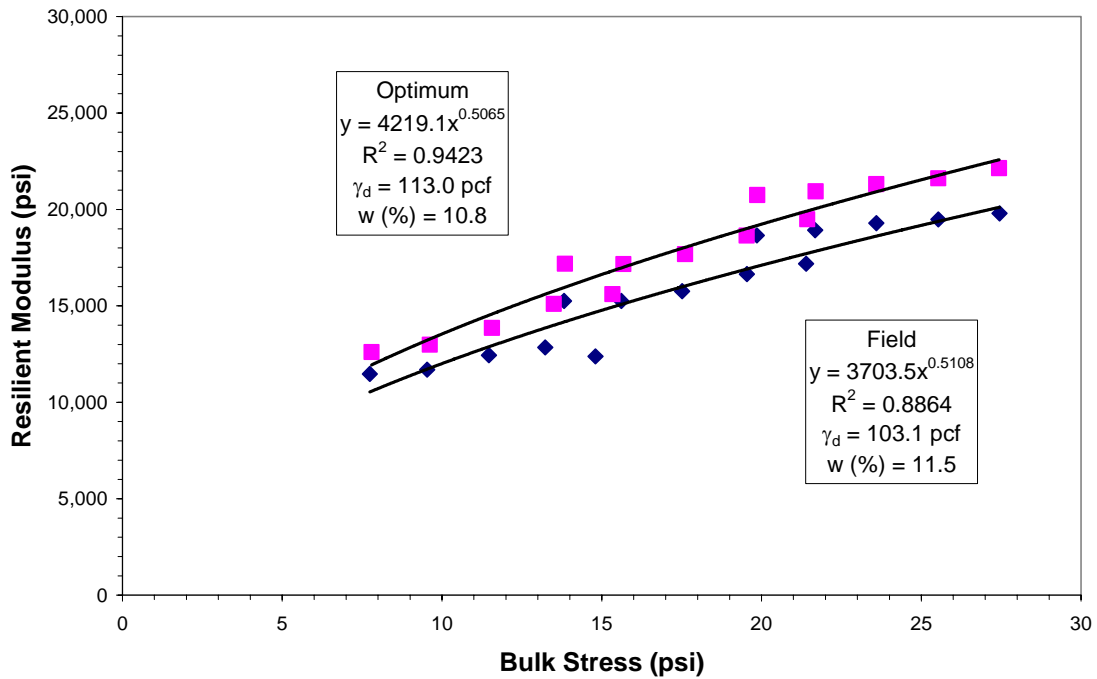


**Figure 4.13. Resilient Modulus for Embankment Material (Section 93310).**

Table 4.7 summarizes soil index properties determined from laboratory tests. Most of the materials obtained from the trenches cut on the calibration sections are non-plastic and classify as A-2-4 and A-3.

Soil suction tests were made using the filter paper method described by Bulut, Lytton, and Wray (2001). Figures from 4.14 to 4.18 show comparisons of soil-water characteristic curves for the embankment soils at sections 26005000, 28040000, and 58060000, 86190000, and 10060000. In each figure, the solid line represents the soil suction curve based on data compiled from the comprehensive review of soil survey reports described in Chapter IV of the Phase I report by Fernando, Oh, and Ryu (2007), while the plotted points represent the data from the soil suction tests conducted in the laboratory. The results shown in the figures are encouraging as the soil suction curves established from published data provides a reasonable fit to the laboratory test data except for Section 10060000. Based on the examination of the test results with published data, researchers determined the soil-water characteristic curves for each county using equations (4.2) and (4.3) and tabulated the soil suction coefficients that are input to the M-E PDG program in Table 4.8.

The soil-water characteristic curve defines the relationship between soil suction and soil moisture content as expressed in the following equations proposed by Fredlund and Xing (1994):

$$\theta_w = C(h) \times \frac{\theta_{sat}}{\left[ \ln \left[ \exp(1) + \left( \frac{h}{a_f} \right)^{b_f} \right] \right]^{c_f}} \quad (4.2)$$

where,

$$C(h) = \left[ 1 - \frac{\ln\left(1 + \frac{h}{h_r}\right)}{\ln\left(1 + \frac{1.45 \times 10^5}{h_r}\right)} \right] \quad (4.3)$$

$\theta_w$  = volumetric water content,

$\theta_{sat}$  = volumetric saturated water content,

$h$  = soil suction in psi, and  
 $a_f, b_f, c_f, \& h_r$  = model parameters.

It should be noted that the soil suction coefficients in Table 4.8 are only for embankment soils. For mechanically stabilized subgrade and base materials, researchers observed that the materials from the trench locations were quite similar. Thus, the decision was made to use a set of specific soil suction coefficients for limerock base and stabilized subgrade. Figures 4.19 and 4.20 show the soil-water characteristic curves for these materials.

**Table 4.7. Summary of Soil Index Properties from Laboratory Tests on Underlying Materials.**

County	District	Roadway ID	Location	Material type	Maximum Density	Optimum w%	LL	PI	Soil class	# 200 Passing
Polk	1	16250000	SR 37	Embankment	114.1	10.8%	NP	NP	A-2-4	12.7%
Polk	1	16003001	SR 563	Base	121.1	10.3%	NP	NP	NA	NA
				Subgrade	123.1	8.5%	NP	NP	A-2-4	15.1%
				Embankment	114.8	10.8%	NP	NP	A-2-4	12.2%
Alachua	2	26005000	SR 222	Base	117.8	10.6%	NP	NP	NA	NA
				Subgrade	120.7	8.5%	NP	NP	A-2-4	12.0%
				Embankment	125.7	9.6%	NP	NP	A-2-4	18.0%
Bradford	2	28040000	SR 18	Subbase	119.0	8.1%	NP	NP	A-2-4	12.0%
				Embankment	117.1	9.4%	NP	NP	A-3	9.0%
Gadsden	3	50010000	US 90	Subbase	130.9	8.8%	21	7.1	A-2-4	17.0%
				Embankment	119.0	12.8%	30.5	16.7	A-6	41.0%
Santa Rosa	3	58060000	SR 89	Base	133.6	7.9%	21	7.4	A-2-4	25.8%
				Subgrade	133.9	7.9%	19.3	4.8	A-2-4	34.1%
				Embankment	126.4	9.7%	21	6.3	A-2-4	34.1%
Broward	4	86190000	SR 823	Base	130.7	7.9%	NP	NP	NA	NA
				Subgrade	129.8	7.0%	NP	NP	A-2-4	17.0%
				Embankment	118.5	9.9%	NP	NP	A-3	8.8%
Palm Beach	4	93100000	SR25/US27	Base	122.0	11.0%	NP	NP	NA	NA
				Subgrade	123.9	11.1%	NP	NP	A-1-b	22.7%
				Embankment	113.5	14.0%	NP	NP	A-2-4	20.5%
Palm Beach	4	93310000	SR 710	Base	129.0	8.0%	NP	NP	NA	NA
				Subgrade	113.2	10.3%	NP	NP	A-3	6.2%
				Embankment	112.7	11.0%	NP	NP	A-3	6.0%
Seminole	5	77040000	SR 46	Subbase	101.3	11.4%	NP	NP	A-3	5.0%
				Embankment	103.7	12.2%	NP	NP	A-3	6.0%

**Table 4.7. Summary of Soil Index Properties from Laboratory Tests on Underlying Materials (continued).**

County	District	Roadway ID	Location	Material type	Maximum Density	Optimum w%	LL	PI	Soil class	# 200 Passing
Volusia	5	79270000	SR 483	Base	120.9	9.9%	NP	NP	NA	NA
				Subgrade	121.4	7.9%	NP	NP	A-2-4	13.6%
				Embankment	103.1	13.8%	NP	NP	A-3	3.7%
Monroe	6	90060000	US 1	Subbase	120.8	9.4%	NP	NP	NA	NA
Dade	6	87060000	A1A	Base	129.4	7.0%	NP	NP	NA	NA
				Embankment	124.9	7.9%	NP	NP	A-2-4	19.2%
Hillsborough	7	10060000	US 41	Base	120.1	10.0%	NP	NP	NA	NA
				Subgrade	112.6	11.2%	NP	NP	A-3	8.2%
				Embankment	116.8	12.4%	NP	NP	A-2-4	16.9%
Hillsborough	7	10160000	SR 60	Base	117.6	11.6%	NP	NP	NA	NA
				Subgrade	105.1	6.6%	NP	NP	A-3	9.0%
				Embankment	104.4	12.5%	NP	NP	A-3	6.6%

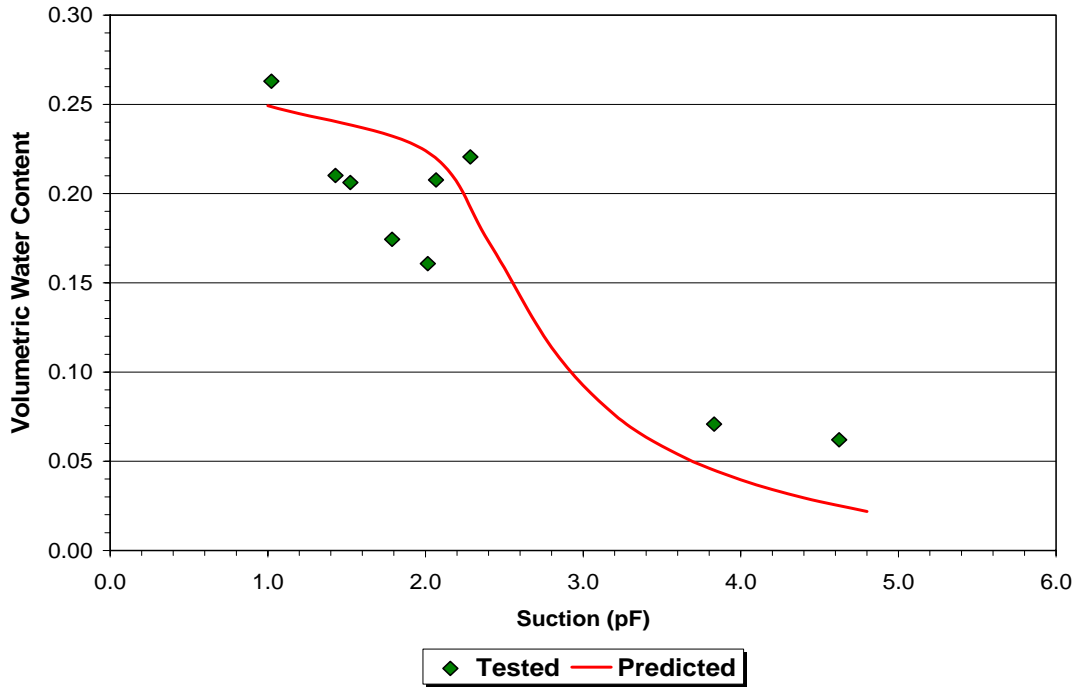


**Figure 4.14. Soil-Water Characteristic Curve of Embankment Soil from Section 26005.**

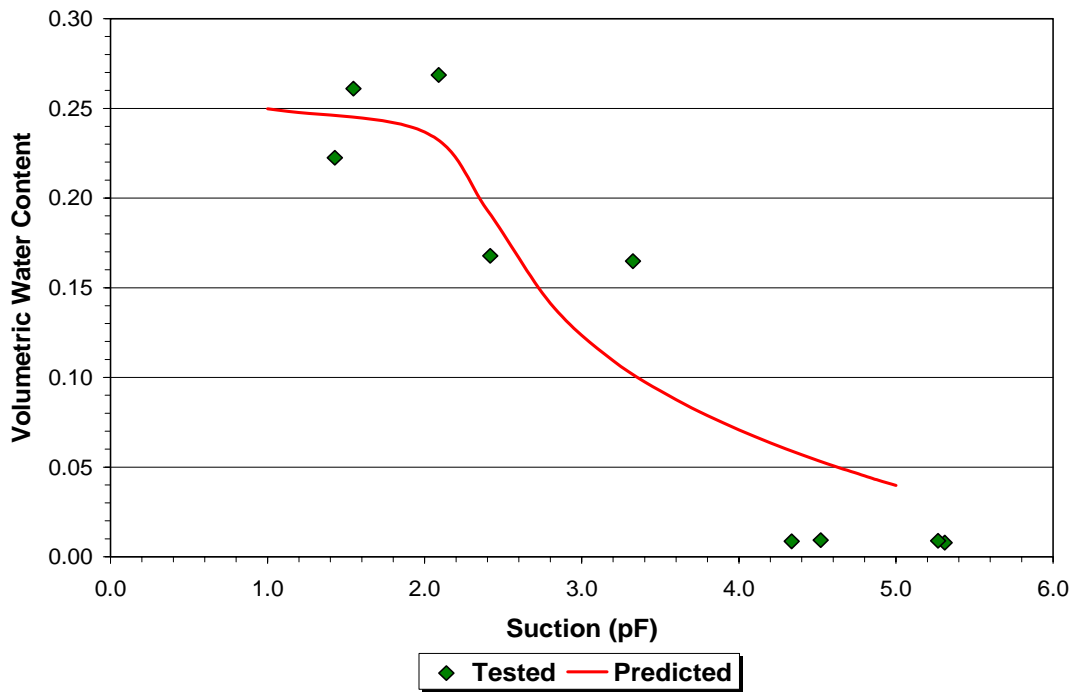


**Figure 4.15. Soil-Water Characteristic Curve of Embankment Soil from Section 28040.**

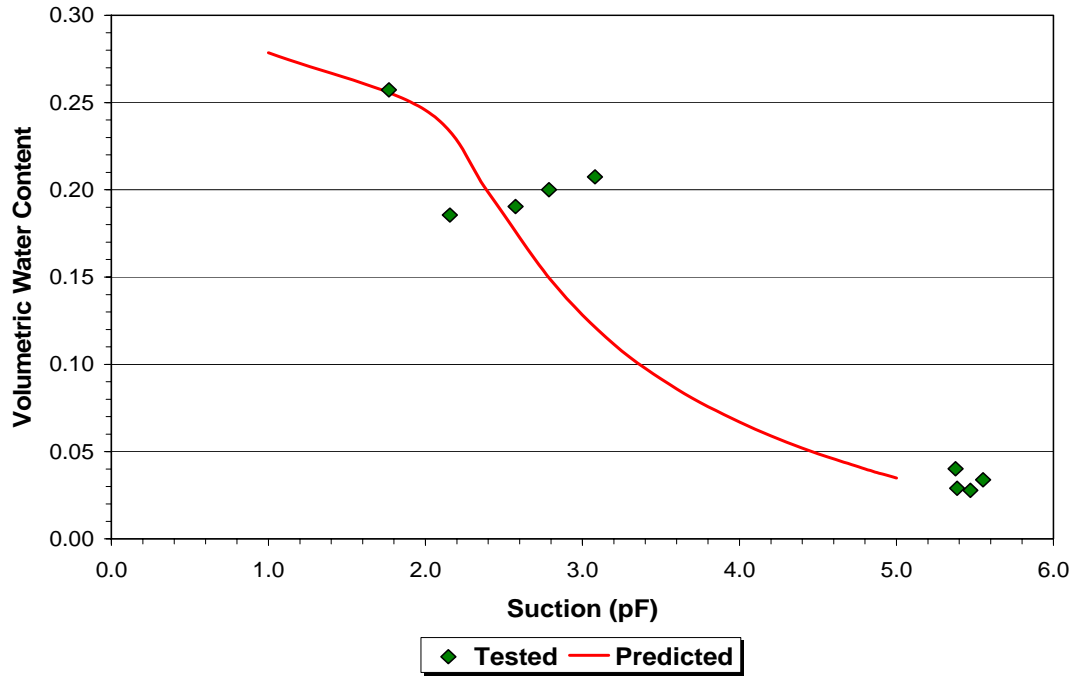


**Figure 4.16. Soil-Water Characteristic Curve of Embankment Soil from Section 58060.**

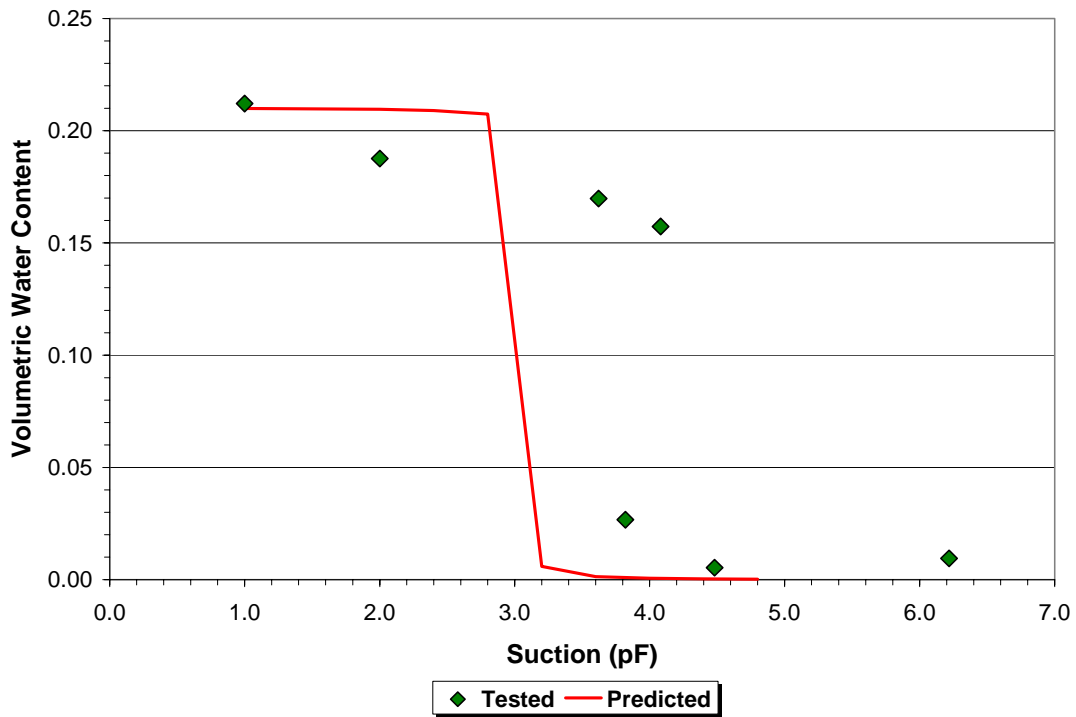


**Figure 4.17. Soil-Water Characteristic Curve of Embankment Soil from Section 86190.**

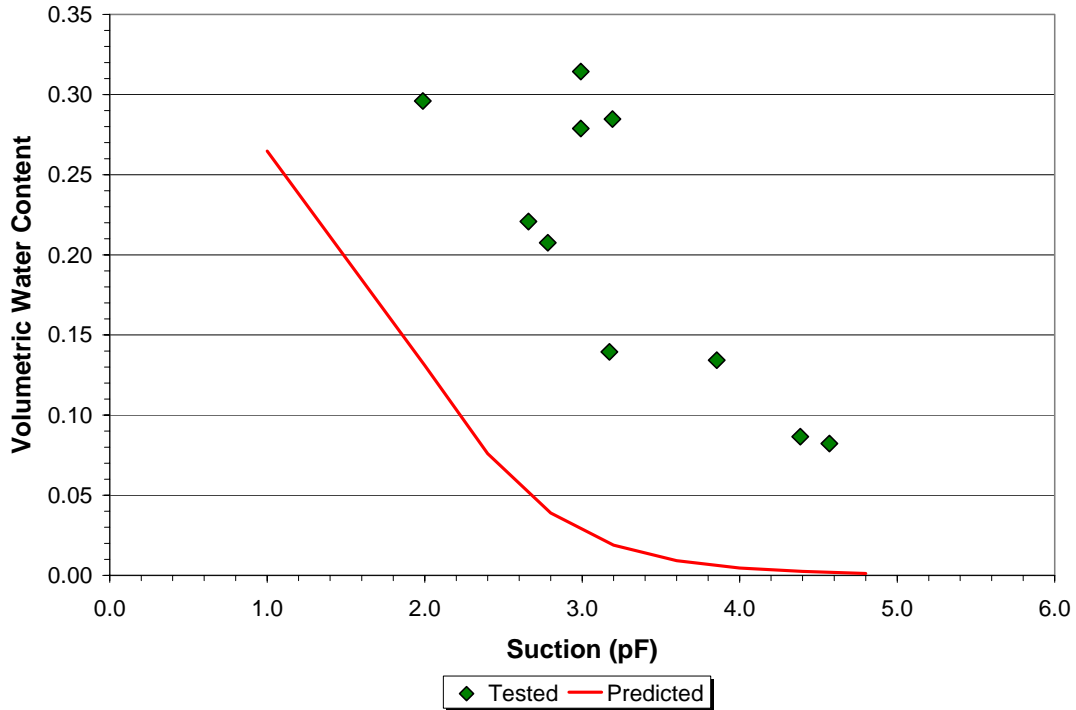


**Figure 4.18. Soil-Water Characteristic Curve of Embankment Soil from Section 10060.**

**Table 4.8. Soil Suction Coefficients for Embankment Soils.**

County Name	Soil Suction Coefficients			
	$a_f$ (psi)	$b_f$	$c_f$	$h_f$ (psi)
Alachua	2.584	0.989	1.224	100.049
Baker	1.715	0.855	2.187	100.049
Bay	6.013	0.542	5.318	100.078
Bradford	2.025	1.515	0.640	100.052
Brevard	4.807	0.414	3.551	100.716
Broward	1.214	0.827	2.857	99.424
Calhoun	0.827	1.267	0.793	99.990
Charlotte	2.857	0.790	1.517	99.427
Citrus	1.378	0.733	3.342	100.765
Clay	1.694	0.846	2.958	100.050
Collier	1.083	0.867	2.374	99.427
Columbia	2.163	0.861	2.290	100.050
Dade	3.359	1.264	0.636	99.415
De Soto	1.730	0.840	2.949	99.424
Dixie	1.565	0.871	2.812	100.050
Duval	1.581	0.905	2.806	100.050
Escambia	7.132	1.608	0.354	99.989
Flagler	3.999	0.624	5.304	100.716
Franklin	6.618	0.629	6.397	99.986
Gadsden	6.013	0.542	5.318	100.078
Gilchrist	1.563	0.871	2.812	100.050

**Table 4.8. Soil Suction Coefficients for Embankment Soils (continued).**

County Name	Soil Suction Coefficients			
	$a_f$ (psi)	$b_f$	$c_f$	$h_f$ (psi)
Glades	1.426	0.768	3.161	99.424
Gulf	7.332	2.451	0.607	99.988
Hamilton	6.708	0.802	1.570	100.035
Hardee	1.423	0.769	3.161	99.424
Hendry	1.912	1.073	1.197	99.425
Hernando	1.303	0.809	3.400	100.765
Highlands	0.865	0.941	2.233	99.425
Hillsborough	1.377	0.730	3.327	100.765
Holmes	10.447	1.979	0.364	99.941
Indian River	2.381	0.681	4.168	99.414
Jackson	5.888	0.646	5.812	99.999
Jefferson	7.327	1.903	0.357	99.424
Lafayette	5.102	0.668	4.453	100.033
Lake	3.999	0.625	5.304	100.716
Lee	1.211	0.822	2.835	99.424
Leon	8.010	2.344	0.288	99.634
Levy	4.783	0.687	5.191	100.033
Liberty	6.618	0.629	6.397	99.986
Madison	6.016	0.495	2.610	100.034
Manatee	1.423	0.769	3.161	99.424
Marion	3.997	0.597	5.242	100.763
Martin	3.997	0.597	5.242	100.763
Monroe	12.862	18.823	1.500	100.040
Nassau	3.997	0.597	5.242	100.763
Okaloosa	6.013	0.542	5.318	100.078
Okeechobee	1.206	0.829	2.843	99.424
Orange	3.998	0.613	5.240	100.763
Osceola	1.674	0.724	3.414	100.765
Palm Beach	2.381	0.681	4.168	99.414
Pasco	1.381	0.728	3.323	100.766
Pinellas	1.378	0.728	3.325	100.765
Polk	6.013	0.542	5.318	100.078
Putnam	4.996	0.674	5.176	100.033
St. Johns	4.863	0.674	5.100	100.033
St. Lucie	5.829	1.560	0.714	100.717
Santa Rosa	7.332	2.451	0.607	99.988
Sarasota	1.149	0.926	2.902	99.424
Seminole	1.655	0.734	3.426	100.765
Sumter	1.405	0.832	3.330	100.765
Suwannee	1.316	0.722	1.419	100.116
Taylor	1.405	1.042	1.602	100.116
Union	7.946	1.845	0.510	100.082
Volusia	1.549	0.594	3.192	100.765
Wakulla	5.888	0.646	5.812	99.999
Walton	6.013	0.542	5.318	100.078
Washington	5.888	0.646	5.812	99.999

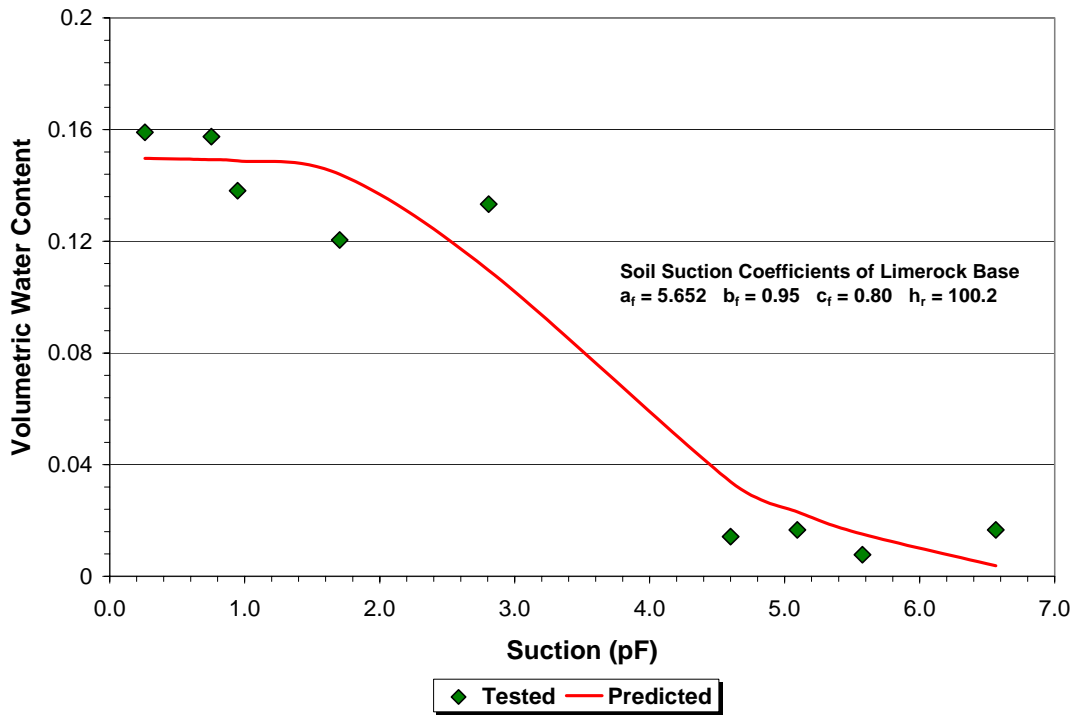


Figure 4.19. Soil-Water Characteristic Curve of Limerock Base.

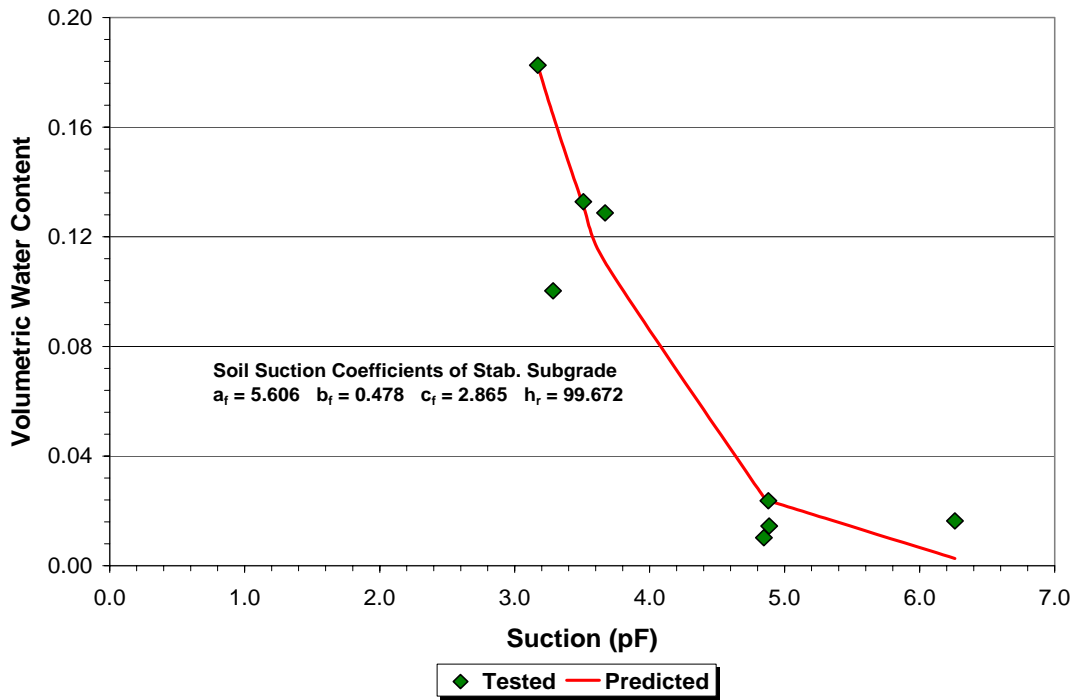


Figure 4.20. Soil-Water Characteristic Curve of Stabilized Subgrade.

## **CHAPTER V. SUPPLEMENTARY FLEXIBLE PAVEMENT THICKNESS DESIGN TABLES BASED ON M-E PDG**

This project aimed to implement the mechanistic-empirical pavement design guide in Florida. For this implementation, the decision was made to provide a set of supplementary pavement thickness design tables based on the M-E PDG to include as an alternative to the current set of thickness design tables used by the Department. Prior to generating the M-E PDG thickness design tables, the need for calibrating the performance models in the M-E PDG program was first considered. Based on discussions with the project advisory panel, no calibrations of the current flexible pavement performance models in M-E PDG version 1.0 were carried out. The advisory panel and researchers recognized that further changes in the performance models will come about from on-going national studies on top-down cracking, reflective cracking, and rutting. Thus, the decision was made to wait until the models developed from these projects were incorporated into a future release of the M-E PDG program, at which time the Florida DOT will re-assess the need for local model calibrations. The advisory panel also agreed with the recommendation to develop the preliminary flexible pavement design tables based on the existing alligator (bottom-up) cracking model in M-E PDG version 1.0. Given these decisions, researchers conducted sensitivity analyses to determine critical variables which have significant influences on alligator cracking predictions. Based on the results, supplementary thickness design tables were established from multiple runs of the M-E PDG program for new construction and overlay projects.

### **SENSITIVITY ANALYSES**

Additional sensitivity analyses were performed to determine key variables that should be considered in establishing the design tables for flexible pavements based on the M-E PDG. It should be noted that all sensitivity analyses focused on alligator cracking since the decision was made to develop the thickness design tables based only on this distress type. The variables selected for the sensitivity analysis, the factor levels used, and results obtained are shown in Table 5.1. Researchers note that the ranges of layer moduli used in the analyses are based on recommendations provided by Dr. David Horhota of the State Materials Office who provided approximate ranges of laboratory resilient moduli for various levels of bulk stress considered to be representative of current FDOT design practice, and data from previous projects.

All runs were executed with a reliability level of 90%, a design life of 20 years, and a performance criterion of 35% on alligator cracking. The pavement structure analyzed consisted of a 1.5-inch friction course, a 4.5-inch structural course over a 10-inch limerock base, 12 inches of mechanically stabilized subgrade, and A-2-4 embankment. Figures 5.1 to 5.8 illustrate the sensitivity of the predicted alligator cracking to the design variables considered in the analyses.

**Table 5.1. Variables and Factor Levels Used in Sensitivity Analyses.**

Variables	Description	Sensitivity**
Environmental*	Miami / Tallahassee	Low
Base Modulus	30, 45 , 60 ksi	High
Stabilized Modulus	12, 14, 16 ksi	Low
Embankment Modulus	8,10,12 ksi	Low
Base Thickness	8, 10, 12 inch	Low
AADTT	11250 for TTC 6 8600 for TTC 1 16000 for TTC 14	Low
Air-Void of AC	7, 7.5, 8 %	High
PG-Grade of AC	64-22, 70-22, 76-22	Low

\*Ground water table depths of 5 and 30 feet were assumed, respectively, for Miami and Tallahassee based on boring data.

\*\*Sensitivity based solely on predicted alligator cracking.

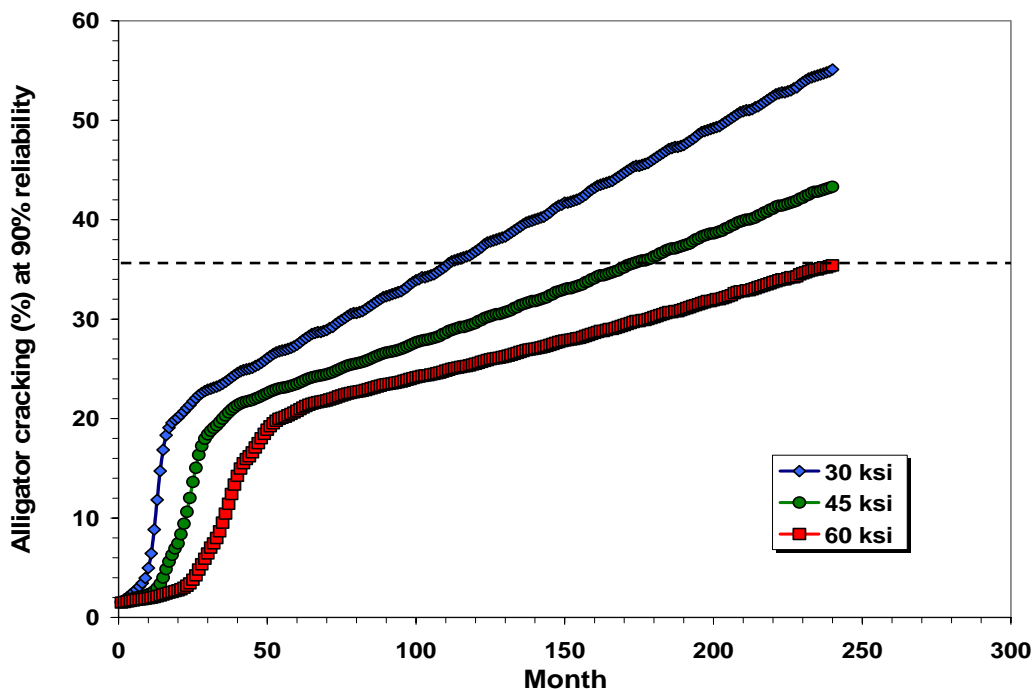


**Figure 5.1. Sensitivity of Alligator Cracking to Base Modulus.**

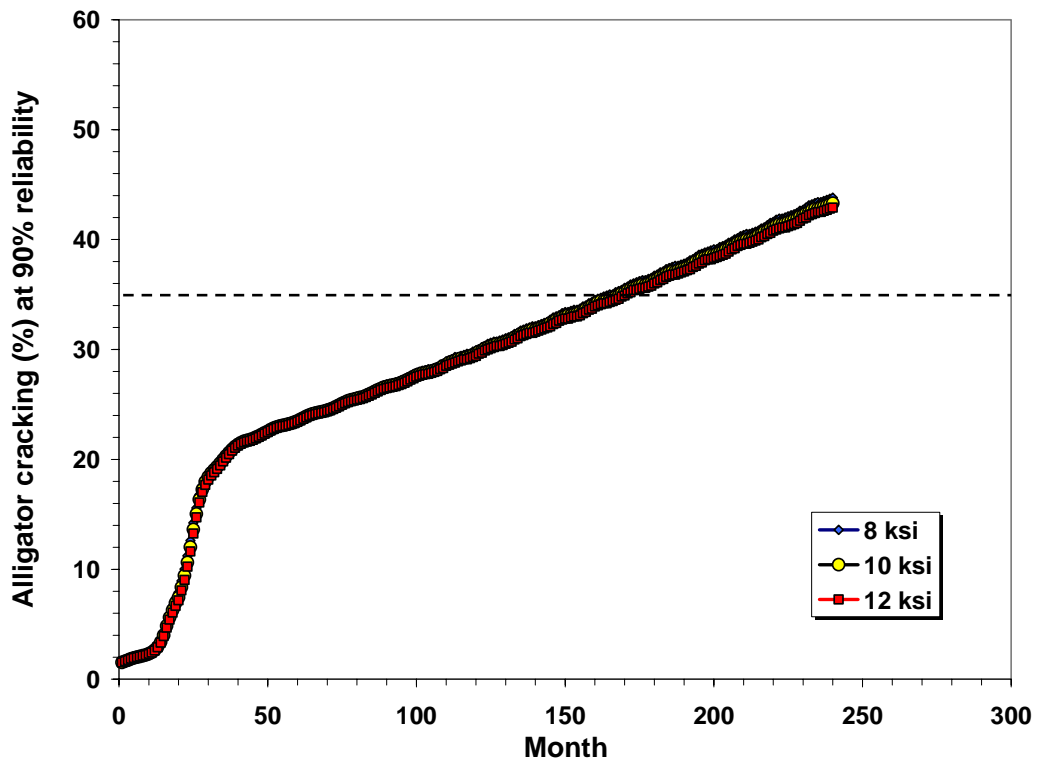


Figure 5.2. Sensitivity of Alligator Cracking to Embankment Modulus.

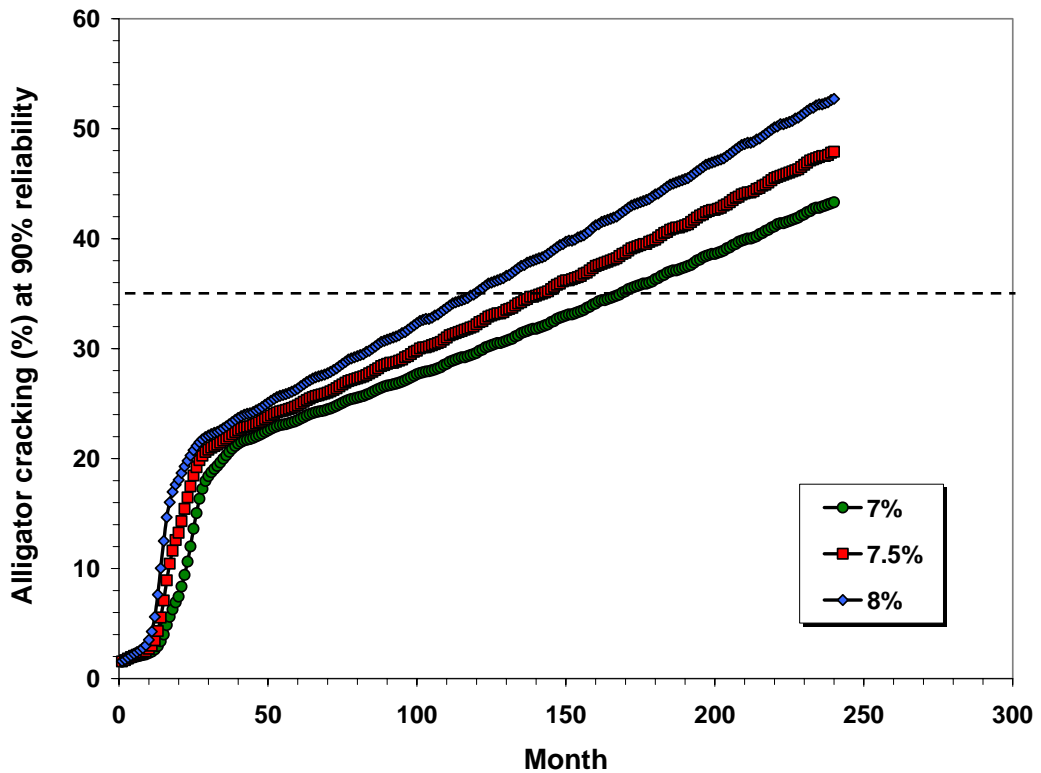


Figure 5.3. Sensitivity of Alligator Cracking to AC Air Voids Content.

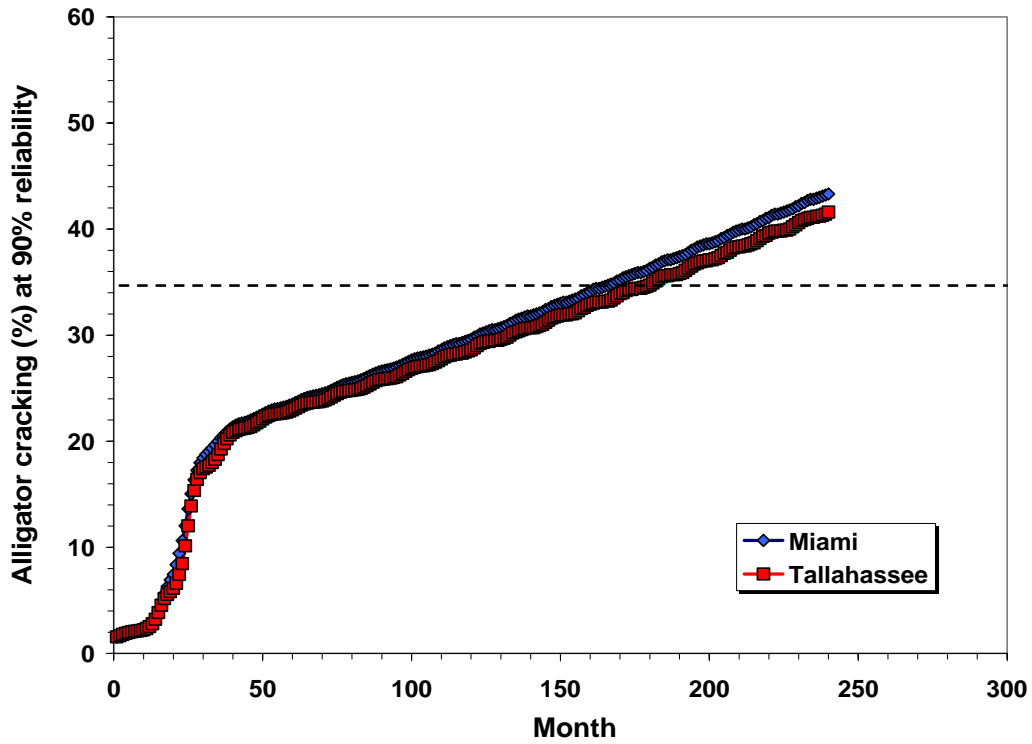


Figure 5.4. Sensitivity of Alligator Cracking to Regional Environmental Differences.

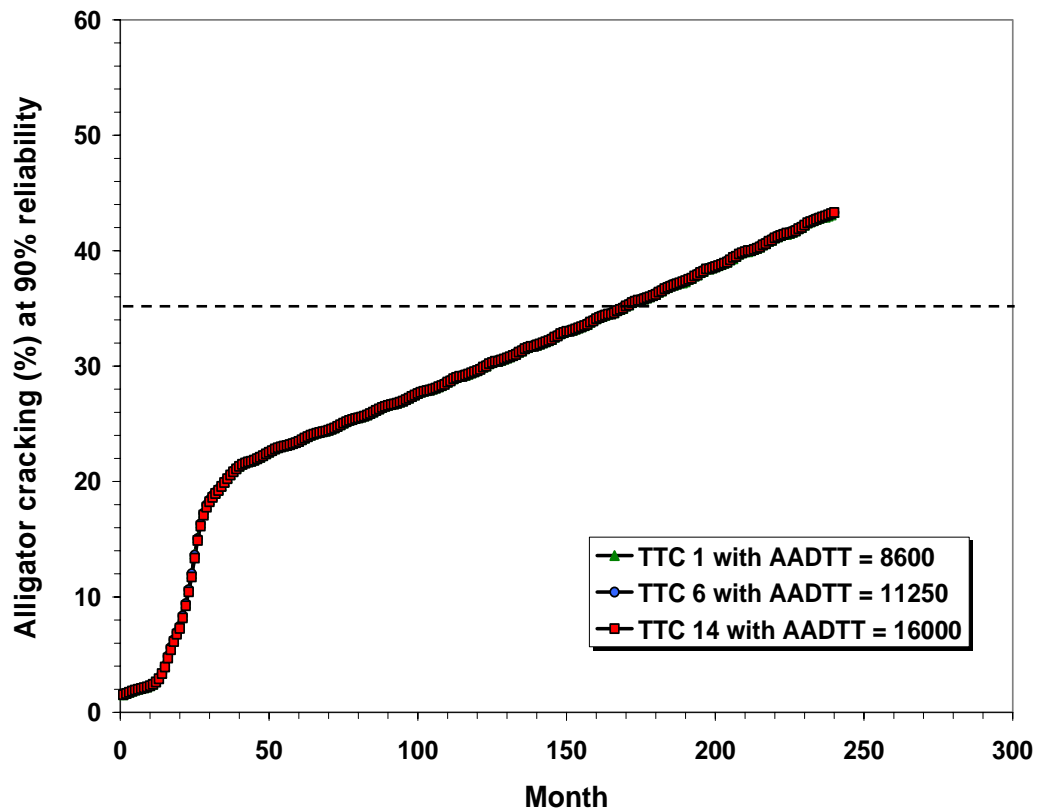


Figure 5.5. Sensitivity of Alligator Cracking to Truck Traffic Classification (TTC).

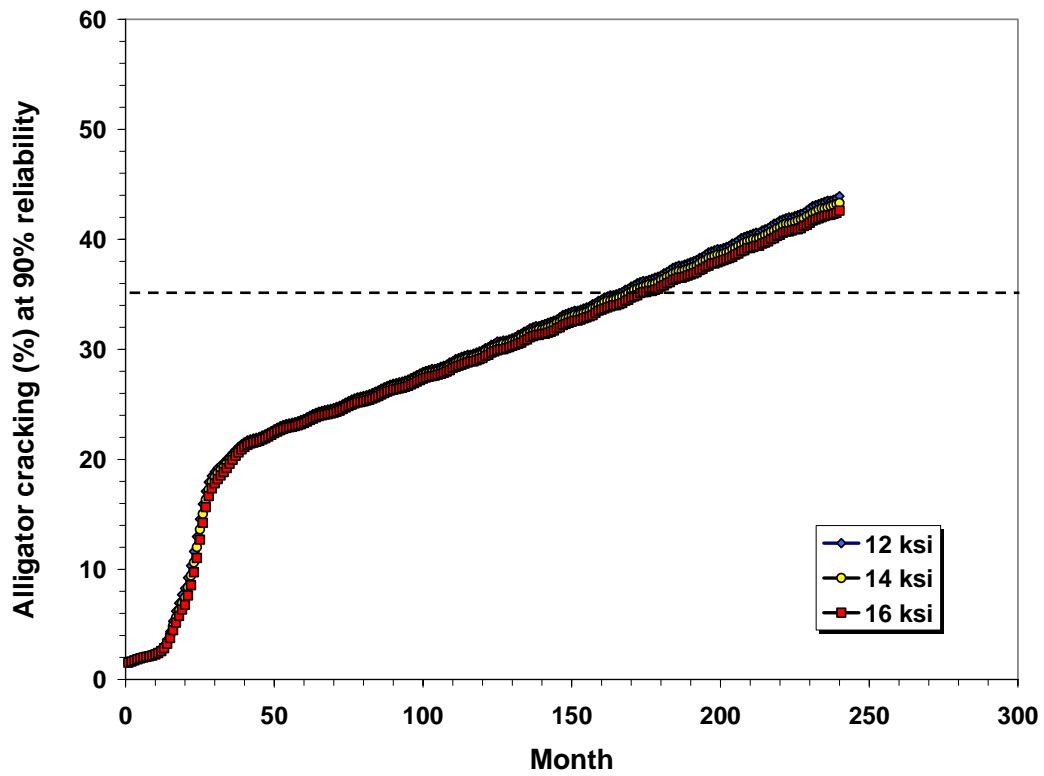


Figure 5.6. Sensitivity of Alligator Cracking to Stabilized Subgrade Modulus.

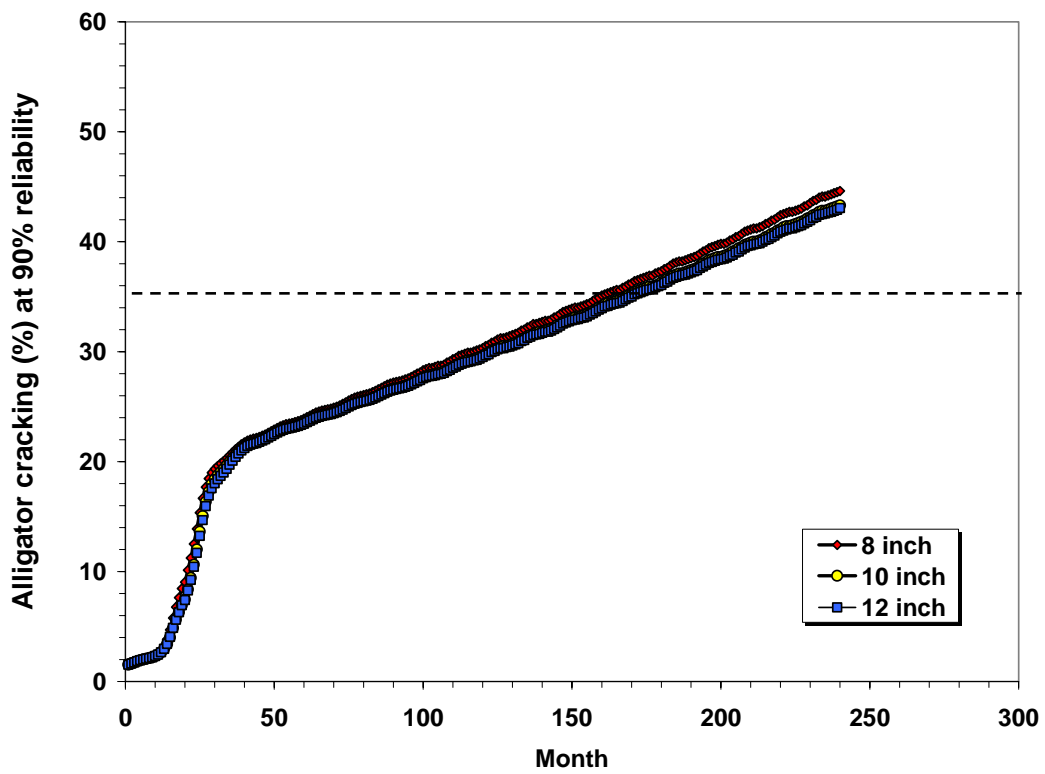
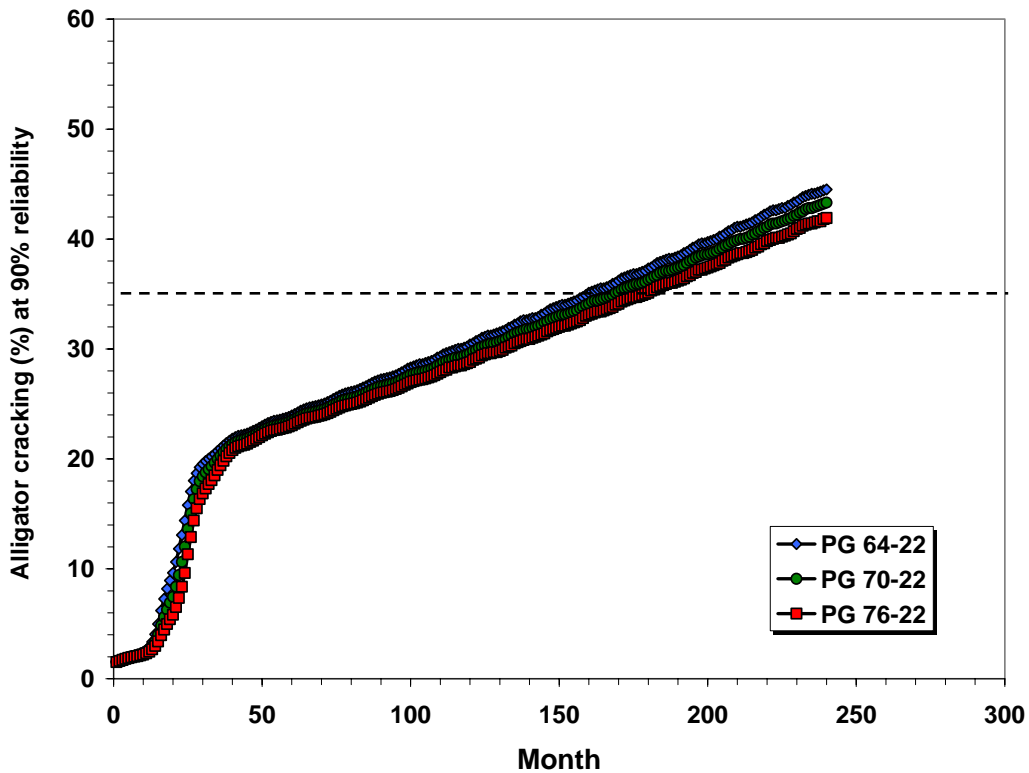


Figure 5.7. Sensitivity of Alligator Cracking to Base Thickness.



**Figure 5.8. Sensitivity of Alligator Cracking to PG Binder Grade.**

It was observed that base modulus and AC air voids content significantly affected the predictions of alligator cracking from the M-E PDG program. The other variables exhibited relatively insignificant effects on alligator cracking over the range by which each factor was varied. The effect of climate on alligator cracking was observed to be not significant as shown in Figure 5.4. The pavement structure in the Miami area, with generally higher temperatures and shallower ground water table depth, was predicted to have slightly larger amounts of alligator cracking compared to the same pavement in the Tallahassee area. With respect to the effect of traffic, the predictions of alligator cracking were found to depend more on the cumulative design ESALs than with the truck traffic classification (TTC) that defines the distribution of the different vehicle types as shown in Figure 5.5. This figure shows that the predicted alligator cracking between TTCs are very similar when the AADTT is varied to produce the same number of cumulative ESALs within the design period.

The sensitivity analyses showed that the predicted alligator cracking did not vary significantly with changes in the embankment modulus. This result is counter-intuitive since the tensile strains at the bottom of the asphalt concrete layer are expected to vary with the

embankment modulus. To verify this result, researchers utilized the layered elastic program BISAR (de Jong et al., 1973) to check the M-E PDG program predictions. Table 5.2 shows the input data used for this analysis. For the wheel load condition, researchers assumed an 18- kip single axle with dual tires spaced 12 inches center-to-center. Two sets of analysis were done with and without the stabilized subgrade layer to examine if there is a difference in the sensitivity of the predicted alligator cracking due to the presence of the mechanically stabilized subgrade.

**Table 5.2. Input Data and Levels for BISAR Runs.**

Layer	Thickness (inch)	M <sub>r</sub> (ksi)
AC	5	500
Base	8, 10, 12, 14, 16	30, 40, 50
Subgrade	12	16
Embankment	infinite	6, 8, 12, 16

For this verification, the calculated tensile strains at the critical positions beneath the load, and the predicted number of load repetitions to failure were plotted versus each variable range. Service life based on alligator cracking was computed using the Asphalt Institute equation (1982), which is given below.

$$N_f = 0.0796(\epsilon_{ac})^{-3.291}(E_{ac})^{-0.854} \quad (6.1)$$

where,

- $N_f$  = allowable number of load repetitions based on fatigue cracking,
- $\epsilon_{ac}$  = calculated tensile strain at the bottom of the AC layer,
- $E_{ac}$  = asphalt concrete modulus (psi).

The results shown in Figures from 5.9 to 5.11 indicate that base modulus is the most critical factor controlling the predicted alligator cracking rather than embankment modulus and base thickness, which concur with the results from the M-E PDG sensitivity analyses. In addition, the pavement structure built directly over the embankment soil was predicted to have a smaller number of load repetitions due to the slightly higher predicted tensile strains at the bottom of the asphalt compared to the case where the pavement is constructed with the stabilized subgrade layer. This finding appears to justify the current practice of placing a mechanically stabilized subgrade in asphalt concrete pavements. Consistent with current practice, the design tables developed for these pavements assume 12 inches of mechanically stabilized subgrade. Overall, the sensitivity of the predicted alligator cracking to

embankment modulus was relatively less significant compared to the sensitivity of the predictions to the base modulus. Thus, the results from this verification appear to support the findings from the M-E PDG sensitivity analyses.

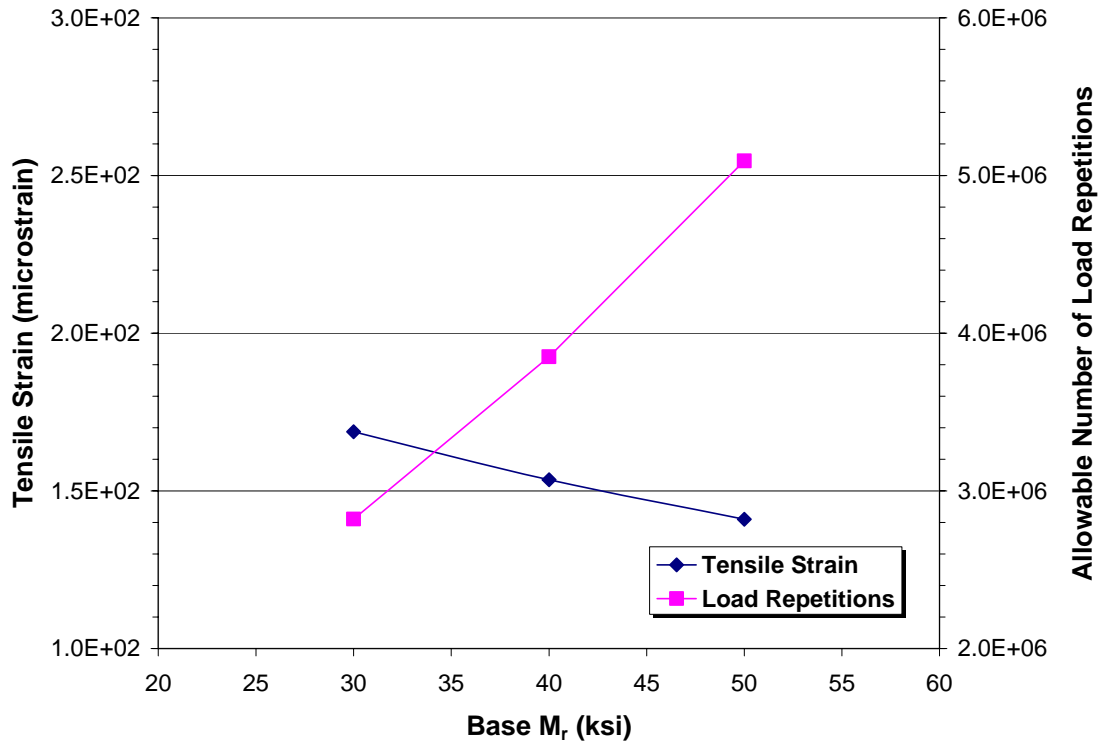


**Figure 5.9. Sensitivity of Predicted Tensile Strains and Number of Load Repetitions to Base Modulus.**

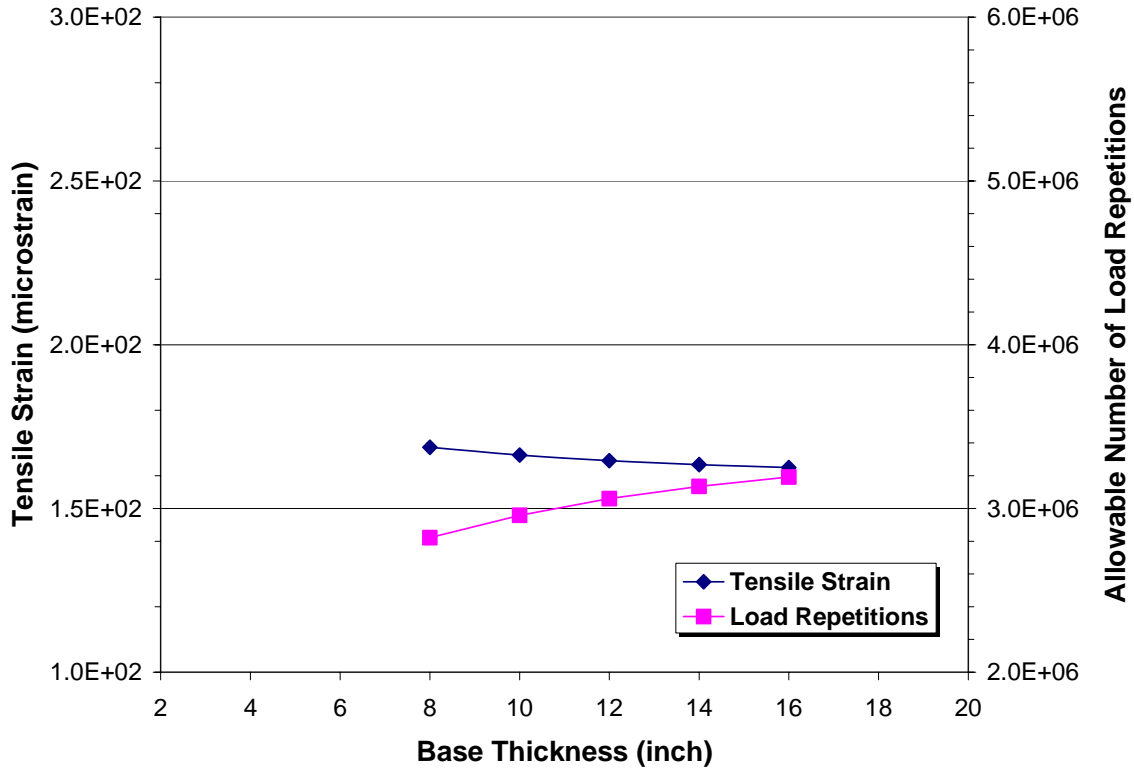


Figure 5.10. Sensitivity of Predicted Tensile Strains and Number of Load Repetitions to Base Thickness.

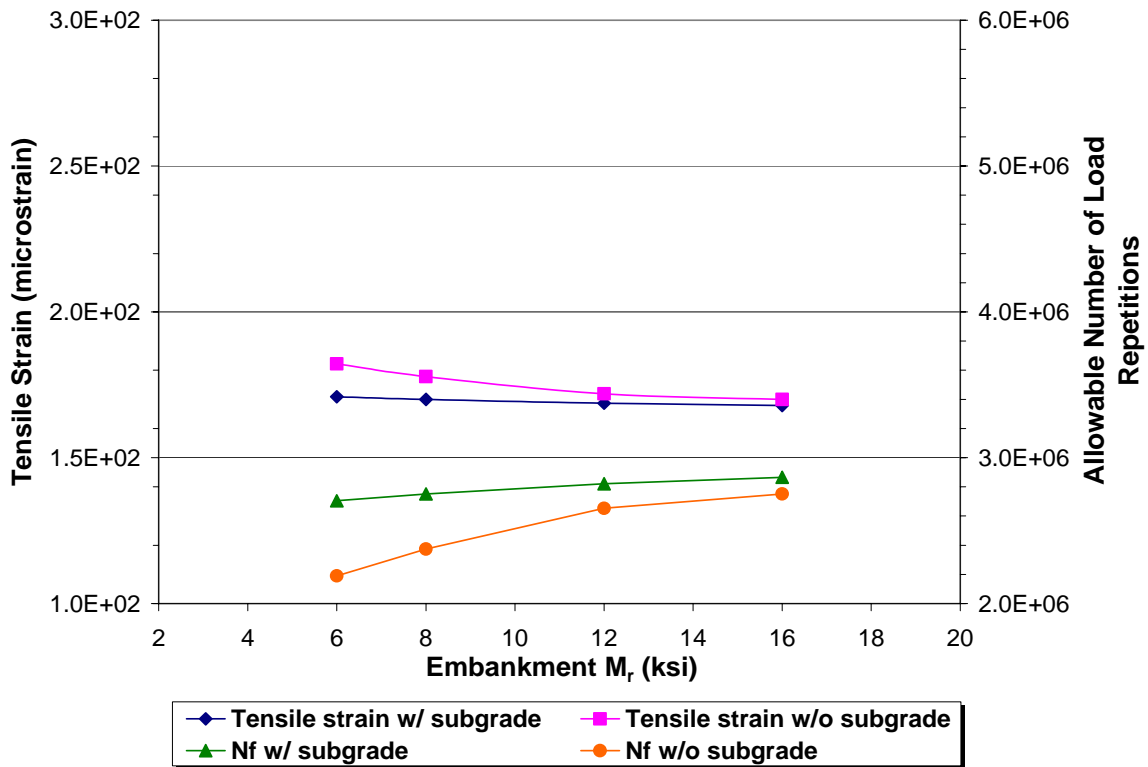


Figure 5.11. Sensitivity of Predicted Tensile Strains and Number of Load Repetitions to Embankment Modulus.

## DEVELOPMENT OF FLEXIBLE PAVEMENT DESIGN TABLES

Prior to generating the design tables, efforts were made to review the current Florida DOT design procedure for flexible pavements. The Florida DOT flexible design tables assign a structural number for different levels of ESALs, embankment resilient modulus, and reliability. For a given structural number corresponding to a specific combination of cumulative 18-kip ESALs, embankment modulus, and reliability, engineers can determine the layer thicknesses for new construction and overlay designs. From the review of the Florida DOT design procedure and the results from the sensitivity analyses of the M-E PDG program, the decision was made to establish design tables following a similar format to the current Florida DOT practice for new construction and overlay projects. Researchers note that the M-E PDG program analyzes new construction and overlay projects separately as shown in Figure 5.12. The design variables for generating the design tables based on alligator cracking were selected as explained in the following sections.

The screenshot shows a software window titled "General Information" with the following fields and options:

- Project Name: ST1\_AC\_TAMPA
- Description: Structure 1
- Design Life (years): 20
- Base/Subgrade Construction Month: November, Year: 2006
- Pavement Construction Month: May, Year: 2007
- Traffic open month: June, Year: 2007
- Type of Design:
  - New Pavement:
    - Flexible Pavement
    - Jointed Plain Concrete Pavement (JPCP)
    - Continuously Reinforced Concrete Pavement (CRCP)
  - Restoration:
    - Jointed Plain Concrete Pavement (JPCP)
  - Overlay:
    - Asphalt Concrete Overlay
    - PCC Overlay

Buttons: OK, Cancel

Figure 5.12. M-E PDG General Information Screen.

### Characterization of Asphalt Concrete Layer

The Florida DOT uses different kinds of friction and structural AC courses. Based on a review of Florida DOT standard specifications, previous research reports, and laboratory tests conducted in this project, the different asphalt concrete materials used by the Department were characterized as tabulated in Table 5.3.

**Table 5.3. Asphalt Concrete Material Properties Used in M-E PDG Runs.**

Property	FC-5	FC-9.5	FC-12.5	SP-9.5	SP-12.5	SP-19.0	Modified SP
Cum. % Ret. 3/4"	0	0	0	0	0	5	5
Cum. % Ret. 3/8"	10	15	15	25	30	35	35
Cum. % Ret. #4	40	30	35	42	45	50	50
% passing #200	6	6	6	5	5	5	5
PG Grade	70-22	70-22	70-22	70-22	70-22	70-22	76-22
A-VTS	10.299 -3.426	10.299 -3.426	10.299 -3.426	10.299 -3.426	10.299 -3.426	10.299 -3.426	9.715 -3.208
AV (%)	7	7	7	7	7	7	7

For PG grade, the Florida DOT uses PG 67-22 in current practice. However, since no default temperature-viscosity coefficients (A-VTS) are available in the M-E PDG program, PG 70-22 was instead specified for the M-E PDG runs made to generate the thickness design tables. For the materials given in Table 5.3, Table 5.4 shows how the predicted alligator cracking varied with different combinations of friction and structural courses. All predictions are based on 95 percent reliability. Table 5.4 shows no significant differences in the amounts of predicted alligator cracking. Thus, researchers selected the most typical combination, consisting of FC 12.5 over SP 12.5, in generating the supplemental thickness design tables for HMAC pavements.

**Table 5.4. Predictions of Alligator Cracking (%) for Different AC Layer Combinations.**

Mixture Combination	FC 5	FC 9.5	FC 12.5
SP 9.5	42.27	41.64	41.81
SP 12.5	42.27	41.64	41.81
SP 19.0	41.99	41.34	41.64
Modified SP	41.27	40.64	40.91

## Characterization of Underlying Layers

For characterizing the moduli of the underlying layers, Dr. David Horhota of the State Materials Office provided approximate ranges of laboratory resilient moduli for various levels of bulk stress considered to be representative of current FDOT design practice, and data from previous projects. From these consultations, researchers used the laboratory test results obtained from this project to determine values of resilient modulus for underlying pavement layers based on the following levels of bulk stress:

- Base – 50 psi,
- Stabilized subgrade – 14 psi, and
- Embankment – 11 psi.

Figure 5.13 shows the distribution of moduli along the calibration sections tested in this project. From this figure, researchers assigned representative modulus values of 30 and 45 ksi for base, 16 ksi for stabilized subgrade, and 12 ksi for embankment, for developing the flexible pavement thickness design tables using the M-E PDG program. Since the predicted alligator cracking from the M-E PDG program was found to be insensitive to the embankment and subgrade moduli, researchers assigned only one level of modulus to each of these factors.

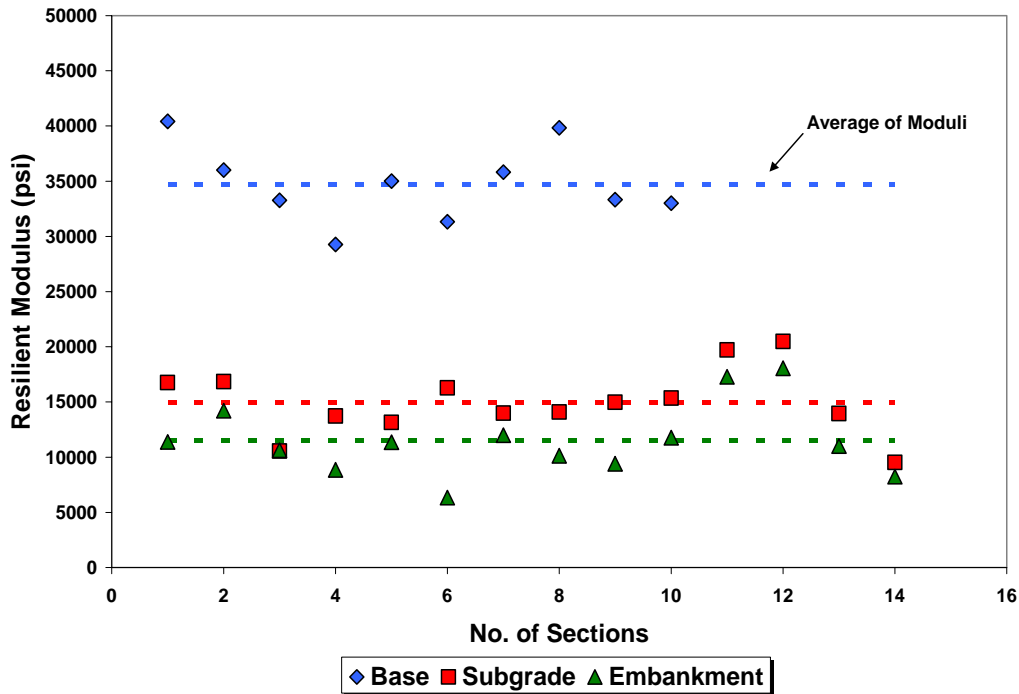


Figure 5.13. Distribution of Underlying Layer Resilient Modulus.

With respect to the effect of base thickness, researchers found that the predicted alligator cracking is insensitive to this design variable. To be free from uncertainty in adopting one level of base thickness, the decision was made to check the design requirements for 8 and 10 inches of limerock base. In this regard, a comparison of the design requirements between 8- and 10-inch base layers showed that the thickness requirements are generally the same but for one case where the 8-inch base results in a 0.5-inch greater HMAC thickness. Since the differences are generally very minimal, researchers are of the opinion that the design tables based on 8-inches of Limerock base would suffice.

### **Consideration of Overlay Projects**

With respect to modeling the performance of HMAC overlays, researchers observed that the program predicts only small amounts of alligator cracking for overlaid pavements when the M-E PDG overlay option shown in Figure 5.12 is employed. Researchers conducted a check wherein the same flexible pavement was input to the program. However, in one case, researchers performed the analysis using the M-E PDG's new construction option while in the other case, the overlay option was used. For the same flexible pavement, the M-E PDG program predicted significantly higher amounts of alligator cracking under the new construction option, but far less cracking under the overlay option. Thus, it appears that the tensile strain at the bottom of the asphalt is being predicted at different locations between the two analysis options. If the horizontal strain is predicted at the bottom of the HMAC layer in the new construction option, the strain is likely to be tensile, resulting in higher predictions of alligator cracking. On the other hand if the same strain is predicted at the bottom of the overlay, smaller tensile strains, and even compressive horizontal strains might be predicted under loading, particularly for thin ( $\leq 2$ -inch) overlays placed on top of an existing milled asphalt concrete layer.

In view of the apparent anomaly in the overlay analysis option, researchers took a different approach in developing the thickness design tables for asphalt concrete overlays. This approach is based on using the new construction option in the M-E PDG program with the existing HMAC layer characterized according to the condition of the material. This approach is similar in concept to the current practice followed within the Florida DOT of assigning a reduced structural coefficient to the existing asphalt layer based on its condition

as established by visual inspection of cores taken during the pre-construction phase of the rehabilitation process.

To simulate the current pavement condition criteria used by the Department, researchers ran the M-E PDG program for different levels of existing HMAC modulus to simulate good, fair, and poor pavement conditions. The HMAC modulus was varied by adjusting the binder and volumetric properties of the existing material, specifically, binder viscosity and air voids content. Of the two factors, researchers found that the air voids content had a greater influence on the predicted HMAC modulus. In view of this finding, and considering that the air voids content simulates the amount of cracking in the existing material, researchers used this variable to simulate the condition of the existing AC layer.

Researchers established criteria to characterize good, fair, and poor pavement conditions by using the M-E PDG program to find the levels of air voids content that result in overlay thicknesses comparable to the existing FDOT flexible pavement design method. From this analysis, researchers established the following correspondence between air voids content and the existing condition of the HMAC material:

- Good – 7.2 percent,
- Fair – 7.5 percent, and
- Poor – 8.0 percent air voids.

### **Final Selection of Variables for Design Tables**

Based on the work described in the preceding, researchers came up with the following selections of variables that were input to the M-E PDG program to generate design tables for flexible pavements:

- Friction course: 1.5 inch of FC-12.5 (PG 70-22, 7 percent air voids)
- Structural course: SP 12.5 (PG 70-22, 7 percent air voids)
- Existing AC material: 2 to 6 inches of SP 12.5 (PG 70-22, 7.2 percent air voids for HMAC material in good condition, 7.5 percent for existing material in fair condition, and 8.0 percent for material in poor condition)
- Base layer: 8 inches of limerock at two modulus levels of 30 and 45 ksi
- Stabilized subgrade: 12 inches with 16 ksi modulus
- Embankment: A-2-4 soil with 12 ksi modulus
- Reliability: 75, 80, 85, 90, 95 percent

- ESALs: 1 to 70 million ESALs
- Weather: Miami weather data with 5 feet ground water table
- Distress Criterion: 35% alligator cracking
- Initial IRI: 58 inches/mile (same assumption used in generating the PCC thickness design tables presented in Chapter VI)
- Design life: 20 years

### **M-E PDG Runs for Generating Design Tables**

Once an input file is generated, the M-E PDG program was executed to determine the required asphalt layer thickness for new construction and overlay projects. For a given combination of design factors, program runs were made until the predicted alligator cracking for the specified reliability level came within tolerance of the 35% cracking threshold. Appendix G presents the flexible pavement design tables established in this project. It is noted that the AC thickness given in the table is the total thickness of the friction and structural layers. As expected, the required AC thickness increases with higher levels of reliability and cumulative 18-kip ESALs. For overlays, the required thickness varied with the existing asphalt layer thickness, pavement condition, and base modulus as shown in the tables given in Appendix G.

### **COMPARISON OF M-E PDG BASED DESIGN TABLES WITH CURRENT FDOT DESIGN TABLES**

Researchers compared the design tables based on the M-E PDG with the current AASHTO pavement design tables used by the Florida DOT (Flexible Pavement Design Manual, 2005). For these comparisons, the required asphalt concrete layer thickness was determined using the current Florida DOT procedure at different levels of reliability and cumulative ESALs. Tables 5.5 and 5.6 show the required asphalt concrete layer thickness based on the current procedure used by the Department. To illustrate, the shaded cells in Tables 5.5 and 5.6 were calculated as follows:

**Table 5.5. Required AC Thickness for New Design Based on Current FDOT Procedure.**

Cum. ESALs ( $\times 10^6$ )	Reliability				
	75	80	85	90	95
1	0.5	0.7	0.9	1.2	1.6
2	1.2	1.5	1.7	2.0	2.5
3	1.7	1.9	2.2	2.5	3.0
4	2.0	2.3	2.5	2.9	3.4
5	2.3	2.5	2.8	3.2	3.9
10	3.3	3.5	3.8	4.2	4.7
15	3.8	4.1	4.4	4.8	5.4
20	4.3	4.5	4.8	5.2	5.8
25	4.6	4.9	5.2	5.6	6.2
30	4.9	5.2	5.5	5.9	6.5
35	5.1	5.4	5.7	6.1	6.7
40	5.3	5.6	6.0	6.3	7.0
45	5.5	5.8	6.1	6.5	7.2
50	5.7	6.0	6.3	6.7	7.4
55	5.8	6.1	6.4	6.9	7.5
60	6.0	6.2	6.6	7.0	7.7
65	6.1	6.4	6.7	7.2	7.8
70	6.2	6.5	6.9	7.3	8.0

**Table 5.6. Required AC Thickness for Overlay Design Based on Current FDOT Procedure (poor condition with 2-inch existing AC).**

Cum. ESALs ( $\times 10^6$ )	Reliability				
	75	80	85	90	95
1	0.0	0.0	0.2	0.5	0.9
2	0.5	0.7	1.0	1.3	1.7
3	1.0	1.2	1.5	1.8	2.3
4	1.3	1.5	1.8	2.2	2.7
5	1.6	1.8	2.1	2.5	3.2
10	2.5	2.8	3.1	3.5	4.0
15	3.1	3.4	3.7	4.0	4.6
20	3.5	3.8	4.1	4.5	5.1
25	3.9	4.1	4.5	4.9	5.5
30	4.2	4.4	4.8	5.1	5.8
35	4.4	4.7	5.0	5.4	6.0
40	4.6	4.9	5.2	5.6	6.3
45	4.8	5.1	5.4	5.8	6.5
50	5.0	5.2	5.6	6.0	6.6
55	5.1	5.4	5.7	6.1	6.8
60	5.3	5.5	5.9	6.3	7.0
65	5.4	5.7	6.0	6.4	7.1
70	5.5	5.8	6.1	6.6	7.2

- 1) For new design,  $SN_R$  can be determined from the design tables in Appendix A of Florida's flexible pavement design manual at 95% reliability level, 70 million ESALs, and 12 ksi resilient modulus. From Table A.7A:  $SN_R = 5.88$
- 2) With  $SN_R$  known, the pavement layer thickness can be calculated. Assumed AC thickness is composed of friction and structural layers. Structural coefficients of 0.44, 0.18, and 0.08 are assigned, respectively, for AC, limerock base, and subgrade layers. Since base thickness and subgrade layer is known as 8 and 12 inch, the AC thickness ( $T_{AC}$ ) is determined using the following equation:  

$$SN_R = 5.88 = (0.44 \times T_{AC}) + (0.18 \times 8) + (0.08 \times 12)$$

$$\therefore T_{AC} = 7.9 \text{ inch} \approx 8.0 \text{ inch}$$
- 3) For overlay design, the existing layer structural number ( $SN_E$ ) needs to be first determined. Since the existing AC thickness after milling is 2 inches with poor condition,  $SN_E$  is calculated as follows:  $SN_E = (0.15 \times 2) + (0.18 \times 8) + (0.08 \times 12) = 2.7$ . The structural coefficient for existing AC at poor condition is determined from Table 5.1 of the flexible pavement design manual.
- 4) The overlay thickness is calculated using the following equation:  

$$SNO = (SN_R - SN_E) / 0.44 = (5.88 - 2.7) / 0.44 = 7.2 \text{ inch.}$$

The above tables were compared to Tables G1, G2, G3, and G18 cell-to-cell.

Figures 5.14 to 5.17 show the distributions of the differences in required AC thicknesses between the M-E PDG and current FDOT thickness design tables. The difference was taken by subtracting the thickness based on the current procedure from the M-E PDG based design thickness. Therefore, negative values imply that the M-E PDG gives thinner pavements than the current FDOT flexible pavement design tables and vice versa.

The comparison for new designs showed that the thickness difference ranged from -2 to +2 inches. In terms of frequency, the required AC thickness based on M-E PDG was slightly conservative when using a limerock base modulus of 30 ksi. The change in base modulus from 30 to 45 ksi shifted the distribution of the differences with the highest frequency shifting from 1 to 0.5 inch. For overlay design, the thickness difference was slightly lower compared to new design with differences of 0 and 0.5 inch showing the highest frequency of occurrence. It should be noted that the comparisons were made assuming a base modulus of 45 ksi and 2 inches of existing AC thickness. With respect to existing

pavement condition, there was a 0.5-inch shift in the highest frequency when the existing AC structure was varied from poor to good condition.

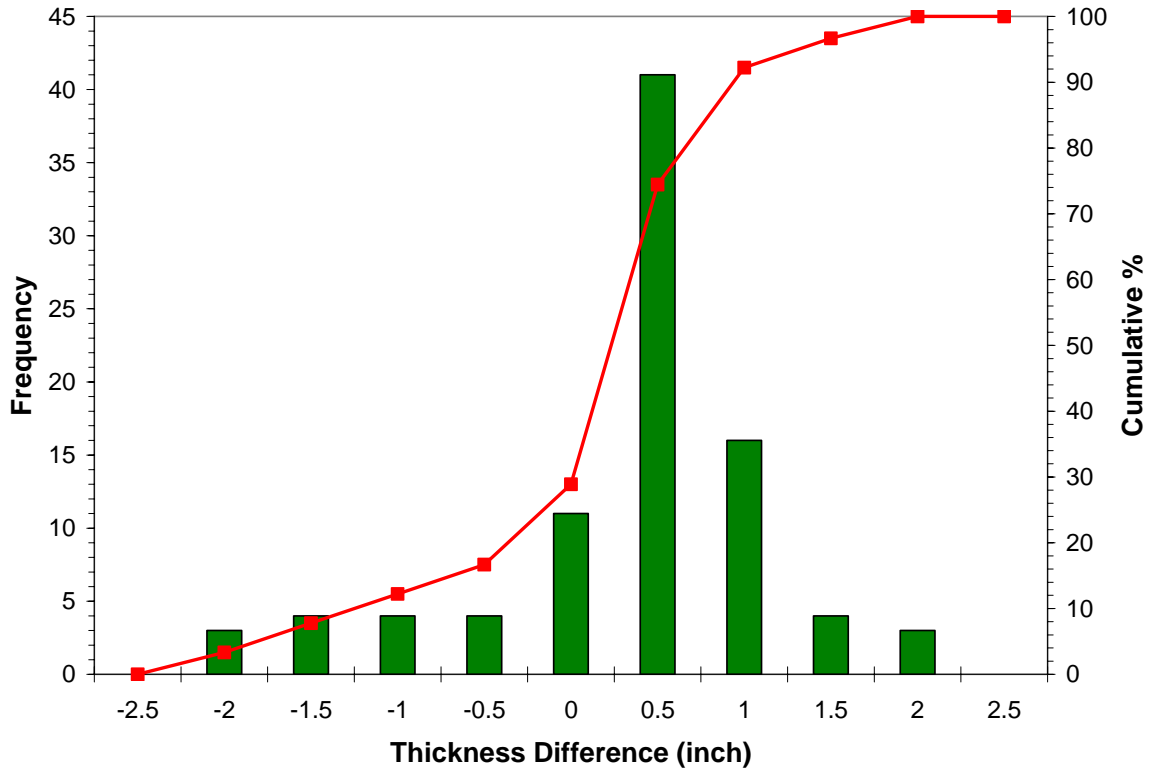


**Figure 5.14. Distribution of Thickness Differences for New Design Assuming 45 ksi Base Modulus.**

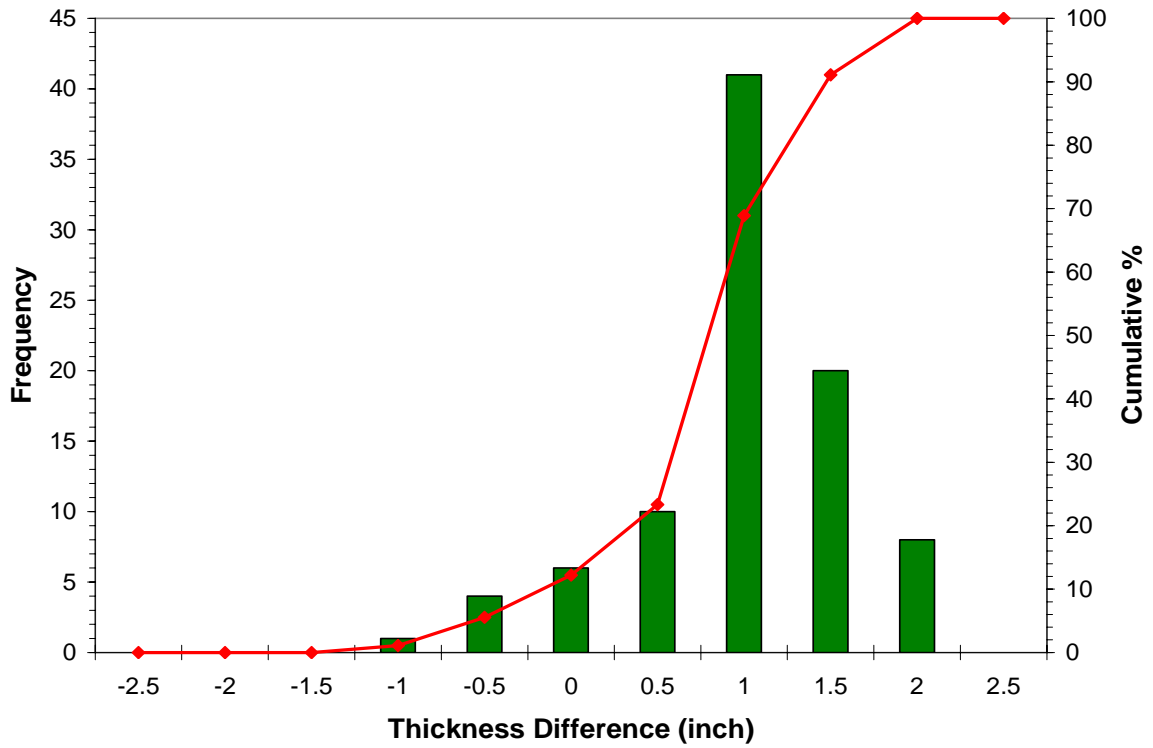


**Figure 5.15. Distribution of Thickness Differences for New Design Assuming 30 ksi Base Modulus.**

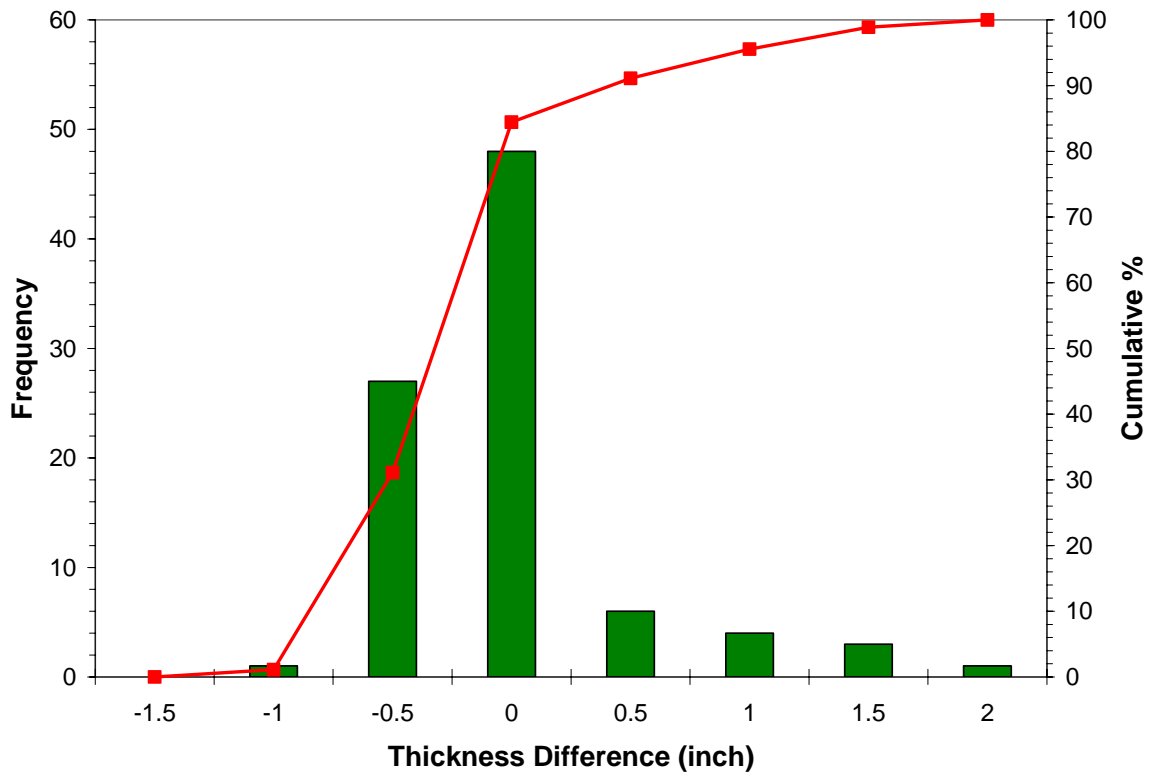


**Figure 5.16. Distribution of Thickness Differences for Overlay Design Assuming 45 ksi Base Modulus and Poor Condition of Existing AC Material.**

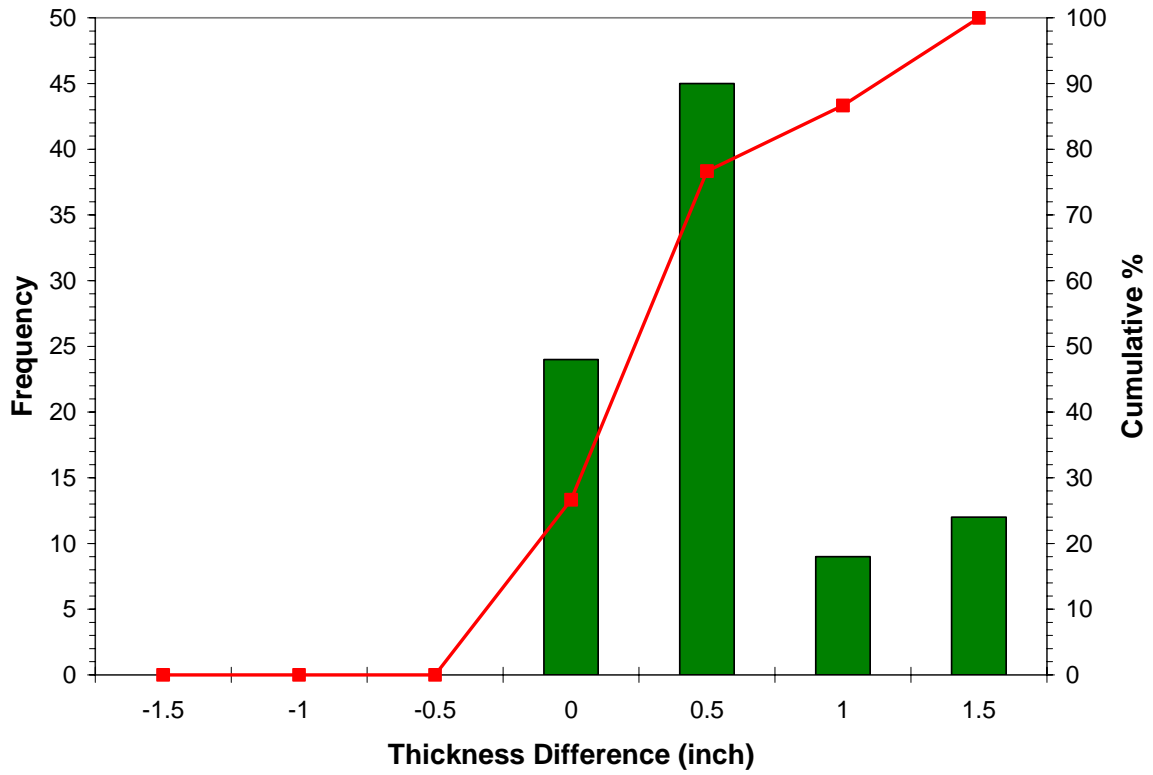


**Figure 5.17. Distribution of Thickness Differences for Overlay Design Assuming 45 ksi Base Modulus and Good Condition of Existing AC Material.**

## **CHAPTER VI. SUPPLEMENTARY RIGID PAVEMENT THICKNESS DESIGN TABLES BASED ON M-E PDG**

This chapter presents the development of new rigid pavement design tables based on the M-E PDG program. For verifying the M-E PDG rigid pavement performance prediction models, TTI researchers compiled input data on the PCC calibration sections, and ran the M-E PDG program to compare performance predictions with actual measurements of transverse cracking, faulting, and international roughness indices (IRIs) provided by the Florida DOT. After reviewing these comparisons, the decision was made to calibrate the performance prediction models for faulting and IRI in order to reduce the bias between the observed and predicted performance on the calibration sections. From results of tasks to identify a representative pavement structure, establish environmental regions tied to climatic condition, and select primary input variables for predicting performance using the M-E PDG program, researchers established two sets of design tables. The tables belonging to the first set (referred to as *Design I*) are intended to be used for most typical applications while the tables in the second set (*Design II*) are intended for design projects that require higher construction quality control of material properties directly impacting predicted pavement performance. The succeeding sections document the development of the PCC design tables.

### **VERIFICATION AND CALIBRATION OF M-E PDG PERFORMANCE MODELS**

Prior to generating the design tables, efforts were made to verify the performance predictions from the M-E PDG program. For this purpose, TTI researchers compared the M-E PDG distress predictions with corresponding FDOT pavement condition measurements on the rigid pavement calibration sections established during this implementation project. Researchers compiled input data for predicting the performance of the calibration sections and assembled measurements of transverse cracking, faulting, and IRI from pavement condition surveys conducted by the Department. Tables 6.1 to 6.3 present the observed pavement performance data, and associated traffic, materials, and pavement structure information for the PCC calibration sections. Table 6.1 presents averages of the most recent data taken within the last 2 to 3 years on each section for comparison with the M-E PDG performance predictions. Table 6.2 shows the truck traffic distributions for the different sections. It is noted that the AADTT values were estimated for the base year to accumulate the number of heavy vehicles or ESALs to the current year of service. The average CTE and

compressive strength values are given in Table 6.3. The properties tabulated were determined using data from CTE and compressive strength tests done on cores taken from the calibration sections. For the performance predictions, it is necessary to backcalculate the in-place compressive strength at the base year. For this purpose, researchers employed a PCC aging model incorporated into the M-E PDG program. This aging model was developed for estimating strength gain in terms of modulus rupture ( $MR$ ) and is given by:

$$MR(t) = (1 + \log(t / 0.0767) - 0.01566 * \log(t / 0.0767)^2) * MR_{28\text{-day}} \quad (7.1)$$

where  $t$  is the pavement age in years. In addition, the M-E PDG program uses equation (7.2) to estimate the compressive strength  $f'_c$  from  $MR$ .

$$f'_c = (MR / 9.5)^2 \text{ in } \textit{psi} \quad (7.2)$$

By substituting equation (7.2) to (7.1), the compressive strength at 28 days can be estimated as follows:

$$f'_{c28\text{-day}} = f'_c(t) / [1 + \log(t / 0.0767) - 0.01566 * \log(t / 0.0767)^2]^2 \quad (7.3)$$

The estimated 28-day compressive strengths are tabulated in Table 6.3. The average 28-day compressive strength was found to be 3800 psi, which is between the specified minimum strength of 3000 psi for pavements based on the FDOT standard specifications, and a compressive strength of about 4350 psi corresponding to the standard concrete design modulus of 4,000,000 psi given in the FDOT rigid pavement design manual (2006).

It should be noted that no consideration was given on the effect of aging on CTE due to absence of published data on this factor. The remaining data in Table 6.3 on PCC thickness, joint spacing, dowel diameter, slab width, and underlying materials were established on the basis of coring and FWD data.

Given the data in Tables 6.1 to 6.3, researchers used the existing performance models in the M-E PDG program to predict the performance of the calibration sections, and compared the performance predictions with the corresponding measured values. These comparisons showed that the M-E PDG program underestimated the measured IRIs and faulting on the calibration sections as shown in Figures 6.1 to 6.3. To correct this bias, the decision was made to calibrate the M-E PDG faulting and IRI models using the observed performance data on the rigid pavement sections. Researchers later used these calibrated models to develop the design tables. With respect to the cracking model, no calibrations were deemed necessary so the original model was used in the development work.

**Table 6.1. Compiled Pavement Performance Data on Calibration Sections.**

<b>County</b>	<b>ID</b>	<b>Section Limit (mile)</b>	<b>Base Year</b>	<b>Transverse Crack (%)</b>	<b>IRI (inch/mile)</b>	<b>Faulting (inch)</b>
Charlotte	10100000	@ 3.092 and 2.563	1978	20.0	123	0.128
Polk	16100000	0.46 ~ 1.74	1970	30.38	124.50	0.16
Hillsborough	10250001	0.0 ~ 1.102	2006	0.26	47.00	0.01
Hillsborough	10075000A	19.0 ~ 20.4	1987	0.43	116.50	0.03
Hillsborough	10075000B	23.4 ~ 24.69	1987	2.24	151.67	0.03
Pinellas	15003000A	0.37 ~ 1.29	1986	18.97	132.67	0.03
Pinellas	15003000B	1.29 ~ 0.37	1986	19.54	148.00	0.03
Pinellas	15190000A	2.287 ~ 4.44	1987	11.60	77.67	0.01
Pinellas	15190000B	4.44 ~ 2.287	1987	12.30	71.67	0.02
St. Johns	78020000	0.7 ~ 0.02	1955	16.50	160.67	0.10
Gadsden	123811	200 and 400 ft (LTPP)	1976	90.40	221.76	0.14
Lake	11020000	14.03 ~ 14.12	1978	0.00	117.00	0.01
Dade	87030000A	8.83 ~ 10.0	1959	16.40	110.33	0.01
Dade	87030000B	10.0 ~ 8.83	1959	12.02	98.67	0.01
Dade	87270000	0.0 ~ 0.98	1963	4.90	112.67	0.01
Dade	87061000	0.21 ~ 0.0	1991	6.45	219.00	0.01

**Table 6.2. Compiled Traffic Data on Calibration Sections.**

<b>ID</b>	<b>Base Year</b>	<b>AADTT</b>	<b>Growth (%)</b>	<b>Class 4 (%)</b>	<b>Class 5 (%)</b>	<b>Class 6 (%)</b>	<b>Class 7 (%)</b>	<b>Class 8 (%)</b>	<b>Class 9 (%)</b>	<b>Class 10 (%)</b>	<b>Class 11 (%)</b>	<b>Class 12 (%)</b>	<b>Class 13 (%)</b>
10100000	1978	203	7.3	2.2	46.8	15.5	8.2	13.2	13.1	0.3	0.3	0.1	0.1
16100000	1970	1109	-0.5	1.6	26	10.5	1.2	10.3	47.8	0.4	0.3	0.1	1.8
10250001	2006	3382	5.0	2.9	22.7	19.6	3.8	6	38	2.6	0	0	4.4
10075000A	1987	3620	6.1	9.7	60.7	0.1	0.1	24.4	2.2	1	1.3	0	0.4
10075000B	1987	5587	3.2	10	38.3	15.7	2.3	16.9	6.3	3.9	0.9	0.3	5.4
15003000A	1986	288	4.7	16	48.3	10	3.1	8.9	7.6	5.2	0.1	0	0.7
15003000B	1986	288	4.7	16	48.3	10	3.1	8.9	7.6	5.2	0.1	0	0.7
15190000A	1987	2091	4.6	13	24.8	6.9	0.9	41.3	9.7	3.2	0.2	0	0.1
15190000B	1987	2091	4.6	13	24.8	6.9	0.9	41.3	9.7	3.2	0.2	0	0.1
78020000	1955	684	1.8	2	37.3	34.8	0.4	13.2	11.1	0.4	0.4	0.3	0.1
123811	1976	3090	0.9	1.2	14.3	3.2	0.5	22.4	55	0.8	1.6	0.7	0.2
11020000	1978	146	8.2	9.3	19.2	20.4	1.3	10.5	32	6.2	0.2	0.2	0.7
87030000A	1959	306	2.3	17	58.5	10.1	0	11.6	2.8	0	0	0	0
87030000B	1959	306	2.3	17	58.5	10.1	0	11.6	2.8	0	0	0	0
87270000	1963	3897	1.6	3.6	36.5	7.2	0.7	14.4	36.6	0.5	0.4	0.1	0.1
87061000	1991	968	1.6	4.2	9.6	10.8	0.8	1.2	63.7	6.8	0	0	3

**Table 6.3. Compiled Material and Structural Data on Calibration Sections.**

ID	Slab Thickness (inches)	CTE (microstrain/°F)	Lab.Comp. Strength (psi)	28 day_Comp. Strength(psi)	Joint (feet)	Dowel dia. (inches)	Slab width (feet)	Base	Subgrade	Embankment
10100000	12.0*	5.64	2604	1793*	15	N/A	12	-	12" A-2-4 (24)**	A-3 (17.5)
16100000	9.0	4.74	6049	4137	20	1.25	12	12" A-1-B (40)	12" A-1-B (40)	A-2-4 (14)
10250001	12.5	4.72	5485	4417	15	1.375	12	4" AC (2000)	12" A-2-4 (16)	A-2-4 (14)
10075000A	13.5	4.91	5615	3909	15	1.25	14	12" A-1-B (40)	8" A-3 (24)	A-2-4 (15.5)
10075000B	12.5	5.18	4978	3465	15	1.25	12	7" Econ (1854)	12" A-2-4 (15.5)	A-2-4 (15.5)
15003000A	9.5	4.89	5177	3599	20	1.25	12	7" Econ (1600)	12" A-3 (14.6)	A-3 (14)
15003000B	9.5	5.00	4952	3442	20	1.25	12	7" Econ (1516)	12" A-3 (14.6)	A-3 (14)
15190000A	9.5	4.81	4728	3292	20	1.25	12	7" Econ (1769)	12" A-3 (14.6)	A-3 (14)
15190000B	9.5	4.80	5743	3998	20	1.25	12	7" Econ (1542)	12" A-3 (14.6)	A-3 (14)
78020000	8.0	4.48	6965	4724	20	1.0	12	12" A-1-B (40)	20" A-2-4 (37.5)	A-2-4 (14.6)
123811	9.5	5.06	5300	3852	20	N/A	12	6.5" Soil Cement (40)	17" A-2-4 (32)	A-2-4 (15)
11020000	12.5	4.56	4508	3103	18	1.25	12	4" Econ (2000)	12" A-2-4 (28)	A-3 (14)
87030000A	8.5	5.57	5669	3852	15	1.0	12	12" A-1-B (40)	10" A-3 (40)	A-2-4 (17.5)
87030000B	8.5	5.42	6014	4087	15	1.0	12	12" A-1-B (40)	10" A-3 (40)	A-2-4 (17.5)
87270000	9.0	5.23	5728	3900	18	1.25	12	12" A-1-B (40)	16" A-3 (40)	A-2-4 (17.5)
87061000	12.0	4.72	5226	3665	18	1.25	12	12" A-1-B (40)	15" A-3 (30)	A-2-4 (15.5)

\* Composite value (PCC + Econcrete)

\*\*Resilient modulus in ksi

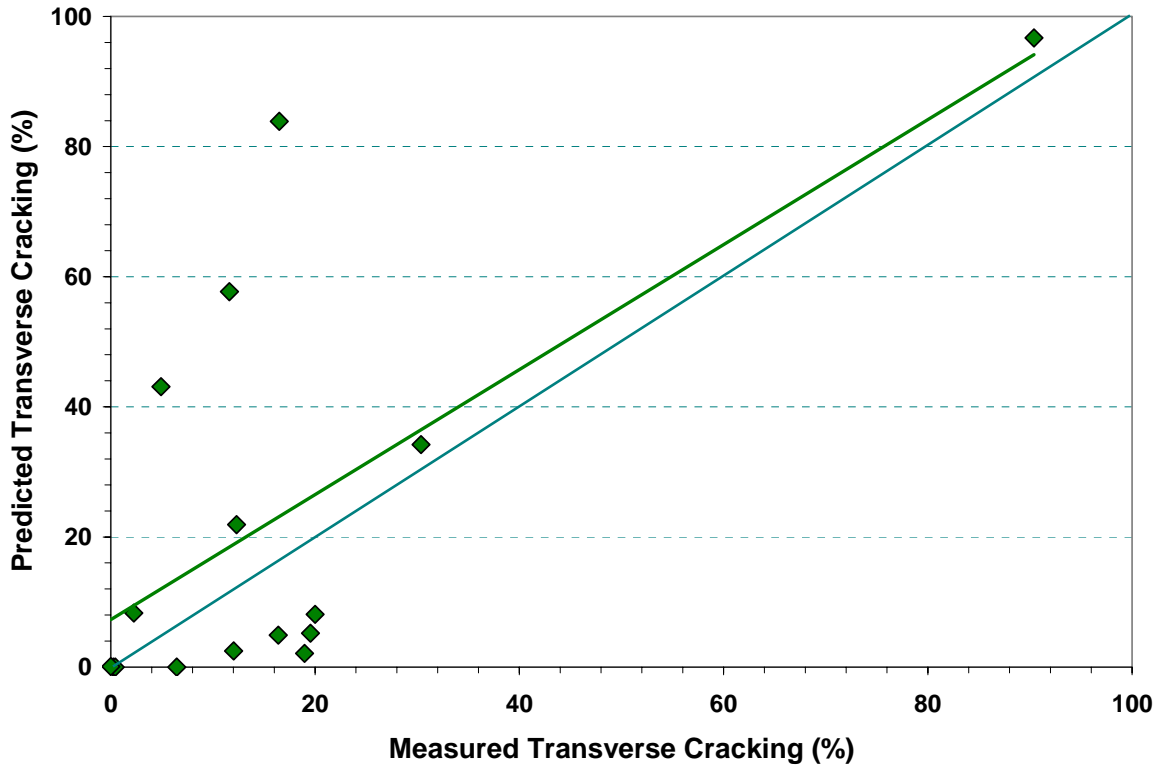


Figure 6.1. Comparison of Predicted and Measured Transverse Cracking.

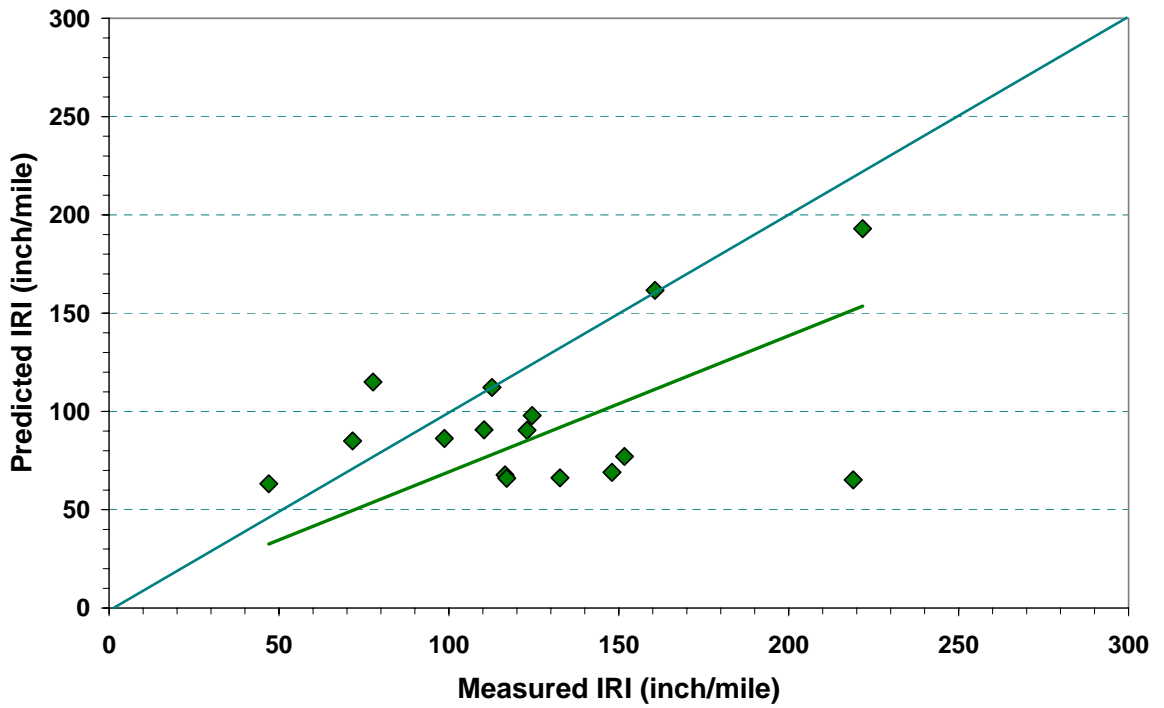
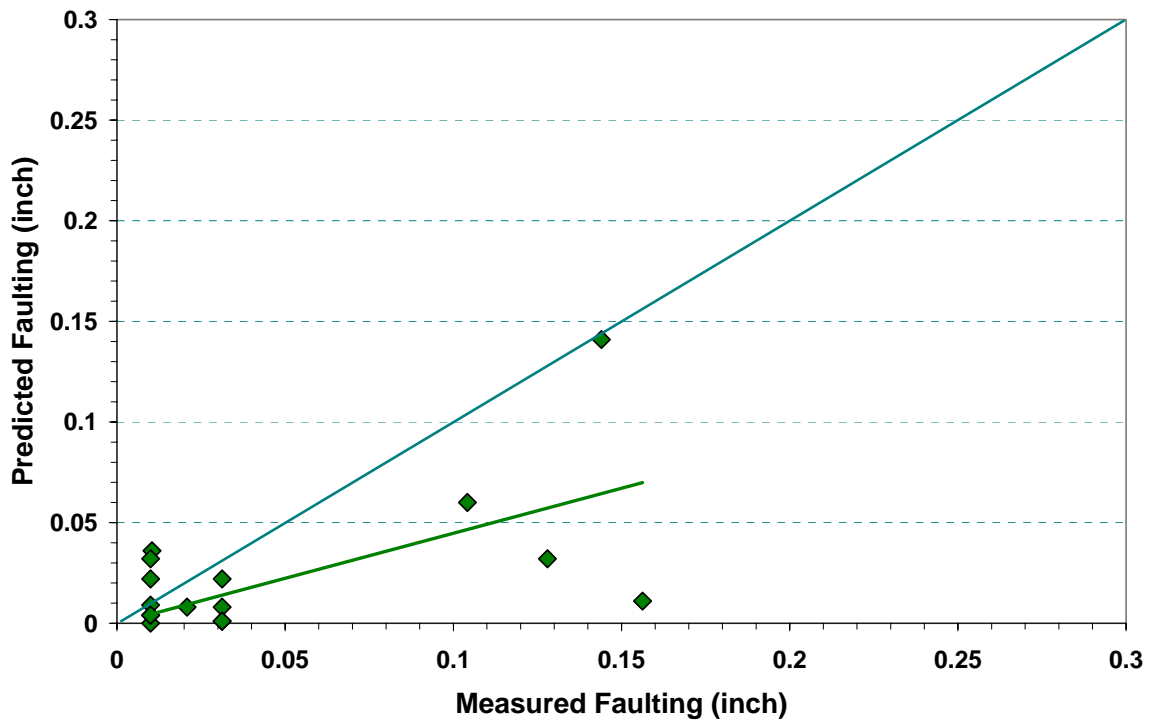


Figure 6.2. Comparison of Predicted and Measured IRI.



**Figure 6.3. Comparison of Predicted and Measured Faulting.**

To calibrate the IRI and faulting models, an investigation was conducted to identify the calibration factors that are critical to predicting these pavement condition indicators. There are 8 coefficients controlling the faulting predictions and 4 coefficients for the IRI model as shown in Figures 6.4 and 6.5. The national calibration factors were regarded as the base or reference values. Researchers then varied each factor  $\pm 40$  percent to determine the sensitivity of the performance predictions to each calibration factor. Note that the percent of cracked slabs and amount of faulting are predicted independently in the pavement design program. Thus, changes in the calibration factors for percent of cracked slabs do not affect the predictions of faulting and vice-versa. However, IRI is calculated as a function of faulting, cracking, and the site factor. Thus, the IRI predictions vary with changes in the calibration factors of the other two rigid pavement distresses predicted in the M-E PDG program. As presented in Table 6.4, researchers found that the faulting coefficients C1 and C6 significantly influenced the faulting and IRI predictions from the M-E PDG program.

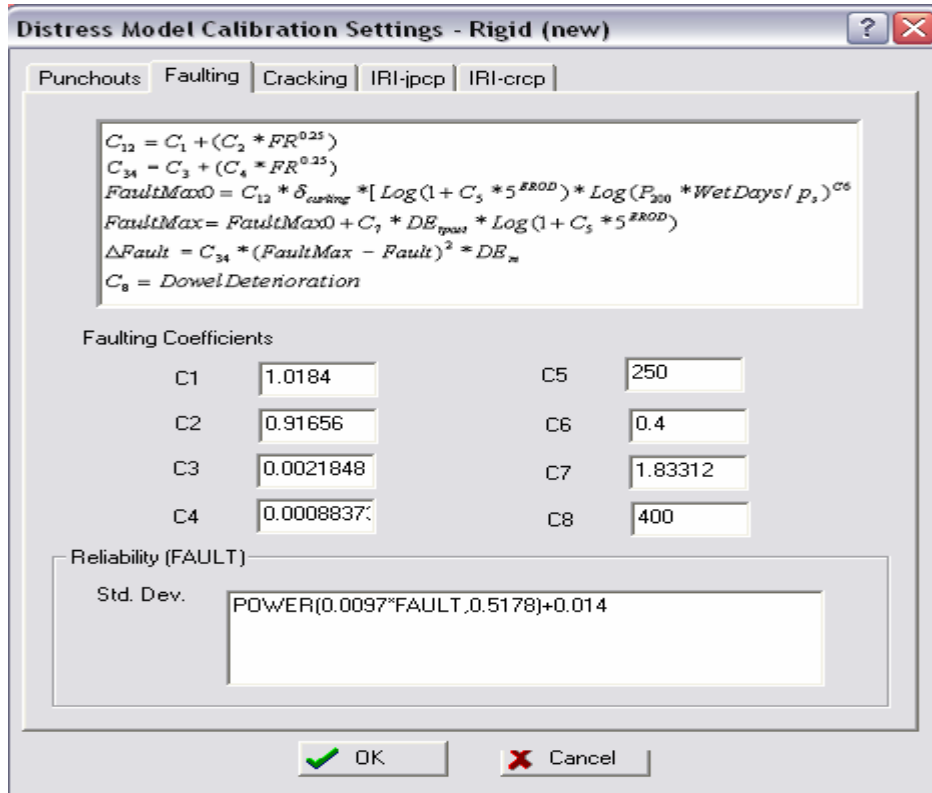


Figure 6.4. M-E PDG Screen of Faulting Model Calibration Settings.

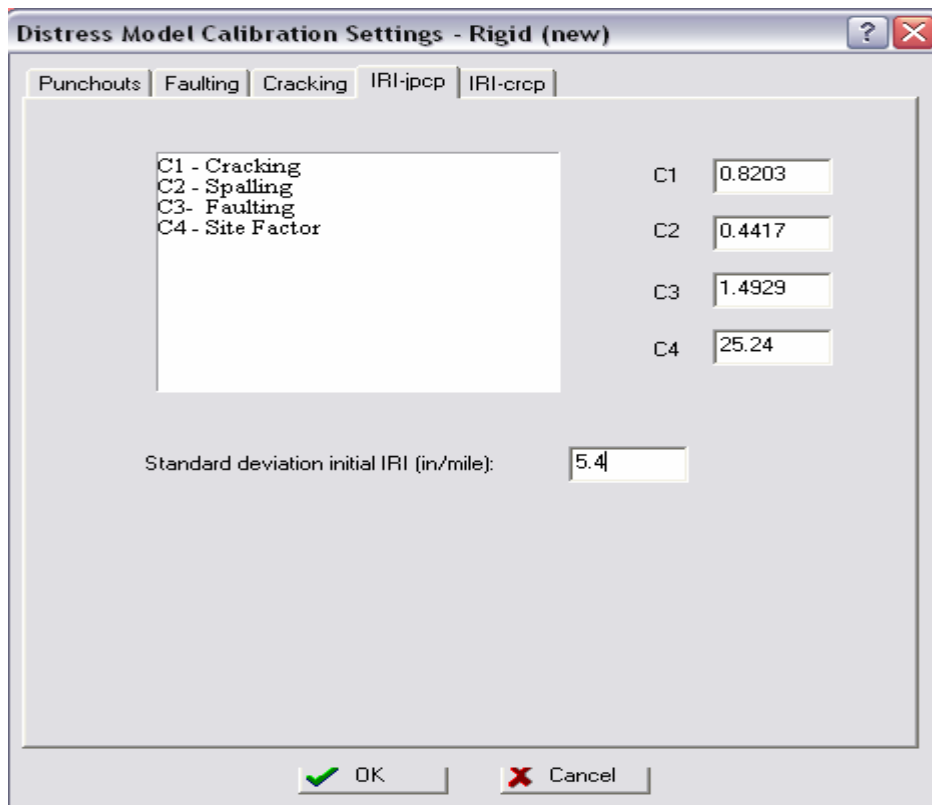


Figure 6.5. M-E PDG Screen of IRI Model Calibration Settings.

**Table 6.4. Sensitivity of Calibration Factors in Faulting Model.**

Run No.	Condition	Faulting (inch)	Crack (%)	IRI (inch/mile)	% of change in faulting	Sensitivity
1	Reference	0.056	35.3	141.7	–	–
2	C1+40	0.086	35.3	163.1	53.5	<b>H</b>
3	C1-40	0.028	35.3	122.6	-50	<b>H</b>
4	C2+40	0.056	35.3	141.7	0	L
5	C2-40	0.056	35.3	141.7	0	L
6	C3+40	0.064	35.3	147.7	14.2	M
7	C3-40	0.042	35.3	132.5	-25	M
8	C4+40	0.056	35.3	141.7	0	L
9	C4-40	0.056	35.3	141.7	0	L
10	C5+40	0.057	35.3	142.5	1.7	L
11	C5-40	0.054	35.3	140.6	-3.5	L
12	C6+40	0.082	35.3	160.1	46.4	<b>H</b>
13	C6-40	0.037	35.3	128.8	-33.9	<b>H</b>
14	C7+40	0.059	35.3	144.2	5.3	L
15	C7-40	0.052	35.3	139.4	-7.1	L
16	C8+40	0.056	35.3	141.7	0	L
17	C8-40	0.055	35.3	141.7	-1.7	L

Based on this finding, researchers calibrated the faulting model to change the coefficient C1 from 1.0184 to 2.0 after calibration. For the IRI model, the coefficient C3 was changed from 1.4929 to 2.5. Figures 6.6 to 6.7 show the results of the calibrations on the faulting and IRI predictions on the rigid pavement test sections. Although a relatively high scatter is observed in each plot, the data points for IRI and faulting are observed to be more evenly distributed around the line of equality after calibration, illustrating the reduction in bias from the original predictions based on the national calibration factors.

Researchers note that an unbonded slab-base interface was assumed in the local calibrations conducted in this project. This assumption is based on published documentation from NCHRP 1-37A. It is noted that in Part 3, Chapter IV (Rigid Design) of the NCHRP 1-37A documentation (ARA, 2004), the developers of the guide did not recommend specifying a debonding age greater than 5 years. In addition, Appendix FF (ARA, 2003) of the original documentation showed that for the Florida calibration sections, the developers of the guide assumed unbonded condition for all but one section in the original calibration, and that for the one section where a bonded interface was used, a bonding age of 12 months was used in the original calibration.

It is noted that the bonding condition is not known at the time of pavement design. Even the original documentation recognized that the effects of environmental and traffic

loading will tend to weaken the bond at the slab-base interface over time and that the bonded-interface assumption over the entire design period may be unconservative. Thus, researchers assumed an unbonded slab-base interface for the local calibrations done in this project.

### ESTABLISHING RIGID PAVEMENT DESIGN TABLES

Using the calibrated performance models, researchers generated the design tables for rigid pavements using the M-E PDG program. Prior to generating the tables, researchers selected the performance criteria on cracking, faulting, and IRI based on reviewing performance data and discussions with the project manager. Preliminary tasks to select a representative PCC pavement structure and establish climatic regions were also conducted. In addition, researchers conducted sensitivity analyses based on version 1.0 (after calibration of the IRI and faulting models) to determine the critical variables that should be considered in generating the thickness design tables.

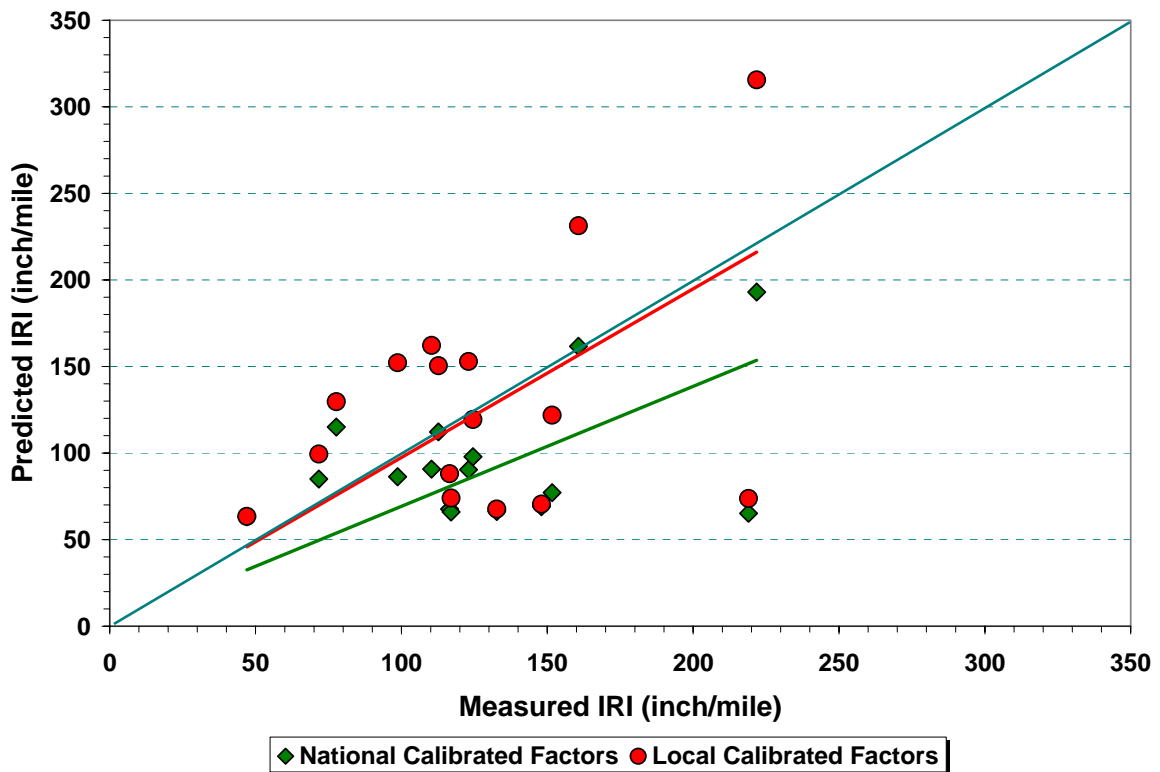
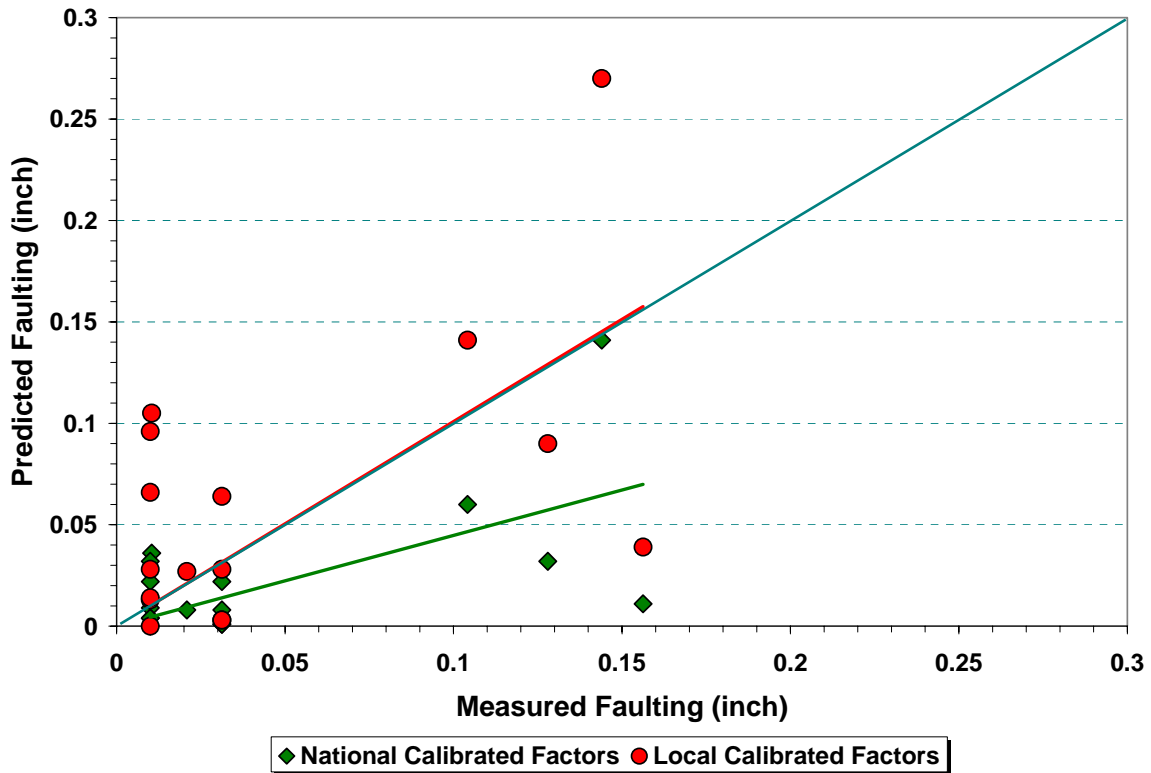


Figure 6.6. Comparison of Measured and Predicted IRIs after Calibration.



**Figure 6.7. Comparison of Measured and Predicted Faulting after Calibration.**

### Selection of Performance Criteria

To establish design thresholds for cracking, faulting, and IRI, researchers examined the pavement condition data on the rigid pavement calibration sections. From this examination, design criteria for cracking and IRI were selected to correspond to the critical pavement rating score that FDOT uses to identify deficient pavement sections. However, no definite relationships were observed between faulting and crack rating, or between faulting and ride rating. Thus, researchers reviewed other on-going M-E PDG implementation efforts to see what performance thresholds are being used. In this regard, the implementation of the M-E PDG in California (Kannekanti and Harvey, 2006) provided criteria that researchers considered in developing the design tables. Based on this review and the evaluation of pavement condition data on the rigid pavement calibration sections, the decision was made to use the following criteria for determining acceptable pavement designs:

- Transverse cracking: 10 percent slabs cracked (based on the California implementation project documented by Kannekanti and Harvey, 2006)
- Faulting: 0.12 inches

- IRI: initial IRI of 58 inch/mile to reflect the current FDOT practice of grinding rigid pavements after placement, and a terminal IRI of 180 inch/mile corresponding to a Ride Number of 2.5 based on the relationship between IRI and Ride Number reported by Fernando, Oh, and Ryu (2007).

In generating the design tables, the performance predictions from the M-E PDG program were checked against the above criteria to determine if a given pavement design passes or fails. For this purpose, a 20-year design life was used, following the current rigid pavement design tables implemented by the Department. In addition, per recommendation of the FDOT project manager, a 0.25-inch thickness allowance was used in generating the design tables. In this way, if a given trial design fails to meet any of the specified performance criteria but does so if the slab thickness is incremented by 0.25 inches, the trial design with the original slab thickness (prior to the 0.25-inch thickness increment) is accepted.

### **Investigation of Rigid Pavement Cross-Sections**

Researchers analyzed the rigid pavement structures shown in Figure 6.8 and compared the required slab thicknesses determined from the M-E PDG program. This analysis showed that, among the pavement cross-sections shown, structure 3 yielded up to 0.5-inch thicker slabs than the other pavement cross-sections, for the range of climatic and soil conditions considered in the analysis. Thus, the decision was made to use rigid pavement structure 3 to generate the design tables for jointed plain concrete pavements using the M-E PDG program.

In practice, the engineer uses the PCC design tables developed in this project to get the required slab thickness. The engineer will then select one of the 5 cross-sections shown in Figure 6.8 to determine the particular pavement cross-section for his/her design.

### **Consideration of Environmental Effects**

To consider the effect of climatic variations in the rigid pavement design method, researchers first identified representative city locations (in terms of longitude, latitude, and elevation) for the different counties comprising Florida. Given these cities, researchers used the climatic data base included with the M-E PDG program to characterize the climatic conditions per county. For each location, the M-E PDG program identifies the six closest weather stations from which the user may select any number of stations to interpolate the

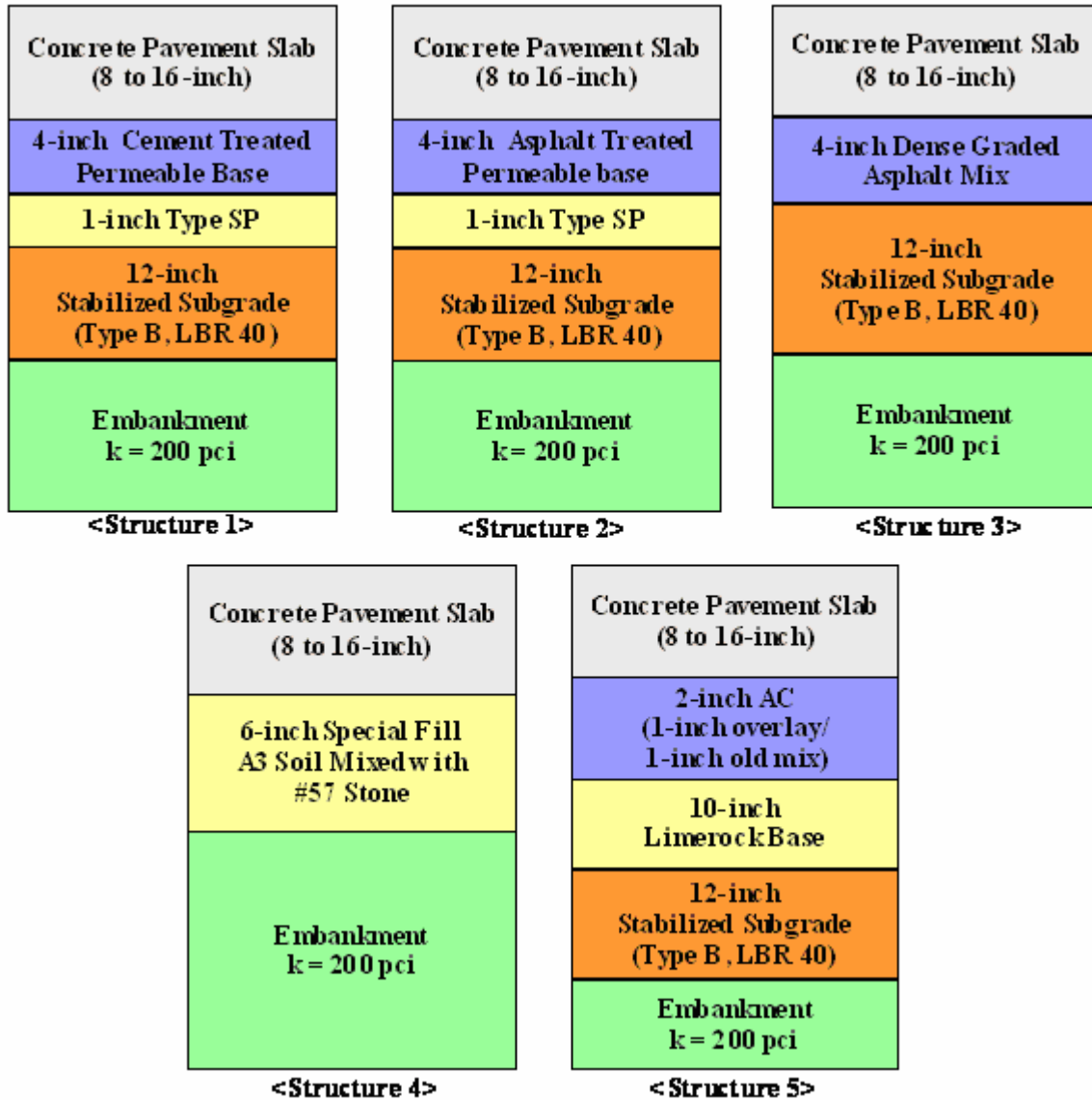


**Figure 6.8. Rigid Pavement Cross-Sections Analyzed for Developing Design Tables.**

climatic data at the location of interest. During this task, researchers noted that the required slab thickness might vary depending on the weather stations selected for the interpolation. Researchers examined the weather station data for these cases, and where anomalies were found, that weather station was not selected in characterizing the climatic conditions for the given county. These weather stations are Marathon, Tampa International Airport, Miami International Airport, and Daytona International Airport.

Figure 6.9 illustrates the variation of design slab thicknesses due to differences in environmental conditions. Researchers used the M-E PDG program to generate the map shown under the following assumptions:

- Projected cumulative ESALs of 50 million
- Vehicle class distribution: Default values in M-E PDG for TTC 1
- Reliability level: 90 %
- Coefficient of thermal expansion of 6.0 microstrain per °F
- 28-day compressive strength: 4000 psi
- Slab width: 13 feet with tied shoulder
- Joint spacing: 15 feet
- Subgrade modulus of reaction: 200 pci
- Initial IRI: 58 inch/mile

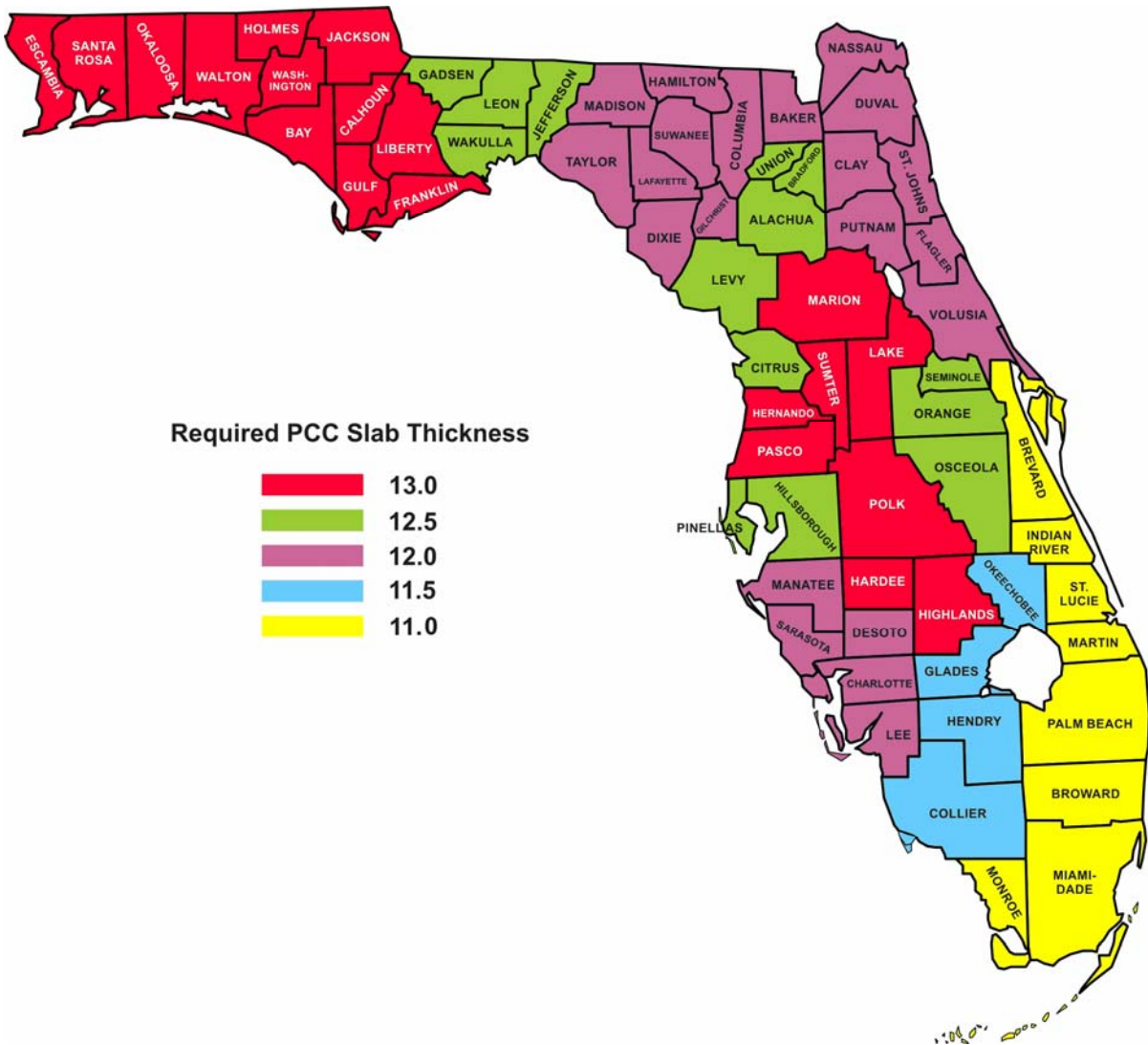
The thickness design map illustrated in Figure 6.9 was generated by running the M-E PDG program on each county in Florida. To reduce software run time, a 12-inch thick slab was initially assumed. Depending on whether or not this initial design met the given criteria for transverse cracking, faulting, and IRI, researchers varied the slab thickness in 0.5-inch increments to determine the design slab thickness. From the numerous runs made, transverse cracking was observed to be the most predominant failure mode that governed the required slab thickness for the design assumptions used.

Figure 6.9 shows the subdivision of the state into five different regions, with design slab thicknesses varying from 11 to 13 inches. Table 6.5 shows the list of counties for each of these five regions. The environmental data compiled for the different regions were used to determine design slab thicknesses with the M-E PDG program.

### **Selection of Design Variables**

The results from the sensitivity analyses presented in Chapter IV showed that the resilient modulus of the underlying materials had minimal influence on the pavement performance predictions. In view of the program update from version 0.9 to 1.0, and the local calibrations of the IRI and faulting models, researchers verified the sensitivity of the performance predictions to the following design variables:

- CTE
- Compressive strength
- Traffic (AADTT, ESALs)
- Slab width
- Subgrade modulus of reaction k-value



**Figure 6.9. Map of Required PCC Slab Thickness at 90% reliability and  $50 \times 10^6$  Cumulative ESALs.**

**Table 6.5. List of Counties for the Different Thickness Regions.**

Region	County No.	County Name	Representative Location for Weather Data
1	46	Bay	Panama city
1	47	Calhoun	Blountstown
1	48	Escambia	Pensacola
1	49	Franklin	Apalachicola
1	51	Gulf	Port. St. Joe
1	6	Hardee	Wauchula
1	8	Hernando	Brooksville
1	9	Highlands	Sebring
1	52	Holmes	Bonifay
1	53	Jackson	Marianna
1	11	Lake	Leesburg
1	56	Liberty	Bristol
1	36	Marion	Ocala
1	57	Okaloosa	Crestview/Destin
1	14	Pasco	Zephyrhills
1	16	Polk	Winter haven
1	58	Santa Rosa	Milton
1	18	Sumter	Wildwood
1	60	Walton	De Funiak Sprs.
1	61	Washington	Chipley
2	26	Alachua	Gainesville
2	28	Bradford	Starke
2	2	Citrus	Inverness
2	50	Gadsden	Quincy
2	10	Hillsborough	Tampa
2	54	Jefferson	Monticello
2	55	Leon	Tallahassee
2	34	Levy	Chiefland
2	35	Madison	Madison
2	75	Orange	Orlando
2	92	Osceola	St. Cloud
2	5	Pinellas	St. Petersburg
2	77	Seminole	Oviedo
2	39	Union	Lake Butler
2	59	Wakulla	Wakulla
3	27	Baker	MacClenny
3	1	Charlotte	Punta Gorda
3	71	Clay	Green Cove Springs
3	29	Columbia	Lake City
3	4	De Soto	Arcadia
3	30	Dixie	Cross City
3	72	Duval	Jacksonville
3	73	Flagler	Bunnell

**Table 6.5. List of Counties for the Different Thickness Regions (continued).**

Region	County No.	County Name	Representative Location for Weather Data
3	31	Gilchrist	Trenton
3	32	Hamilton	Jasper
3	33	Lafayette	Mayo
3	12	Lee	Fort Myers
3	13	Manatee	Ellenton
3	74	Nassau	Hillard
3	76	Putnam	Palatka
3	78	St. Johns	St. Augustine
3	17	Sarasota	Sarasota/Bradenton
3	37	Suwannee	Live Oak
3	38	Taylor	Perry
3	79	Volusia	Daytona beach
4	3	Collier	Naples
4	5	Glades	Moore Haven
4	7	Hendry	La Belle
4	91	Okeechobee	Okeechobee
5	70	Brevard	Melbourne
5	86	Broward	Fort Lauderdale, Hollywood
5	87	Dade	Miami
5	88	Indian River	Vero beach
5	89	Martin	Stuart
5	90	Monroe	Keywest, Marathon, Flamingo
5	93	Palm Beach	West Palm beach
5	94	St. Lucie	Fort Pierce

For this verification, researchers assumed a pavement structure consisting of a 12-inch slab, 4-inch dense graded asphalt mix, 12-inch mechanically stabilized subgrade, and sandy soil embankment. This pavement structure is considered typical of Florida rigid pavements. Figures 6.10 to 6.14 illustrate the sensitivity of the transverse cracking predictions to the design factors that were varied in the sensitivity analyses. The performance predictions are for a 20-year design life with 50 million cumulative 18-kip ESALs.

The impact of CTE and compressive strength on transverse cracking predictions is highly significant. Higher CTE and lower compressive strength yield to more transverse cracking. Based on the review of laboratory test results and FDOT material specifications, discussions with FDOT engineers, and comments from industry representatives, two levels of CTE (5.75 and 6.0  $\mu\epsilon/^\circ\text{F}$ ), and two levels of compressive strength (4000 and 4500 psi) were selected for generating the final set of design tables based on the M-E PDG program.

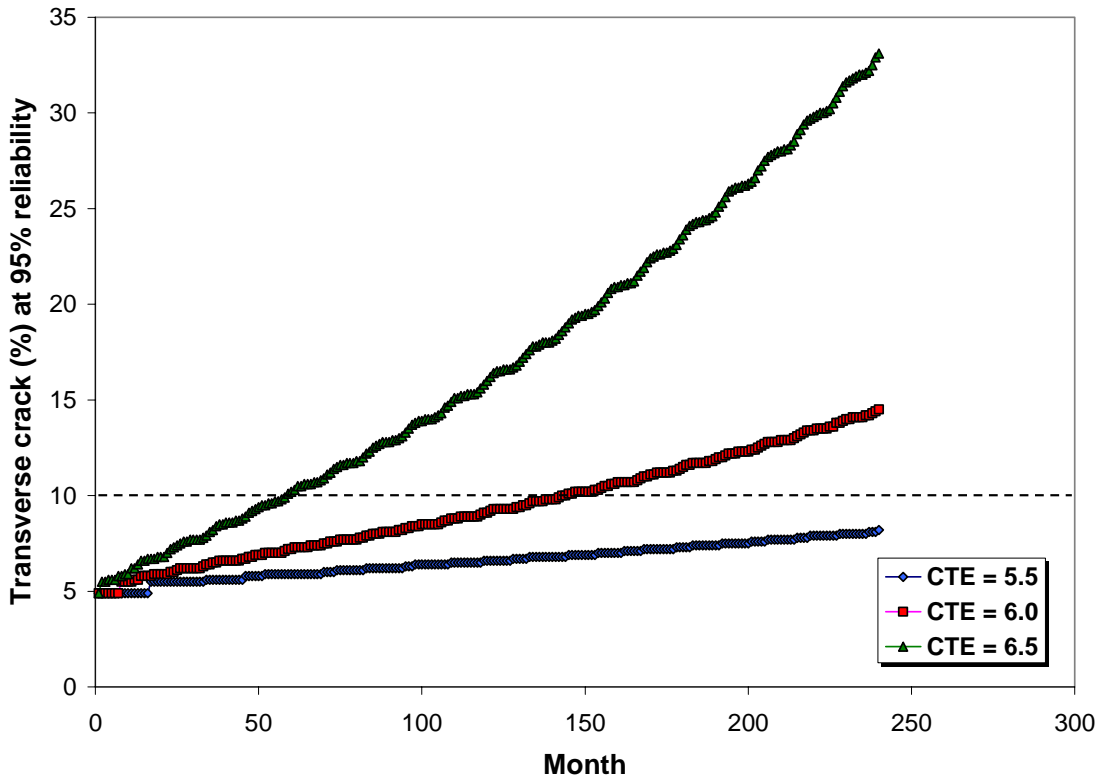


Figure 6.10. Sensitivity of Transverse Cracking Predictions to CTE.

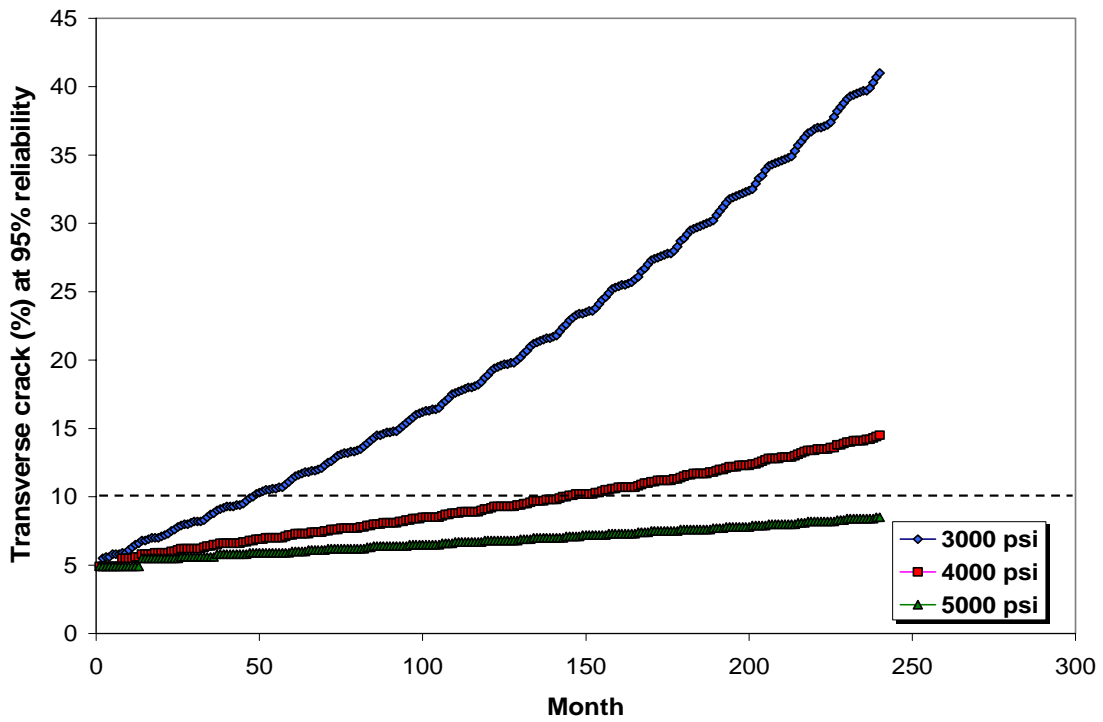


Figure 6.11. Sensitivity of Transverse Cracking Predictions to Compressive Strength.

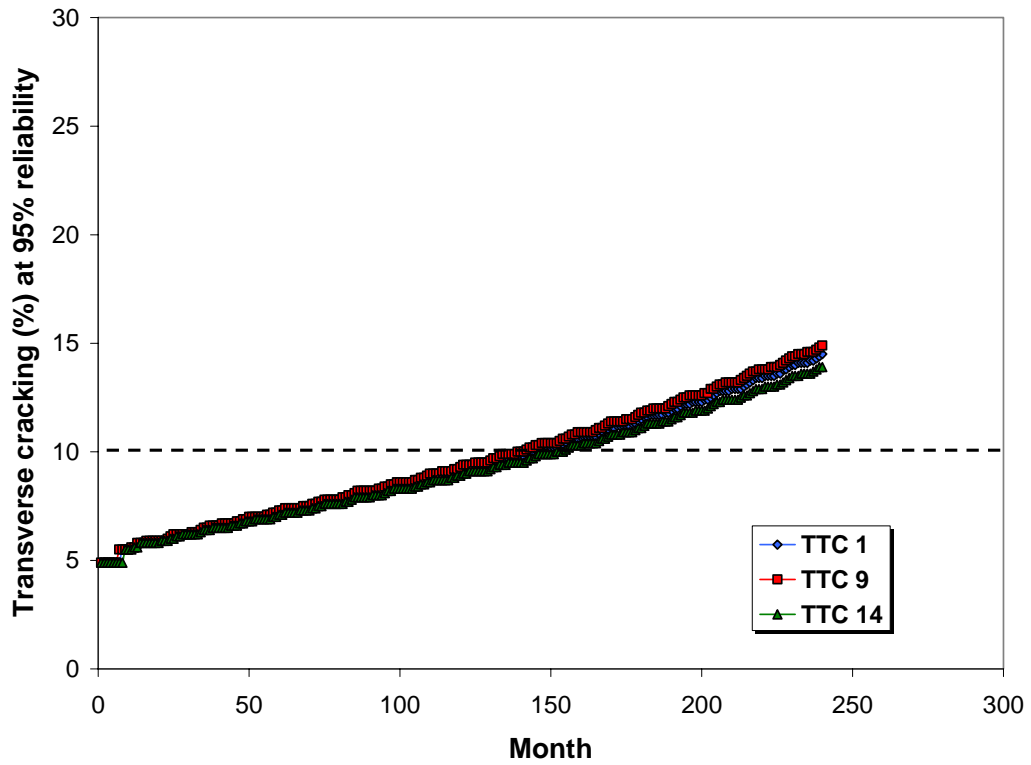


Figure 6.12. Sensitivity of Transverse Cracking Predictions to the TTC.

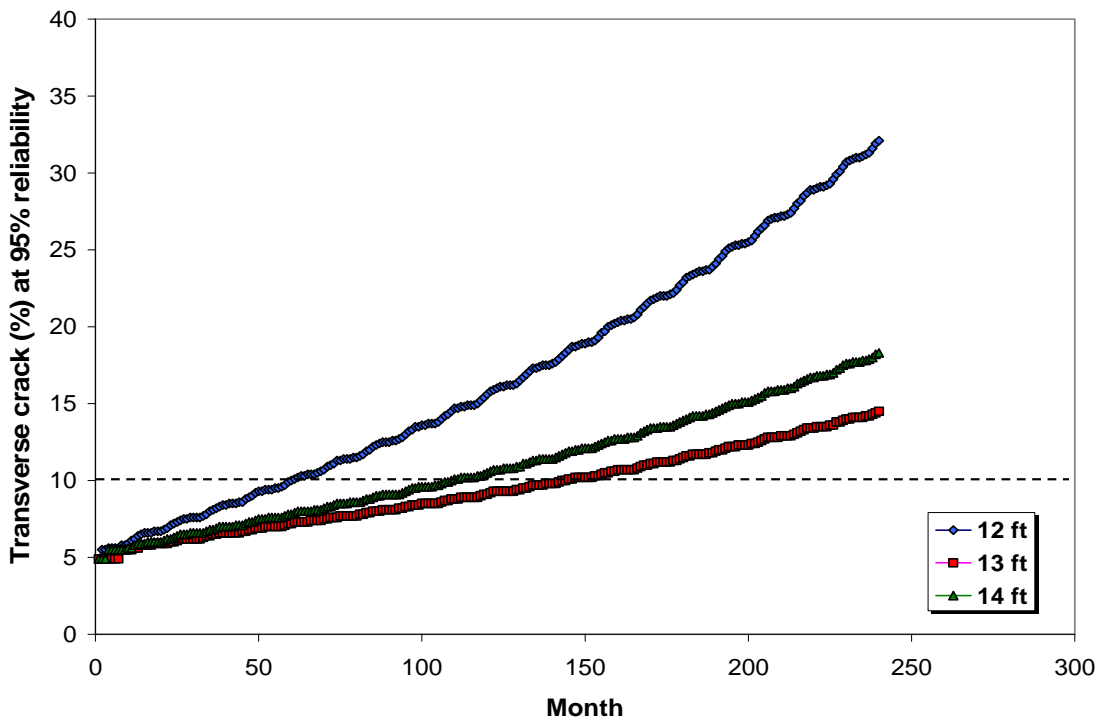
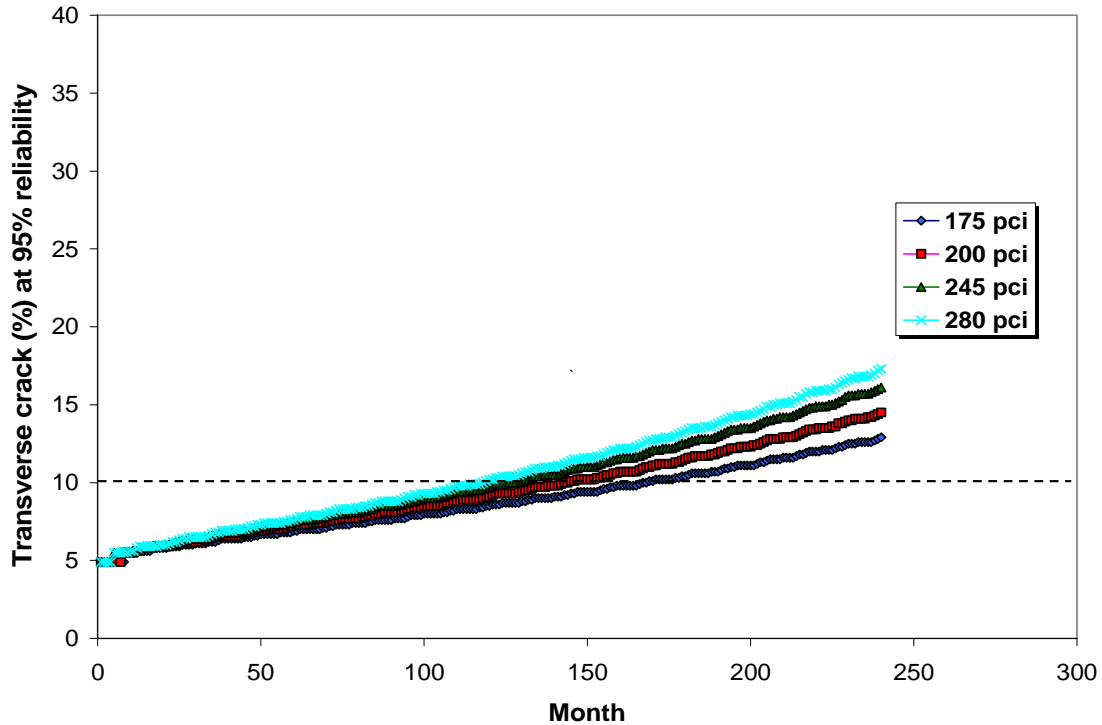


Figure 6.13. Sensitivity of Transverse Cracking Predictions to Slab Width.



**Figure 6.14. Sensitivity of Transverse Cracking Predictions to Subgrade Modulus of Reaction.**

Slab widths from 12 to 14 feet were considered to check the sensitivity to transverse cracking. This investigation identified a 13 feet wide slab (with tied shoulder) as being optimal in terms of resulting in the least amount of transverse cracking. Thus, the design tables were generated based on this slab width and assuming a tied shoulder. Similar to the finding that ESALs are critical in terms of determining the required AC thickness, researchers found that the predicted transverse cracking was not significantly affected by the TTC when the AADTT is varied to provide the same number of cumulative ESALs for the different TTCs assumed in the analyses. Since the ESAL was determined to be a useful index for quantifying the joint effects of truck traffic and axle load distributions, the decision was made to generate the design tables as a function of cumulative 18-kip ESALs, similar to the format of the current FDOT rigid pavement design tables. For this purpose, researchers used TTC 1 to characterize the vehicle distribution and varied the average annual daily truck traffic to determine the required slab thicknesses for different cumulative ESALs as shown in Table 6.6.

**Table 6.6. Cumulative ESALs vs. Number of Heavy Trucks.**

Average Annual Daily Truck Traffic	Cumulative ESALs ( $\times 10^6$ )	Cumulative Number of Heavy Trucks
1145	10	5,915,430
2290	20	11,830,900
3435	30	17,746,300
4580	40	23,661,700
5725	50	29,577,100
6870	60	35,492,600
8015	70	41,408,000
9160	80	47,323,400
10,305	90	53,238,800
11,450	100	59,154,300

While it is recognized that the M-E PDG is set up to use axle load spectra, considerable research by the Department's Transportation Statistics Office would be required to develop appropriate axle load distributions for pavement design. As a transition to the new guide, the decision was made to use the ESAL forecasts currently produced by Planning, and which engineers presently use with the Department's current design method. The M-E PDG does provide an ESAL estimate that is tied to the cumulative number of trucks for a particular project. While this ESAL estimate is based on a 9-inch slab, the equivalency factors from which this estimate is determined do not vary significantly for the ranges of axle loads within legal limits and the range of slab thicknesses in the proposed design tables. Thus, the error in the required slab thickness is expected to be minimal in the researchers' opinion.

From the sensitivity analyses, the following variables were selected to generate the rigid pavement design tables:

- Projected cumulative ESALs from 1 to 100 million
- Vehicle class distribution: Default values in M-E PDG for TTC 1
- Reliability level: Five levels for Design I (75, 80, 85, 90, and 95 %) and 90% for Design II
- CTE of 6.0  $\mu\epsilon$  per  $^{\circ}\text{F}$  for Design I and 5.75 of CTE for Design II,
- 4000 psi of 28-day compressive strength for Design I and 4500 psi for Design II
- Slab width: 13 feet with tied shoulder
- Joint spacing: 15 feet
- Subgrade modulus of reaction: 200 pci

- Initial IRI: 58 inch/mile (based on current FDOT practice of grinding rigid pavements after placement)
- Three dowel diameter sizes based on current FDOT practice: 1-inch dowel diameter for 8 to 8.5-inch slabs, 1.25-inch dowel diameter for 9 to 10.5-inch slabs, and 1.5-inch dowel diameter for 11-inch and thicker slabs.

## **COMPARISON OF M-E PDG BASED DESIGN TABLES WITH CURRENT FDOT DESIGN TABLES**

The rigid pavement design tables established from this implementation project are presented in the Appendix H of this report. Two sets of tables, *Design I* and *Design II*, were developed based on the levels of CTE and compressive strength used in running the M-E PDG program. The tables given in Appendix H show that the required slab thickness ranges from 8 to 14.5 inches for the range of variables used in their development. Researchers note that a minimum slab thickness of 8 inches was adopted in developing these tables. The required slab thicknesses in *Design II* generally showed 1- to 1.5-inch reductions from corresponding thicknesses in the Design I tables due to the lower CTE and higher compressive strength values assumed for *Design II*.

Researchers also compared the new thickness design tables with the current FDOT design tables based on the 1993 AASHTO pavement design guide. For this comparison, the required slab thicknesses at 90 percent reliability level for regions 1 and 5 were examined. It is noted that these two regions cover the range of required slab thicknesses in the new design tables. Figure 6.15 shows how the differences in required slab thickness varied between the new and current set of thickness design tables. The differences plotted in this figure were determined by subtracting the thickness based on the existing FDOT design tables from the corresponding thickness obtained from M-E PDG program. Figure 6.15 shows that the differences ranged from -4.0 to 1.0 inches, with the M-E PDG-based design thicknesses generally being thinner than the corresponding slab thicknesses from the current FDOT PCC design tables. The required slab thicknesses based on the *Design I* table for region 1 are observed to be the most comparable with the existing design method, generally resulting in the least differences. It is evident that the required PCC slab thicknesses for region 5 are generally thinner than the corresponding thicknesses based on the current method for both the *Design I* and *Design II* tables.

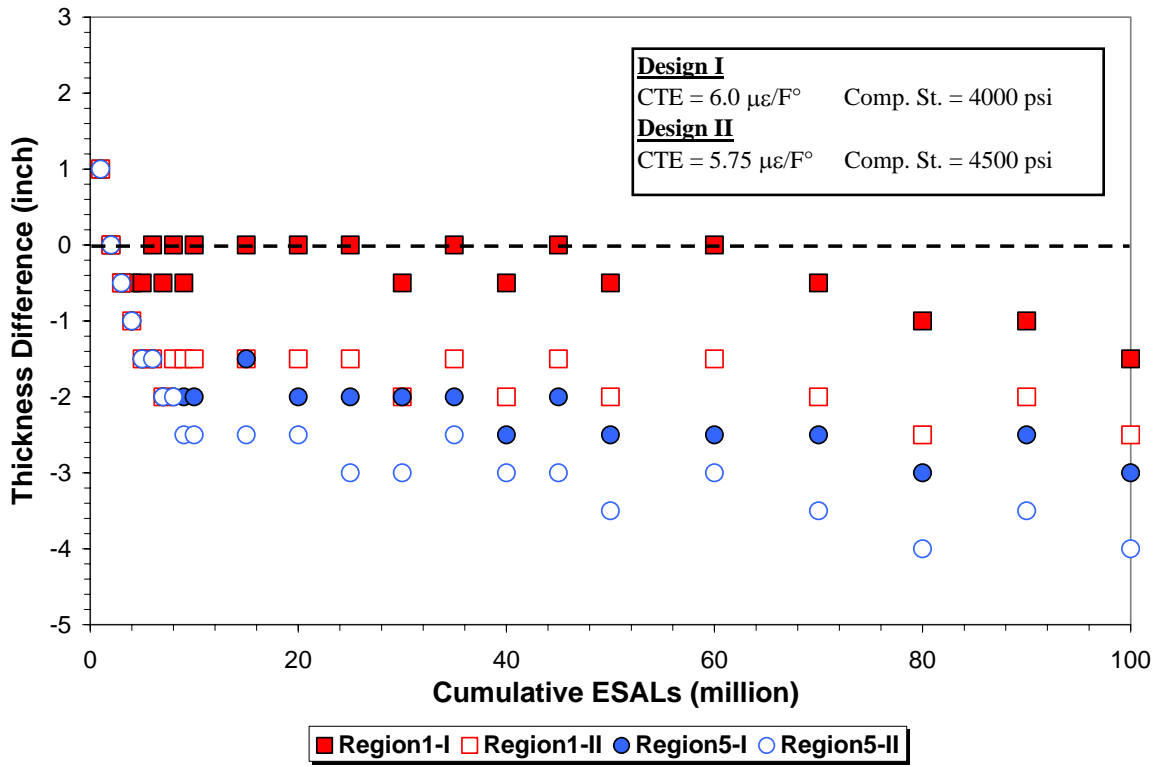


**Figure 6.15. Distributions of Differences in Required Slab Thicknesses.**



## CHAPTER VII. PROJECT SUMMARY AND RECOMMENDATIONS

The primary objectives of this project were to provide a database for verifying and calibrating, as necessary, the performance models in the existing M-E PDG program and to establish a new Florida pavement design method based on the M-E PDG. To accomplish these tasks, researchers executed a comprehensive work plan that included the following:

- examination of Florida's pavement condition survey database to identify in-service pavement sections for model calibrations,
- sensitivity analyses to identify critical factors affecting predicted pavement performance from the M-E PDG program,
- field and laboratory tests to characterize material properties of in-service pavement sections for model calibration,
- compilation of database for model calibration,
- local calibration of faulting and IRI models for rigid pavement designs; and
- development of M-E PDG-based pavement thickness design tables for flexible and rigid pavements

Based on the research conducted, the following findings are noted:

- From the review of M-E PDG input requirements and sensitivity analyses, researchers identified the laboratory and field tests needed to characterize material properties for calibrating the performance models in the design guide program. The test plan is based on characterizing design factors that were found to significantly affect predicted pavement performance from the M-E PDG program. These factors include mixture properties that determine the dynamic modulus of the asphalt concrete material, specifically, gradation, air voids content, effective binder content, and the asphalt viscosity-temperature relationship. The sensitivity analyses also identified properties of the underlying unbound layers in flexible pavements that significantly affect predicted pavement performance based on longitudinal and alligator cracking, rutting, and IRI. These properties include the resilient moduli of the base, subgrade, and embankment materials, and the soil-water characteristic curve, that may be characterized from soil suction tests or estimated using prediction equations that relate soil suction parameters to gradation, soil moisture-density relationship, and Atterberg limits.

- For jointed plain concrete pavements, the sensitivity analyses identified the concrete coefficient of thermal expansion (CTE), and compressive strength as significant predictors of PCC pavement performance. On this project, these properties were characterized from laboratory tests done on concrete cores taken from in-service pavement sections established for model calibrations. In addition, joint spacing, dowel diameter, and slab width were found to significantly affect the performance predictions from the M-E PDG program. However, the moduli of the underlying unbound materials as well as the modulus of subgrade reaction were found to have minimal effect on the PCC performance predictions.
- M-E PDG runs made to evaluate the effect of ground water table depth showed that the effect of this factor on the performance predictions diminishes with depths greater than 20 feet. Thus, for the field tests done on the calibration sections, borings to determine the depth of the water table were made to a depth of 20 feet or until the water table was reached, whichever came earlier.
- For characterizing asphalt layers, extraction and DSR testing was performed on cored samples. Since the cored asphalt samples comprised several lifts, the properties were characterized for each lift. For calibration, the original air voids were estimated using the global aging model incorporated in the M-E PDG. However, since the decision was made to forego local calibrations pending the development of improved prediction models for top-down cracking, reflection cracking, and rutting, the database compiled on the asphalt calibration sections were not used in this project. This database might be used in a follow-up project to revise the asphalt thickness design tables from this study based on the improved prediction models from on-going national development efforts.
- For characterizing PCC materials, the CTE and compressive strength were determined for each core. The CTE values tested at FDOT and TTI were compared and showed good agreement between measurements made on corresponding cores. Since the PCC performance predictions are highly influenced by the concrete coefficient of thermal expansion, researchers made a careful selection of the CTE values for generating the PCC thickness design tables based on the M-E PDG. This decision considered CTE measurements obtained from tests on molded specimens and cores from FDOT construction projects; the

standard deviations of repeat CTE measurements reported in the literature; and work conducted in other M-E PDG implementation projects. In characterizing concrete compressive strength, this project tested concrete cores taken from in-service Florida pavements. Researchers used the compressive strengths determined from cores with an aging model incorporated in the M-E PDG program to backcalculate the 28-day strength for local model calibrations. The average of the estimated 28-day compressive strengths was found to be 3800 psi, which is between the specified 28-day minimum compressive strength of 3000 psi and a compressive strength of about 4350 psi corresponding to the standard concrete design modulus of 4000 ksi given in the FDOT rigid pavement manual.

- For characterizing underlying materials, resilient modulus and soil suction tests were conducted. The sensitivity analyses indicated that the resilient moduli of the underlying materials are not significant in controlling PCC predicted pavement performance. For flexible pavements, researchers found that the base modulus significantly influences the predicted amounts of alligator (bottom-up) cracking from the M-E PDG program. The sensitivity analyses also revealed a moderate benefit to placing a mechanically stabilized subgrade over the embankment, particularly for embankment moduli of 10 ksi or less. Based on these findings, laboratory resilient modulus test data, and recommendations provided by the technical advisory panel, researchers assigned representative modulus values of 30 and 45 ksi for base, 16 ksi for stabilized subgrade, and 12 ksi for the embankment material to develop the flexible pavement thickness design tables based on the M-E PDG. Researchers also conducted a limited comparison of soil suction curves determined from laboratory tests and curves established based on published information on Florida soils. This comparison generally showed reasonable agreement between the data obtained from soil suction tests conducted in this project and those determined from published information. Given this finding, researchers established a database of soil suction properties for the embankment materials found in the different Florida counties.
- For characterizing traffic loading, this project compiled data on percent trucks, heavy vehicle distributions, AADTT, and traffic growth rates on the calibration sections. The sensitivity analyses indicated that predicted pavement performance

is highly tied to the cumulative ESALs, which was found to be a suitable index for quantifying the aggregate effect of traffic design variables, i.e., AADTT, heavy vehicle distribution, and axle load spectra on predicted pavement performance. While it is recognized that the M-E PDG is set up to use axle load spectra for pavement design, considerable research by the Department's Transportation Statistics Office would be required to develop appropriate axle load distributions for pavement design. As a transition to the new guide, the decision was made to use the ESAL forecasts currently produced by Planning, and which engineers presently use with the Department's current design method.

- To account for climatic effects, researchers used the weather data embedded in the M-E PDG to investigate the effects of climatic factors on predicted pavement performance. The sensitivity analyses showed that climatic factors have a more pronounced effect on the performance predictions for rigid pavements in Florida. For flexible pavements, the effects of these factors were minimal in terms of the predicted alligator cracking under Florida climatic conditions. From the investigations of climatic effects, researchers established five climatic regions for developing the thickness design tables for rigid pavements based on the M-E PDG.
- Researchers compared the faulting and IRI predictions on the PCC calibration sections to establish the need for local calibrations prior to developing the thickness design tables. This comparison showed that the faulting and IRI predictions tended to underestimate the measured values on these sections. Thus, researchers recalibrated the faulting and IRI models based on the observed performance data on the PCC calibration sections. Based on the results from a sensitivity analysis of the model coefficients, the C1 coefficient of the faulting model was adjusted to 2.0 and the C3 coefficient of the IRI model to 2.5 to reduce the bias between the model predictions and the observed performance data. No calibration was done for transverse cracking model.
- Based on examining the pavement performance data from condition surveys done by the Department and work conducted in other M-E PDG implementation efforts, researchers established performance criteria for generating thickness design tables based on the M-E PDG. For rigid pavements, the performance criteria selected for generating the final set of design tables were 10 percent transverse cracking,

0.12 inches of faulting, and a terminal IRI of 180 inches/mile corresponding to a predicted Ride Number of 2.5. Researchers assumed an initial IRI of 58 inches/mile for generating the design tables for both PCC and asphalt pavements. For developing the asphalt thickness design tables, a limiting criterion of 35 percent on the predicted alligator cracking was used.

- For flexible pavements, this project established design tables for new construction and overlay projects. To simulate the current pavement condition criteria used by the Department, researchers ran the M-E PDG program for different levels of existing HMAC modulus to simulate good, fair, and poor pavement conditions. The HMAC modulus was varied by adjusting the binder and volumetric properties of the existing material, specifically, binder viscosity and air voids content. Of the two factors, researchers found that the air voids content had a greater influence on the predicted HMAC modulus. In view of this finding, and considering that the air voids content simulates the amount of cracking in the existing material, researchers used this design variable to simulate the condition of the existing AC layer. Researchers established criteria to characterize good, fair, and poor pavement conditions by using the M-E PDG program to find the levels of air voids content that result in overlay thicknesses comparable to the existing FDOT flexible pavement design method. From this analysis, researchers established the following correspondence between air voids content and the existing condition of the HMAC material: Good – 7.2 percent, Fair – 7.5 percent, and Poor – 8.0 percent air voids.
- Based on results of sensitivity analyses, a review of current practice, and consultations with the project advisory panel, researchers came up with following selections of variables to generate the design tables for flexible pavements based on the M-E PDG:
  - Friction course: 1.5 inches of FC-12.5 (PG 70-22, 7 percent air voids)
  - Structural course: SP 12.5 (PG 70-22, 7 percent air voids)
  - Existing AC material: 2 to 6 inches of SP 12.5 (PG 70-22, 7.2 percent air voids for HMAC material in good condition, 7.5 percent for existing material in fair condition, and 8.0 percent for material in poor condition)

- Base layer: 8 inches of limerock at two levels of base modulus (30 and 45 ksi)
  - Stabilized subgrade: 12 inches with 16 ksi modulus
  - Embankment: A-2-4 soil with 12 ksi modulus
  - Reliability: 75, 80, 85, 90, 95 percent
  - ESALs: 1 to 70 million ESALs
  - Weather: Miami weather data with 5-foot depth of ground water table
  - Distress criterion: 35% alligator cracking
  - Vehicle class distribution: default values in M-E PDG for TTC 6
  - Design life: 20 years
- For rigid pavement design, researchers compared the required slab thicknesses for different PCC pavement structures found in the Florida highway network. From this comparison, researchers selected a pavement structure consisting of a concrete slab surface overlying 4 inches of dense graded asphalt mix, 12 inches of Type B stabilized subgrade, and the embankment soil. This pavement structure yielded approximately 0.5-inch thicker slabs compared to the thickness requirements for the other PCC pavement structures investigated. The following selections of design variables were used for generating rigid pavement design tables:
    - Projected cumulative ESALs ranging from  $1 \times 10^6$  to  $100 \times 10^6$
    - Vehicle class distribution: Default values in M-E PDG for TTC 1
    - Reliability level: Five levels for *Design I* tables (75, 80, 85, 90, and 95 %) and 90% for the *Design II* table
    - CTE of  $6.0 \mu\epsilon$  per  $^{\circ}\text{F}$  for *Design I* tables and  $5.75 \mu\epsilon$  per  $^{\circ}\text{F}$  for *Design II*
    - 4000 psi 28-day compressive strength for *Design I* and 4500 psi for *Design II*
    - Slab width: 13 feet with tied shoulder
    - Joint spacing: 15 feet
    - Subgrade modulus of reaction: 200 pci
    - Three dowel diameter sizes based on current FDOT practice: 1-inch dowel diameter for 8 to 8.5-inch slabs, 1.25-inch dowel diameter for 9 to 10.5-inch slabs, and 1.5-inch dowel diameter for 11-inch and thicker slabs.

- The required AC thicknesses based on the M-E PDG ranged from 2 to 9 inches for new pavement designs and 1.5 to 7.5 inches for asphalt concrete overlays. These requirements were determined over a range of ESALs from  $1 \times 10^6$  to  $70 \times 10^6$  for a 20-year design period. The comparison of the required AC thickness based on the design tables derived from the M-E PDG and the thickness determined using the current FDOT design method showed differences ranging from -2 to +2 inches for new pavement designs. For these cases, the required AC thicknesses based on the M-E PDG tables were slightly conservative when using a limerock base modulus of 30 ksi. The change of base modulus from 30 ksi to 45 ksi shifted the distribution of the differences with the highest frequency shifting from 1 to 0.5 inch. For overlay design, the thickness difference was slightly lower compared to new design with differences of 0 and 0.5 inch showing the highest frequency of occurrence. However, it is noted that the comparisons were made assuming a base modulus of 45 ksi and 2 inches of existing AC thickness. With respect to existing pavement condition, there was a 0.5-inch shift in the highest frequency when the existing AC structure was varied from poor to good condition.
- Two sets of PCC tables, *Design I* and *Design II*, were developed based on the levels of CTE and compressive strength used in running the M-E PDG program. The PCC design tables given in Appendix H show that the required slab thickness ranges from 8 to 14.5 inches for the range of variables used in their development. Researchers note that a minimum slab thickness of 8 inches was adopted in developing these tables. The required slab thicknesses in *Design II* generally showed 1- to 1.5-inch reductions from corresponding thicknesses in the *Design I* tables due to the lower CTE and higher compressive strength values assumed for *Design II*. As expected, the slab thickness requirement increases with higher reliability and cumulative 18-kip ESALs. Researchers also compared the new thickness design tables with the current FDOT design tables based on the 1993 AASHTO pavement design guide. For this comparison, the required slab thicknesses at 90 percent reliability level for regions 1 and 5 were examined. The differences in the required slab thickness between the two methods ranged from -4.0 to 1.0 inches, with the M-E PDG-based design thicknesses generally being

thinner than the corresponding slab thicknesses from the current FDOT PCC design tables. The required slab thicknesses based on the *Design I* table for region 1 were observed to be the most comparable with the existing design method, generally resulting in the least differences. Among the five regions, Region 1 also required the greatest design slab thickness. The required PCC slab thicknesses for region 5 were found to be generally thinner than the corresponding thicknesses based on the current method for both the *Design I* and *Design II* tables.

Given the above findings, researchers offer the following recommendations with respect to implementing the initial M-E PDG-based pavement design method for the Florida DOT:

- Since performance prediction models for longitudinal (top-down) cracking, reflection cracking, and rutting are expected to be developed and incorporated into a future release of the M-E PDG program, researchers recommend that a follow-up project be undertaken to review and revise the flexible pavement thickness design tables developed in this study to incorporate other performance criteria based on the improved models developed from on-going national studies. Until then, FDOT flexible pavement designs can be achieved using the current design method with the M-E PDG-based design tables used for comparative checks.
- In line with above recommendation, the Department needs to consider establishing a data base of verification/calibration sections on selected FDOT resurfacing or new construction projects. This recommendation would entail assembling materials and construction information within a selected section of each project that, with the performance data collected over time, can be used to verify the predictions from the M-E PDG program, and perform calibrations in the future, as necessary. These sections might possibly require performance monitoring separate from the PCS surveys that are done annually by the Department to measure the pavement condition and track the performance of each specific verification/calibration section. The recommendation would also cover the work of assembling a materials library to permit molding specimens used during construction for running tests to characterize material properties for future model verification/calibration.

- The concrete coefficient of thermal expansion was found to be a critical factor controlling the predicted performance of jointed plain concrete pavements. Researchers recommend that a CTE materials specification be established as part of quality assurance tests to be conducted on PCC pavement construction projects. Implementation of this specification will require training of inspectors and contractor personnel on the test method adopted to verify CTE values achieved from construction.
- The PCC design tables developed from this project are based on a 13-foot slab width, which was found to be optimal from sensitivity analyses of predicted PCC pavement performance. Thus, researchers recommend building 13-foot wide slabs (with tied shoulders) unless right-of-way restrictions dictate a narrower slab width. For such cases, the current PCC design method may be used or a slab 1.5-inch thicker than the corresponding required thickness based on a 13-foot wide slab may be placed for cumulative ESALs of 50 million or less. This recommendation is based on runs made of the M-E PDG program to compare thickness requirements between 12- and 13-foot wide slabs. Tables 7.1 and 7.2 show the results from these runs. Researchers note that slabs with tied shoulders were assumed in the comparisons given in Tables 7.1 and 7.2. Researchers also note that the engineer can choose to run the M-E PDG program to establish the PCC design thickness for a 12-foot slab width.

**Table 7.1. Comparison of Thickness Requirements between 12- and 13-foot Wide Slabs for *Design I*.**

ESALs ( $\times 10^6$ )	Region (95% Reliability)				
	1	2	3	4	5
5	11 (9.5)*	10.5 (9.5)	10 (9)	10 (8.5)	9.5 (8)
10	12 (11)	11.5 (10.5)	11 (10)	10.5 (9.5)	10.5 (9)
30	13.5 (12.5)	13 (12)	12.5 (11.5)	12 (11)	12 (10.5)
50	14.5 (13.5)	14 (13)	13.5 (12.5)	13 (12)	12.5 (11.5)

\*The number in parentheses indicates the thickness with a 13-foot wide slab.

**Table 7.2. Comparison of Thickness Requirements between 12- and 13-foot Wide Slabs for *Design II*.**

ESALs ( $\times 10^6$ )	Region (90% Reliability)				
	1	2	3	4	5
5	9.5 (8)*	9 (8)	9 (8)	9 (8)	9 (8)
10	10.5 (9)	10 (8.5)	9.5 (8)	9.5 (8)	9 (8)
30	12 (10.5)	11.5 (10.5)	11 (10)	11 (9.5)	10.5 (9.5)
50	13 (11.5)	12.5 (11)	12 (10.5)	11.5 (10.5)	11 (10)

\*The number in parentheses indicates the thickness with a 13-foot wide slab.

## REFERENCES

American Association of State Highway and Transportation Officials. *AASHTO Guide for Design of Pavement Structures*. Washington, D.C., 1993.

Applied Research Associates. *Guide for Mechanistic-Empirical Design of New and Rehabilitated Pavement Structures – Appendix CC-2: Estimating Original Air Voids in GPS-LTPP Sections*. Final Document, National Cooperative Highway Research Program, Transportation Research Board, Washington, D.C., 2001.

Applied Research Associates. *Guide for Mechanistic-Empirical Design of New and Rehabilitated Pavement Structures - Appendix FF: Calibration Sections for Rigid Pavements*. National Cooperative Highway Research Program, Transportation Research Board, Washington, D.C., 2003.

Applied Research Associates. *Guide for Mechanistic-Empirical Design of New and Rehabilitated Pavement Structures*. Final Report, National Cooperative Highway Research Program Project 1-37A, Transportation Research Board, Washington, D.C., 2004.

Applied Research Associates. *Guide for Mechanistic-Empirical Design of New and Rehabilitated Pavement Structures – Appendix II-2: Sensitivity Analysis for Asphalt Concrete Fatigue Alligator Cracking*. Final Document, National Cooperative Highway Research Program, Transportation Research Board, Washington, D.C., 2004.

Asphalt Institute. *Research and Development of the Asphalt Institute's Thickness Design Manual (MS-1) Ninth Edition*. Research Report No. 82-2, Asphalt Institute, Lexington, Ky., 1982.

Bulut, R., R. L. Lytton, and W. K. Wray. *Suction Measurements by Filter Paper*. Expansive Clay Soils and Vegetative Influence on Shallow Foundations, ASCE Geotechnical Special Publication No. 115 (eds. C. Vipulanandan, M. B. Addison, and M. Hasen), American Society of Civil Engineers, Reston, Va., pp. 243-261, 2001.

De Jong, D. L., M. G. F. Peutz, and A. R. Korswagen. *Computer Program BISAR*. External Report, Koninklijke/Shell-Laboratorium, The Netherlands, 1973.

Fernando, E.G., J. Oh, and D. Ryu. *Phase I of M-E PDG Program Implementation in Florida*. Research Report No. D04491/PR15281-1, Texas Transportation Institute, The Texas A&M University System, College Station, Tex., 2007

Florida Department of Transportation. *Rigid Pavement Design Manual*, Document No. 625-010-006-d, Pavement Management Office, Tallahassee, Fla., 2006.

Florida Department of Transportation. *Flexible Pavement Design Manual*, Document No. 625-010-002-f, Pavement Management Office, Tallahassee, Fla., 2005.

Florida Department of Transportation. *Flexible Pavement Condition Survey Handbook*, 2003.

Florida Department of Transportation. *Rigid Pavement Condition Survey Handbook*, 2003

Florida Department of Transportation. *Standard Specifications for Road and Bridge Construction*, 2004

Fredlund, D. G., and A. Xing. *Equations for the Soil-Water Characteristic Curve*. Canadian Geotechnical Journal, Vol. 31, No. 4, pp. 521-532, 1994.

Kannekanti, V., and J. Harvey. Sample Rigid Pavement Design Tables Based on Version 0.8 of the Mechanistic Empirical Pavement Design Guide. Technical Memorandum (UCPRC-TM-2006-04), University of California Pavement Research Center, 2006.

Mirza, M. W. and M. W. Witzczak. *Development of a Global Aging System for Short and Long Term Aging of Asphalt Cements*. Journal of the Association of Asphalt Paving Technologists, Vol. 64, pp. 393-430, 1995.

Olidis, C. and D. Hein. *Guide for the Mechanistic-Empirical Design of New and Rehabilitated Pavement Structures Material Characterization Is your Agency Ready?* Annual Conference of the Transportation Association of Canada, Quebec City, Quebec, 2004

Stubstad, R. N., E. O. Lukanen, C. A. Richter, and S. Baltzer. *Calculation of AC Layer Temperatures from FWD Field Data*. Proceedings, Fifth International Conference on the Bearing Capacity of Roads and Airfields, Vol. 2, Trondheim, Norway, pp. 919-928, 1998.

Witzczak, M. W. and O. A. Fonseca. *Revised Predictive Model for Dynamic (Complex) Modulus of Asphalt Mixtures*. Transportation Research Record 1540, Transportation Research Board, Washington, D.C., pp. 15-23, 1996.

## **APPENDIX A**

### **CANDIDATE PCS SEGMENTS FOR MODEL CALIBRATIONS**



**Table A1. Candidate AC Segments.**

Road Identification				Road Condition				Mean RSS				WIM		Application			
RDWYID	BEG	END	S	PCR	CR	RI	RU	PCR	CR	RI	RU	SITE	Dist. (mi)	P	C	I	U
<b>Arterial District 1</b>																	
12020000	4.35	5.13	L	6.5	6.5	7.2	9.0	0.20	0.13		0.20	9917	14.20		x		
12020000	4.35	5.13	R	6.5	6.5	6.8	9.0	0.25	0.14	0.27	0.12	9917	14.20		x		
16110000	15.39	15.74	R	6.5	7.0	6.5	8.0	0.16	0.49	0.06		9927	15.46			x	
16030000	29.06	29.69	L	6.5	7.0	6.5	7.0	0.29	0.63	0.23	0.13	9927	16.66				x
16180000	15.54	16.49	L	6.5	6.5	8.0	8.0	0.43	0.46		0.09	9927	22.64				x
16250000	4.62	7.38	C	6.5	6.5	7.1	8.0	0.22	0.58	0.10		9927	22.75			x	
04010000	6.19	13.16	C	6.5	6.5	7.8	8.0	0.10	0.37		0.12	9917	24.80	x			x
04040000	11.80	12.11	C	6.5	6.5		9.0	0.12	0.21	0.23		9917	27.76	x			
13020000	4.55	6.67	L	6.5	6.5	6.9	8.0	0.12	0.78	0.08		9926	30.66	x			
13140000	0.00	10.74	C	6.5	6.5	7.7	8.0	0.28	0.91		0.10	9926	34.07				x
91070000	0.00	8.11	C	6.5	6.5	7.9	7.0	0.13	0.87		0.15	9918	34.76	x			
13160000	6.27	9.73	C	6.5	6.5	8.0	8.0	0.13	0.55		0.42	9926	36.77	x			
13160000	9.73	15.57	C	6.5	6.5	8.0	8.0	0.13	0.59		0.24	9926	37.59	x			
09060000	0.36	3.53	C	6.5	6.5	7.7	8.0	0.15	0.48	0.09	0.17	9917	37.61	x			
13010000	2.96	5.33	L	6.6	9.0	6.6	9.0	0.10	0.08	0.10		9926	38.51	x		x	
06010000	11.91	13.54	C	6.5	6.5	7.9	9.0	0.13	0.27	0.09	0.20	9927	38.67	x			
03010000	5.91	8.36	L	6.5	6.5	7.5	9.0	0.27	0.53		0.11	9917	43.60				x
17030000	1.20	2.54	L	6.6	8.0	6.6	9.0	0.16	0.09	0.18		9926	46.41		x		
03001000	3.14	4.70	R	6.5	6.5	7.2	9.0	0.09	0.24			9917	49.90	x			
03080000	0.00	2.91	C	6.5	6.5	7.1	8.0	0.11	0.39	0.08		9935	57.93	x			
03030000	0.00	1.12	L	6.5	7.5	6.5	8.0	0.14	0.13	0.14	0.13	9917	62.63	x	x	x	x
<b>Arterial District 2</b>																	
26010000	0.00	11.64	L	6.5	6.5	7.4	9.0	0.08	0.27	0.15	0.25	9904	0.56	x			
72017000	1.49	2.10	R	6.6	7.5	6.6	9.0	0.06	0.27	0.08	0.28	9914	5.96	x		x	
72170000	5.64	6.32	L	6.5	6.5	7.4	9.0	0.13	0.14	0.07		9914	6.11		x		

**Table A1. Candidate AC Segments (continued).**

Road Identification				Road Condition				Mean RSS				WIM		Application			
RDWYID	BEG	END	S	PCR	CR	RI	RU	PCR	CR	RI	RU	SITE	Dist. (mi)	P	C	I	U
<b>Arterial District 2 (continued)</b>																	
72170000	4.11	5.64	R	6.5	6.5	6.9	9.0	0.13	0.28	0.23		9914	6.98	x			
26070068	0.61	1.51	C	6.5	6.5	6.6	7.0	0.13	0.53		0.15	9904	8.53	x			
26010000	13.44	16.63	R	6.6	7.0	6.6	9.0	0.11	0.48	0.11		9904	9.08	x		x	
34110000	12.61	14.68	C	6.5	6.5	7.3	9.0	0.14	0.28	0.05	0.13	9909	9.35	x			
26005000	7.95	10.69	L	6.5	6.5	7.2	9.0	0.09	0.29	0.06		9904	10.68	x			
34040000	12.74	19.64	C	6.5	6.5	7.7	9.0	0.14	0.22	0.07		9904	10.91	x			
26005000	0.35	3.50	L	6.5	6.5	7.4	9.0	0.11	0.20	0.08		9904	12.22	x			
27010000	10.08	11.90	C	6.5	6.5	7.4	9.0	0.04	0.08	0.05		9936	13.86	x	x		
76050000	2.03	8.20	C	6.5	6.5	7.1	8.0	0.11	0.28	0.07		9904	21.31	x		x	
71050000	10.45	16.12	C	6.5	6.5	7.1	9.0	0.09	0.16	0.05		9905	21.61	x			
76080000	0.36	5.70	C	6.5	6.5	7.4	9.0	0.07	0.40	0.04	0.17	9904	22.94	x			
71110000	4.39	5.86	C	6.5	6.5	6.9	9.0	0.15	0.40	0.10		9904	23.53	x			
34050000	9.83	24.03	R	6.5	6.5	8.1	9.0	0.15	0.19		0.13	9909	24.61	x			
28040000	0.00	5.51	C	6.5	6.5	7.6	9.0	0.14	0.33	0.05		9936	25.02	x			
37040000	0.00	0.34	C	6.6	10.0	6.6	9.0	0.07		0.07	0.08	9909	28.03	x		x	
76010000	5.17	6.41	C	6.5	6.5	7.7	9.0	0.04	0.30	0.04	0.11	9925	29.84	x			
28030000	0.00	0.69	C	6.5	8.0	6.5	9.0	0.18	0.12	0.18		9904	31.55		x		
78090000	14.37	14.49	C	6.5	6.5		8.0		0.52		0.10	9905	31.83				x
76010000	29.28	30.37	R	6.5	6.5	6.7	7.0	0.09	0.56	0.09	0.11	9905	35.36	x		x	x
32010000	30.75	31.18	C	6.5	7.0	6.5	9.0	0.07	0.40	0.10		9901	40.30	x		x	
<b>Arterial District 3</b>																	
48003000	6.12	6.75	L	6.5	6.5	6.8	10.0	0.09	0.17	0.06		9924	2.69	x			
48003000	6.12	6.75	R	6.5	6.5	6.7	10.0	0.15	0.54	0.09		9924	2.69	x		x	
50010000	16.48	18.57	R	6.5	6.5	8.1	9.0	0.05	0.11	0.01	0.18	9940	3.34	x	x		
48012000	7.38	7.70	C	6.5	8.5	6.5	10.0	0.09	0.10	0.08		9924	3.69			x	
58010000	11.05	11.68	L	6.5	6.5	7.3	10.0	0.14	0.15	0.08		9937	4.48	x	x		
48020000	7.87	9.65	L	6.5	6.5	6.8	7.0	0.25	0.76	0.12	0.25	9924	4.70			x	

**Table A1. Candidate AC Segments (continued).**

Road Identification				Road Condition				Mean RSS				WIM		Application			
RDWYID	BEG	END	S	PCR	CR	RI	RU	PCR	CR	RI	RU	SITE	Dist. (mi)	P	C	I	U
<b>Arterial District 3 (continued)</b>																	
48020000	13.45	16.15	L	6.6	7.5	6.6	8.0	0.22	0.67	0.07	0.14	9924	4.94			x	
58010000	9.32	10.75	L	6.5	6.5	8.1	9.0	0.14	0.15	0.03		9937	5.43	x	x		
48010000	2.15	2.90	R	6.5	6.5	6.7	9.0	0.10	0.11	0.09		9916	7.59	x	x	x	
61002000	2.86	3.25	C	6.5	6.5	6.7	8.0	0.20	0.55	0.17	0.12	9939	11.46				x
50040000	0.81	3.05	R	6.5	6.5	7.4	9.0	0.05	0.38	0.02		9940	11.89	x			
61010000	13.33	16.33	C	6.5	6.5	7.5	8.0	0.16	0.13		0.15	9939	12.96		x		
61010000	17.55	19.08	L	6.5	6.5	6.6	9.0	0.17	0.58	0.02	0.08	9939	13.35			x	
46060000	9.10	11.96	C	6.5	6.5	7.8	8.0	0.11	0.61	0.03	0.08	9907	14.29	x			
58060000	20.72	21.80	C	6.5	6.5	7.8	9.0	0.09	0.12	0.03		9937	18.96	x	x		
46040000	0.00	1.12	C	6.5	6.5	6.7	8.0	0.09	0.26	0.07	0.07	9907	20.80	x			
57130000	0.00	1.33	L	6.5	6.5	8.4	8.0	0.62	0.73		0.08	9937	29.31				x
57130000	0.00	1.33	R	6.5	6.5	8.0	8.0	0.62	0.73		0.10	9937	29.31				x
<b>Arterial District 4</b>																	
86190000	2.33	3.67	R	6.5	6.5	7.3	9.0	0.08	0.08	0.05		9934	5.37		x		
86100000	1.53	2.73	R	6.5	6.5	6.7	8.0	0.11	0.41	0.06		9930	7.02	x		x	
86230000	0.00	2.61	R	6.6	7.5	6.6	9.0	0.06	0.26	0.06		9930	8.85	x		x	
94050000	0.00	2.78	C	6.5	6.5	6.9	8.0	0.17	0.51	0.10		9913	9.04			x	
86090000	6.00	8.64	R	6.5	6.5	6.5	8.0	0.08	0.54	0.05		9933	10.40	x		x	
94050000	2.78	8.75	C	6.5	6.5	7.1	9.0	0.10	0.72	0.09		9913	10.62	x			
93001000	3.88	5.81	L	6.5	8.0	6.5	9.0	0.20	0.08	0.20		9921	11.06		x		
86010001	0.00	2.55	L	6.5	6.5	6.7	9.0	0.10	0.32	0.08		9930	11.34	x			
93310000	7.99	12.22	L	6.5	6.5	8.0	8.0	0.14	0.41		0.31	9921	12.56	x			
93310000	12.22	17.80	L	6.5	6.5	7.7	8.0	0.08	0.23		0.12	9921	12.75	x			x
86012000	0.00	0.45	R	6.5	6.5	6.5	8.0	0.11	0.55	0.11		9933	13.00	x		x	
86020000	7.91	9.00	L	6.6	9.0	6.6	8.0	0.04	0.07	0.04	0.09	9933	13.02				x
86020000	7.91	9.00	R	6.6	7.5	6.6	8.0	0.04	0.14	0.04	0.10	9933	13.02		x		x
93100000	11.90	12.62	L	6.5	6.5	6.8	9.0	0.16	0.40	0.14		9935	13.56			x	

**Table A1. Candidate AC Segments (continued).**

Road Identification				Road Condition				Mean RSS				WIM		Application			
RDWYID	BEG	END	S	PCR	CR	RI	RU	PCR	CR	RI	RU	SITE	Dist. (mi)	P	C	I	U
<b>Arterial District 4 (continued)</b>																	
93200000	0.00	1.37	C	6.5	6.5	6.9	9.0	0.09	0.13	0.09		9933	24.96		x		
<b>Arterial District 5</b>																	
18010000	19.48	21.60	C	6.5	6.5	7.9	8.0	0.11	0.60		0.14	9931	3.07	x			x
79181000	0.38	2.86	R	6.5	6.5	8.1	8.0	0.46	0.88		0.11	9906	5.61				x
77030000	5.09	6.04	R	6.5	6.5	7.5	9.0	0.09	0.14	0.06	0.22	9906	6.06	x	x		
70060000	11.99	14.29	C	6.5	6.5	7.8	9.0	0.28	0.12			9919	6.90		x		
70060000	0.00	11.07	C	6.5	6.5	7.8	9.0	0.14	0.14			9919	7.47	x	x		
79070000	26.97	29.29	R	6.6	7.0	6.6	9.0	0.09	0.34	0.08		9929	7.54	x		x	
11010047	0.00	2.09	R	6.5	6.5	7.0	9.0	0.16	0.39	0.07		9931	7.58			x	
77010000	5.94	11.65	L	6.5	6.5	7.6	9.0	0.10	0.22	0.02	0.13	9906	9.59	x			x
11010000	6.04	9.70	R	6.5	6.5	7.8	8.0	0.15	0.12		0.15	9931	10.28	x	x		
79270000	1.62	2.39	L	6.5	8.0	6.5	10.0	0.10	0.09	0.10	0.14	9925	11.32		x		
77040000	5.81	11.05	C	6.5	6.5	7.4	7.0	0.11	0.33	0.03	0.08	9906	11.93	x			x
77010000	1.85	2.53	L	6.5	6.5	6.5	7.0	0.13	0.49	0.15	0.27	9906	15.67	x		x	
79080000	5.13	6.79	L	6.5	6.5	6.6	9.0	0.08	0.36	0.07	0.08	9925	16.16	x			
77040000	11.05	16.10	C	6.5	6.5	8.1	8.0	0.12	0.24	0.02	0.06	9906	16.84	x			
36009000	3.96	5.46	C	6.6	8.5	6.6	9.0	0.09	0.14	0.09	0.13	9931	22.88	x		x	
36110000	6.60	22.51	C	6.5	6.5	7.4	8.0	0.12	0.22	0.08	0.09	9904	25.02	x			x
36060000	4.79	11.93	C	6.5	6.5	8.3	8.0	0.14	0.37		0.10	9904	26.51	x			x
75003000	2.05	5.00	R	6.5	6.5	7.8	10.0	0.10	0.12	0.03		9906	26.63	x	x		
75003000	2.05	4.92	L	6.5	6.5	7.7	10.0	0.12	0.12	0.05		9906	26.67	x	x		
36080000	5.17	6.53	L	6.5	6.5	7.4	8.0	0.09	0.56	0.10	0.08	9904	26.82	x			
36080000	2.36	3.31	L	6.5	6.5	7.8	7.0	0.09	0.43	0.08	0.11	9904	27.04	x			x
36080000	2.36	3.31	R	6.5	6.5	7.4	7.0	0.13	0.60	0.08	0.12	9904	27.04	x			x
70070002	0.00	0.38	L	6.5	6.5	6.6	7.0	0.05	0.10	0.09		9919	32.32		x		
92030000	0.00	0.61	R	6.5	6.5	7.6	7.0	0.14	0.24	0.08	0.10	9927	40.68	x			X

**Table A1. Candidate AC Segments (continued).**

Road Identification				Road Condition				Mean RSS				WIM		Application			
RDWYID	BEG	END	S	PCR	CR	RI	RU	PCR	CR	RI	RU	SITE	Dist. (mi)	P	C	I	U
<b>Arterial District 6</b>																	
87170000	3.70	5.23	L	6.5	6.5	7.3	9.0	0.11	0.46			9930	1.34	x			
87060000	14.05	14.87	L	6.6	9.0	6.6	9.0	0.12	0.08	0.12	0.20	9930	2.37	x		x	
87090000	0.79	3.69	R	6.6	7.0	6.6	7.0	0.06	0.26	0.07		9934	2.74			x	
87030000	24.96	25.38	R	6.5	6.5	7.4	8.0	0.10	0.52		0.29	9930	4.10	x			
87038000	0.00	0.96	R	6.5	6.5	6.8	8.0	0.07	0.44	0.13	0.10	9934	4.21				x
87080000	0.69	2.68	R	6.5	6.5	6.8	9.0	0.15	0.11	0.14		9930	4.44		x	x	
87080001	2.29	3.08	C	6.6	10.0	6.6	9.0	0.05		0.05	0.08	9930	5.66	x		x	
87002000	7.55	9.70	L	6.5	6.5	7.5	9.0	0.12	0.22			9934	6.14	x			
87060000	0.87	2.72	L	6.5	6.5	7.5	8.0	0.20	0.43	0.06	0.10	9930	9.38				x
87220000	2.29	3.86	L	6.6	7.5	6.6	8.0	0.14	0.30	0.15	0.12	9934	9.74	x		x	x
87281000	2.62	3.86	L	6.5	6.5	6.5	9.0	0.15	0.18	0.15		9930	12.15	x		x	
90060000	13.03	16.38	C	6.5	6.5	7.4	9.0	0.08	0.18			9934	65.33	x			
90030000	6.13	7.10	C	6.5	6.5	7.5	10.0	0.10	0.19			9934	101.94	x			
<b>Arterial District 7</b>																	
10160000	0.00	6.77	R	6.5	6.5	7.4	8.0	0.21	0.32	0.04	0.11	9922	3.62				x
10340000	1.28	2.67	C	6.5	9.0	6.5	8.0	0.09		0.09	0.13	9922	6.32				x
10110000	0.00	0.44	R	6.6	8.5	6.6	9.0	0.07	0.15	0.07		9926	6.37	x		x	
14150000	0.00	1.79	C	6.5	6.5	7.3	8.0	0.07	0.17	0.05	0.11	9920	7.14	x			
10070000	4.28	4.58	L	6.5	6.5	7.5	9.0	0.05	0.58	0.01		9927	7.92	x			
14130000	0.48	0.80	C	6.5	6.5	7.5	9.0	0.11	0.76	0.02	0.08	9920	11.39	x			
10060000	8.91	17.43	R	6.5	6.5	7.9	9.0	0.15	0.09		0.11	9926	13.09	x	x		
15009000	1.81	2.32	C	6.5	6.5	6.9	9.0	0.11	0.26	0.13	0.25	9922	17.88	x		x	
15007000	0.00	3.06	L	6.6	8.0	6.6	9.0	0.05	0.33	0.05	0.10	9922	22.31	x		x	
15010000	1.34	4.50	R	6.6	7.0	6.6	8.0	0.03	0.50	0.03	0.12	9922	24.82				x
02030000	14.65	15.53	L	6.5	6.5	6.5	9.0	0.08	0.27	0.10	0.12	9931	36.43	x		x	x
15070001	0.00	0.48	L	6.6	10.0	6.6	8.0	0.06		0.06	0.11	N/A	N/A				x

**Table A1. Candidate AC Segments (continued).**

Road Identification				Road Condition				Mean RSS				WIM		Application			
RDWYID	BEG	END	S	PCR	CR	RI	RU	PCR	CR	RI	RU	SITE	Dist. (mi)	P	C	I	U
<b>Interstate</b>																	
79110000	14.67	25.27	L	6.5	6.5	8.3	8.0	0.29	0.83		0.11	9925	2.84				x
53002000	13.61	19.50	L	6.5	6.5	8.4	9.0	0.26	0.14		0.08	9943	7.44	x			
53002000	13.61	19.50	R	6.5	6.5	8.2	8.0	0.30	0.14		0.10	9943	7.44	x			x
36210000	22.50	23.51	L	6.5	6.5	7.1	7.0	0.07	0.41	0.02	0.06	9904	18.95	x			x
75280000	22.37	24.67	R	6.5	6.5	8.2	8.0	0.11	0.20	0.06		9906	19.36	x			
15170000	5.94	7.66	R	6.5	6.5	8.1	9.0	0.06	0.13		0.16	9926	28.01		x		
73001000	0.00	18.73	L	6.5	6.5	7.8	9.0	0.30	0.11		0.22	9925	29.56		x		
93220000	16.45	17.00	L	6.5	6.5	7.8	8.0	0.09	0.30			9933	29.76	x			
93220000	16.45	17.00	R	6.5	6.5	7.9	9.0	0.12	0.30			9933	29.76	x			
75280000	1.00	8.84	L	6.5	6.5	8.5	9.0	0.09	0.08			9920	35.02	x	x		
<b>Turnpike</b>																	
87470000	0.00	0.17	R	6.5	6.5	6.6	10.0	0.13	0.42	0.11		9930	3.61	x			
87470000	0.00	0.24	L	6.5	6.5	7.0	9.0	0.13	0.24	0.13		9930	3.64	x			
86470000	8.51	15.16	L	6.5	6.5	8.4	9.0	0.04	0.52			9933	6.10	x			
86470000	8.51	15.16	R	6.5	6.5	8.4	8.0	0.07	0.45			9933	6.10	x			
86470000	15.16	16.95	L	6.5	6.5	8.4	9.0	0.05	0.41			9933	6.26	x			
86470000	0.00	0.55	R	6.5	6.5	7.9	9.0	0.06	0.28			9930	6.30	x			
86470000	18.89	22.30	R	6.5	6.5	8.0	8.0	0.43	0.57		0.12	9933	9.88				x
87471000	14.37	17.37	L	6.5	6.5	7.5	9.0	0.16	0.24		0.10	9934	19.67				x

**Table A2. Candidate PCC Segments.**

Subsystem	Road Identification				Road Condition			Mean RSS			WIM		Application		
	RDWYID	BEG	END	S	PCR	CR	RI	PCR	CR	RI	SITE	Dist. (mi)	P	C	I
Arterial 2	72030000	9.43	10.39	R	6.4	7.3	6.4	0.12		0.12	9914	4.42			x
	72030000	7.46	8.71	R	6.8	8.4	6.8	0.11		0.13	9914	4.80	x		x
	72090000	8.23	11.14	R	6.1	8.7	6.1	0.13		0.13	9905	10.19	x		x
Arterial 5	79010000	9.60	11.46	L	6.6	9.4	6.6	0.07		0.07	9929	0.08	x		x
Arterial 6	87030000	8.83	10.10	L	6.5	6.5	6.7	0.03	0.05	0.02	9930	11.01	x	x	
	87030000	8.83	10.10	R	6.1	6.1	6.5	0.38	0.06	0.42	9930	11.01		x	
Arterial 7	10150000	12.59	12.84	L	6.3	8.0	6.3	0.56	0.08	0.56	9922	5.30		x	
Interstate	72280000	6.08	7.48	L	6.3	6.3	7.2	1.52	1.52	0.10	9905	2.24			x
	72280000	7.48	13.10	L	6.5	6.5	7.7	1.63	1.67	0.06	9905	5.62			x
	72001000	34.52	35.51	R	6.7	9.0	6.7	0.11		0.13	9914	9.65			x
	87270000	0.00	0.98	R	6.9	6.9	7.6		0.11		9930	11.47		x	
	15002000	0.00	0.16	R	6.3	7.0	6.3	0.60	0.04	0.60	9926	23.93		x	
	15003000	0.37	1.29	R	6.5	6.9	6.5	0.05	0.10	0.05	9926	24.03		x	
	15190000	2.29	4.43	R	6.3	6.3	7.2	0.08	0.36		9926	25.37	x		

**Table A3. Candidate AC Segments with Long Service Lives.**

Subsystem	RDWYID	BEG	END	S	PCR	CR	RI	RU	SITE	Dist. (mi)	Age
Arterial 1	03080000	0.00	2.91	C	6.5	6.5	7.1	8.0	9935	57.93	29
	05020000	6.38	8.29	C	6.5	6.5	7.5	8.0	9918	13.44	22
	05090000	2.66	12.44	C	6.5	6.5	7.1	9.0	9918	20.53	28
	13020000	4.55	6.67	L	6.5	6.5	6.9	8.0	9926	30.66	21
	13030000	0.51	1.91	R	6.5	6.5	6.7	8.0	9926	32.63	22
	13050000	22.39	27.12	C	6.5	6.5	7.5	7.0	9926	39.61	28
	13160000	6.27	9.73	C	6.5	6.5	8.0	8.0	9926	36.77	29
	13160000	9.73	15.57	C	6.5	6.5	8.0	8.0	9926	37.59	27
	16040000	11.27	13.59	C	6.5	6.5	7.2	9.0	9927	33.98	26
	16040000	13.99	15.06	C	6.5	6.5	7.0	9.0	9927	35.92	26
	16090000	6.26	12.37	C	6.5	6.5	7.0	8.0	9927	33.30	29
	17010000	4.30	7.85	R	6.5	6.5	7.4	8.0	9917	25.19	29
	17030000	2.54	2.80	L	6.5	6.5	6.7	8.0	9926	46.51	28
	91070000	0.00	8.11	C	6.5	6.5	7.9	7.0	9918	34.76	24
Arterial 2	26010000	12.54	13.18	R	6.5	6.5	7.3	10.0	9904	6.93	23
	26010000	13.44	16.63	R	6.6	7.0	6.6	9.0	9904	9.08	23
	26020000	3.25	6.07	C	6.5	9.5	6.5	9.0	9904	10.03	29
	26050000	0.62	3.91	L	6.5	6.5	7.2	8.0	9904	7.18	29
	26070068	0.61	1.51	C	6.5	6.5	6.6	7.0	9904	8.53	24
	26090000	15.77	15.96	L	6.5	6.5		9.0	9904	7.56	29
	26220000	9.19	11.10	L	6.5	6.5	6.7	9.0	9904	5.96	28
	27010000	10.08	11.90	C	6.5	6.5	7.4	9.0	9936	13.86	21
	32010000	30.75	31.18	C	6.5	7.0	6.5	9.0	9901	40.30	23
	34070000	9.30	16.54	C	6.5	6.5	7.6	9.0	9909	20.18	29
	38030000	2.34	3.98	C	6.5	6.5	7.3	9.0	9901	27.64	28
	38030000	3.98	4.64	C	6.5	6.5	7.1	8.0	9901	28.64	28
	72018000	1.99	2.84	L	6.5	6.5	7.1	10.0	9914	5.85	23

**Table A3. Candidate AC Segments with Long Service Lives (continued).**

Subsystem	RDWYID	BEG	END	S	PCR	CR	RI	RU	SITE	Dist. (mi)	Age
Arterial 2	72050000	13.95	15.74	L	6.5	6.5	6.5	9.0	9914	7.81	29
	72080000	7.83	8.44	R	6.5	6.5	8.3	10.0	9914	3.70	26
	72170000	0.00	0.70	L	6.5	6.5	6.8	9.0	9914	11.38	29
	74130000	0.81	3.09	C	6.5	6.5	6.9	9.0	9914	22.61	27
	76050000	0.00	2.03	C	6.5	6.5	7.4	9.0	9904	17.29	23
	78030000	1.95	18.89	C	6.5	6.5	6.7	7.0	9905	15.55	28
	78090000	14.37	14.49	C	6.5	6.5		8.0	9905	31.83	26
Arterial 3	48020000	12.08	13.03	C	6.5	6.5	6.6	8.0	9924	5.00	29
	55020000	0.51	1.13	L	6.5	7.0	6.5	9.0	9908	4.93	26
	55020000	0.51	1.13	L	6.5	7.0	6.5	9.0	201	4.93	26
	57050000	0.00	1.25	L	6.5	6.5	6.5	8.0	9928	21.41	27
Arterial 4	86006000	0.00	2.14	R	6.6	9.0	6.6	8.0	9933	5.98	29
	86018000	0.00	1.21	R	6.6	9.0	6.6	8.0	9930	7.98	27
	86020000	3.45	4.16	R	6.5	6.5	6.7	9.0	9933	11.86	29
	86020000	7.91	9.00	L	6.6	9.0	6.6	8.0	9933	13.02	22
	86020000	7.91	9.00	R	6.6	7.5	6.6	8.0	9933	13.02	22
	86100000	1.53	2.73	R	6.5	6.5	6.7	8.0	9930	7.02	24
	86100000	13.84	14.78	R	6.5	6.5	7.0	9.0	9933	6.38	23
	86230000	3.44	3.64	R	6.5	10.0	6.5	9.0	9930	8.85	27
	93006000	1.28	2.08	L	6.5	7.5	6.5	8.0	9921	26.64	29
	93010000	2.87	5.10	L	6.6	8.0	6.6	9.0	9933	19.80	26
	93012000	0.00	0.37	R	6.6	9.0	6.6	9.0	9921	14.78	26
	93012000	1.96	2.86	L	6.6	7.0	6.6	8.0	9921	14.99	26
	93030000	7.16	8.27	L	6.5	6.5	6.7	9.0	9933	23.89	26
	93040000	0.84	2.19	L	6.6	7.0	6.6	9.0	9921	12.49	29
	93120000	19.75	20.33	L	6.5	6.5	6.5	9.0	9921	22.21	29
	94050000	0.00	2.78	C	6.5	6.5	6.9	8.0	9913	9.04	26
94050000	2.78	8.75	C	6.5	6.5	7.1	9.0	9913	10.62	24	

**Table A3. Candidate AC Segments with Long Service Lives (continued).**

Subsystem	RDWYID	BEG	END	S	PCR	CR	RI	RU	SITE	Dist.	Age
Arterial 5	11080000	1.52	4.82	C	6.5	6.5	7.4	8.0	9931	14.94	28
	18010000	28.74	30.26	C	6.5	6.5	7.6	8.0	9931	10.41	22
	36060000	4.79	11.93	C	6.5	6.5	8.3	8.0	9904	26.51	22
	36110000	6.60	22.51	C	6.5	6.5	7.4	8.0	9904	25.02	24
	70002000	0.24	2.09	R	6.6	7.0	6.6	9.0	9929	21.34	26
	70004000	2.86	4.59	L	6.5	6.5	6.7	8.0	9919	17.98	28
	70020000	9.45	9.82	R	6.6	7.0	6.6	8.0	9919	17.64	24
	75003000	5.00	7.30	R	6.5	6.5	6.6	8.0	9906	24.02	29
	75011000	0.66	2.49	L	6.5	6.5	6.9	8.0	9906	18.21	26
	75080000	17.42	17.66	C	6.5	9.0	6.5	9.0	9906	24.48	29
	75250000	4.81	7.27	L	6.5	8.0	6.5	8.0	9906	22.94	24
	77010000	16.53	16.93	R	6.5	9.5	6.5	9.0	9906	4.57	23
	77161000	0.00	0.90	C	6.6	9.0	6.6	9.0	9906	7.64	22
	79070000	26.97	29.29	R	6.6	7.0	6.6	9.0	9929	7.54	24
	79190000	8.21	9.62	L	6.5	6.5	6.5	7.0	9925	12.47	26
	79190000	8.21	9.62	R	6.5	6.5	6.9	8.0	9925	12.47	26
79230000	2.38	4.00	R	6.5	7.5	6.5	8.0	9925	13.03	26	
Arterial 6	87015000	0.35	1.93	C	6.6	8.5	6.6	8.0	9934	26.27	26
	87019000	0.00	2.91	L	6.5	6.5	7.0	8.0	9930	5.50	29
	87030000	8.23	8.83	L	6.5	6.5	6.5	10.0	9930	11.65	29
	87046000	0.00	1.29	R	6.6	10.0	6.6	9.0	9934	16.89	22
	87047000	8.54	9.51	R	6.5	9.0	6.5	9.0	9934	10.58	24
	87091000	7.09	8.06	L	6.6	10.0	6.6	9.0	9934	21.37	24
	87260000	18.96	22.27	R	6.5	6.5	8.3	7.0	9930	6.71	25
	90030000	6.13	7.10	C	6.5	6.5	7.5	10.0	9934	101.9	24
Arterial 7	15010000	8.98	10.42	L	6.5	6.5	6.7	8.0	9922	26.72	24
	15060000	5.42	5.62	L	6.5	6.5	6.5	7.0	9922	21.55	29
	15060000	5.42	5.62	R	6.5	6.5	6.5	7.0	9922	21.55	29
	15140000	3.30	4.06	R	6.5	9.0	6.5	10.0	9922	28.40	24
Turnpike	86471000	4.21	6.54	R	6.5	6.5	7.8	8.0	9930	7.61	24

**Table A4. Candidate PCC Segments with Long Service Lives.**

Subsystem	RDWYID	BEG	END	S	PCR	CR	RI	SITE	Dist. (mi)	Age
Arterial 1	01010000	0.49	4.98	L	6.7	6.7	7.0	9917	1.85	22
	16100000	2.22	2.89	L	6.3	7.8	6.3	9927	1.75	22
	16100000	2.22	2.89	R	6.8	6.9	6.8	9927	1.75	22
	16100000	3.93	5.05	L	6.2	6.2	7.0	9927	3.68	22
	16100000	3.93	5.05	R	6.1	6.1	7.2	9927	3.68	22
Arterial 2	72030000	7.46	8.71	R	6.8	8.4	6.8	9914	4.80	22
	72030000	9.43	10.39	R	6.4	7.3	6.4	9914	4.42	22
	72090000	8.23	11.14	L	6.3	8.9	6.3	9905	10.19	22
	72090000	8.23	11.14	R	6.1	8.7	6.1	9905	10.19	22
	72090445	0.50	0.91	R	6.7	8.2	6.7	9914	7.76	22
	78010000	16.12	18.73	R	6.1	8.2	6.1	9905	22.39	22
Arterial 3	48080060	0.00	1.83	L	6.5	8.8	6.5	9924	6.08	24
Arterial 5	75008000	5.78	7.88	R	6.2	8.6	6.2	9906	24.54	28
	75008000	8.20	9.67	L	6.7	9.2	6.7	9906	24.18	28
	75008000	8.20	9.67	R	6.9	8.5	6.9	9906	24.18	28
	79010000	26.87	28.71	L	6.6	8.6	6.6	9925	13.57	24
	79010000	26.87	28.71	R	6.8	8.8	6.8	9925	13.57	23
Arterial 6	87004000	0.00	0.49	R	6.2	7.8	6.2	9930	7.64	22
Arterial 7	10150000	12.59	12.84	L	6.3	8.0	6.3	9922	5.30	22
Interstate	72001000	34.52	35.51	L	6.2	9.0	6.2	9914	9.65	22
	72001000	34.52	35.51	R	6.7	9.0	6.7	9914	9.65	22
	72270000	17.05	21.00	L	6.4	7.9	6.4	9914	3.45	29
	72270000	17.16	21.00	R	6.3	7.5	6.3	9914	3.46	29
	75280000	14.73	18.78	L	6.5	8.9	6.5	9906	25.41	29
	87004000	0.49	0.79	R	6.2	9.1	6.2	9930	7.49	22
	87004000	0.79	1.28	L	6.3	8.6	6.3	9930	7.36	22
	87270000	0.00	0.98	L	6.3	8.9	6.3	9930	11.47	22
	10320000	0.42	4.72	L	6.3	8.4	6.3	9922	5.00	22

**Table A4. Candidate PCC Segments with Long Service Lives (continued).**

Subsystem	RDWYID	BEG	END	S	PCR	CR	RI	SITE	Dist. (mi)	Age
Interstate	15002000	0.60	0.99	L	6.2	7.6	6.2	9926	23.33	22
	15003000	0.37	1.29	R	6.5	6.9	6.5	9926	24.03	22
	15190000	2.29	4.43	R	6.3	6.3	7.2	9926	25.37	22
	15190000	5.29	10.96	L	6.2	8.1	6.2	9922	21.86	22

**APPENDIX B**  
**SUMMARY OF FWD AND PCS DATA**



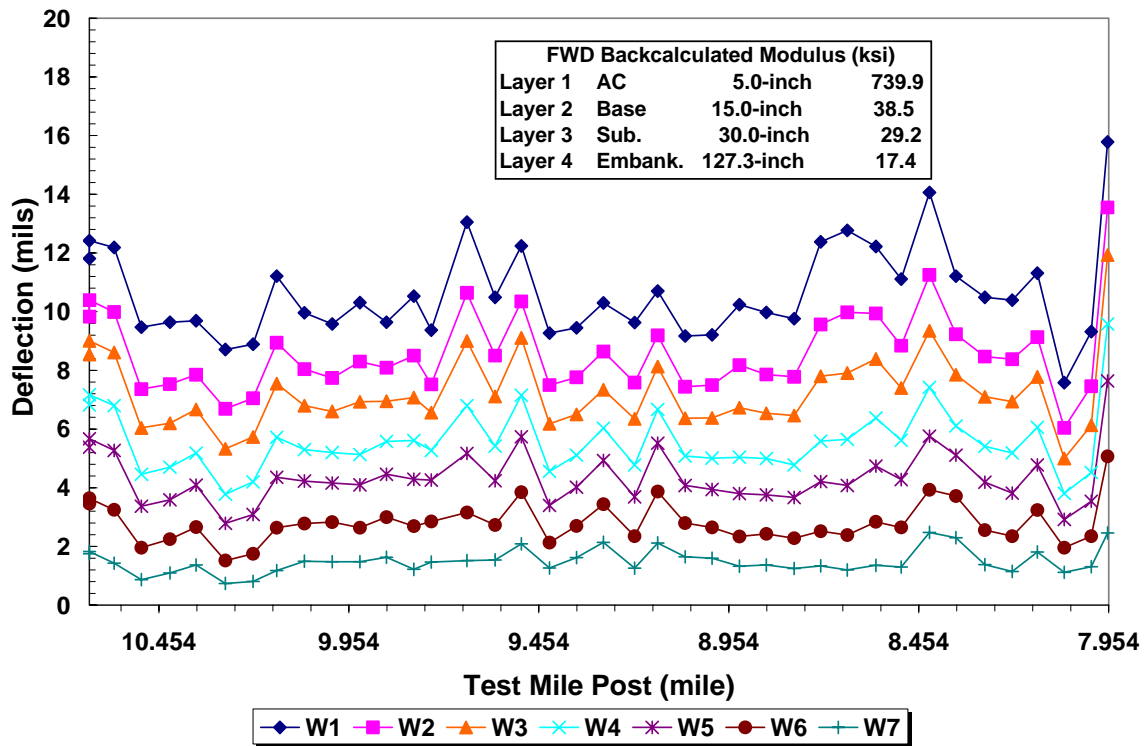


Figure B1. Illustration of FWD Data of 260050000 at Alachua County.

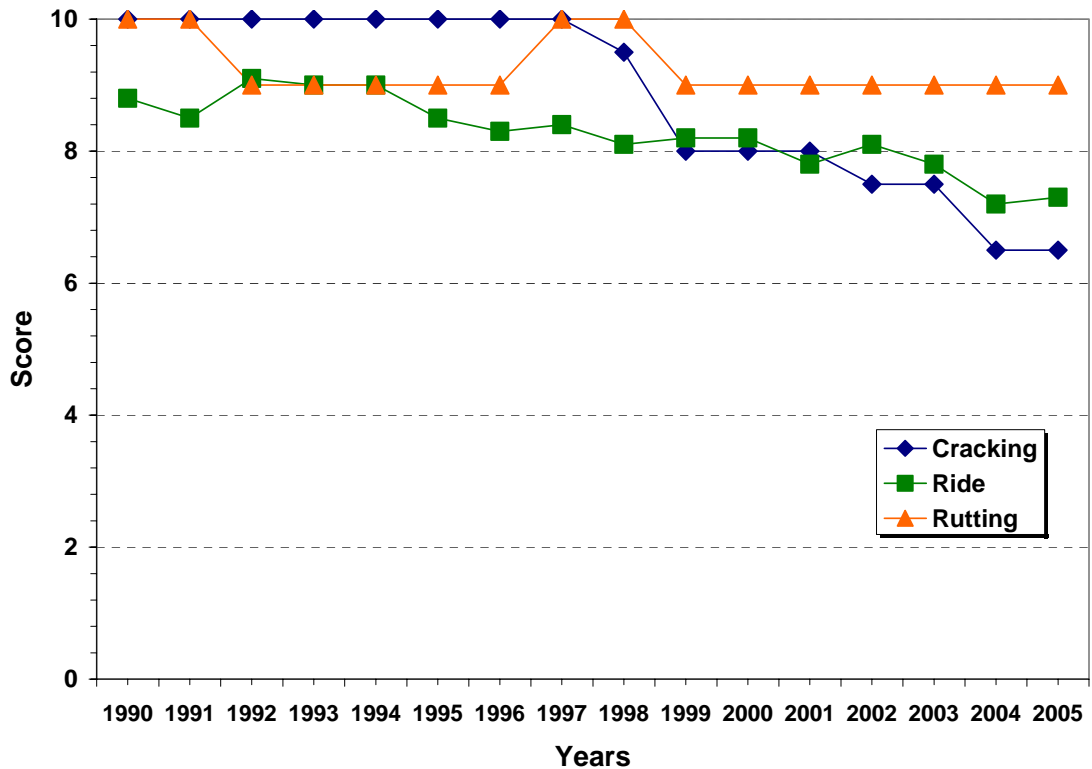


Figure B2. PCS Data of 26005000 at Alachua County.

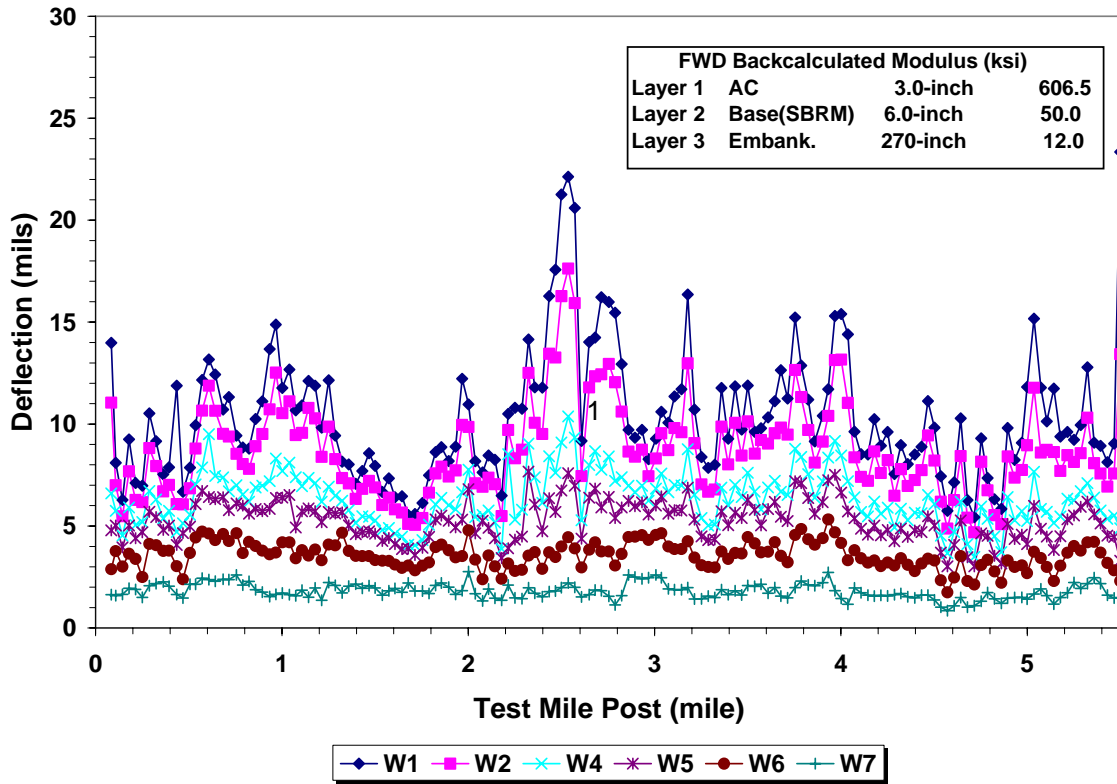


Figure B3. Illustration of FWD Data of 28040000 at Bradford County.

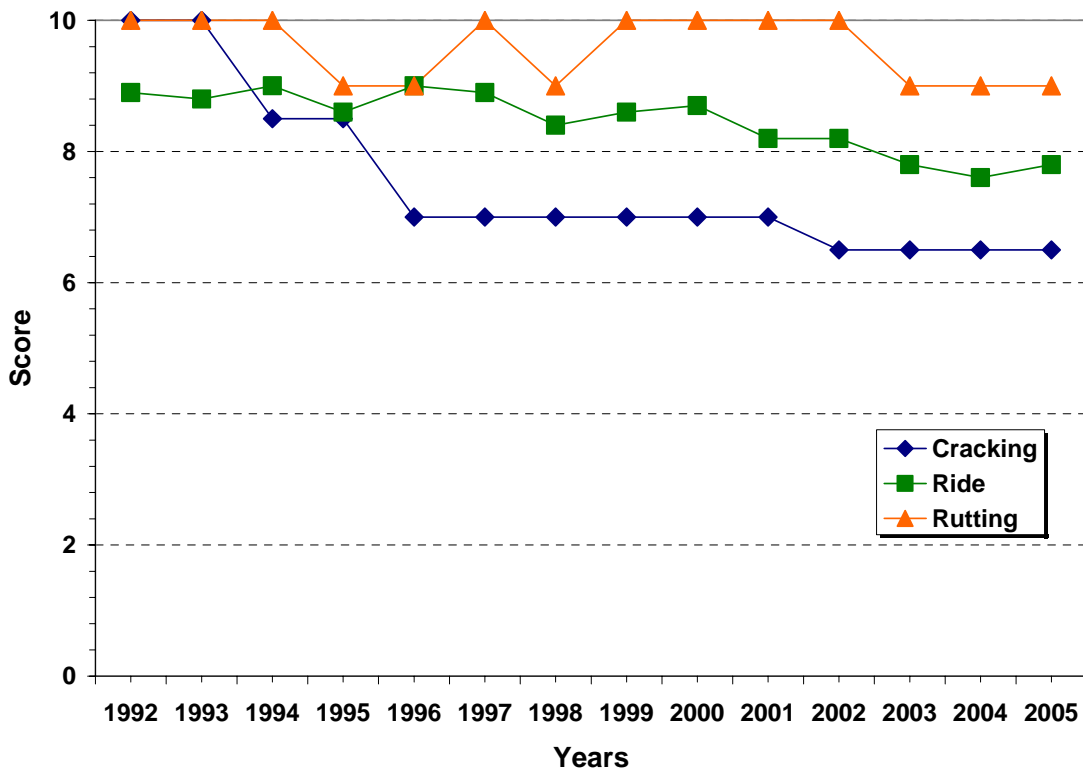


Figure B4. PCS Data of 28040000 at Bradford County.

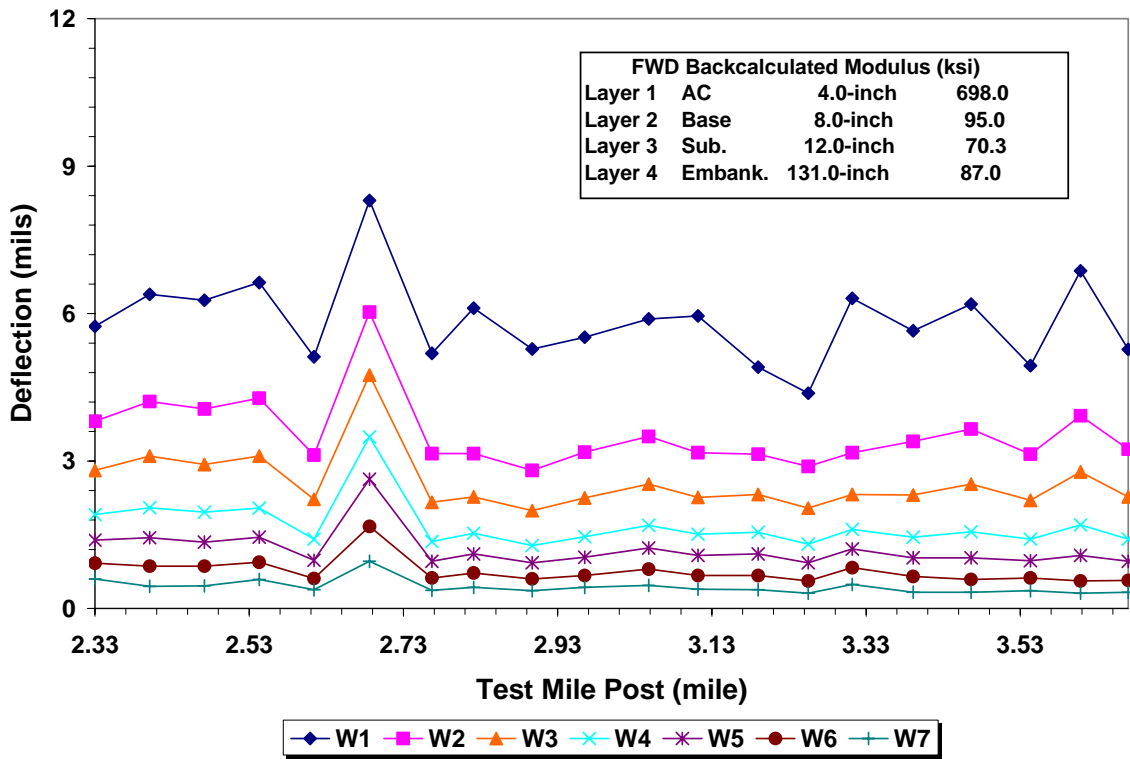


Figure B5. Illustration of FWD Data of 86190000 at Broward County.

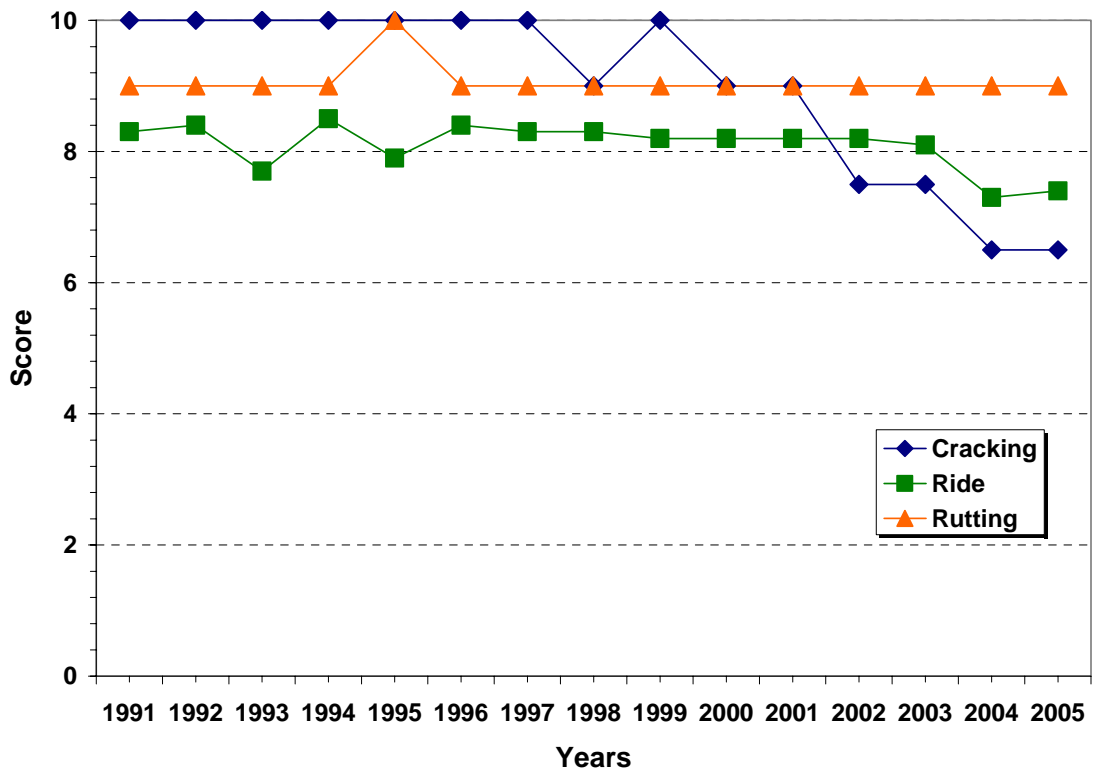


Figure B6. PCS Data of 86190000 at Broward County.

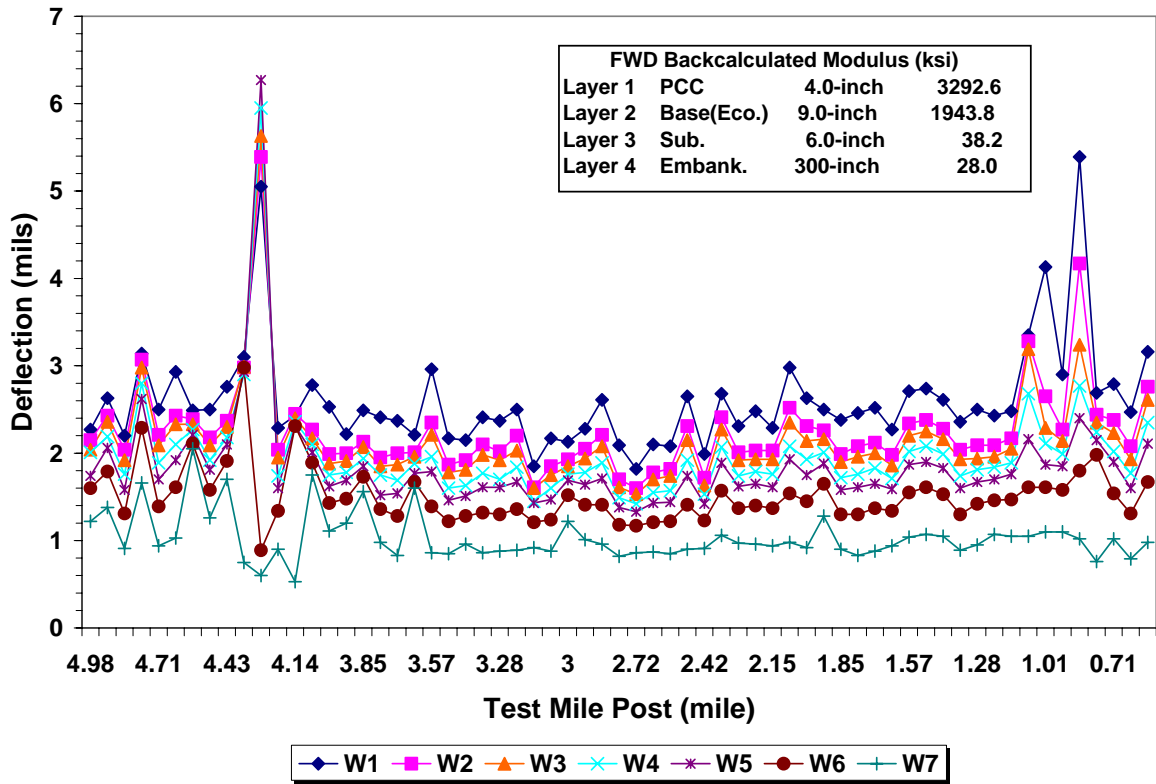


Figure B7. Illustration of FWD Data of 01010000 at Charlotte County.

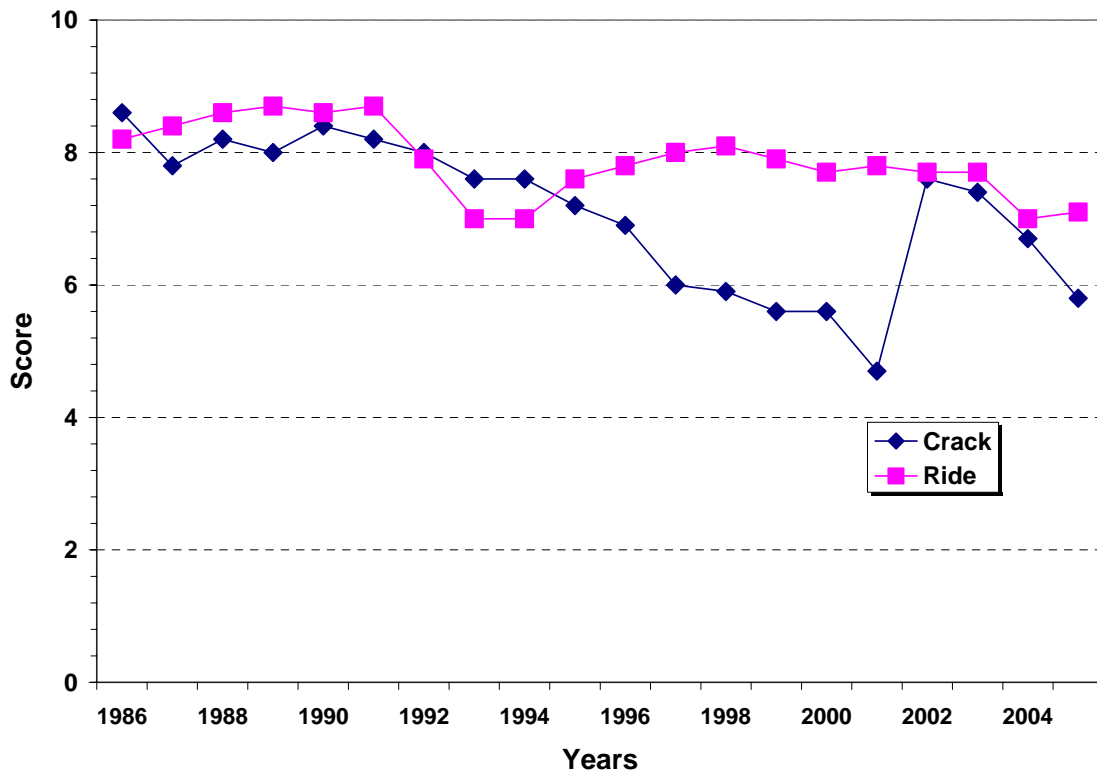


Figure B8. PCS Data of 01010000 at Charlotte County.

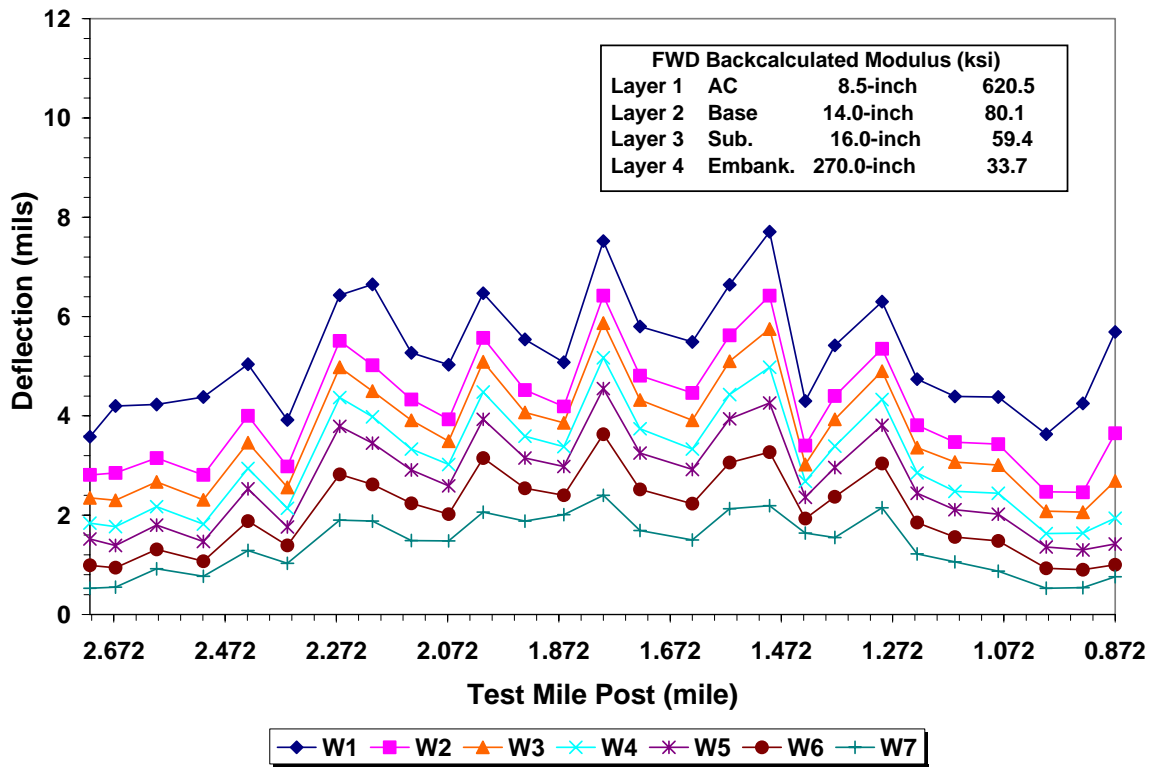


Figure B9. Illustration of FWD Data of 87060000 at Dade County.

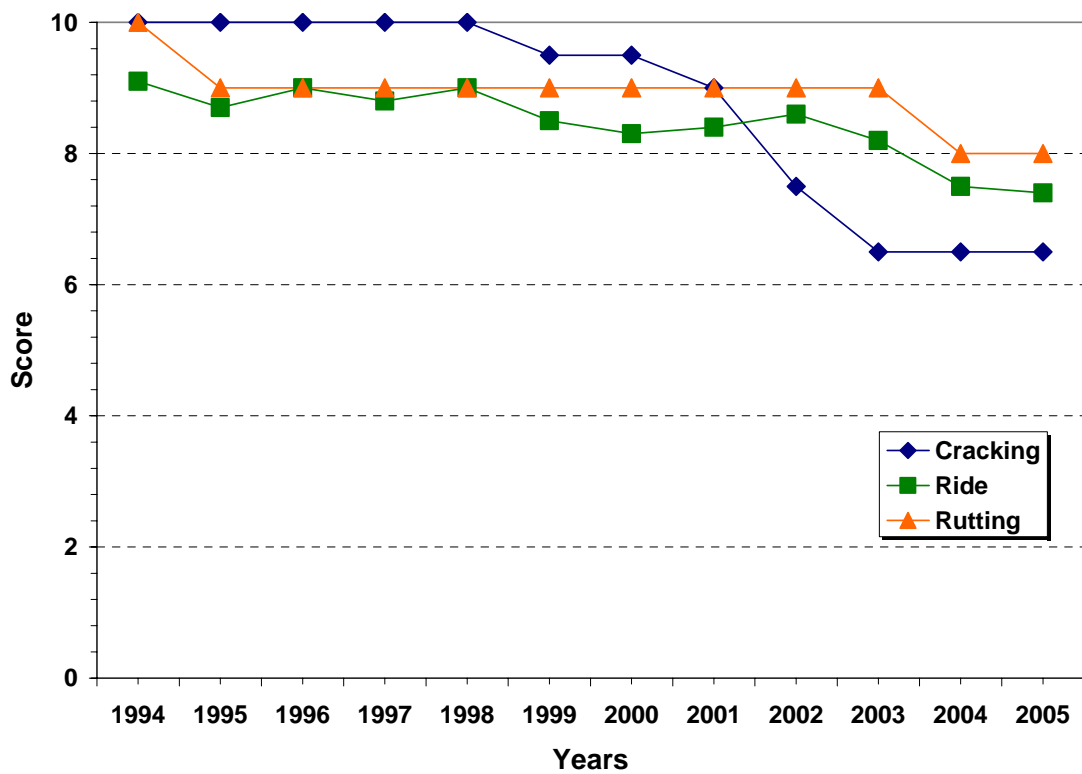


Figure B10. PCS Data of 87060000 at Dade County.

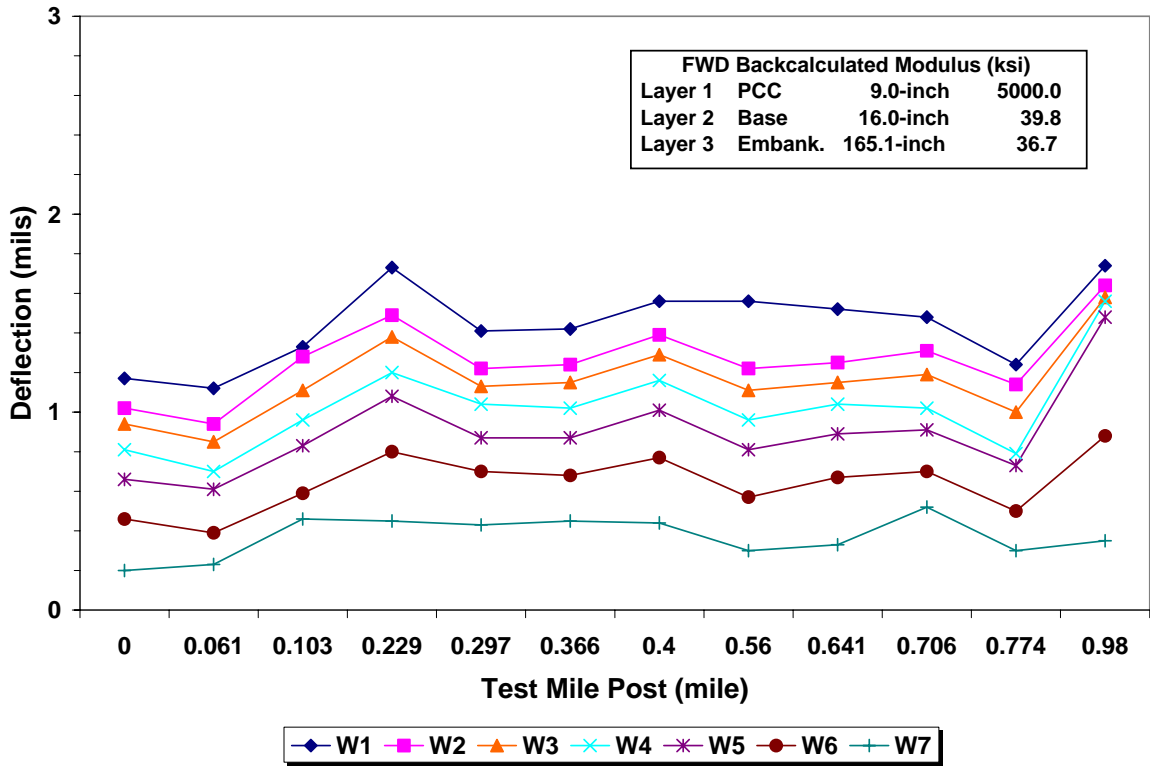


Figure B11. Illustration of FWD Data of 87270000 at Dade County.

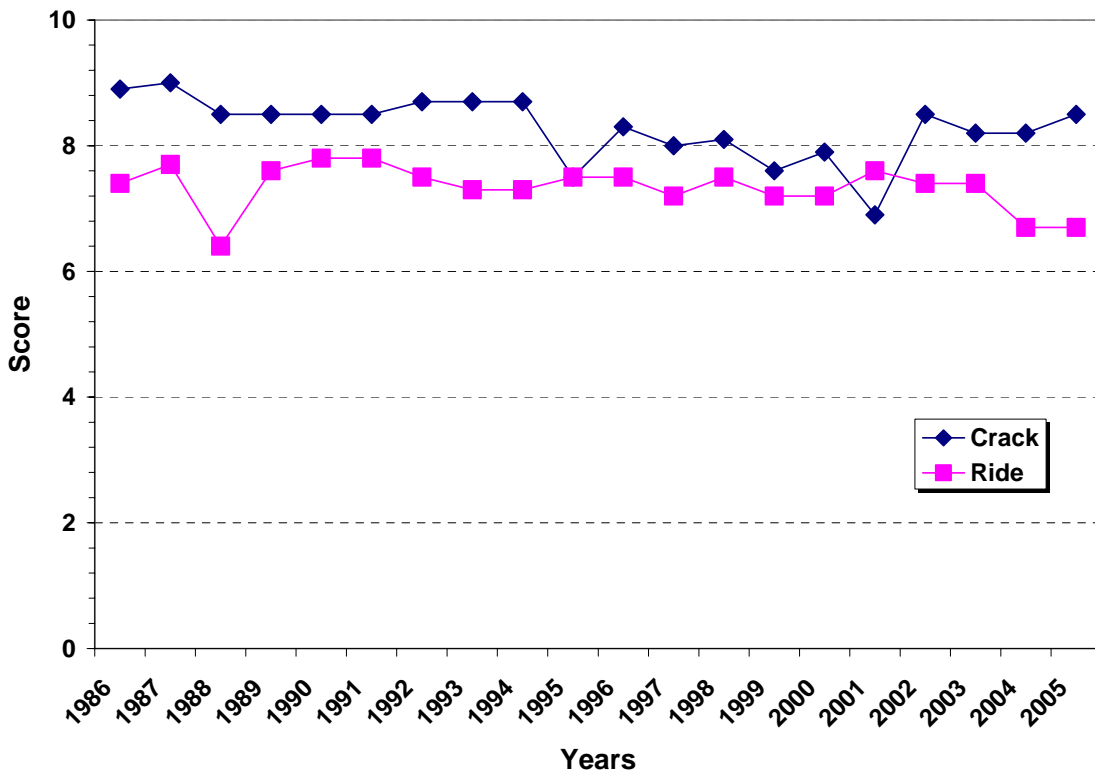


Figure B12. PCS Data of 87270000 at Dade County.

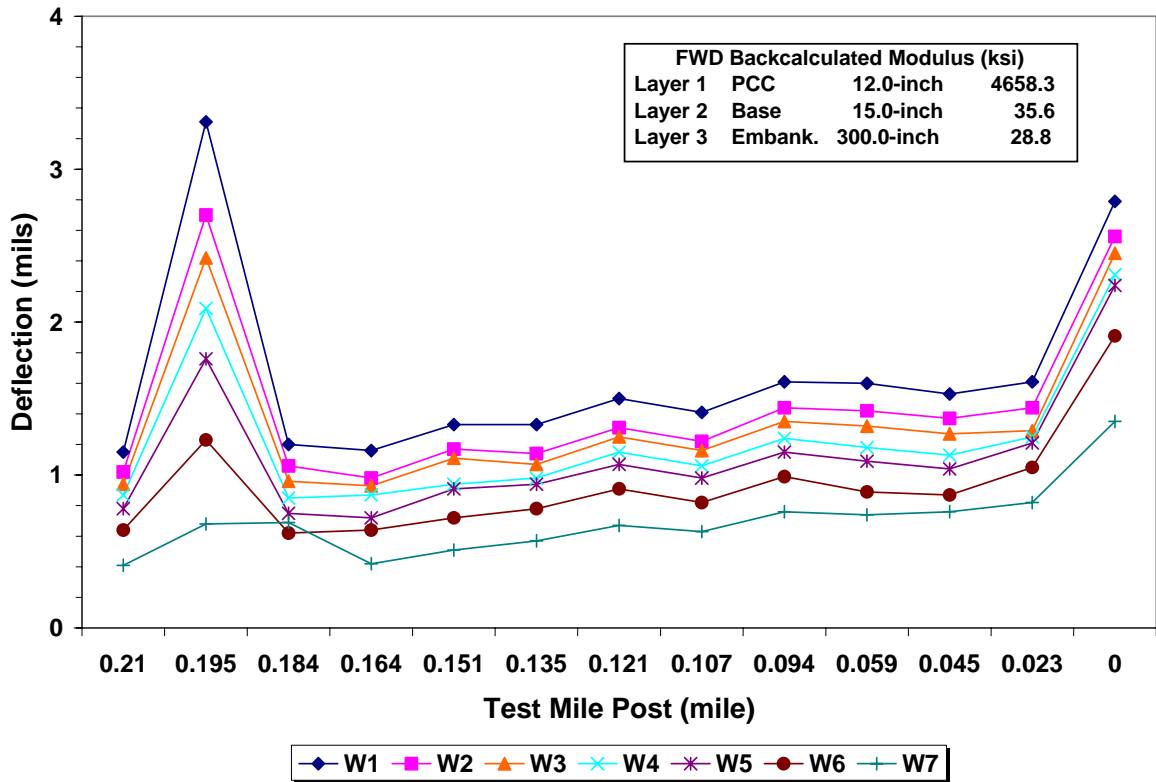


Figure B13. Illustration of FWD Data of 87061000 at Dade County.

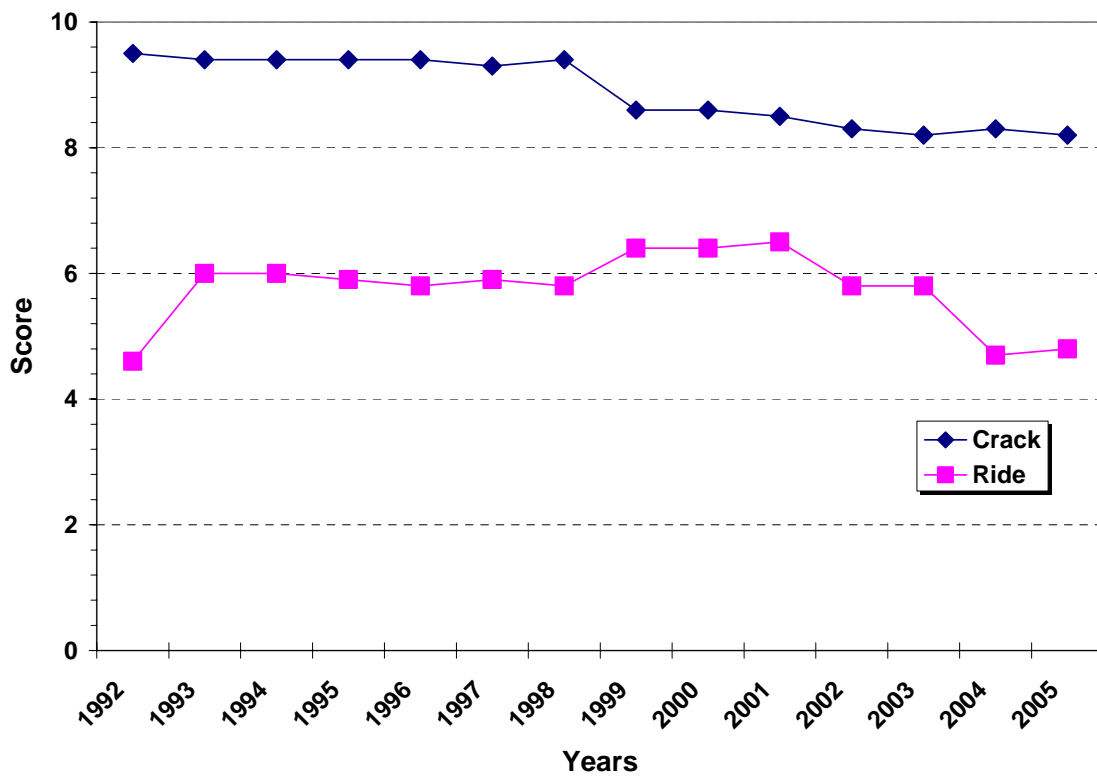


Figure B14. PCS Data of 87061000 at Dade County.

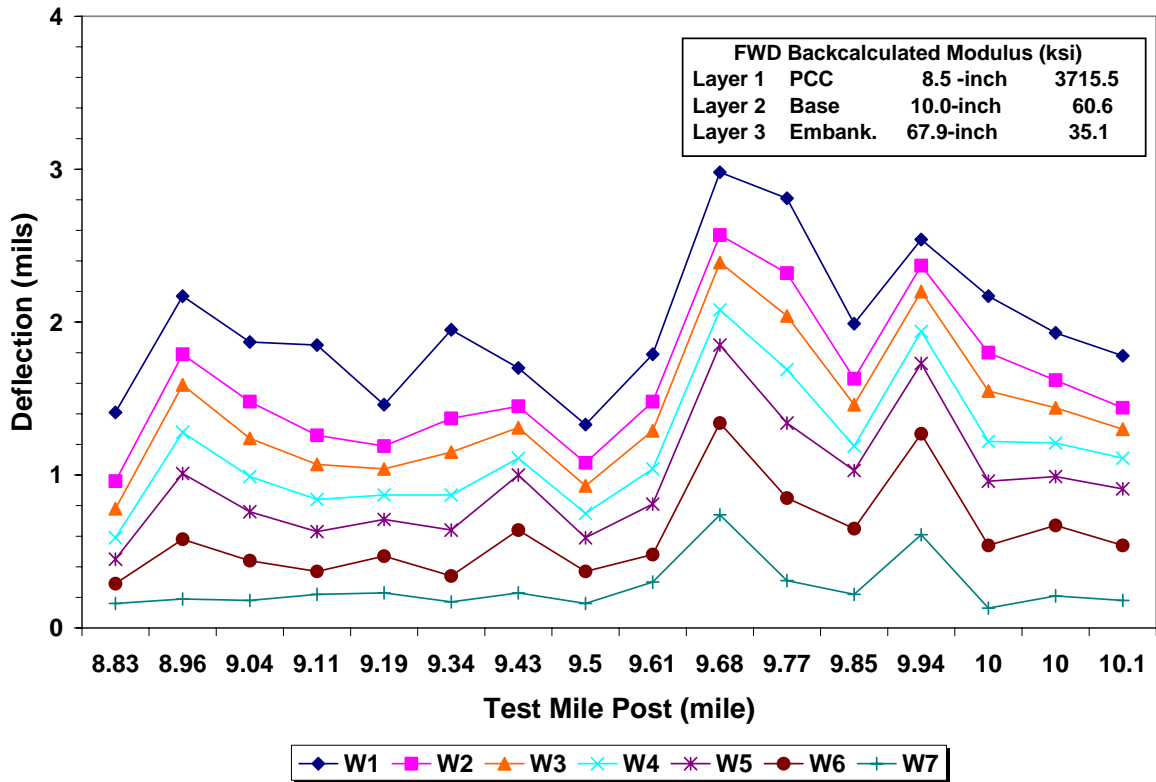


Figure B15. Illustration of FWD Data of 87030000R at Dade County.

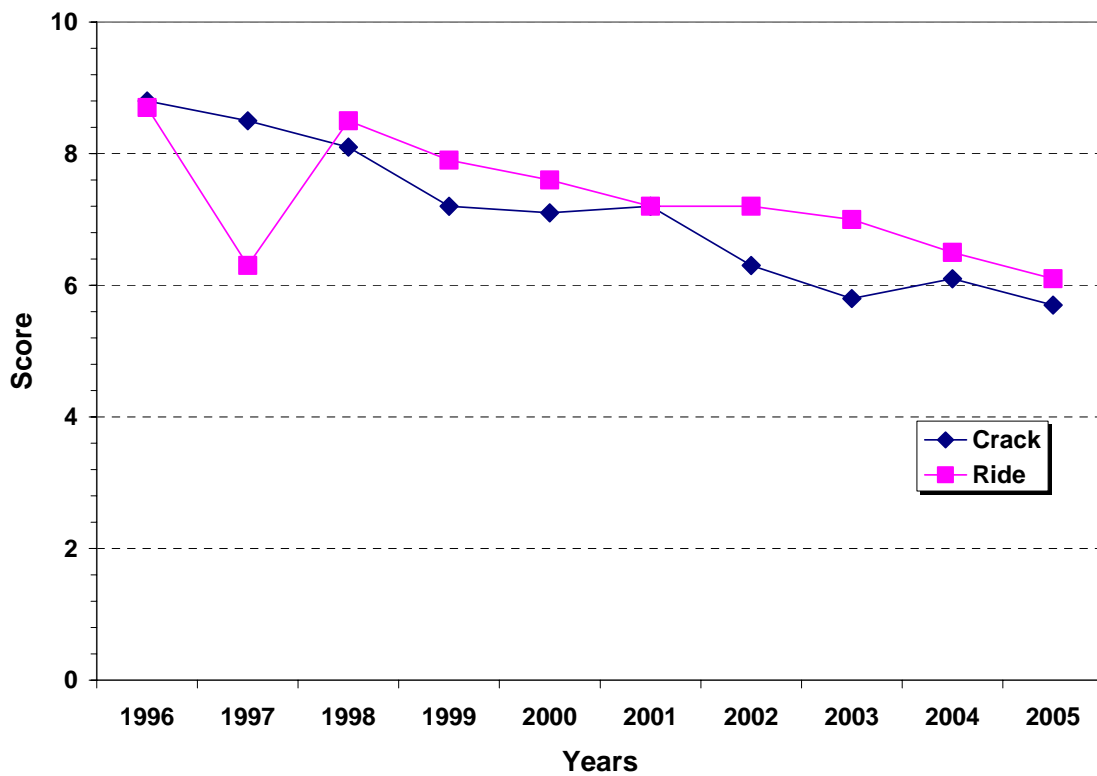


Figure B16. PCS Data of 87030000R at Dade County.

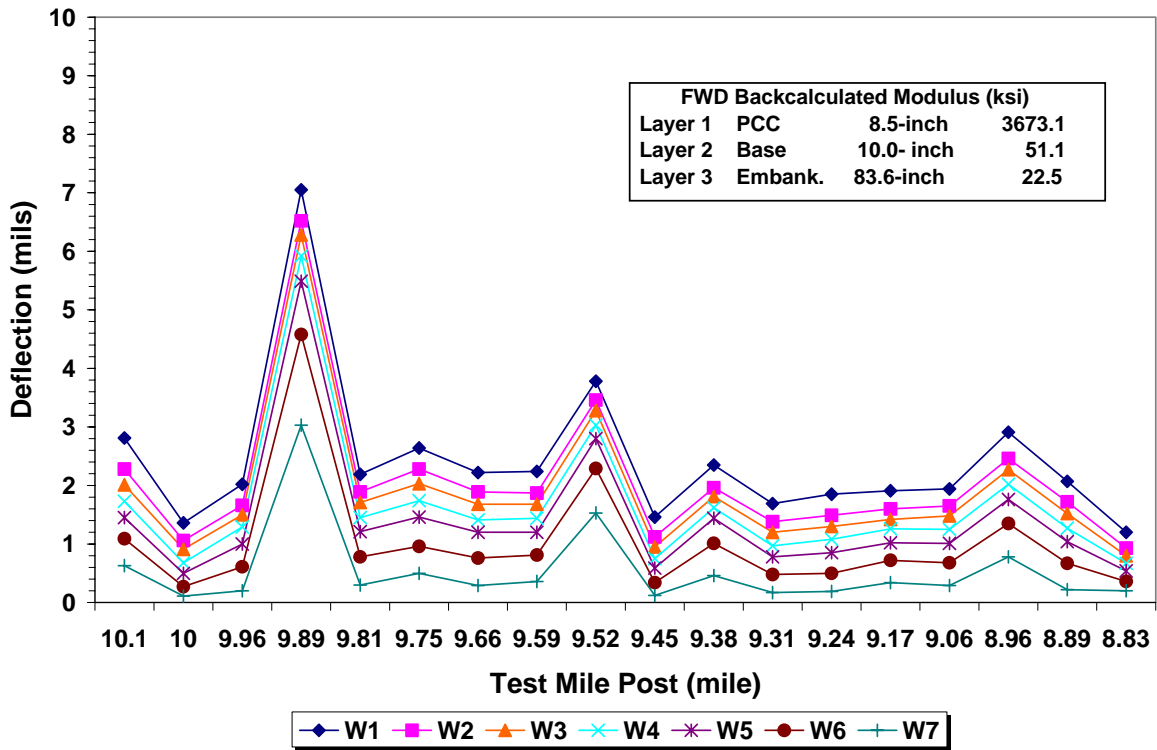


Figure B17. Illustration of FWD Data of 87030000L at Dade County.

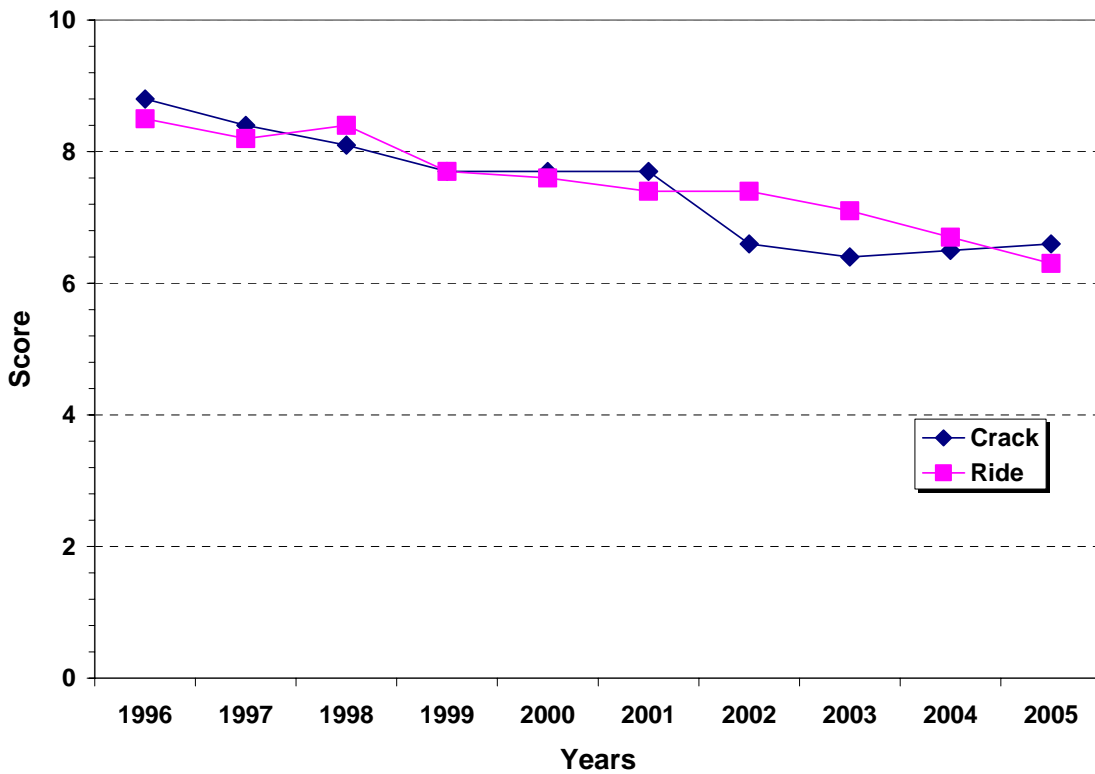


Figure B18. PCS Data of 87030000L at Dade County.

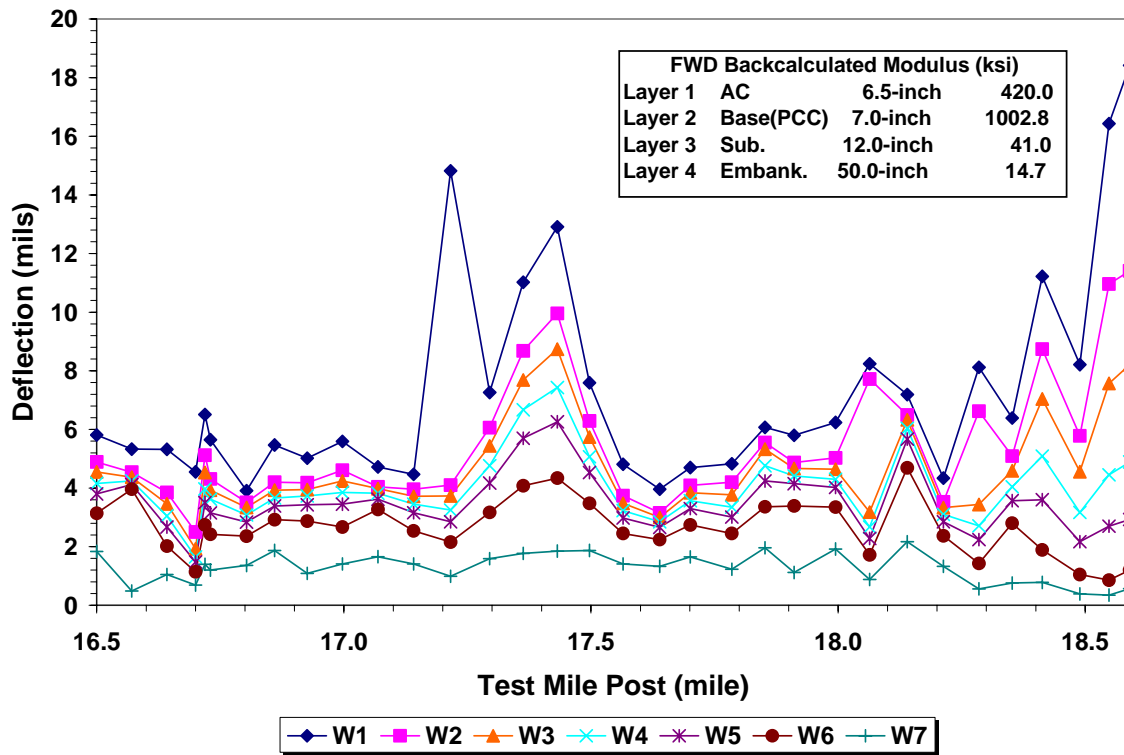


Figure B19. Illustration of FWD Data of 50010000 at Gadsden County.

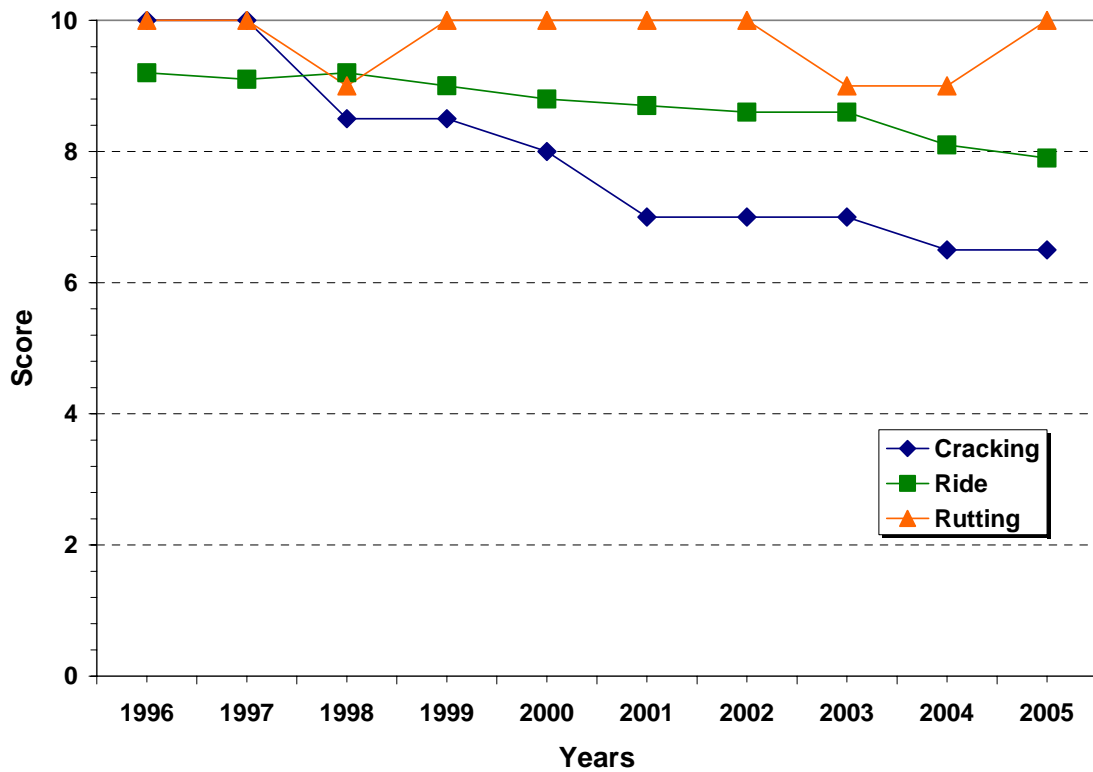


Figure B20. PCS Data of 50010000 at Gadsden County.

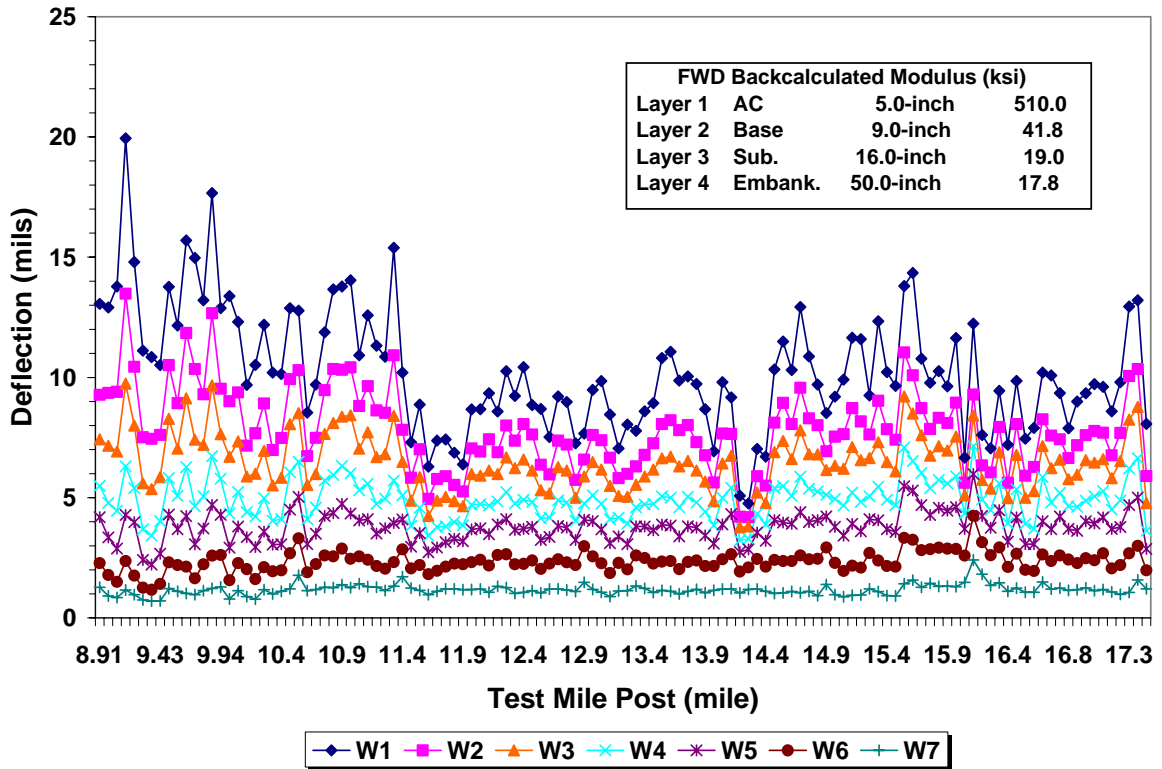


Figure B21. Illustration of FWD Data of 10060000 at Hillsborough County.

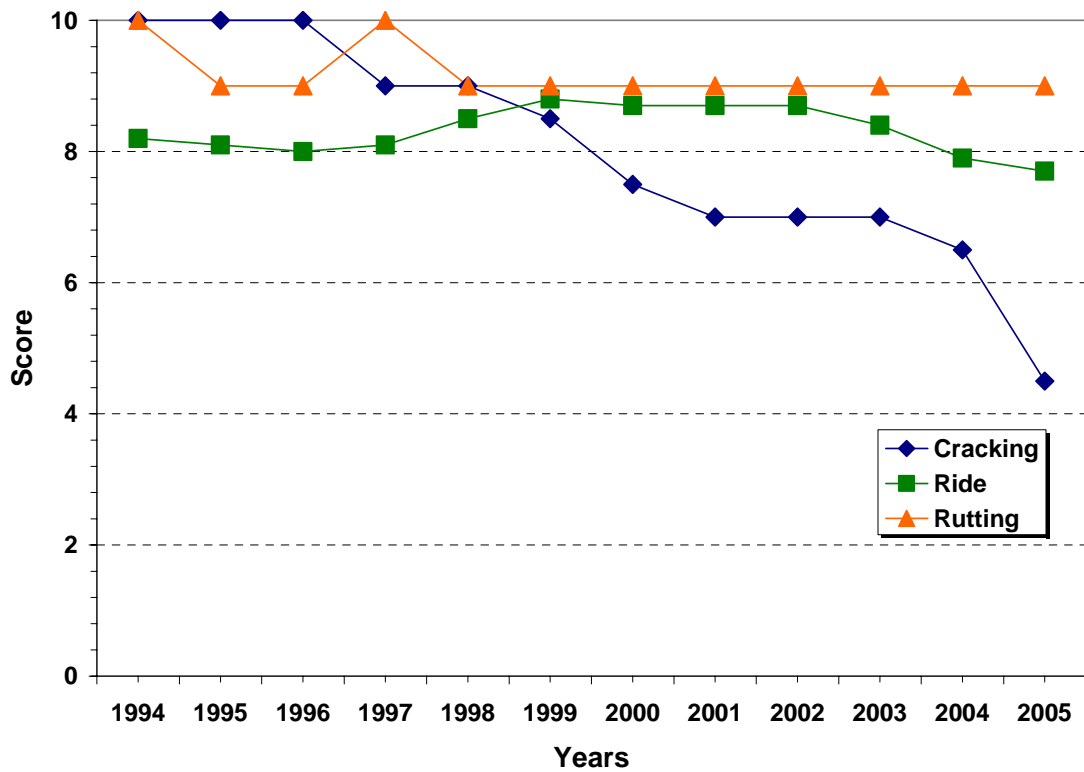


Figure B22. PCS Data of 10060000 at Hillsborough County.

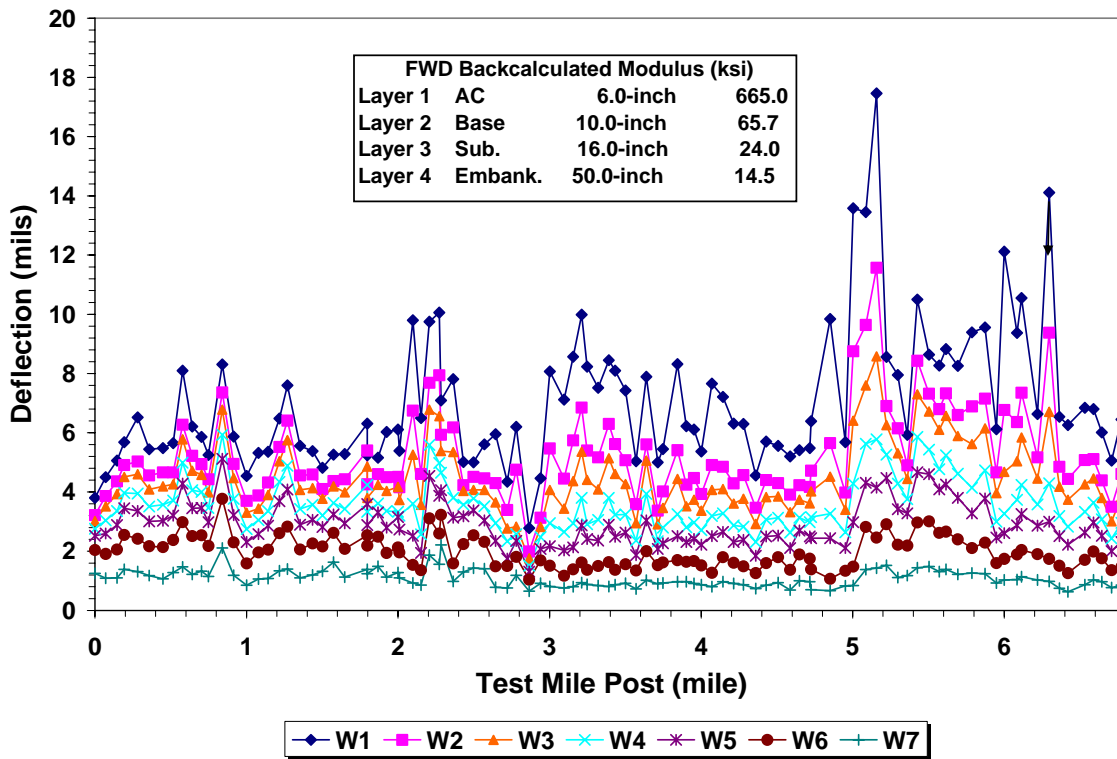


Figure B23. Illustration of FWD Data of 10160000 at Hillsborough County.

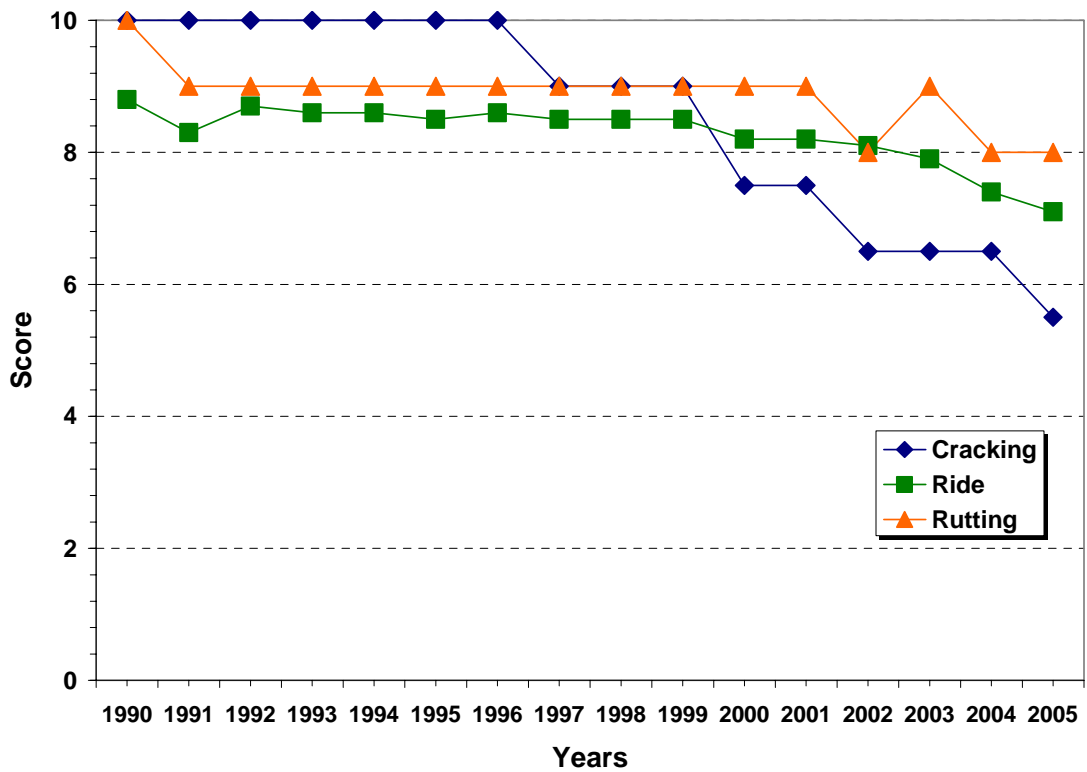


Figure B24. PCS Data of 10160000 at Hillsborough County.

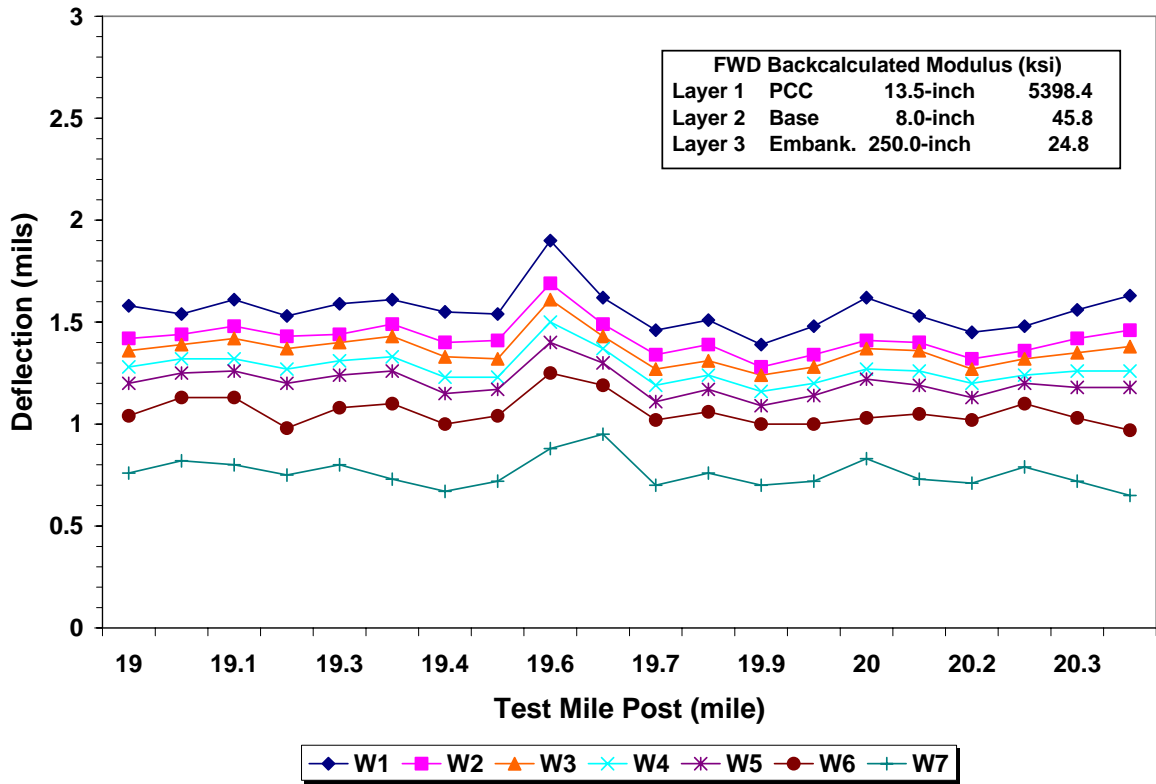


Figure B25. Illustration of FWD Data of 10075000A at Hillsborough County.

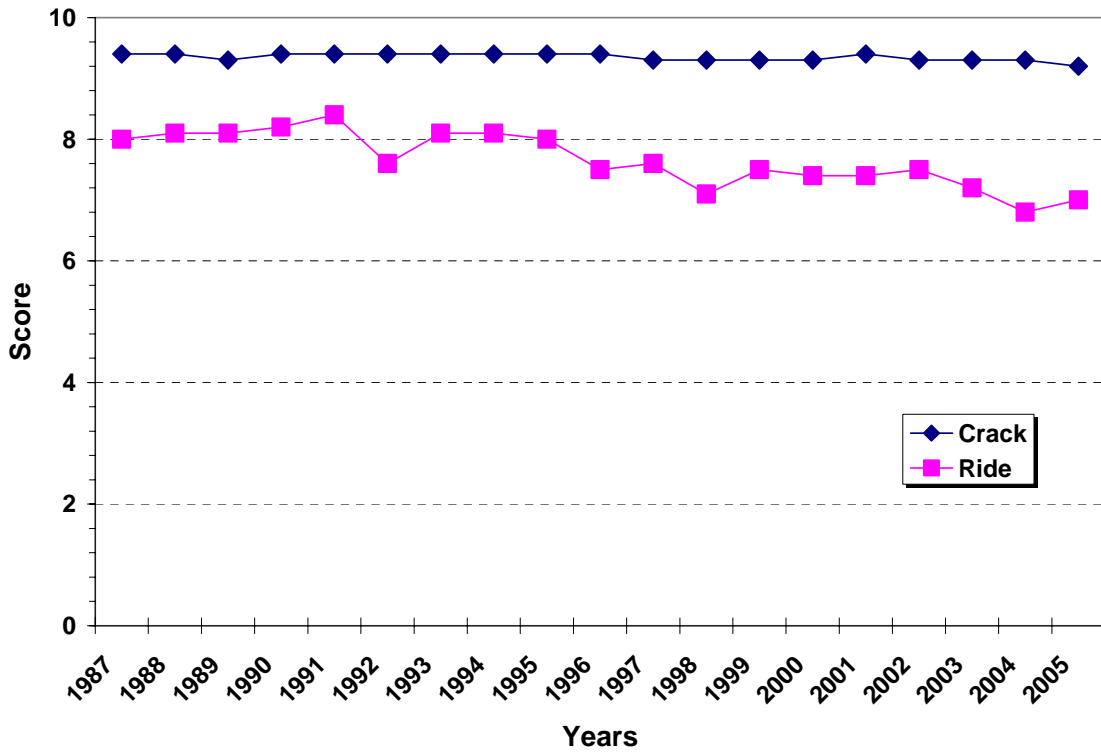


Figure B26. PCS Data of 10075000A at Hillsborough County.

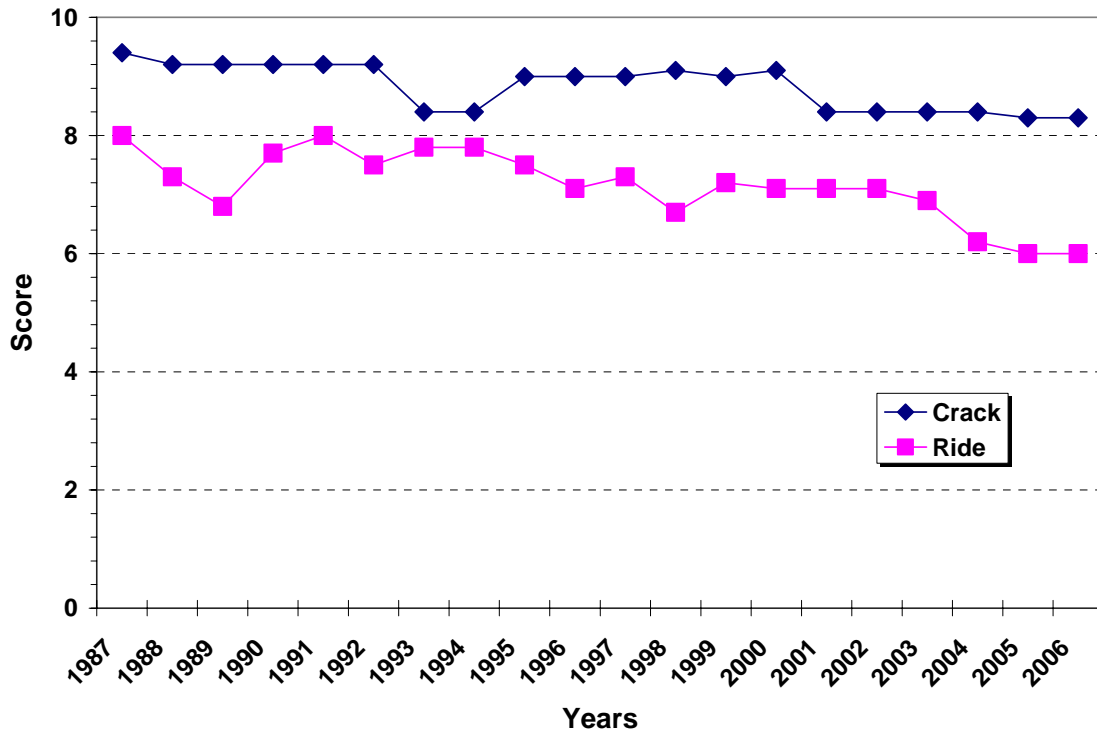


Figure B27. PCS Data of 10075000B at Hillsborough County.

Note: This section limit is from 23.4 to 24.69 miles. The section was added later during the project so FWD test was not performed.

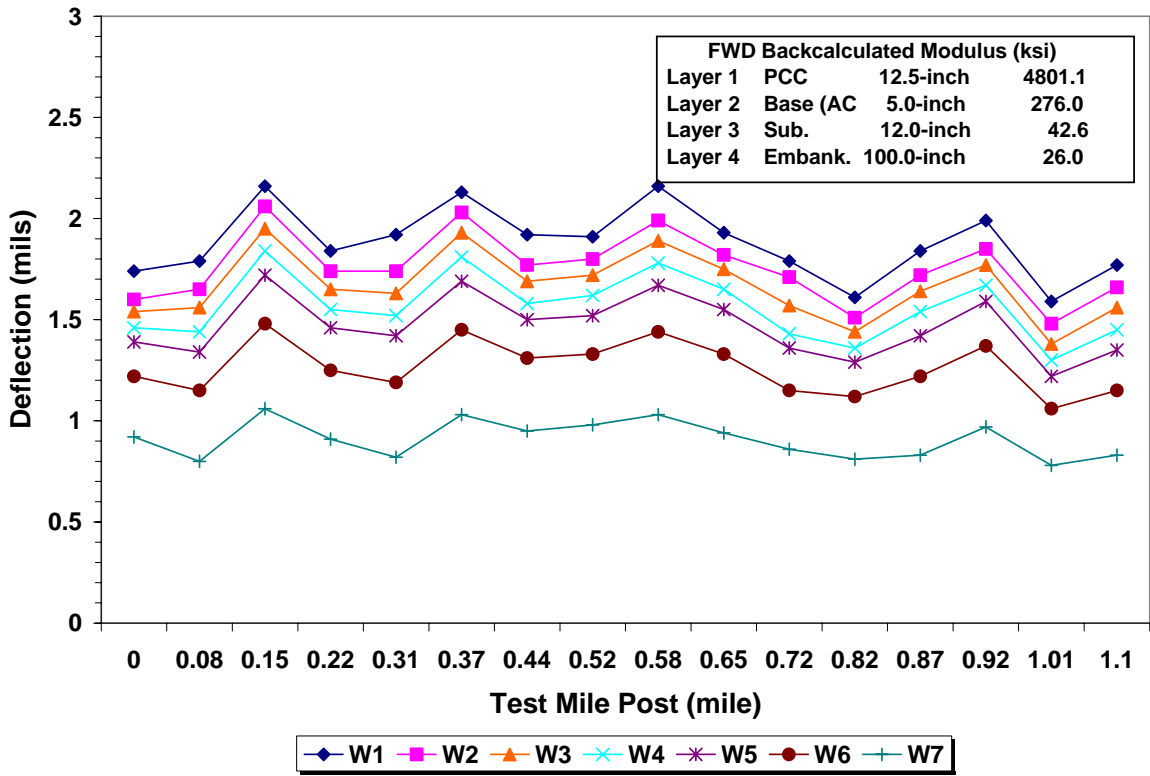


Figure B28. Illustration of FWD Data of 10250001 at Hillsborough County.

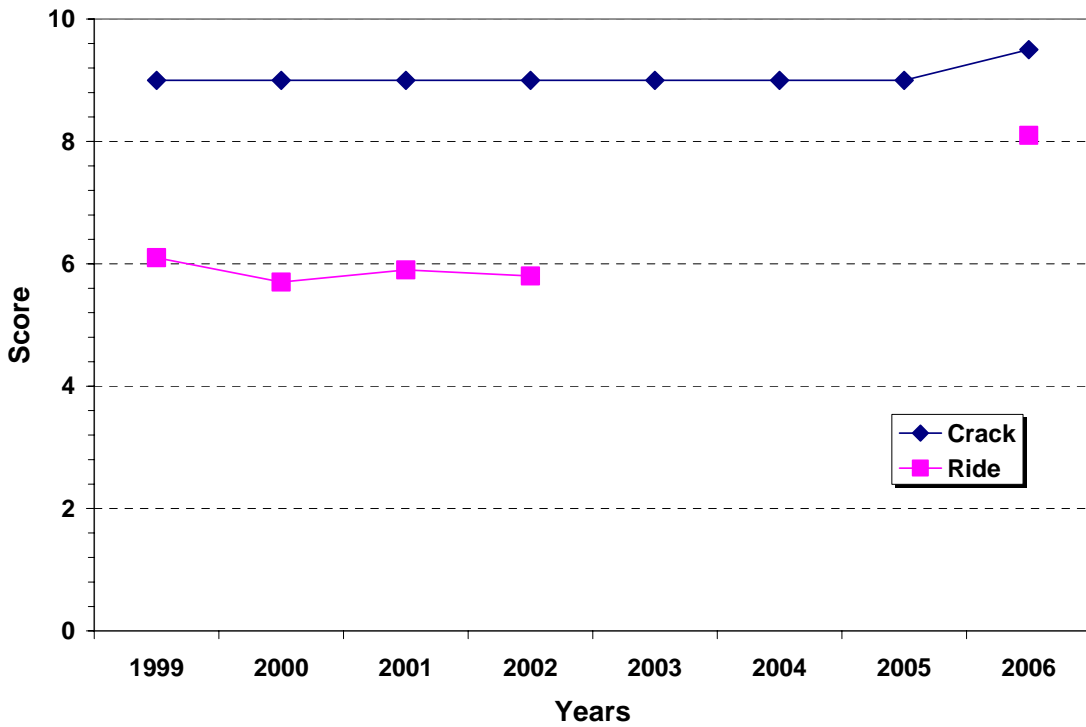


Figure B29. PCS Data of 10250001 at Hillsborough County.

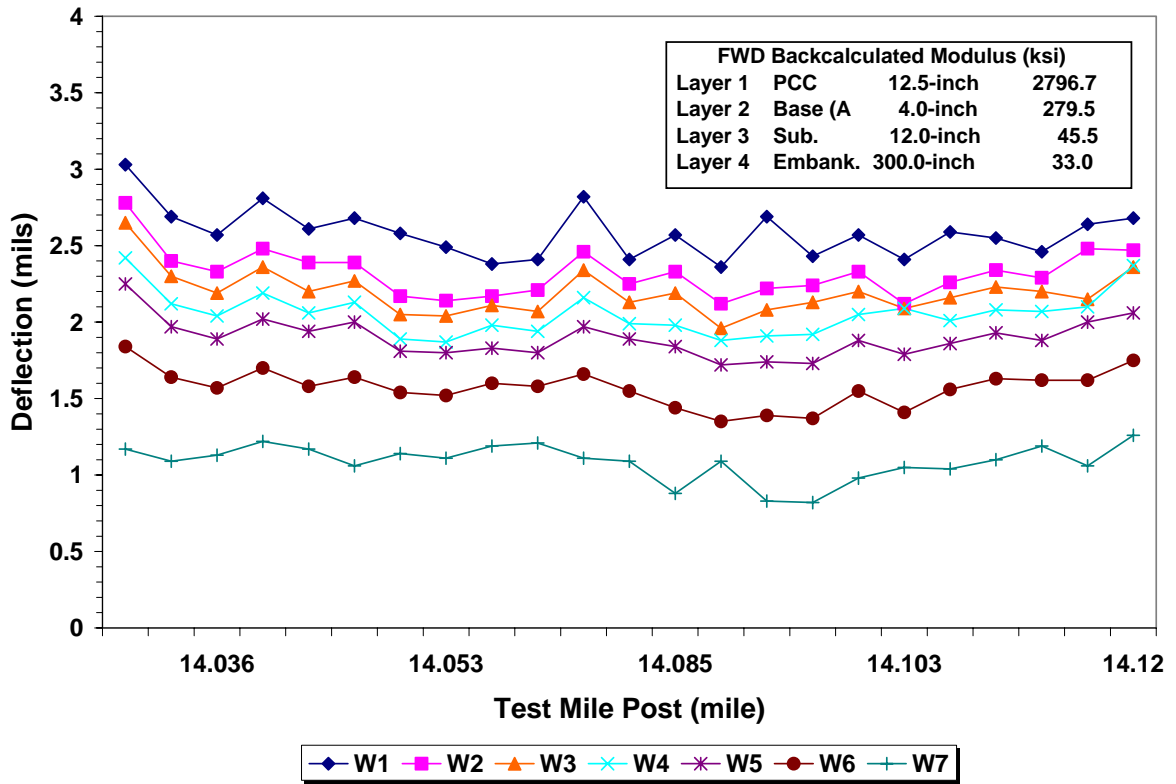


Figure B30. Illustration of FWD Data of 11020000 at Lake County.

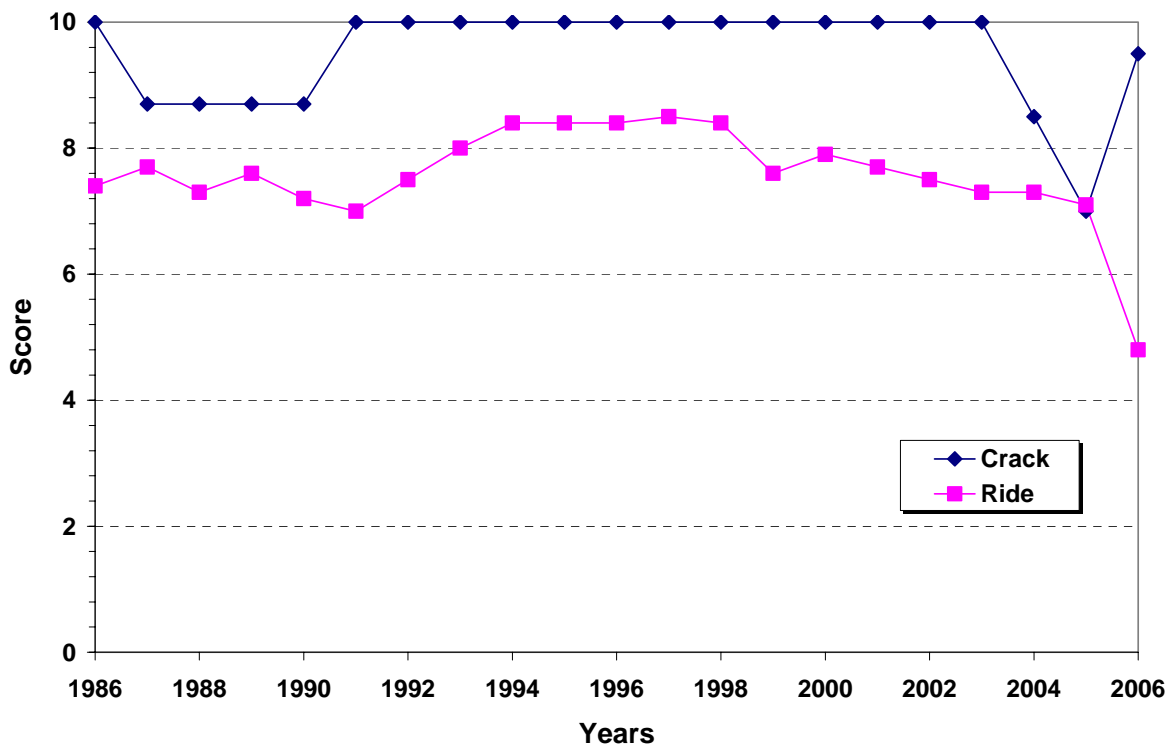


Figure B31. PCS Data of 11020000 at Lake County.

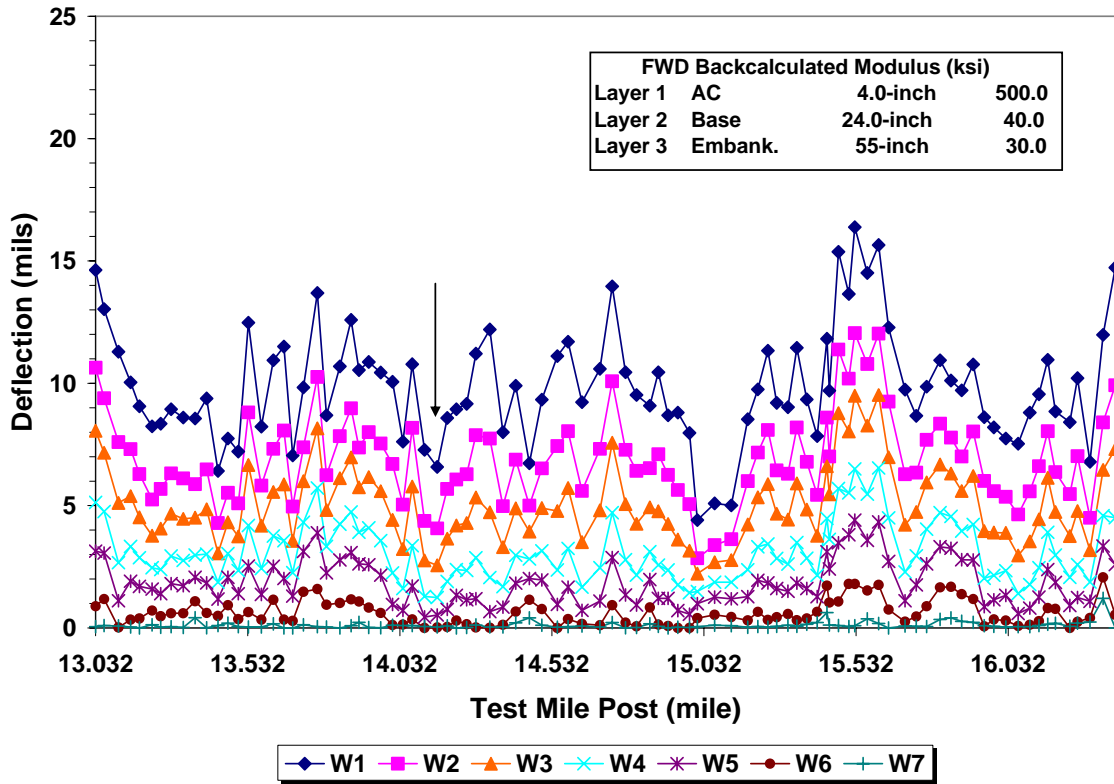


Figure B32. Illustration of FWD Data of 90060000 at Monroe County.

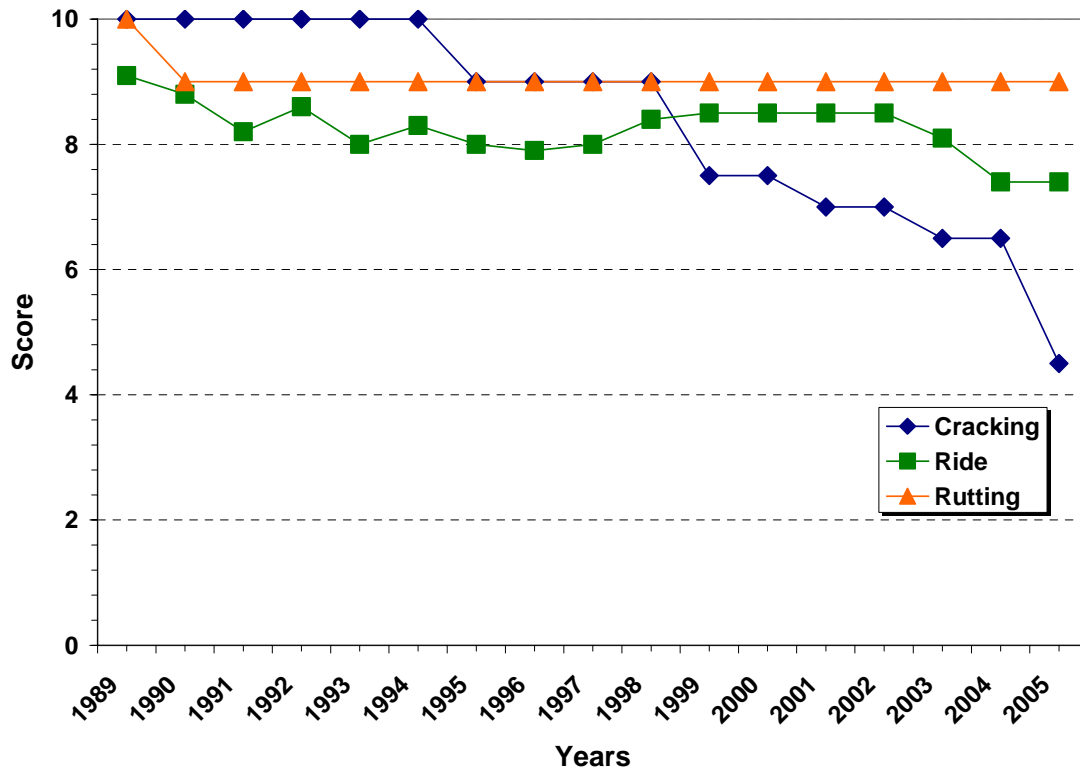


Figure B33. PCS Data of 90060000 at Monroe County.

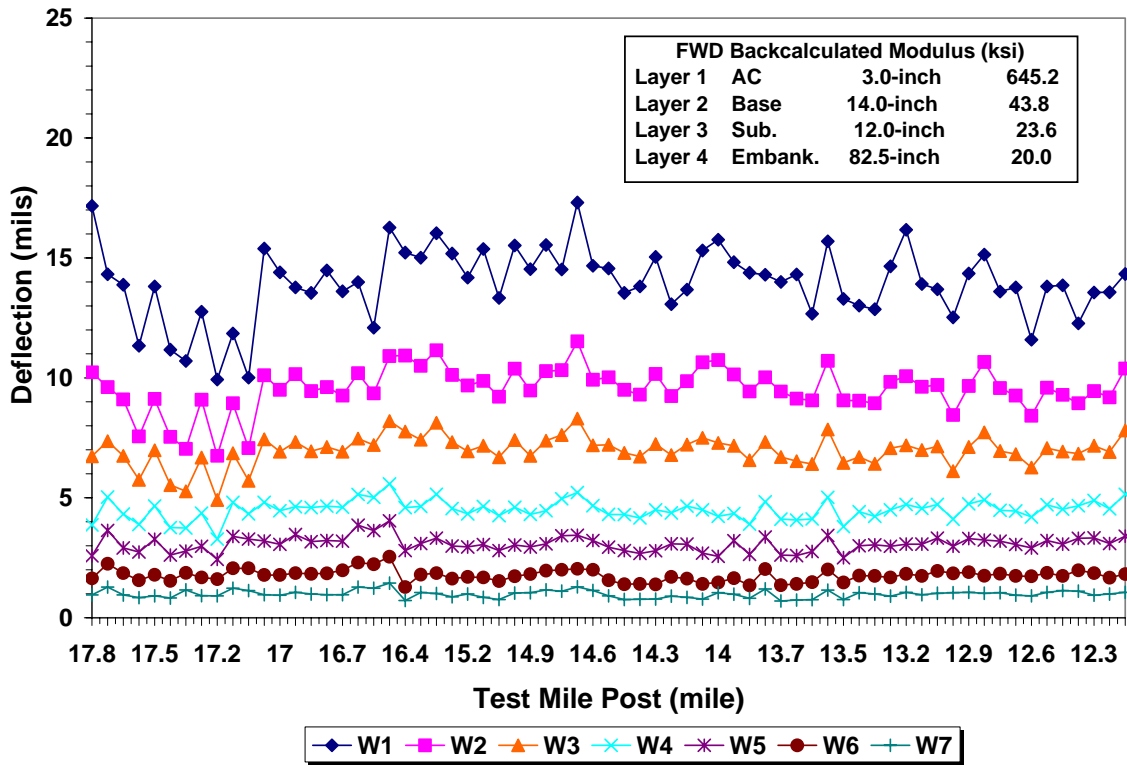


Figure B34. Illustration of FWD Data of 93310000 at Palm Beach County.

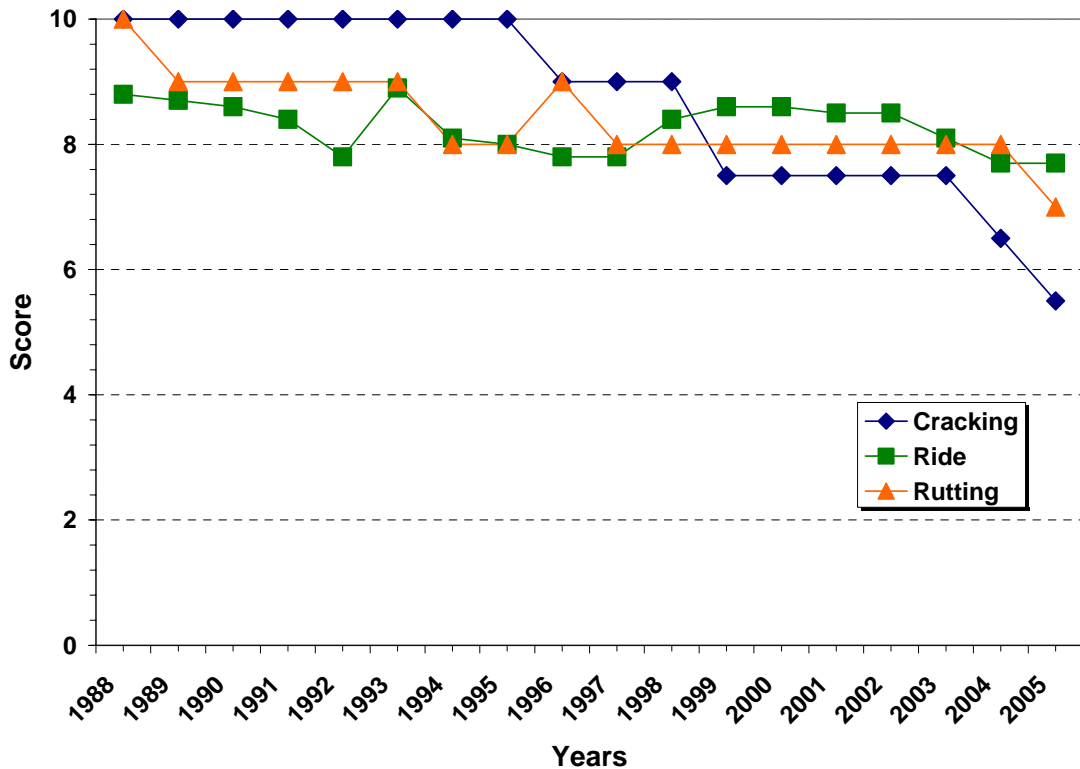


Figure B35. PCS Data of 93310000 at Palm Beach County.

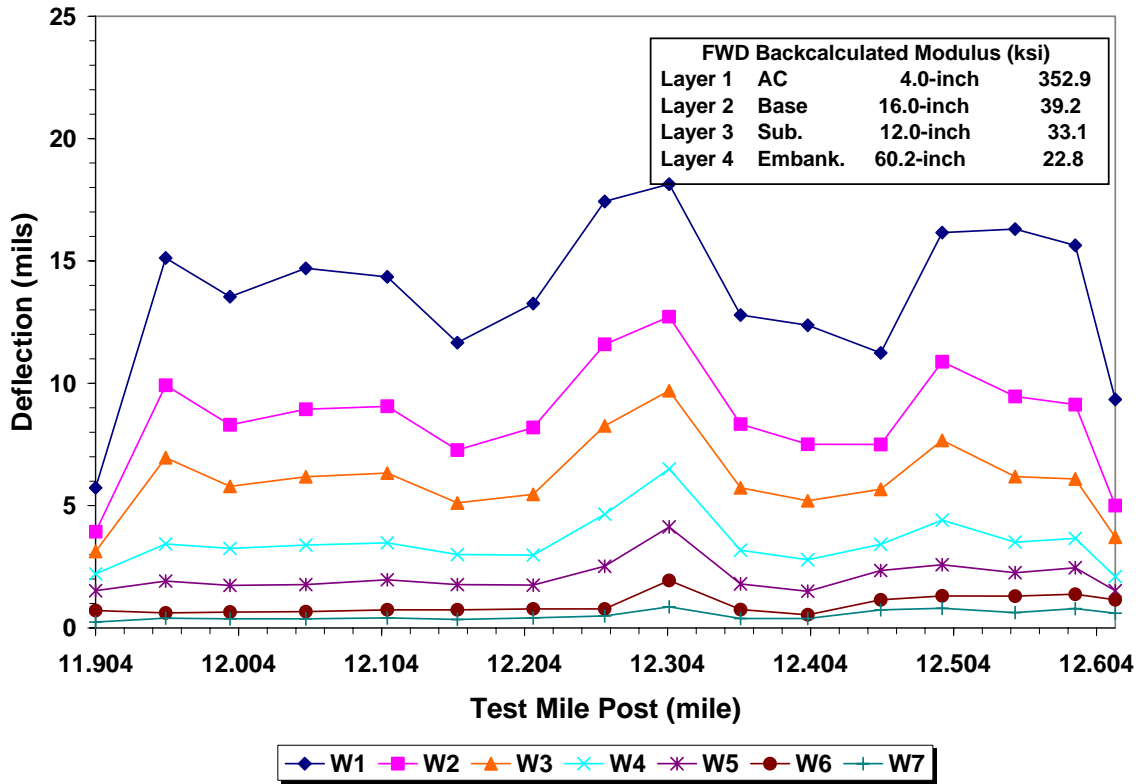


Figure B36. Illustration of FWD Data of 93100000 at Palm Beach County.

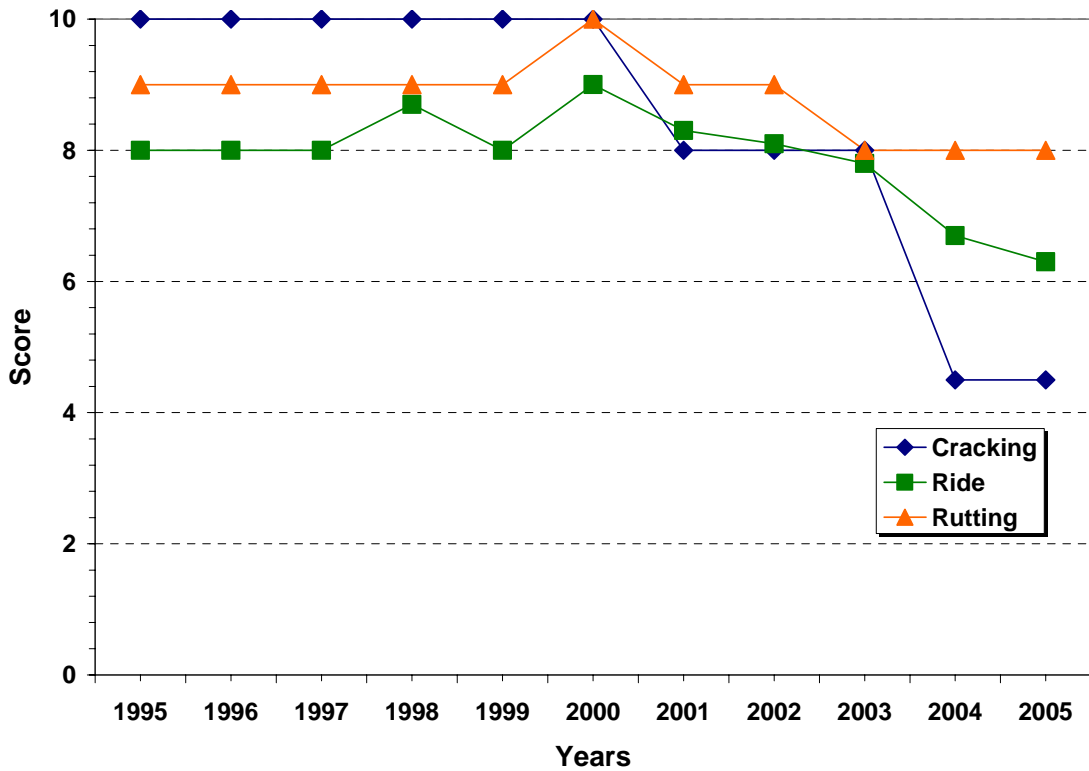


Figure B37. PCS Data of 93100000 at Palm Beach County.

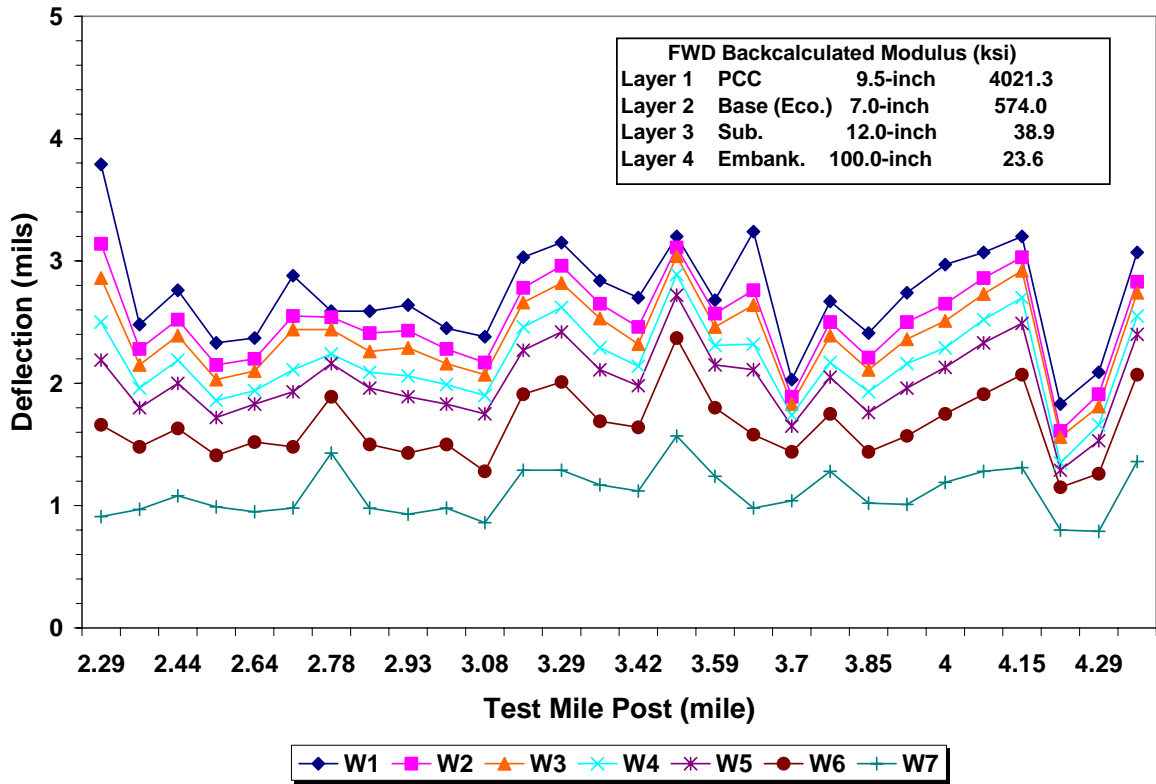


Figure B38. Illustration of FWD Data of 15190000R at Pinellas County.

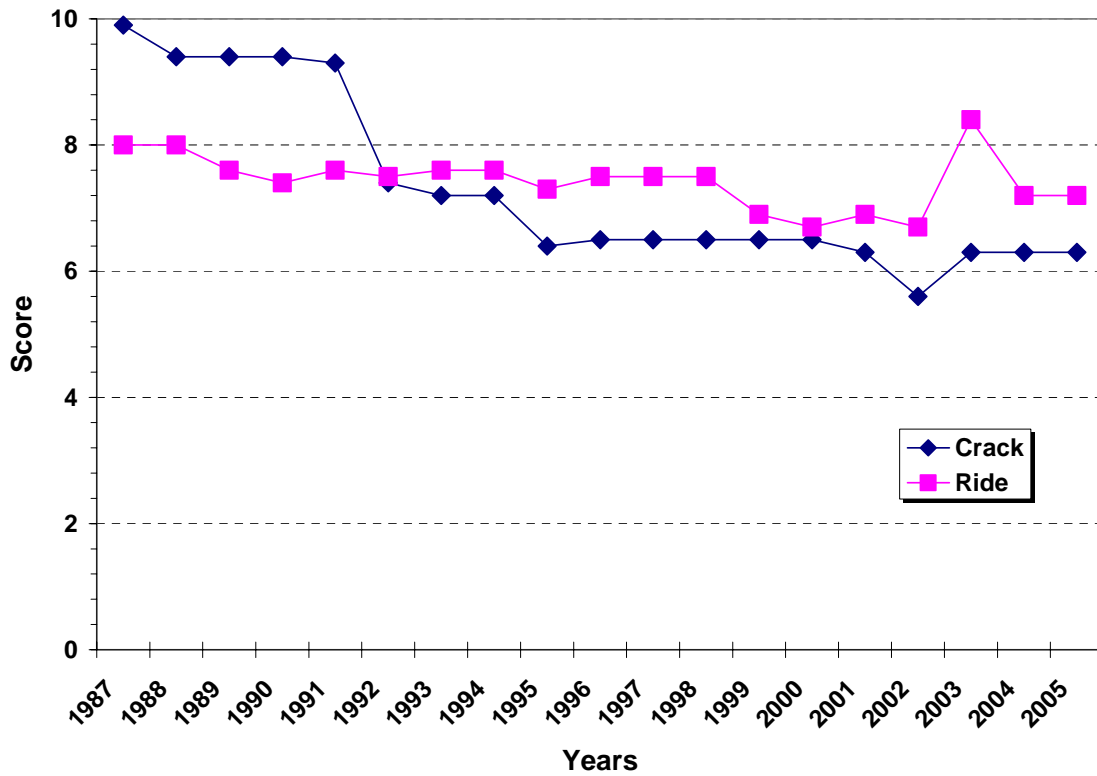


Figure B39. PCS Data of 15190000R at Pinellas County.

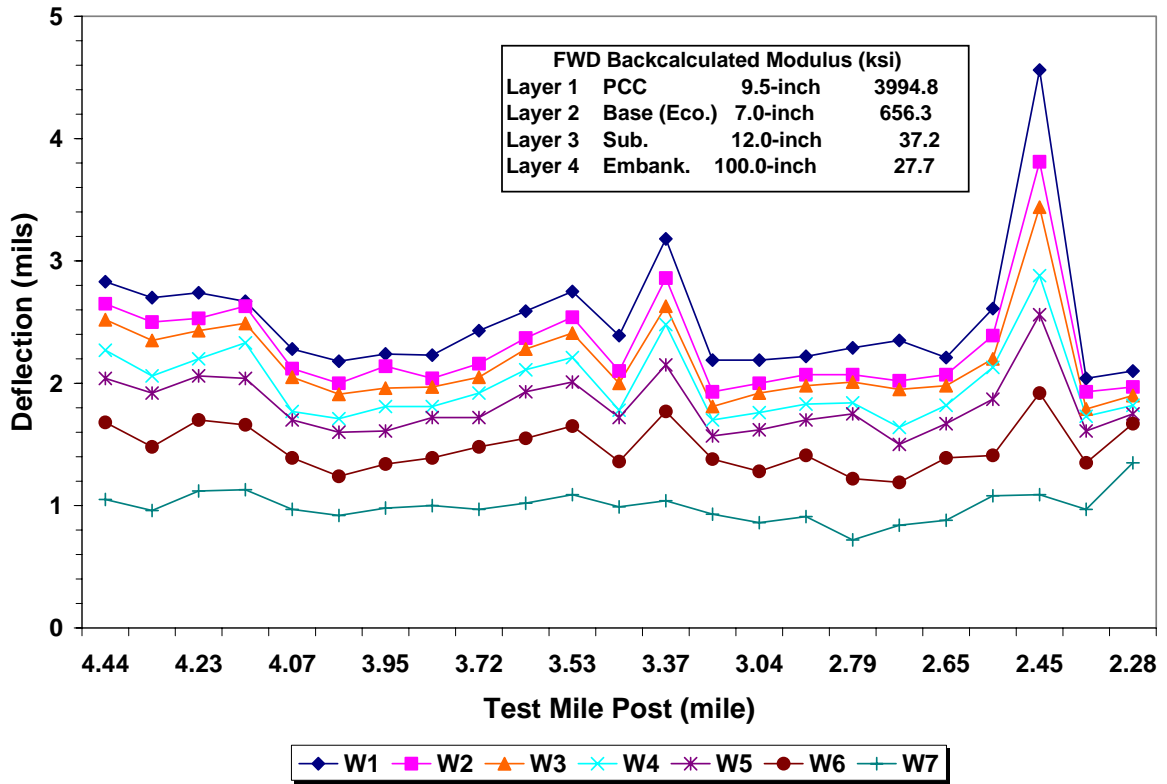


Figure B40. Illustration of FWD Data of 15190000L at Pinellas County.

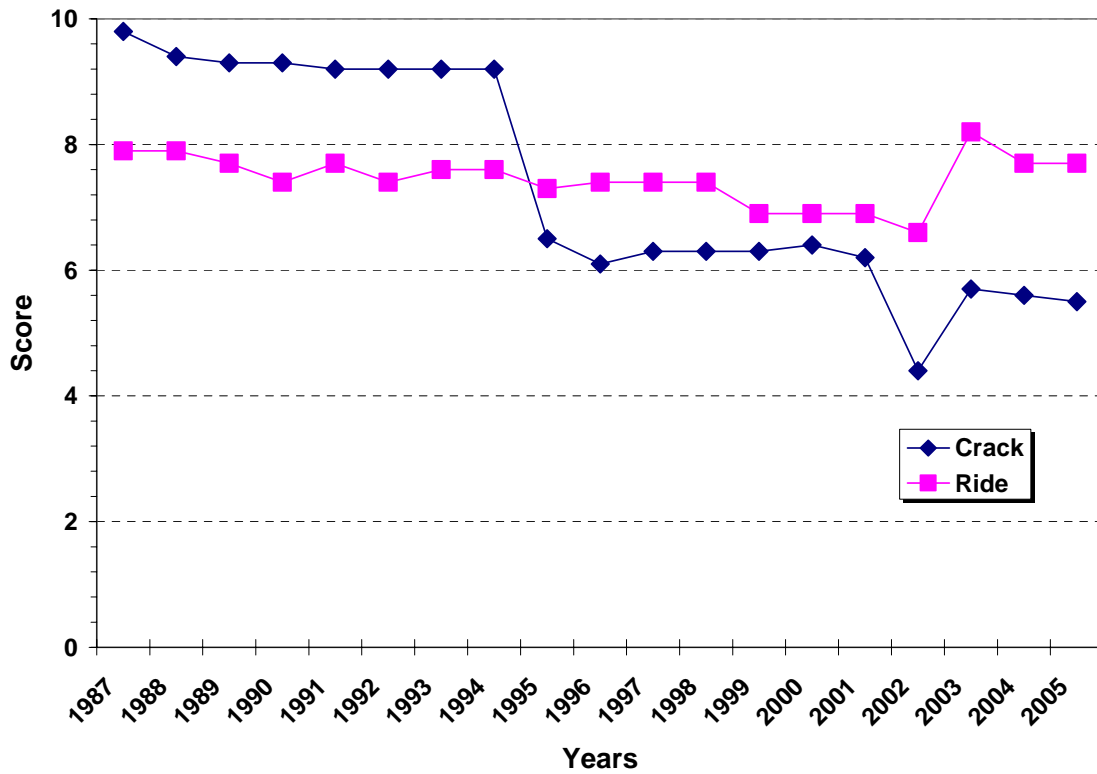


Figure B41. PCS Data of 15190000L at Pinellas County.

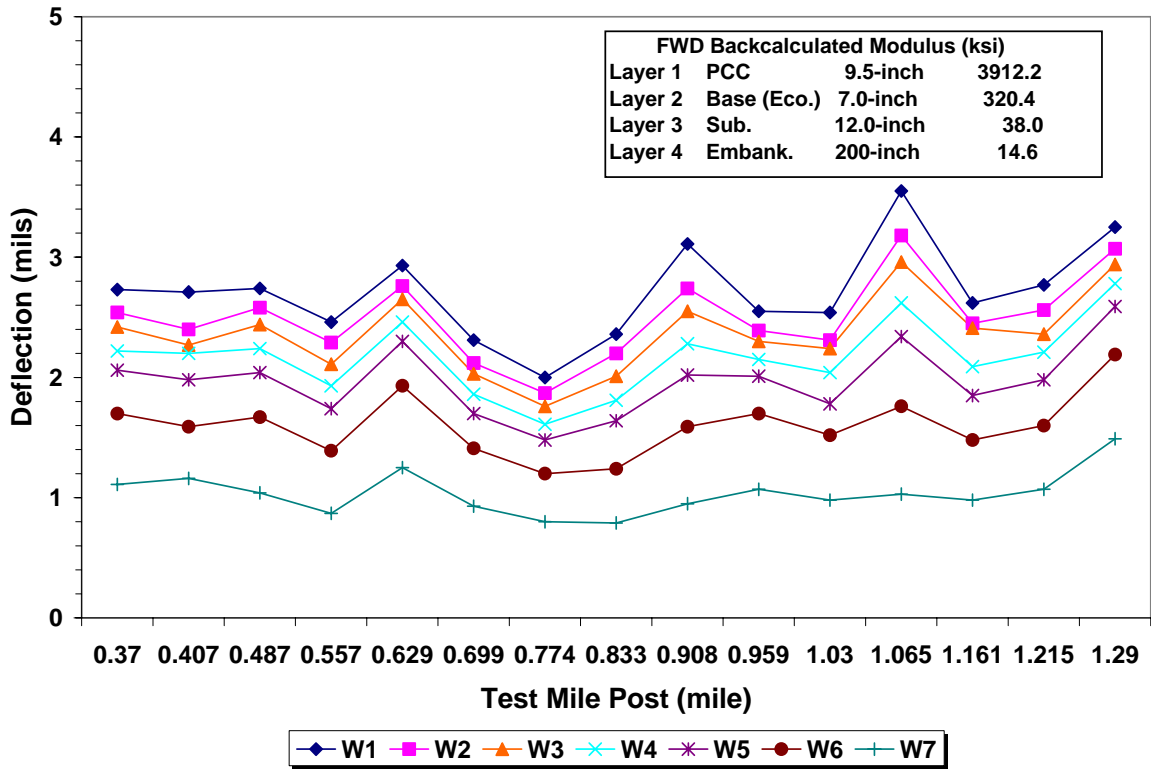


Figure B42. Illustration of FWD Data of 15003000R at Pinellas County.

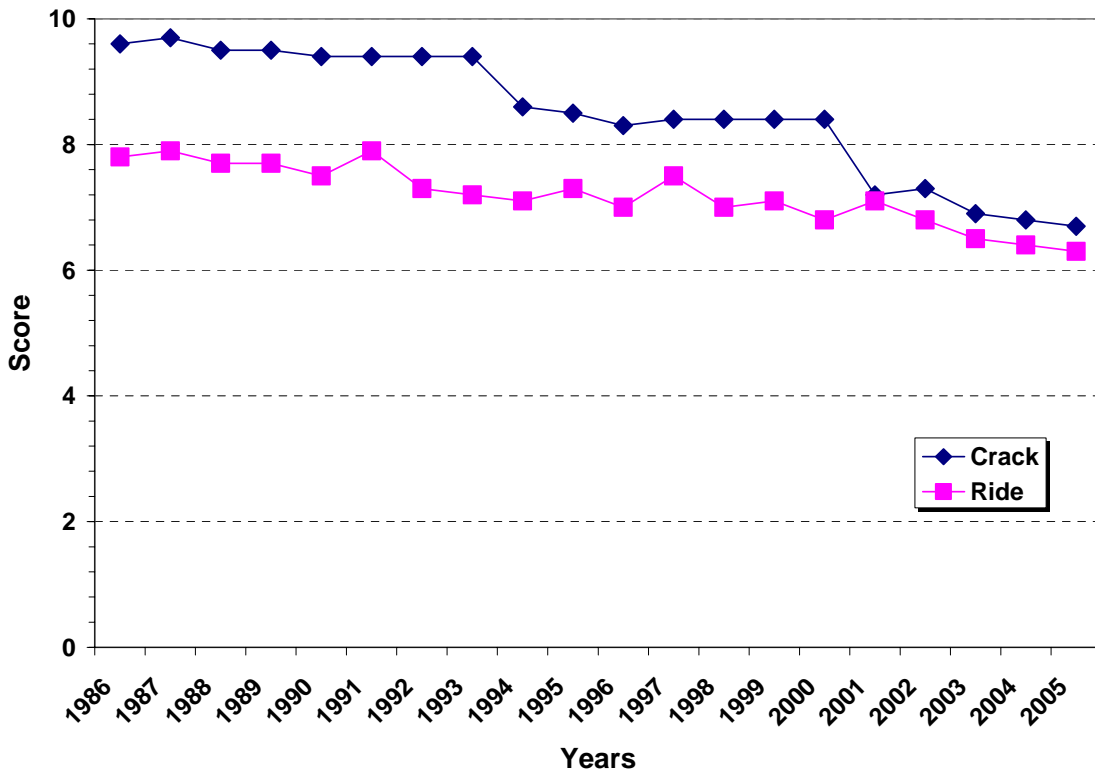


Figure B43. PCS Data of 15003000R at Pinellas County.

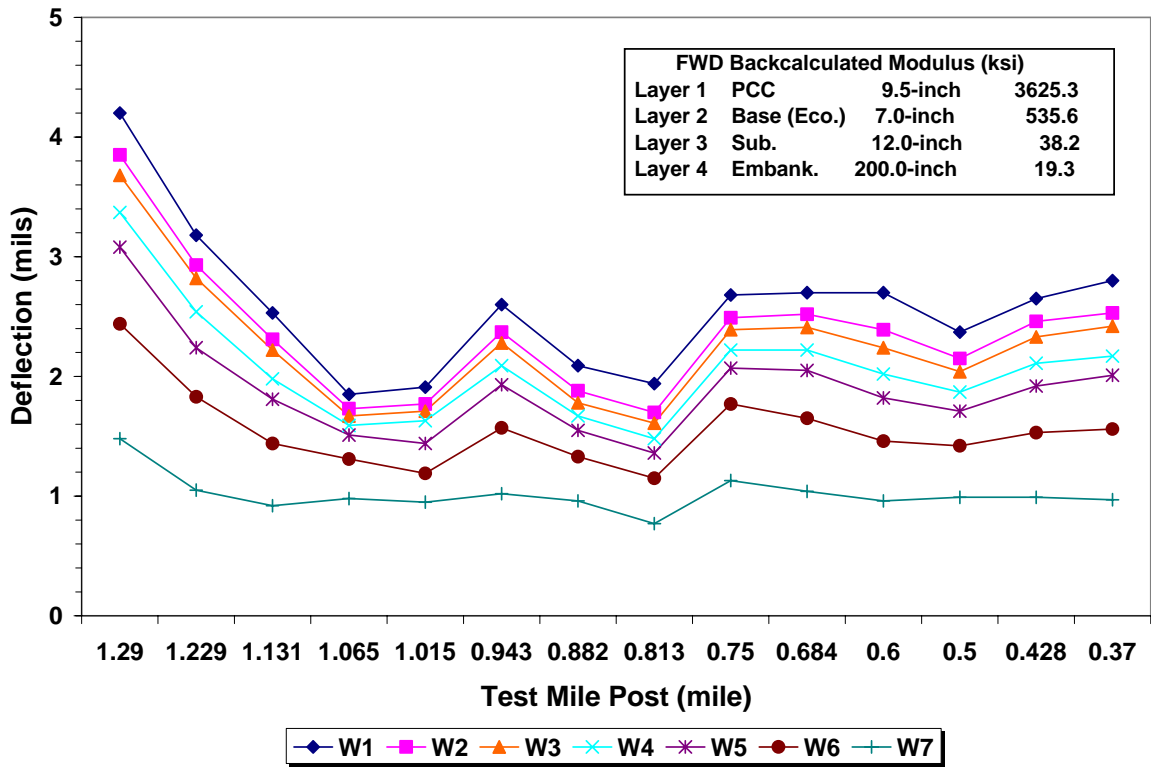


Figure B44. Illustration of FWD Data of 15003000L at Pinellas County.

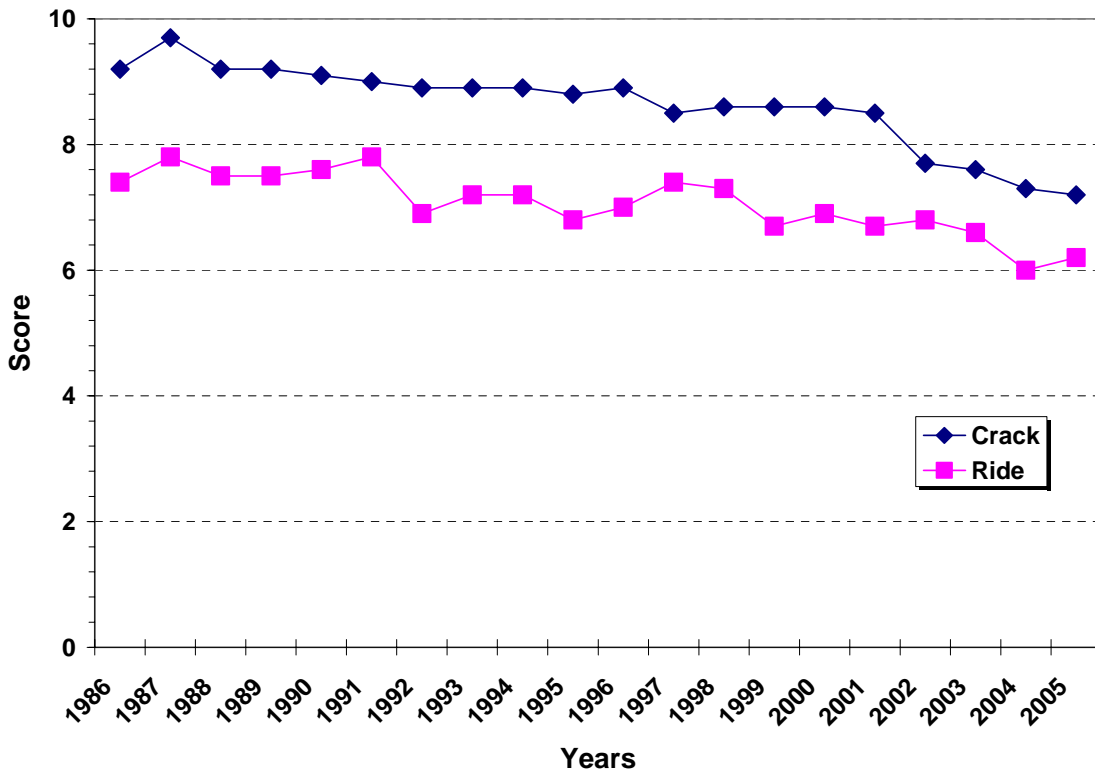


Figure B45. PCS Data of 15003000L at Pinellas County.

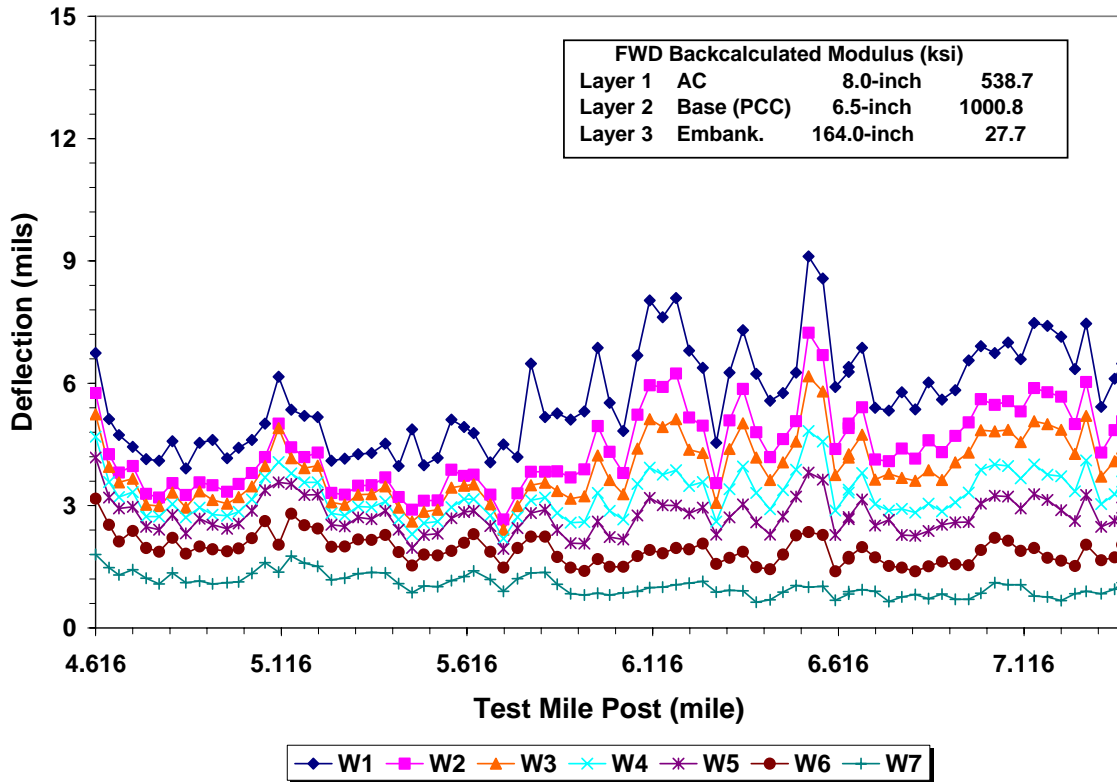


Figure B46. Illustration of FWD Data of 16250000 at Polk County.

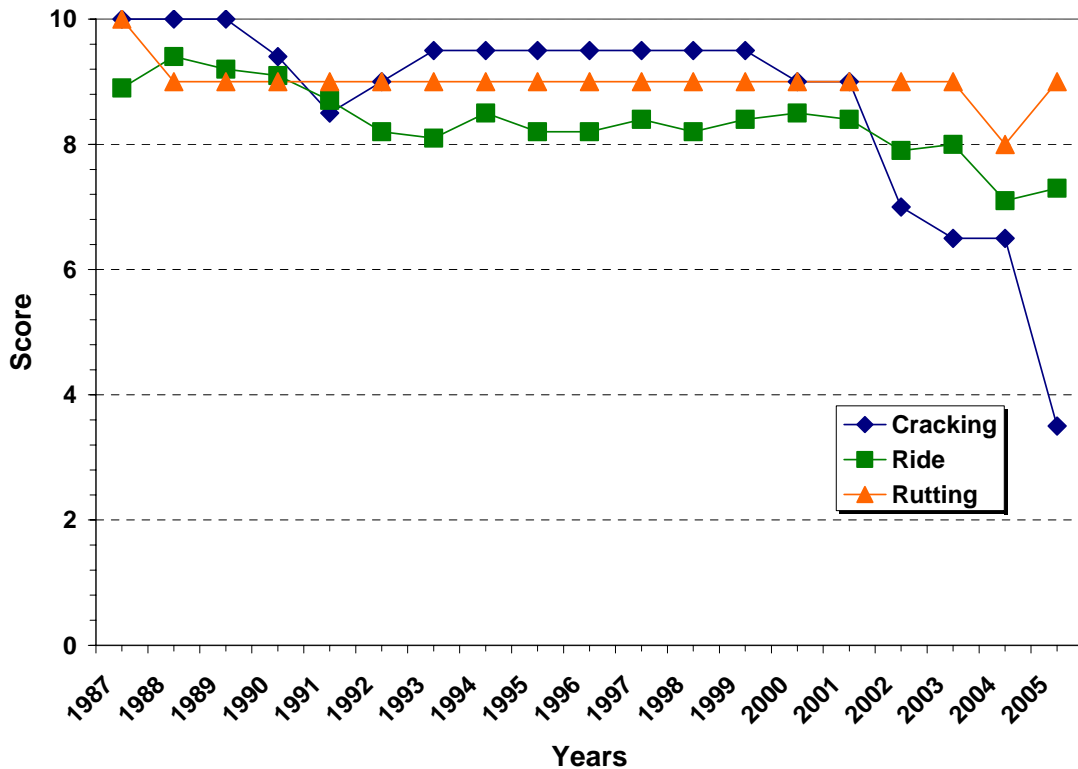


Figure B47. PCS Data of 16250000 at Polk County.

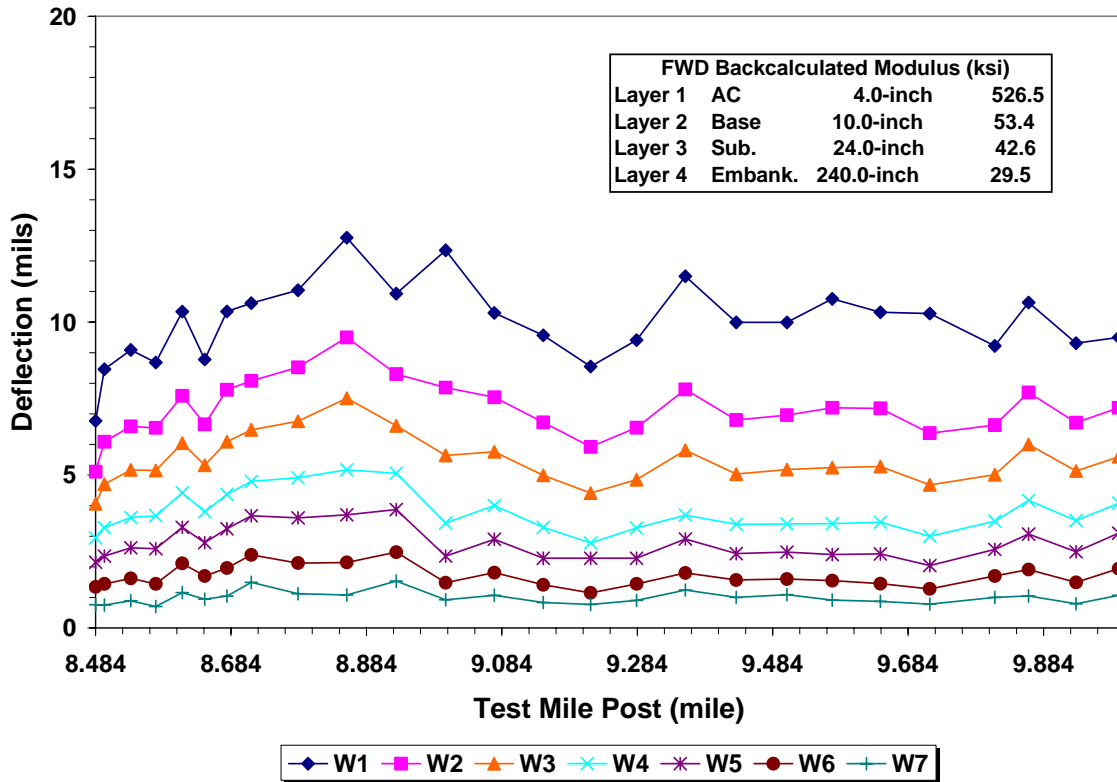


Figure B48. Illustration of FWD Data of 16003001 at Polk County.

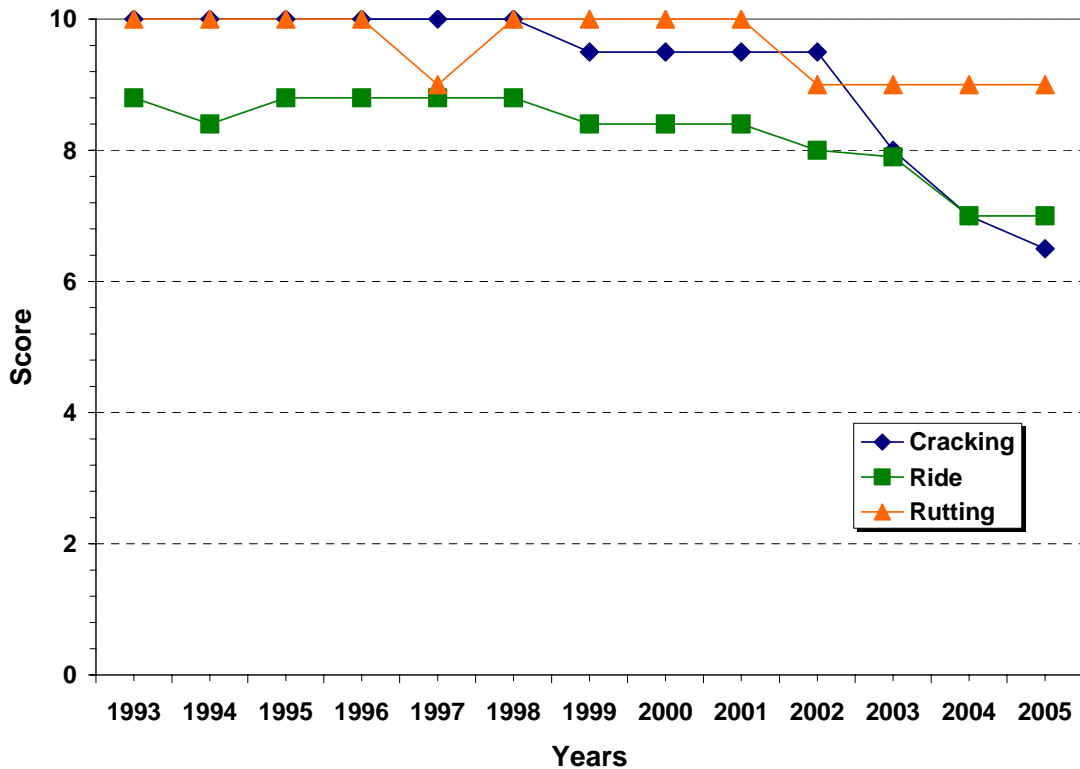


Figure B49. PCS Data of 16003001 at Polk County.

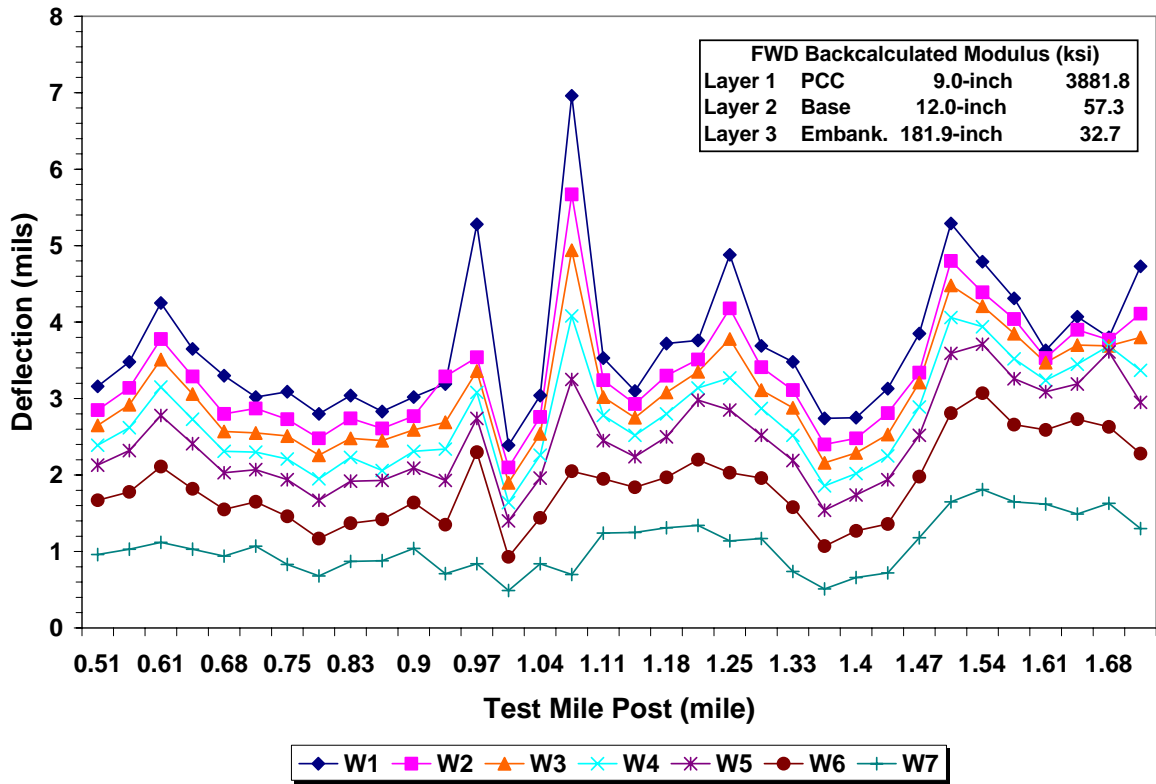


Figure B50. Illustration of FWD Data of 16100000 at Polk County.

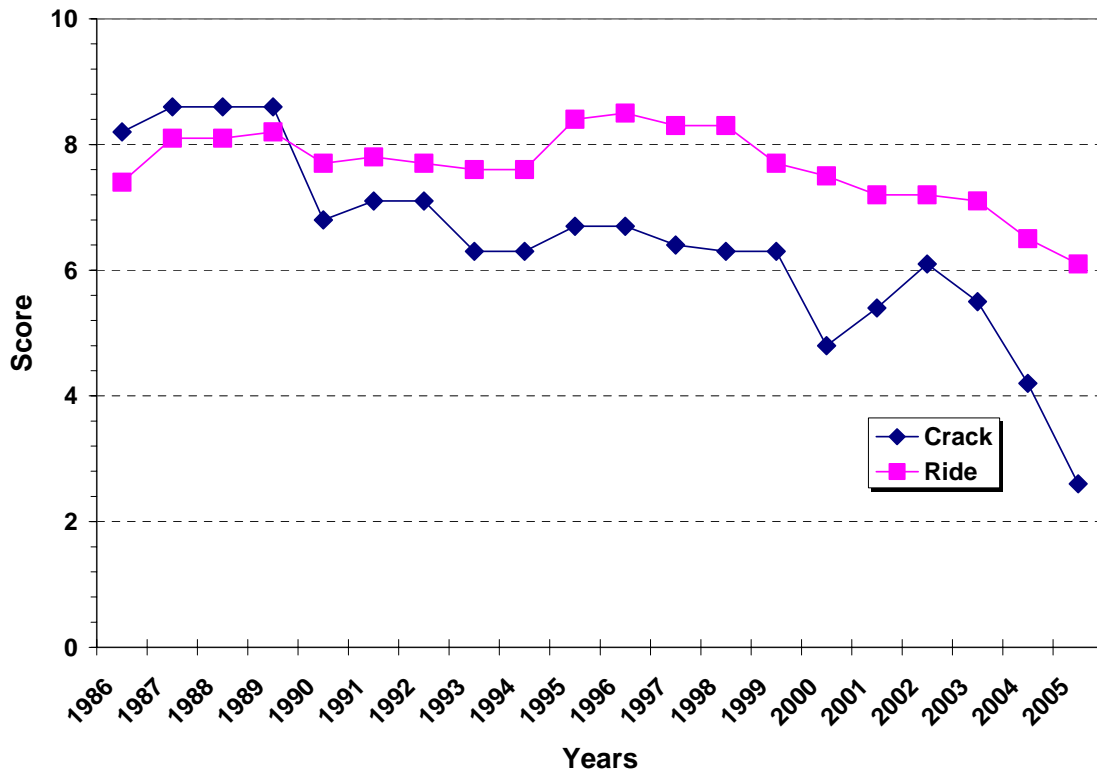


Figure B51. PCS Data of 16100000 at Polk County.

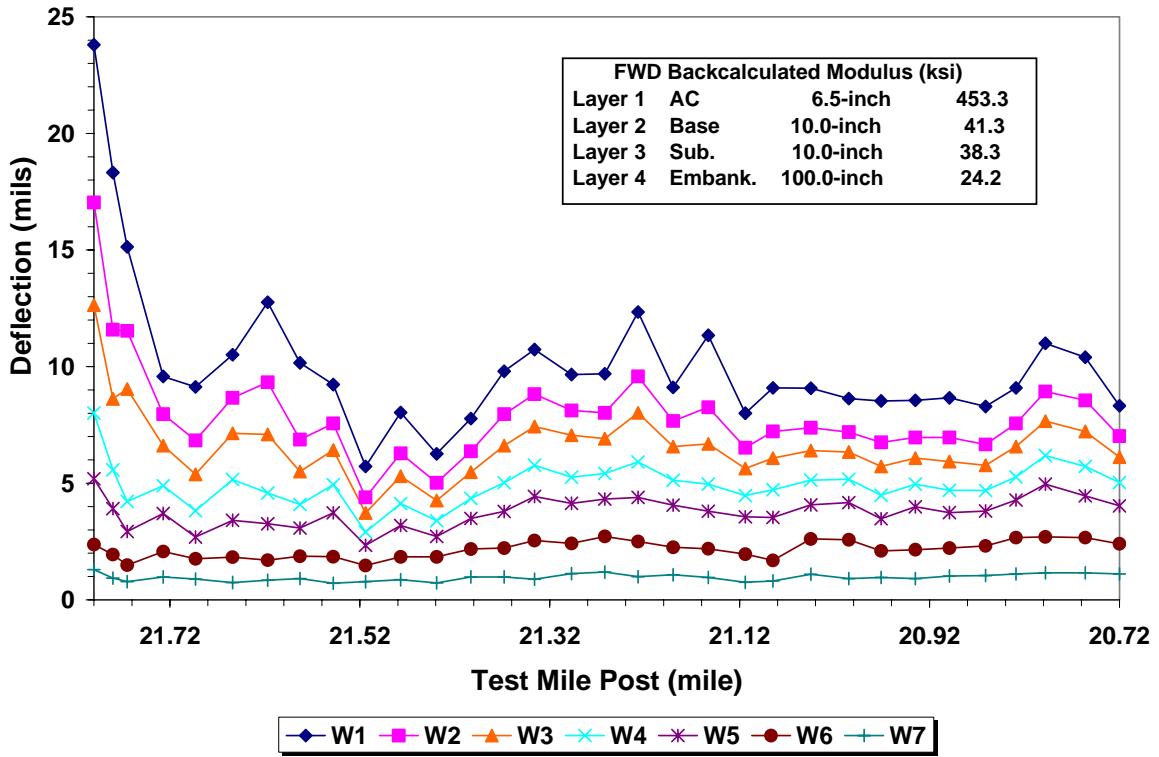


Figure B52. Illustration of FWD Data of 58060000 at Santa Rosa County.

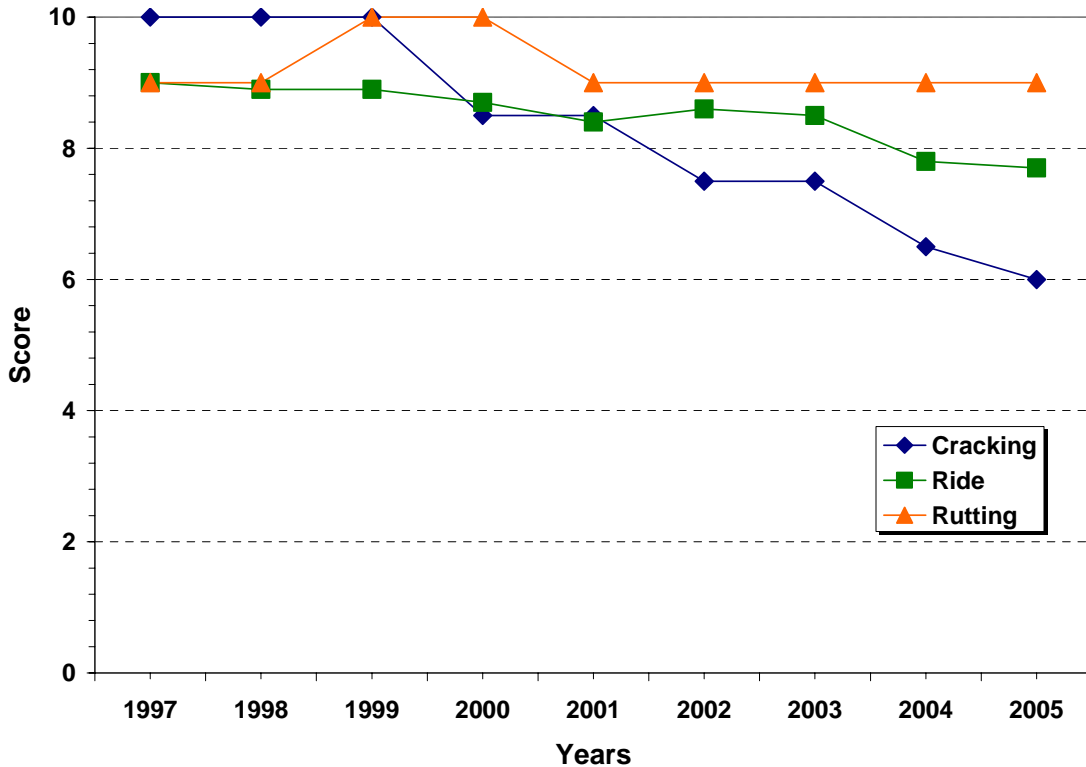


Figure B53. PCS Data of 58060000 at Santa Rosa County.

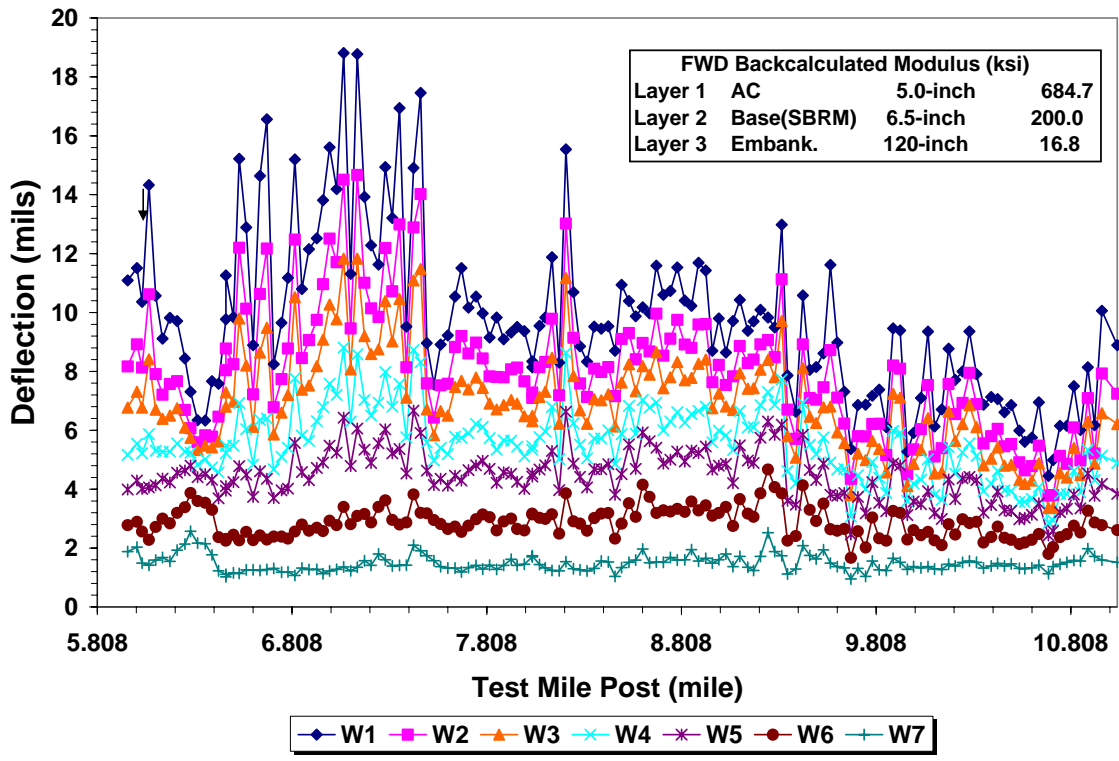


Figure B54. Illustration of FWD Data of 77040000 at Seminole County.

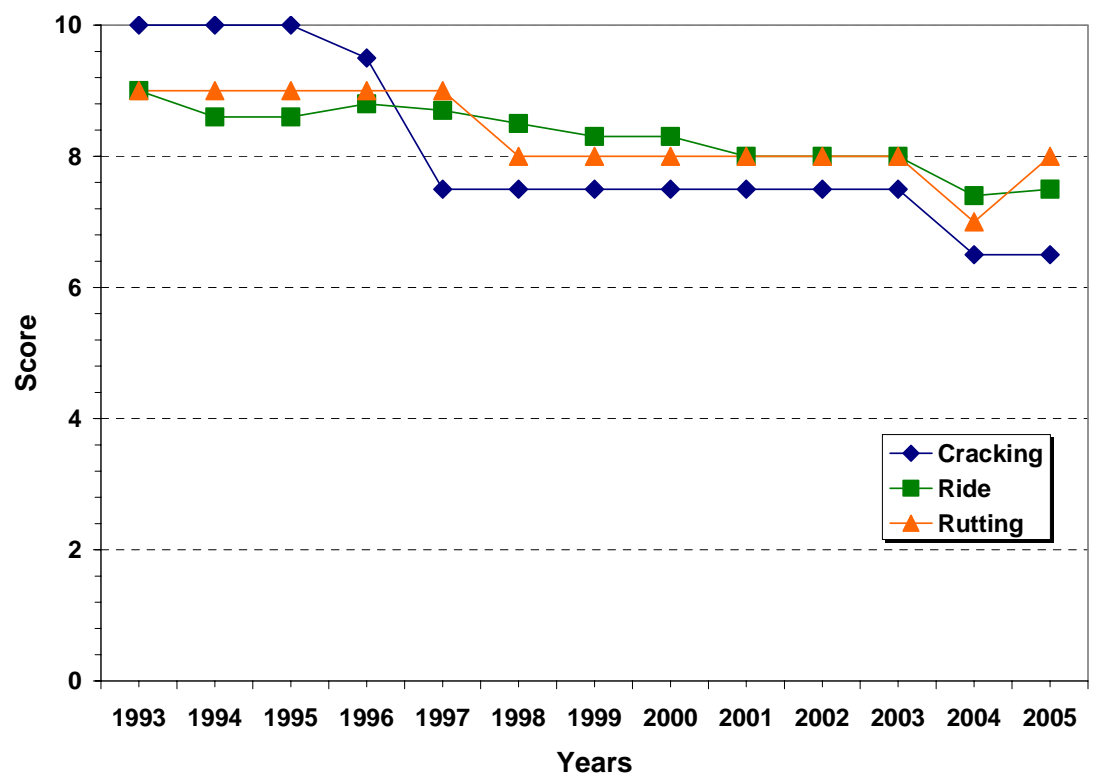


Figure B55. PCS Data of 77040000 at Seminole County.

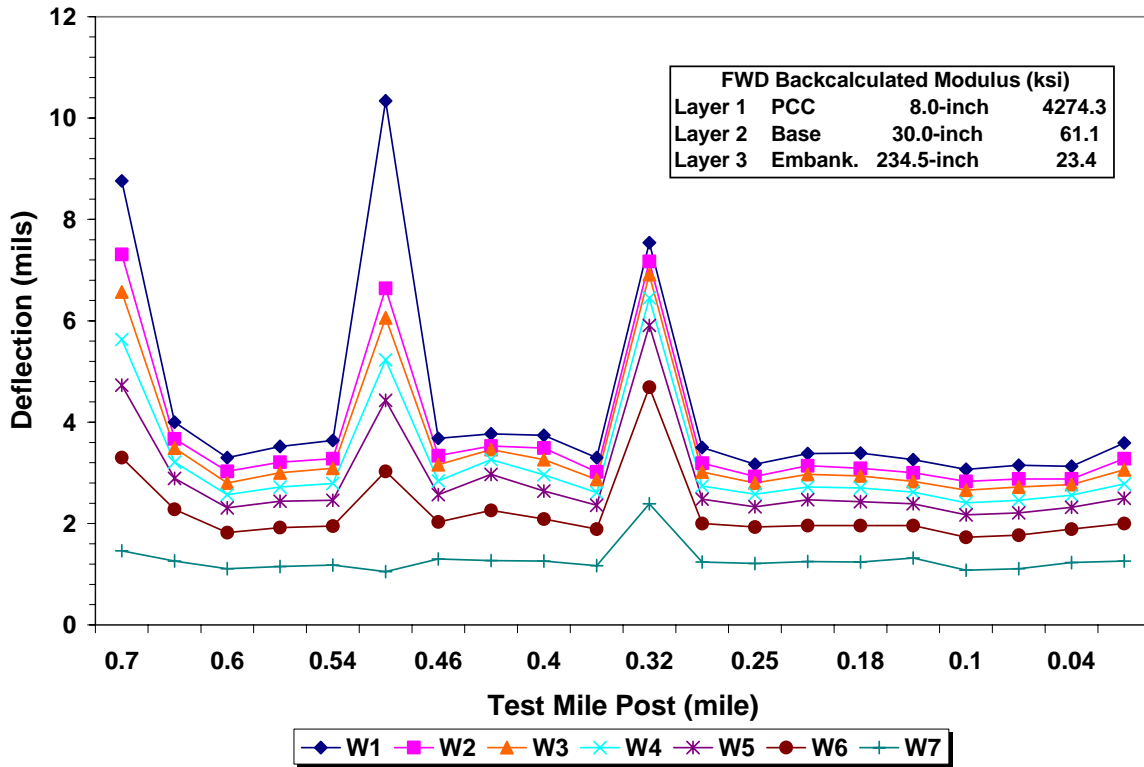


Figure B56. Illustration of FWD Data of 78020000 at St. Johns County.

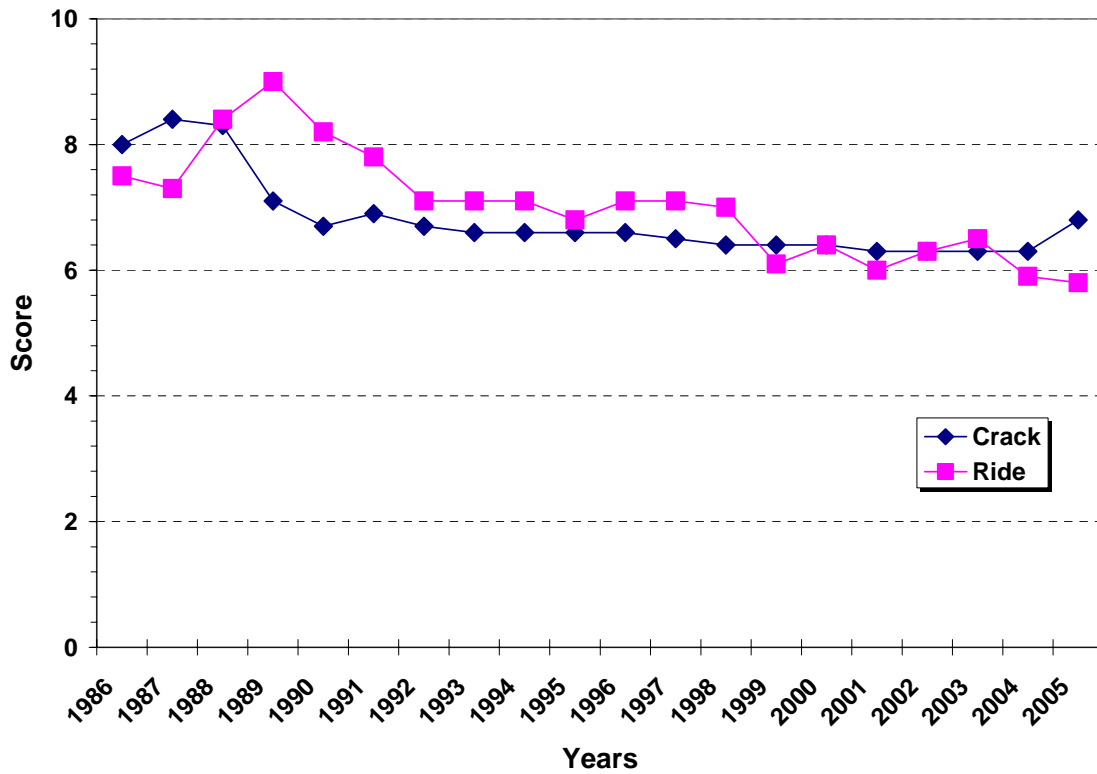


Figure B57. PCS Data of 78020000 at St. Johns County.

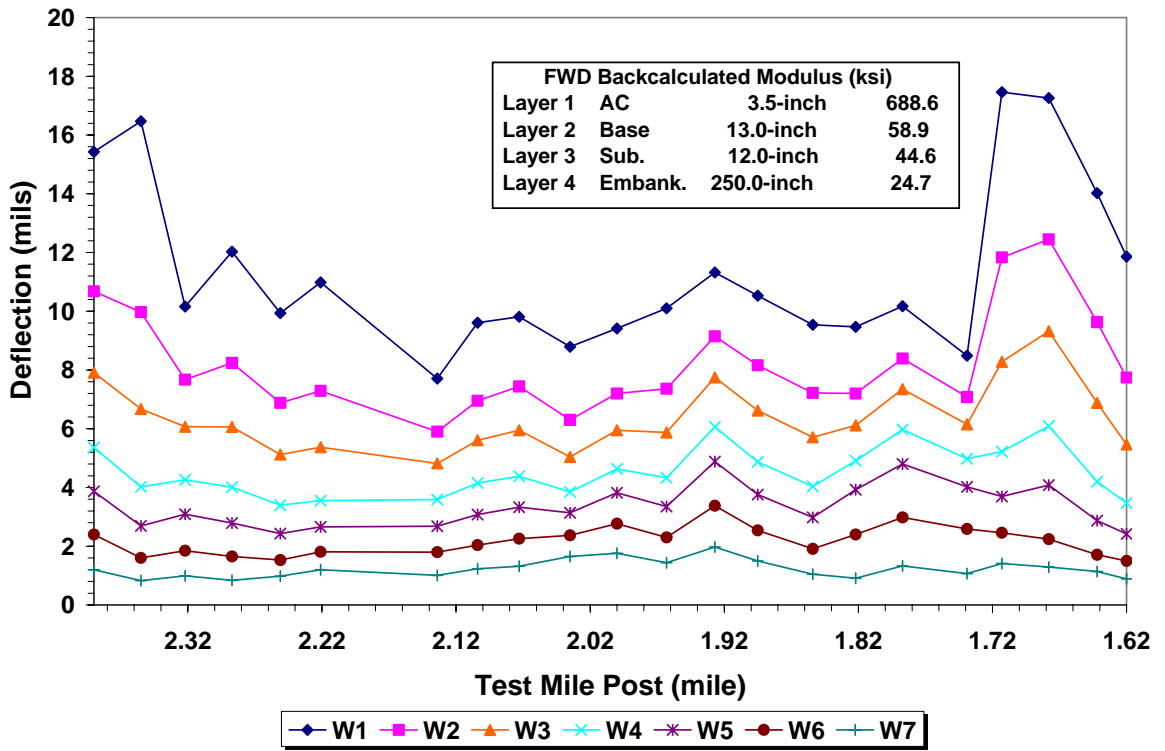


Figure B58. Illustration of FWD Data of 79270000 at Volusia County.

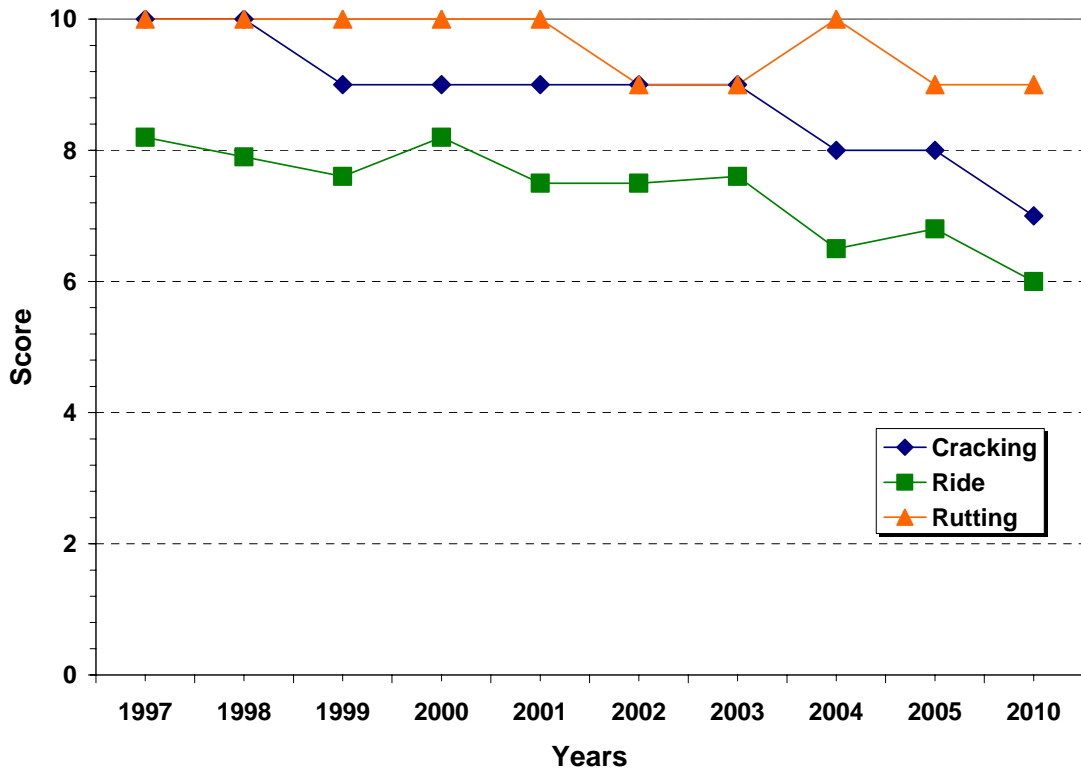


Figure B59. PCS Data of 79270000 at Volusia County.

**APPENDIX C**  
**SUMMARY OF CORE DATA**



**Table C1. Core Data of 58060000 at SR 89 in Santa Rosa County.**

Core No.	Mile Post	FC3	S3	T2	S1	T1	HMAC Core Length (inch)	Base		Comments
								SCLY	ST	
1-A-T	21.78	0.9	1	1	1.5	0.7	5.1	10	10	
1-B-F		0.9	1.2	1.1	1.4	0.6	5.2			
1-C-T		0.9	1.3	1.1	1.5	0.6	5.4			
2-A-T	21.693	0.8	1	1.1	2.1	0.6	5.6			
2-B-F		0.8	1	1.1	2.1	0.6	5.6			
3-A-T	21.617	1.1	0.7	2.1	2.2	0.6	6.7			
3-B-F		1	1	2	2.4	0.9	7.3			
3-C-T		1	1	2	2.3	0.7	7			
4-A-T	21.53	1.2	1	2	2.7	0.6	7.5			
4-B-F		1.1	1	2	2.8	0.6	7.5			
5-A-T	21.4	1.3	0.7	1.6	2.7	0.6	6.9			Top Down
5-B-F		1.3	0.7	1.6	2.7	0.6	6.9			
5-C-T		1.3	0.7	1.5	2.8	0.6	6.9			
5-D-T		1.2	0.9	1.75	2.5	0.6	6.95			
6-A-T	21.336	0.8	0.5	1.6	1.8	0.6	5.3			Top Down
6-B-F		1	0.6	1.7	1.6	0.6	5.5			
6-C-T		0.9	0.6	1.6	1.6	0.6	5.3			
7-A-T	21.227	0.7	0.8	2.3	2.1	0.5	6.4	10	9	Ground water table (GWT) = 30'
7-B-F		0.7	0.9	2.1	1.9	0.7	6.3			
7-C-T		0.8	0.8	2.1	2.1	0.7	6.5			
8-A-T	20.971	0.8	0.5	3	1.8	0.6	6.7			
8-B-F		0.9	0.4	2.9	1.7	0.6	6.5			
9-A-T	20.798	0.8	0.4	2.6	3.2	0.6	7.6			
9-B-F		0.7	0.4	2.5	3	0.6	7.2			
9-C-T		0.7	0.4	2.6	3.4	0.7	7.8			

**Table C2. Core Data of 50010000 at US90 and SR10 in Gadsden County.**

Core No.	Mile Post	FC3	S3	T2	S1	HMAC Core Length (inch)	Base		Comments
							CONC	ST	
1-A-T	16.699	0.5	2.4	1.3	3.5	7.7			Cracks down through all the way
1-B-F		0.5	2.4	1.3	3.5	7.7			
1-C-T		0.5	2.1	1.7	3.4	7.7			
2-A-T	16.977	0.6	2	0.7	2.8	6.1			Cracks down through all the way
2-B-F		0.6	2	0.7	2.8	6.1			
2-C-T		0.6	2	0.7	2.8	6.1			
2-D-T		0.6	2	0.7	2.8	6.1			
3-A-T	17.196	0.5	1.8	0.9	2.6	5.8			Cracks down through all the way
3-B-F		0.5	1.8	0.9	2.6	5.8			
3-C-T		0.6	1.6	1	2.5	5.7			
4-A-T	17.275	0.5	2	1	2.2	5.7			
4-B-F		0.7	1.8	1	2.2	5.7			
4-C-T		0.7	2	1	2.3	6			
5-A-T	17.412	0.6	2	1	2.5	6.1	7	12	Trench Location Cracks down through all the way GWT = 30'
5-B-F		0.6	2	1	2.5	6.1			
5-C-T		0.6	1.9	1	2.5	6			
5-D-T		0.6	2	1	2.5	6.1			
6-A-T	17.765	0.6	2	1.4	2.3	6.3			
6-B-F		0.5	2	1.1	3	6.6			
7-A-T	18.04	0.5	1.6	1.3	2.3	5.7			
7-B-F		0.5	1.6	0.8	2.6	5.5			
8-A-T	18.393	0.5	1.6	1.5	2.4	6			
8-B-F		0.5	1.5	1.1	2.6	5.7			
8-C-T		0.5	1.6	1.6	2.1	5.8			

**Table C3. Core Data of 123811 at I-10 in Gadsden County.**

Core No.	Mile Post	PCC Core Length (inch)	Base		Comments
			Soil Cement		
1-A-T	200 ft	9.8	7		GWT = 27' Joint = 20' AC Shoulder = 10' Lane = 12'
1-B-F		9.5	6.5		
1-C-F		9.75	7		
2-A-T	400 ft	9	6.5		
2-B-F		9.2	7.6		
2-C-F		9.1	7		

**Table C4. Core Data of 26005000 at SR 222 in Alachua County.**

Core No.	Mile Post	FC3	S3	T2	S1	Core Length (inch)	Base		Comments
							LR	ST	
1-A-T	10.61	1	3	1.75		5.75			
1-B-F		1	3	1.75		5.75			
2-A-T	10.4	0.9	1	1.6	1.5	5			
2-B-F		0.9	1	1.6	1.5	5			
2-C-T		0.9	1	1.6	1.5	5			
3-A-T	10.1	1.1	1.1	1.3	1.7	5.2			
3-B-F		1.1	1.1	1.3	1.7	5.2			
4-A-T	9.925	1	1.3	1.2	1.4	4.9			
4-B-F		1	1.3	1.2	1.4	4.9			
5-A-T	9.507	0.9	1.2	1.2	1.6	4.9			Top Down
5-B-F		0.9	1.2	1.2	1.6	4.9			
5-C-T		0.9	1.2	1.2	1.6	4.9			
6-A-T	9.3	0.9	1.3	1.4	1.3	4.9			
6-B-F	9.3	0.9	1.3	1.4	1.3	4.9			
6-C-T		0.9	1.3	1.4	1.3	4.9			
6-D-T		0.9	1.3	1.4	1.3	4.9			
7-A-T	9.1	0.8	1.5	1.3	1.6	5.2			

**Table C4. Core Data of 26005000 at SR 222 in Alachua County (continued).**

Core No.	Mile Post	FC3	S3	T2	S1	Core	Base		Comments
						Length (inch)	LR	ST	
7-B-F		0.8	1.5	1.3	1.6	5.2			
7-C-T		0.8	1.5	1.3	1.6	5.2			
8-A-T	8.58	0.5	1.5	2.5		4.5	15	30	Trench 5.5' GWT Top Down
8-B-F		0.5	1.5	2.5		4.5			
8-C-T		0.5	1.5	2.5		4.5			
9-A-T	8.426	0.9	1.2	1.4	1.3	4.8			
9-B-F	8.426	0.9	1.2	1.4	1.3	4.8			
10-A-T	8.142	1.1	1.2	1.5	1.3	5.1			
10-B-F		1.1	1.2	1.5	1.3	5.1			
10-C-T		1.1	1.2	1.5	1.3	5.1			
10-D-T		1.1	1.2	1.5	1.3	5.1			
11-A-T	8.071	1.1	1.6	0.9	1.5	5.1			
11-B-F		1.1	1.6	0.9	1.5	5.1			
11-C-T		1.1	1.6	0.9	1.5	5.1			

**Table C5. Core Data of 28040000 at SR 18 in Bradford County.**

Core No.	Mile Post	FC3	S3	T2	Core Length (inch)	Base	Comments
						SBRM	
1-A-T	0.1	1	0.8	1.2	3		
1-B-F		1	0.8	1.2	3	7	
2-A-T	0.288	0.6	1	1.75	3.35		
2-B-F		0.6	1	1.75	3.35		
2-C-T		0.6	1	1.75	3.35	6	
3-A-T	0.7	0.5	1.25	1.5	3.25		
3-B-F		0.5	1.25	1.5	3.25	5.5	
4-A-T	0.967	0.7	0.9	1.5	3.1		
4-B-F		0.7	0.9	1.5	3.1	6	
5-A-T	1.4	0.8	0.7	1.5	3		Cracks all the way down
5-B-F		0.8	0.7	1.5	3		
5-C-T		0.8	0.7	1.5	3		
5-D-T		0.8	0.7	1.5	3	5.5	
6-A-T	1.7	0.8	1.2	1.3	3.3		
6-B-F		0.8	1.2	1.3	3.3	6.2	
7-A-T	1.967	0.7	0.9	1.5	3.1		
7-B-F		0.7	0.9	1.5	3.1	6.3	
8-A-T	2.357	0.9	0.9	1.5	3.3		
8-B-F		0.9	0.9	1.5	3.3	6	
9-A-T	2.536	0.7	0.6	2	3.3		Trench GWT = 4.5'
9-B-F		0.7	0.6	2	3.3		
9-C-T		0.7	0.6	2	3.3		
9-D-T		0.7	0.6	2	3.3	6	
10-A-T	2.7	0.7	0.7	1.4	2.8		
10-B-F		0.7	0.7	1.4	2.8	6	
11-A-T	3.288	0.6	0.9	1.6	3.1		
11-B-F		0.6	0.9	1.6	3.1	5.3	
12-A-T	3.754	0.8	0.7	1.2	2.7		
12-B-F		0.8	0.7	1.2	2.7		
12-C-T		0.8	0.7	1.2	2.7	5.8	
13-A-T	4.4	0.5	0.8	1.3	2.6		

**Table C5. Core Data of 28040000 at SR 18 in Bradford County (continued).**

Core No.	Mile Post	FC3	S3	T2	Core	Base	Comments
					Length (inch)	SBRM	
13-B-F		0.5	0.8	1.3	2.6	6	
14-A-T	4.7	0.8	1.4	1.6	3.8		
14-B-T		0.8	1.4	1.6	3.8	6.3	
15-A-T	5.1	0.5	0.8	1.3	2.6		
15-B-F		0.5	0.8	1.3	2.6		
15-C-T		0.5	0.8	1.3	2.6	8.4	
16-A-T	5.323	0.6	0.8	1.3	2.7		
16-B-F		0.6	0.8	1.3	2.7		
16-C-T		0.6	0.8	1.3	2.7		
16-D-T		0.6	0.8	1.3	2.7	6.2	

**Table C6. Core Data of 78020000 at US 1 in St. Johns County.**

Core No.	Mile Post	Core Length (inch)	Base		Comments
				Sand	
1-A-T	0.502	8.25			
1-B-F		8.2			
1-C-F		8			
1-D-F		8			
2-A-T	0.323	7.5			Joint = 20', Dowel = 1.25" GWT = 4.5' Sand Embankment
2-B-F		7.6			
2-C-F		7.5			
2-D-F		7.7			
3-A-T	0.125	8			
3-B-F		7.9			
3-C-F		7.8			
3-D-F		8			

**Table C7. Core Data of 77040000 at SR46 in Seminole County.**

Core No.	Mile Post	FC4	S3	S1	T1			Core Length (inch)	Base		Comments
										SBRM	
1-A-T	6.073	1	1	2	0.5			4.5	6.7		
1-B-F		1	1	2	0.5			4.5			
1-C-T		1	1	2	0.5			4.5			Crack all the way down
		<b>FC4</b>	<b>S3</b>	<b>S</b>	<b>S1</b>	<b>T</b>					
2-A-T	6.222	0.7	1.25	0.8	2.75	0.7		6.2	6		
2-B-F		0.7	1.25	0.8	2.75	0.7		6.2			
2-C-T		0.7	1.25	0.8	2.75	0.7		6.2			Bottom up
		<b>FC4</b>	<b>S3</b>	<b>S1</b>	<b>T</b>						
3-A-T	6.352	0.5	1.8	7.5	1.2			11	6	Widened section	
3-B-F		0.8	3.5	5.5	1.5			11.3		Different core layer	
4-A-T	6.682	0.8	0.8	1.8	0.9			4.3	6		

**Table C7. Core Data of 77040000 at SR46 in Seminole County (continued).**

Core No.	Mile Post	FC4	S3	S1	T1			Core	Base	Comments
								Length (inch)	SCLY	
4-B-F		0.8	0.8	1.8	0.9			4.3		
5-A-T	7.143	0.6	1.1	2	1.1			4.8	6	
5-B-F		0.6	1	1.5	1			4.1		
6-A-T	7.466	0.5	0.8	2	1.4			4.7	6	Trench Location Crack all the way down GWT = 10'
6-B-F		0.5	0.8	2	1.4			4.7		
6-C-T		0.5	0.8	2	1.4			4.7		
7-A-T	7.643	0.5	1	1.7	0.8			4	6	Top down
7-B-F		0.5	1	1.7	0.8			4		
7-C-T		0.5	1	1.7	0.8			4		
7-D-T		0.5	1	1.7	0.8			4		
		<b>FC4</b>	<b>S3</b>	<b>S1</b>	<b>T2</b>	<b>T3</b>				
8-A-T	8.214	0.8	0.9	1.75	0.6	1.3		5.35	4.5	
8-B-F		0.8	0.9	1.75	0.6	1.3		5.35		
9-A-T	8.643	0.6	0.75	1.5	0.7	1.5		5.05	5.5	
9-B-F		0.6	0.75	1.5	0.7	1.5		5.05		
9-C-T		0.6	0.75	1.5	0.7	1.5		5.05		
10-A-T	9.323	0.5	0.7	1.5	1	1.1		4.8	6	
10-B-F		0.5	0.7	1.5	1	1.1		4.8		
		<b>FC4</b>	<b>S3</b>	<b>S1</b>	<b>T</b>					
11-A-T	9.672	0.9		2.5	1.2			4.6	6.25	
11-B-F		0.8		2.5	1.4			4.7		
11-C-T		0.9		2.5	1.2			4.6		
12-A-T	10.282	0.6	1	1.2	1.2			4	5.5	
12-B-F		0.7	1.1	1.5	1.1			4.4		
12-C-T		0.6	1	1.2	1.2			4		
13-A-T	10.69	0.8	1	1.7	1.4			4.9		
13-B-F		0.8	1	1.7	1.4			4.9	7	
		<b>FC4</b>	<b>FC3</b>	<b>S3</b>	<b>S1</b>	<b>T3</b>	<b>T2</b>			
14-A-T	10.922	1	0.7	1	1.5	0.6	0.6	4.8	5.5	Different layers due to the location close to intersection centerline widened
14-B-F		1	0.7	1	1.5	0.6	0.6	4.8		
14-C-T		1	0.7	1	1.5	0.6	0.6	4.8		
14-D-T		1	0.7	1	1.5	0.6	0.6	4.8		

**Table C8. Core Data of 11020000 at SR50 in Lake County.**

Core No.	Mile Post	Core Length (inch)	Base	Comments
			Permeable Base	
1-A-T	14.06	12	4	
1-B-F		11.5		
1-C-F		12		
2-A-T	14.14	13	4	Joint = 18', Dowel = 1.25" Lane width = 12' GWT = 15' 8.5' PCC shoulder
2-B-F		13		
2-C-F		13		

**Table C9. Core Data of 79270000 at SR483 in Volusia County.**

Core No.	Mile Post		T3	T2	Core	Base		Comments
					Length (inch)	LR	STAB	
1-A-T	2.34		1.25	1	2.25			
1-B-F			1.25	1	2.25			
		<b>FC3</b>	<b>S1</b>	<b>T2</b>				
2-A-T	2.327	0.75	1.3	1.75	3.8			
2-B-F		0.75	1.3	1.75	3.8			
2-C-T		0.75	1.3	1.75	3.8			
3-A-T	2.134	0.9	1.4	1.8	4.1			
3-B-F		0.9	1.4	1.8	4.1			
4-A-T	2	1.2	1.2	1.9	4.3			
4-B-F		1.2	1.2	1.9	4.3			
		<b>FC3</b>	<b>S3</b>	<b>S1</b>				
5-A-T	1.927	1.2	1	2	4.2			
5-B-F		1.2	1	2	4.2			
			<b>FC3</b>	<b>S1</b>				
6-A-T	1.713		0.8	8	8.8			Different layers Widened section Top down
6-B-F			0.8	8	8.8			
6-C-T				0.8	8	8.8		
7-A-T	1.655		0.7	1.75	2.45	13	12	Trench Top down GWT = 7.6'
7-B-F			0.7	1.75	2.45			
7-C-T			0.7	1.75	2.45			
7-D-T			0.7	1.75	2.45			

**Table C10. Core Data of 16250000 at SR37 in Polk County.**

Core No.	Mile Post	FC4	S	T1	ST	Core Length (inch)	Base	Comments
							CONC	
1-A-T	4.652	0.6	2.2	1.7	2.7	7.2		
1-B-F		0.6	2.2	1.7	2.7	7.2		
2-A-T	4.881	0.8	3.5	3		7.3		
2-B-F		0.8	3.5	3		7.3		
3-A-T	5.247	0.8	3.3	2.5		6.6	6.5	Trench Bottom up crack
3-B-F		0.8	3.5	2.2		6.5		
3-C-T		0.5	3.5	10		14		
4-A-T	5.432	0.8	3.5	3.8		8.1		
4-B-F		0.8	3.5	3.8		8.1		
4-C-T		0.8	3.5	3.8		8.1		
5-A-T	5.789	0.8	3.6	3.5		7.9		Most cracks are along with widened lane GWT = TBD
5-B-F		0.7	4	3.2		7.9		
5-C-T		0.8	3.6	3.5		7.9		
5-D-T		0.6	4.2	3.5		8.3		
6-A-T	5.895	1	3.6	4		8.6		
6-B-F		1	3.6	4		8.6		
7-A-T	6.143	1	4.8	2.3	0.5	8.6		
7-B-F		1	4.8	2.3	0.5	8.6		
8-A-T	6.287	1	5.2	2.5	0.5	9.2		
8-B-F		1	5.2	2.5	0.5	9.2		
9-A-T	6.536	1	5	2.5	0.6	9.1		
9-B-F		1	5	2.5	0.6	9.1		
10-A-T	6.859	1	4	2.5	0.6	8.1		
10-B-F		1	4	2.5	0.6	8.1		
10-C-T		0.7	4	2.5	0.6	7.8		
11-A-T	7.143	0.7	4	2.5	0.6	7.8		
11-B-F		0.7	4	2.5	0.6	7.8		

**Table C11. Core Data of 16003000 at SR563 in Polk County.**

Core No.	Mile Post	FC4	S	Core Length (inch)	Base		Comments
					LR	ST	
1-A-T 1-B-F	8.606	0.6 0.6	3 3	3.6 3.6			
2-A-T 2-B-F 2-C-T	8.736	0.8 0.8 0.8	3.2 3.2 3.2	4 4 4	10	24	Trench GWT =TBD Top down crack
3-A-T 3-B-F 3-C-T	8.8	0.7 0.7 0.7	3.5 3.5 3.5	4.2 4.2 4.2			
4-A-T 4-B-F 4-C-T	8.996	0.7 0.7 0.7	3 3 3	3.7 3.7 3.7			Top down crack
5-A-T 5-B-F	9.2	0.7 0.7	2.8 2.8	3.5 3.5			
6-A-T 6-B-F 6-C-T 6-D-T	9.6	0.7 0.7 0.7 0.7	3.5 3.5 3.5 3.5	4.2 4.2 4.2 4.2			Top down crack
7-A-T 7-B-F	9.886	0.7 0.7	3.2 3.2	3.9 3.9			

**Table C12. Core Data of 16100000 at US 92 in Polk County.**

Core No.	Mile Post	Core Length (inch)	Base		Comments
			ECONC	ST	
1-A-T	0.75	8			
1-B-F		8			
1-C-F		7.8			
2-A-T	0.95	7.8			
2-B-F		7.8	12		
2-C-F		7.8			
3-A-T	0.967	7.6			20' joint space 12' lane width 1" dowel bar
3-B-F		7.6			
3-C-F		7.6			
4-A-T	1.074	7.5			4' AC widened shoulder
4-B-F		7.5			
4-C-F		7.7			
5-A-T	1.538	6.5			
5-B-F		8	12		
5-C-F		8			
6-A-T	1.59	9.1			
6-B-T		10			
6-C-F		9			

**Table C13. Core Data of 01010000 at US 41 in Charlotte County.**

Core No.	Mile Post	Core Length (inch)	Base		Comments
			ECONC	ST	
1-A-T	3.092	4			
1-B-F		3.8	9		
1-C-F		5	9.2	6	
2-A-T	2.563	4	7.7		15' joint space No dowel 4.5' AC widen, 12' lane
2-B-F		3.8	8.3		
2-C-F		3.8	8.2	6	

**Table C14. Core Data of 10075000A at I-75 in Hillsborough County.**

Core No.	Mile Post	Core Length (inch)	Base		Comments
			#57 stone stab		
1-A-T	19.071	13.5	8		
1-B-F		13.5			
1-C-F		13.5			
2-A-T	19.67	13.5	8		13.5' and 16.5' Joint 1.25" Dowel 9.5' PCC shoulder 12' Lane width
2-B-F		13.5			
2-C-F		13.5			
3-A-T	20.003	14.2	8		
3-B-F		14.2			
3-C-F		14.2			

**Table C15. Core Data of 10075000B at I-75 in Hillsborough County.**

Core No.	Mile Post	Core Length (inch)	Base		Comments
			ECONC	Embank	
1-A-T	23.56	12.5			
1-B-F		12.8			
1-C-F		12.5			
2-A-T	23.74	12.6			13.5' and 16.5' Joint 1.25" Dowel 9.5' PCC shoulder
2-B-F		12.4			
2-C-F		12.6			
3-A-T	23.99	12.8	7.0		12' Lane width
3-B-F		12.7			
3-C-F		12.8			
4-A-T	24.5	12.5	6.5	sand	
4-B-F		12.5			
4-C-F		12.5			

**Table C16. Core Data of 10250001 at 22<sup>nd</sup> St. at SR 60 in Hillsborough County.**

Core No.	Mile Post	Core Length (inch)	Base AC Permeable	Comments
1-A-T	0.365	12.5	4	
1-B-F		12.5		
1-C-F		12.5		
2-A-T	0.565	12.5	5	15' Joint 12' Lane 1.375" Dowel 9.5' PCC shoulder
2-B-F		12.5		
2-C-F		12.5		
3-A-T	0.92	12	4	
3-B-F		14.2		
3-C-F		12.2		

**Table C17. Core Data of 10060000 at US 41 in Hillsborough County.**

Core No.	Mile Post	FC	S	T1	ST	Core Length (inch)	Base		Comments
							LR	STAB	
1-A-T	9.37	0.3	1.2	0.5	2.1	4.1			Top down crack
1-B-F		0.3	1.2	0.5	2.1	4.1			
1-C-T		0.3	1.2	0.5	2.1	4.1			
2-A-T	9.84	0.3	1.2	0.5	2	4			Top down crack
2-B-F		0.3	1.2	0.5	2	4			
2-C-T		0.3	1.2	0.5	2	4			
3-A-T	10.281	0.4	1.1	0.6	1.9	4			
3-B-F		0.4	1.1	0.6	1.9	4			
4-A-T	10.5	0.5	1.5	0.6	2	4.6	9	16	Trench
4-B-F		0.5	1.5	0.6	2	4.6			
4-C-T		0.5	1.5	0.6	2	4.6			
4-D-T		0.5	1.5	0.6	2	4.6			
5-A-T	10.642	0.5	1.4	0.6	2.2	4.7			Top down crack
5-B-F		0.5	1.4	0.6	2.2	4.7			
5-C-T		0.5	1.4	0.6	2.2	4.7			

**Table C17. Core Data of 10060000 at US 41 in Hillsborough County (continued).**

Core No.	Mile Post	FC	S	T1	ST	S	Core Length (inch)	Base		Comments
								LR	STAB	
6-A-T	11.377	0.5	1.4	0.6	2.1		4.6			
6-B-F		0.5	1.3	0.6	2.2		4.6			
7-A-T	11,785		4.5	0.8	2.2		7.5			
7-B-F			4.5	0.8	2.2		7.5			
8-A-T	12.4		3.6	0.8	2		6.4			
8-B-F			3.6	0.8	2		6.4			
8-C-T			3.6	0.8	2		6.4			
9-A-T	13.085	1.9	1.9	1.7	2.5	3	11			
9-B-F		1.9	1.9	1.7	2.5	3	11			
10-A-T	13.661		2.9	2	1.5	3	9.4			
10-B-F			2.9	2	1.5	3	9.4			
10-C-T										Broken
11-A-T	14.05	4	0.5	1.3	2	3.2	11			
11-B-F		4	0.5	1.3	2	3.2	11			
12-A-T	14.238	3.5	1.5	1	2.2	3	11.2			Cores at section 13, 14, and 16 were withdrawn
12-B-F		3.5	1.5	1	2.2	3	11.2			
15-A-T	16.634		3.5	1	2	3.3	9.8			due to partially broken &
15-B-F				3.5	1	2	3.3	9.8		

**Table C18. Core Data of 10160000 at SR 60 in Hillsborough County.**

Core No.	Mile Post		FC4	S	T1	BIND		Core Length (inch)	Base		Comments
									LR	ST	
1-A-T	0.282		1	2.8	4.5	1.7		10			.5 " TOP IS APART  TOP DOWN
1-B-F			1	3	4.5	1.8		10.3			
1-C-T			1	3	4.5	1.8		10.3			
2-A-T	0.84		0.5	3.5	3	3.6		10.6			
2-B-F			0.5	3.5	3.5	3.5		11			
2-C-T			0.5	3.5	3.5	3.5		11			
3-A-T	1.436		0.5	3.5	3.5	3.5		11			
3-B-F			0.5	3.5	3.5	3.5		11			
4-A-T	2.17		0.7	1.7	1.1	1.9		5.4	10	16	TRENCH
4-B-F			0.7	1.75	1	2		5.45			TOP DOWN
4-C-T			0.7	1.75	1	2		5.45			
5-A-T	2.5		1	7.5	5.5			14			
5-B-F			1	7.5	5.5			14			
6-A-T	2.98		0.6	1.1	1.3	2.1		5.1			TOP DOWN
6-B-F			0.6	1	1.2	2		4.8			
6-C-T			0.6	1	1.2	2		4.8			
6-D-T			0.6	1	1.2	2	<b>BIND</b>	4.8			
7-A-T	3.45		0.8	0.8	1.2	2	2	6.8			ALLIGATOR
7-B-F			0.8	0.8	1.2	2	2	6.8			
7-C-T		<b>FC4</b>	0.8	0.8	1.2	2	2	6.8			
8-A-T	3.98	0.5	1.3	1.21	1.4	1.9	2	8.31			
8-B-F		0.5	1.3	1.21	1.4	1.9	2	8.31			
8-C-T		0.5	1.3	1.21	1.4	1.9	2	8.31			
9-A-T	4.214	0.75	1.4	1.2	1.3	1.3	2.3	8.25			
9-B-F		0.75	1.4	1.2	1.3	1.3	2.3	8.25			

**Table C19. Core Data of 15003000 at I-175 in Pinellas County.**

Core No.	Mile Post	Core Length (inch)	Base	Comments
			ECONC	
1-A-T	0.7	10		
1-B-F		10		
1-C-F		10		
2-A-T	0.805	9.6	7	20' Joint 1.25" Dowel 6' PCC shoulder
2-B-F		9.6		
2-C-F		9.6		
3-A-T	0.935	9		12' Lane width
3-B-F		9		
3-C-F		9		
Core No.	Mile Post	Core Length (inch)	Base	Comments
			ECONC	
1-A-T	1.123	9		
1-B-F		9		
1-C-F		9		
2-A-T	0.889	9.8	7	20' Joint 1.25" Dowel 6' PCC shoulder
2-B-F		9.8		
2-C-F		9.8		
3-A-T	0.817	9.5		12' Lane width
3-B-F		9.5		
3-C-F		9.5		

**Table C20. Core Data of 15190000 at I-275 in Pinellas County.**

Core No.	Mile Post	Core	Base	Comments
		Length (inch)	ECONC	
1-A-T	2.5	9	7	
1-B-F		9		
1-C-F		9		
2-A-T	2.92	9		20' Joint 1.25" Dowel 8.3' PCC shoulder
2-B-F		9		
2-C-F		9		
3-A-T	3.5	8.8		12' Lane width
3-B-F		8.8		
3-C-F		8.8		
4-A-T	4.1	9.5	7 broken	Frequent transverse cracks
4-B-F		9.5		
4-C-F		9.5		
Core No.	Mile Post	Core	Base	Comments
		Length (inch)	ECONC	
1-A-T	4.285	9.2		
1-B-F		9.2		
1-C-F		9.2		
2-A-T	3.5	9	7.5	20' Joint 1.25" Dowel 8.3' PCC shoulder
2-B-F		9		
2-C-F		9		
3-A-T	3.1	9.3		12' Lane width
3-B-F		9.3		
3-C-F		9.3		
4-A-T	2.45	9.4	7	
4-B-F		9.4		
4-C-F		9.4		
5-A-T	2.4	9.2		
5-B-F		9.2		
5-C-F		9.2		

**Table C21. Core Data of 86190000 at SR 823 in Broward County.**

Core No.	Mile Post	FC2	S1	S1	Core Length (inch)	Base		Comments
						LR	ST	
1-A-T	2.401	0.7	1.3	2.1	4.1			
1-B-F		0.7	1.3	2.1				
2-A-T	2.686	0.7	1.4	2.1	4.2			
2-B-F		0.7	1.4	2.1				
3-A-T	2.837	0.5	1.3	2	3.8			TOP DOWN
3-B-F		0.4	1.2	2				
3-C-T		0.5	1.3	2				
3-D-T		0.5	1.3	2				
4-A-T	3.15	0.8	3.2		4	8	12	Trench 6' GWT TOP DOWN
4-B-F		0.7	3.2					
4-C-T		0.7	3.2					
5-A-T	3.2	0.6	1.4	2	4			
5-B-F		0.5	1.5	2.1				
6-A-T	3.3	0.5	1.5	2	4			
6-B-F		0.5	1.5	2				
6-C-T		0.4	1.6	2.1				

**Table C22. Core Data of 93310000 at SR 710 in Palm Beach County.**

Core No.	Mile Post	FC2	S1	S2	Core Length (inch)	Base		Comments
						LR	ST	
1-A-T	17.52	0.6	1.6	0.8	3	14	12	7.8' GWT TRENCH
1-B-F		0.7	1.5	1.6	3.8			
1-C-T		0.7	1.5	0.75	2.95			
2-A-T	17.2	0.8	1	1.1	2.9			
2-B-F		0.8	1	1.1	2.9			
2-C-T		0.8	1	1.1	2.9			
3-A-T	16.444	0.5	1.1	1.2	2.8			
3-B-F		0.5	1.1	1.2	2.8			
3-C-T		0.5	1.1	1.2	2.8			
4-A-T	15.195	0.5	1	0.5	2			
4-B-F		0.3	1.1	0.55	1.95			
4-C-T		0.5	1	0.5	2			

**Table C23. Core Data of 93100000 at SR 710 in Palm Beach County.**

Core No.	Mile Post		FC2	S1	T1	ST		Core Length (inch)	Base		Comments
									LR	ST	
1-A-T	11.904		0.7	1	1.5	0.9		4.1	16	12	Trench 9' GWT Top down
1-B-F			0.7	1.1	1.5	1	4.3				
1-C-T			0.7	1	1.5	0.9	4.1				
2-A-T	12.157		0.8	1.1	1.4	1.1		4.4			
2-B-F			0.7	1.3	1.4	0.9	4.3				
2-C-T			0.8	1.1	1.4	1.1	4.4				
3-A-T	12.305		0.6	0.9	1.3	0.8		3.6			Top down
3-B-F			0.6	0.9	1.3	0.8	3.6				
3-C-T			0.6	0.9	1.2	0.8	3.5				
3-D-T			0.6	0.9	1.2	0.8	3.5				
4-A-T	12.4		0.7	1.2	1.8	0.8		4.5			Top down
4-B-F			0.6	1.2	1.6	0.9	4.3				
4-C-T			0.7	1.2	1.8	0.8	4.5				
5-A-T	12.547		0.8	0.9	1.3	0.9		3.9			
5-B-F			0.8	0.9	1.3	0.9	3.9				
5-C-T			0.8	0.9	1.3	0.9	3.9				

**Table C24. Core Data of 87061000 at SR 886 in Dade County.**

Core No.	Mile Post	Core Length (inch)	Base		Comments
			LR		
1-A-T	0.195	12.5	15		12' lane
1-B-F		12.5			
1-C-F		12.5			
2-A-T	0.126	12	15		18' Joint We could not find dowel  No shoulder
2-B-F		12			
2-C-F		12			

**Table C25. Core Data of 87270000 at SR 9/9A in Dade County.**

Core No.	Mile Post	Core Length (inch)	Base		Comments
			LR		
1-A-T	0.229	9			5 ~ 8' GWT 12' lane
1-B-F		8.8			
1-C-F		8.9			
2-A-T	0.46	9.1	16		18' Joint We could not find dowel  Conc Shoulder (9')
2-B-F		9.1			
2-C-F		9.1			

**Table C26. Core Data of 87030000 at SR 5 in Dade County.**

Core No.	Mile Post	Core Length (inch)	Base		Comments	
			LR			
1-A-T	8.96	8	10			
1-B-F		8.2				
1-C-F		8.3				
2-A-T	9.13	7.9			15.4' Joint We could not find dowel  No shoulder	
2-B-F		8.5				
2-C-F		8.2				
3-A-T	9.5	10.5	10		12' Lane width Transverse cracks Patched slabs	
3-B-F		8.2				
3-C-F		8.8				

Core No.	Mile Post	Core Length (inch)	Base		Comments	
			LR			
1-A-T	9.888	7.2				
1-B-F		7				
1-C-F		7.2				
2-A-T	9.517	8	8.5		15.4' Joint We could not find dowel  No shoulder	
2-B-F		8.2				
2-C-F		8.2				
3-A-T	9.288	9.3			12' Lane width Transverse cracks Patched slabs	
3-B-F		8.5				
3-C-F		8.5				
4-A-T	8.962	8.5	11			
4-B-F		8				
4-C-F		8				

**Table C27. Core Data of 87060000 at SR A1A in Dade County.**

Core No.	Mile Post	FC2	S1	T	Core Length (inch)	Base		Comments
						LR	STAB	
1-A-T	2.595	0.6	2.3	5.4	8.3			
1-B-F		0.6	2.4	5.5	8.5			
2-A-T	2.266	0.6	2.9	5.1	8.6			
2-B-F		0.6	2.9	5.1	8.6			
2-C-T		0.7	2.8	5.2	8.7			
3-A-T	2.149	0.5	2.7	5.1	8.3	14	16	Trench GWT = 5.3'
3-B-F		0.5	2.7	5.1	8.3			
3-C-T		0.5	2.7	5.1	8.3			
4-A-T	2.009	0.6	3.3	5.1	9			
4-B-F		0.6	3.3	5.1	9			
5-A-T	1.792	0.5	3	5.4	8.9			We trenched all the way down up to 3' and still it was LR. Top down crack
5-B-F		0.4	2.9	5.5	8.8			
5-C-T		0.4	2.9	5.5	8.8			
5-D-T		0.3	3	5.5	8.8			
6-A-T	1.629	0.5	3.3	4.8	8.6			
6-B-F		0.5	3.2	4.7	8.4			
7-A-T	1.493	0.4	2.9	4.5	7.8			
7-B-F		0.5	3	4.7	8.2			
7-C-T		0.5	3.1	4.8	8.4			
8-A-T	1.429	0.5	3.6	5.4	9.5			
8-B-F		0.5	3.6	5.4	9.5			
8-C-T		0.6	3.5	5.3	9.4			
9-A-T	1.289	0.5	3.1	5.4	9			
9-B-F		0.4	3	5.3	8.7			
9-C-T		0.4	3	5.3	8.7			
10-A-T	0.996	0.5	2.9	5.3	8.7			
10-B-F		0.5	2.9	5.3	8.7			

**Table C28. Core Data of 90060000 at US1 in Monroe County.**

Core No.	Mile Post	FC2	S1	T1	ST	Core Length (inch)	Base		Comments
							LR	Embank.	
1-A-T	13.3	0.4	1.8	0.9	0.4	3.5			
1-B-F		0.5	1.7	1	0.5	3.7			
2-A-T	13.534	0.6	1.3	1.1		3			
2-B-F		0.7	1.3	0.9	0.2	3.1			
3-A-T	13.76	0.5	1.5	0.5	1.5	4			
3-B-F		0.5	1.5	0.5	1.5	4			
3-C-T		0.5	1.5	0.5	1.5	4			
4-A-T	14.08	0.4	1	1.5	1	3.9			
4-B-F		0.4	1	1.5	1	3.9			
4-C-T		0.4	1	1.5	1	3.9			
5-A-T	14.155	0.4	1	2		3.4			
5-B-F		0.4	1	2		3.4			
5-C-T		0.5	1	2.5		4			
6-A-T	14.328	0.3	3.5	1		4.8			Alligator crack
6-B-F		0.3	3.5	1		4.8			
6-C-T		0.3	3.5	1		4.8			
6-D-T		0.3	3.5	1		4.8			
7-A-T	14.73	0.3	1	1.8		3.1			
7-B-F		0.3	1	1.8		3.1			
8-A-T	15.067	0.2	1	2.2	0.2	3.6			
8-B-F		0.2	1	2.2	0.2	3.6			
9-A-T	15.337	0.4	1.1	1	1.4	3.9			
9-B-F		0.4	1.1	1	1.4	3.9			
9-C-T		0.4	1.1	1	1.4	3.9			

**Table C28. Core Data of 90060000 at US1 in Monroe County (continued).**

Core No.	Mile Post	FC2	S1	T1	ST	Core Length (inch)	Base		Comments
							LR	Embank.	
10-A-T	15.528	0.5	0.9	1.8	0.9	4.1			Trench
10-B-F		0.5	0.9	1.8	0.9	4.1	24		Top Down
10-C-T		0.5	0.9	1.8	0.9	4.1			
11-A-T	15.917	0.4	1.1	2.5		4			GWT = 6.1'
11-B-F		0.4	1.1	2.5		4			
12-A-T	16.2	0.4	1.1	2.5		4			
12-B-F		0.4	1.1	2.5		4			
12-C-T		0.4	1.1	2.5		4			

**APPENDIX D**

**SUMMARY OF EXTRACTION AND DSR DATA ON AC CORES**



**Table D1. Properties Determined from Extractions and DSR Tests on Core Samples from Section 16250000 in Polk County.**

Sample No.	G <sub>mb</sub>	G <sub>mm</sub>	P <sub>b</sub> (%)	G <sub>se</sub>	G <sub>sb</sub>	V <sub>be</sub> (%)	% AV
1-1	2.08	2.39	5.90	2.60	2.57	10.94	12.87
1-2	2.13	2.33	6.71	2.56	2.54	13.09	8.68
1-3	2.18	2.31	7.42	2.56	2.51	14.05	5.47
1-4	2.06	2.33	6.84	2.57	2.44	9.63	11.91
1-5	1.98	2.33	5.41	2.51	2.40	7.11	14.83
2-1	2.08	2.39	5.90	2.60	2.57	10.93	12.93
2-2	2.15	2.33	6.71	2.56	2.54	13.20	7.91
2-3	2.15	2.31	7.42	2.56	2.51	13.86	6.70
2-4	2.01	2.33	6.84	2.57	2.44	9.43	13.73
2-5	2.02	2.33	5.41	2.51	2.40	7.24	13.27
3-1	2.05	2.39	5.90	2.60	2.57	10.76	14.29
3-2	2.15	2.33	6.71	2.56	2.54	13.20	7.89
3-3	2.20	2.31	7.42	2.56	2.51	14.19	4.52
3-4	2.04	2.33	6.84	2.57	2.44	9.53	12.80
3-5	1.97	2.33	5.41	2.51	2.40	7.07	15.33
4-1	2.08	2.39	5.90	2.60	2.57	10.90	13.13
4-2	2.18	2.33	6.71	2.56	2.54	13.40	6.55
4-3	2.21	2.31	7.42	2.56	2.51	14.27	3.97
4-4	2.01	2.33	6.84	2.57	2.44	9.43	13.72
4-5	2.00	2.33	5.41	2.51	2.40	7.17	14.05
5-1	2.10	2.39	5.90	2.60	2.57	11.02	12.17
5-2	2.20	2.33	6.71	2.56	2.54	13.50	5.84
5-3	2.18	2.31	7.42	2.56	2.51	14.02	5.64
5-4	2.06	2.33	6.84	2.57	2.44	9.64	11.87
5-5	1.98	2.33	5.41	2.51	2.40	7.10	14.97
6-1	2.06	2.39	5.90	2.60	2.57	10.81	13.86
6-2	2.17	2.33	6.71	2.56	2.54	13.35	6.88
6-3	2.18	2.31	7.42	2.56	2.51	14.06	5.35
6-4	2.00	2.33	6.84	2.57	2.44	9.38	14.22
6-5	1.99	2.33	5.41	2.51	2.40	7.13	14.57
7-1	2.16	2.39	5.90	2.60	2.57	11.37	9.38
7-2	2.13	2.33	6.71	2.56	2.54	13.09	8.67
7-3	2.22	2.31	7.42	2.56	2.51	14.32	3.61
7-4	2.08	2.33	6.84	2.57	2.44	9.72	11.09
7-5	2.28	2.33	5.41	2.51	2.40	8.16	2.21
8-1	2.08	2.39	5.90	2.60	2.57	10.92	13.01
8-2	2.10	2.33	6.71	2.56	2.54	12.88	10.18
8-3	2.19	2.31	7.42	2.56	2.51	14.10	5.10
8-4	2.03	2.33	6.84	2.57	2.44	9.50	13.08
8-5	2.33	2.33	5.41	2.51	2.40	8.36	-0.18
9-1	2.12	2.39	5.90	2.60	2.57	11.11	11.45
9-2	2.14	2.33	6.71	2.56	2.54	13.14	8.36
9-3	2.24	2.31	7.42	2.56	2.51	14.42	2.98
9-4	2.15	2.33	6.84	2.57	2.44	10.07	7.87
9-5	2.30	2.33	5.41	2.51	2.40	8.26	1.03

**Table D1. Properties Determined from Extractions and DSR Tests on Core Samples from Section 16250000 in Polk County (continued).**

Sample No.	G <sub>mb</sub>	G <sub>mm</sub>	P <sub>b</sub> (%)	G <sub>se</sub>	G <sub>sb</sub>	V <sub>be</sub> (%)	% AV
10-1	2.08	2.39	5.90	2.60	2.57	10.91	13.05
10-2	2.17	2.33	6.71	2.56	2.54	13.34	6.97
10-3	2.14	2.31	7.42	2.56	2.51	13.79	7.21
10-4	2.03	2.33	6.84	2.57	2.44	9.53	12.82
10-5	2.15	2.33	5.41	2.51	2.40	7.71	7.59
11-1	2.06	2.39	5.90	2.60	2.57	10.80	13.93
11-2	2.19	2.33	6.71	2.56	2.54	13.48	5.97
11-3	2.17	2.31	7.42	2.56	2.51	14.01	5.75
11-4	2.03	2.33	6.84	2.57	2.44	9.51	12.98
11-5	2.30	2.33	5.41	2.51	2.40	8.25	1.13

**Gradation**

Property	Layer 1	Layer 2	Layer 3	Layer 4	Layer 5
Retained 3/4	0	0	0	0	0
Retained 3/8	0.06	0	0.38	0.65	0.06
Retained #4	6.13	21.88	25.39	17.17	12.11
% #200	6.27	6.4	6.48	6.63	6.19
Ave. V <sub>be</sub> (%)	10.95	13.24	14.10	9.58	7.59
Ave. AV (%)	12.9	7.5	5.4	12.5	9.0

**DSR**

Temp.(°C)	Layer 1			Layer 2			Layer 3		
	Vis.(cP)	G* (Pa)	δ°	Vis.(cP)	G* (Pa)	δ°	Vis.(cP)	G* (Pa)	δ°
52	31,891,000	319,760	54.90	25,433,300	254,333	55.53	11,633,300	116,667	61.17
58	14,611,000	146,490	60.20	11,000,000	110,000	60.43	5,020,000	50,200	65.66
64	6,703,100	67,208	64.50	5,013,300	50,133	64.90	2,356,700	23,567	69.97
70	3,048,900	30,569	68.70	2,293,300	22,933	69.21	1,066,700	10,667	74.00
76	1,422,800	14,265	73.00	1,116,700	11,200	73.49	507,000	5,070	77.87
82	637,700	6,394	76.50	484,000	4,840	77.37	200,000	2,000	81.54
88	299,200	3,000	79.60	222,000	2,200	80.57	106,000	1,060	83.89
A-VTS	9.17 -2.19			9.38 -3.07			9.89 -3.26		

Temp.(°C)	Layer 4			Layer 5		
	Vis.(cP)	G* (Pa)	δ°	Vis.(cP)	G* (Pa)	δ°
52	27,666,700	276,667	55.57	102,500,000	1,025,000	51.92
58	11,900,000	119,000	60.39	44,966,700	500,000	55.67
64	5,486,700	54,867	64.85	23,633,300	236,333	58.97
70	2,490,000	24,967	69.24	11,500,000	115,000	62.06
76	1,160,000	11,600	73.66	5,686,700	56,933	65.60
82	527,300	5,273	77.40	2,256,700	22,567	69.21
88	245,000	2,450	80.86	1,153,300	11,533	72.22
A-VTS	9.33 -3.05			8.21 -2.64		

**Table D2. Properties Determined from Extractions and DSR Tests on Core Samples from Section 26005000 in Alachua County.**

Sample No.	G <sub>mb</sub>	G <sub>mm</sub>	P <sub>b</sub> (%)	G <sub>se</sub>	G <sub>sb</sub>	V <sub>be</sub> (%)	% AV
1-1	2.04	2.40	6.08	2.62	2.56	10.13	14.85
1-2	2.18	2.36	6.04	2.58	2.47	9.38	7.74
1-3	2.15	2.38	7.42	2.65	2.46	9.76	9.38
1-4			5.74		2.46		
2-1	2.11	2.40	6.08	2.62	2.56	10.47	12.04
2-2	2.15	2.36	6.04	2.58	2.47	9.25	9.03
2-3	2.22	2.38	7.42	2.65	2.46	10.08	6.39
2-4	2.16	2.37	5.74	2.57	2.46	8.52	8.90
3-1	2.02	2.40	6.08	2.62	2.56	10.03	15.73
3-2	2.05	2.36	6.04	2.58	2.47	8.84	13.09
3-3	2.15	2.38	7.42	2.65	2.46	9.75	9.46
3-4	2.13	2.37	5.74	2.57	2.46	8.42	10.01
4-1	2.05	2.40	6.08	2.62	2.56	10.16	14.65
4-2	2.16	2.36	6.04	2.58	2.47	9.29	8.58
4-3	2.22	2.38	7.42	2.65	2.46	10.08	6.41
4-4	2.19	2.37	5.74	2.57	2.46	8.65	7.51
5-1	1.98	2.40	6.08	2.62	2.56	9.81	17.54
5-2	2.17	2.36	6.04	2.58	2.47	9.33	8.25
5-3	2.19	2.38	7.42	2.65	2.46	9.92	7.91
5-4	2.18	2.37	5.74	2.57	2.46	8.60	8.05
6-1	2.01	2.40	6.08	2.62	2.56	9.99	16.04
6-2	2.21	2.36	6.04	2.58	2.47	9.48	6.70
6-3	2.21	2.38	7.42	2.65	2.46	10.02	6.94
6-4	2.19	2.37	5.74	2.57	2.46	8.66	7.40
7-1	1.99	2.40	6.08	2.62	2.56	9.87	17.08
7-2	2.19	2.36	6.04	2.58	2.47	9.42	7.31
7-3	2.23	2.38	7.42	2.65	2.46	10.10	6.20
7-4	2.23	2.37	5.74	2.57	2.46	8.82	5.71
8-1	2.06	2.40	6.08	2.62	2.56	10.22	14.11
8-2	2.14	2.36	6.04	2.58	2.47	9.20	9.52
8-3	2.10	2.38	7.42	2.65	2.46	9.52	11.57
8-4	2.14	2.37	5.74	2.57	2.46	8.43	9.85
9-1	1.97	2.40	6.08	2.62	2.56	9.79	17.72
9-2	2.19	2.36	6.04	2.58	2.47	9.41	7.45
9-3	2.22	2.38	7.42	2.65	2.46	10.09	6.32
9-4	2.02	2.37	5.74	2.57	2.46	7.99	14.58
10-1	1.98	2.40	6.08	2.62	2.56	9.85	17.27
10-2	2.13	2.36	6.04	2.58	2.47	9.16	9.84
10-3	2.10	2.38	7.42	2.65	2.46	9.53	11.54
10-4	2.13	2.37	5.74	2.57	2.46	8.39	10.28
11-1	2.01	2.40	6.08	2.62	2.56	10.00	16.01
11-2	2.19	2.36	6.04	2.58	2.47	9.41	7.39
11-3	2.07	2.38	7.42	2.65	2.46	9.38	12.89
11-4	2.13	2.37	5.74	2.57	2.46	8.43	9.89

### Gradation

Property	Layer 1	Layer 2	Layer 3	Layer 4
Retained 3/4	0	0	0	0
Retained 3/8	0.97	9.23	0.38	4.88
Retained #4	12.29	21.01	25.39	21.58
% #200	7.27	8.81	6.48	9.11
Ave. $V_{bc}$ (%)	10.03	9.29	9.84	8.49
Ave. AV (%)	15.7	8.6	8.6	9.2

### DSR

Temp.(°C)	Layer 1			Layer 2			Layer 3		
	Vis.(cP)	G* (Pa)	$\delta^\circ$	Vis.(cP)	G* (Pa)	$\Delta^\circ$	Vis.(cP)	G* (Pa)	$\delta^\circ$
52	42,033,300	420,333	50.92	19,900,000	199,333	59.48	18,566,700	185,667	57.61
58	20,300,000	203,000	54.95	8,933,300	89,367	63.53	8,243,300	82,433	62.13
64	9,876,700	98,800	58.61	4,090,000	40,900	67.50	3,806,700	38,067	66.29
70	4,783,300	47,833	62.15	1,886,700	18,867	71.57	1,770,000	17,700	70.18
76	2,330,000	23,300	65.96	886,300	8,870	75.14	839,000	8,397	74.01
82	1,000,000	10,000	70.35	436,000	4,363	78.13	401,000	4,010	77.68
88	505,700	5,060	73.99	202,000	2,020	81.10	184,000	1,840	80.91
A-VTS	8.55 -2.77			9.23 -3.02			9.30 -3.05		

Temp.(°C)	Layer 4		
	Vis.(cP)	G* (Pa)	$\delta^\circ$
52	18,666,700	187,000	58.29
58	8,506,700	85,100	62.09
64	3,863,300	38,633	65.97
70	1,786,700	17,867	69.47
76	849,000	8,490	73.14
82	384,000	3,840	77.69
88	201,000	2,010	80.18
A-VTS	9.24 -3.03		

**Table D3. Properties Determined from Extractions and DSR Tests on Core Samples from Section 28040000 in Bradford County.**

Sample No.	G <sub>mb</sub>	G <sub>mm</sub>	P <sub>b</sub> (%)	G <sub>se</sub>	G <sub>sb</sub>	V <sub>be</sub> (%)	% AV
1-1	1.95	2.36	6.67	2.60	2.52	10.46	17.62
1-2	2.16	2.40	4.69	2.56	2.51	8.01	9.97
1-3	2.09	2.41	5.48	2.60	2.55	9.50	13.16
2-1	1.97	2.36	6.67	2.60	2.52	10.58	16.66
2-2	2.22	2.40	4.69	2.56	2.51	8.23	7.49
2-3	2.04	2.41	5.48	2.60	2.55	9.29	15.06
3-1	1.97	2.36	6.67	2.60	2.52	10.59	16.57
3-2	2.22	2.40	4.69	2.56	2.51	8.23	7.49
3-3	2.04	2.41	5.48	2.60	2.55	9.28	15.13
4-1	1.96	2.36	6.67	2.60	2.52	10.55	16.92
4-2	2.19	2.40	4.69	2.56	2.51	8.15	8.38
4-3	1.99	2.41	5.48	2.60	2.55	9.03	17.43
5-1	1.96	2.36	6.67	2.60	2.52	10.51	17.19
5-2	2.18	2.40	4.69	2.56	2.51	8.08	9.17
5-3	2.05	2.41	5.48	2.60	2.55	9.32	14.73
6-1	1.94	2.36	6.67	2.60	2.52	10.42	17.93
6-2	2.21	2.40	4.69	2.56	2.51	8.20	7.80
6-3	2.06	2.41	5.48	2.60	2.55	9.37	14.31
7-1	1.93	2.36	6.67	2.60	2.52	10.38	18.29
7-2	2.20	2.40	4.69	2.56	2.51	8.17	8.15
7-3	2.01	2.41	5.48	2.60	2.55	9.15	16.28
8-1	1.98	2.36	6.67	2.60	2.52	10.67	15.93
8-2	2.23	2.40	4.69	2.56	2.51	8.27	7.00
8-3	2.03	2.41	5.48	2.60	2.55	9.24	15.54
9-1	1.97	2.36	6.67	2.60	2.52	10.57	16.77
9-2	2.22	2.40	4.69	2.56	2.51	8.24	7.39
9-3	2.01	2.41	5.48	2.60	2.55	9.14	16.38
10-1	1.98	2.36	6.67	2.60	2.52	10.65	16.13
10-2	2.20	2.40	4.69	2.56	2.51	8.17	8.17
10-3	2.01	2.41	5.48	2.60	2.55	9.13	16.48
11-1	1.96	2.36	6.67	2.60	2.52	10.53	17.10
11-2	2.21	2.40	4.69	2.56	2.51	8.22	7.66
11-3	1.99	2.41	5.48	2.60	2.55	9.07	17.09
12-1	2.02	2.36	6.67	2.60	2.52	10.84	14.59
12-2	2.21	2.40	4.69	2.56	2.51	8.21	7.76
12-3	2.02	2.41	5.48	2.60	2.55	9.21	15.82
13-1	1.98	2.36	6.67	2.60	2.52	10.65	16.14
13-2	2.21	2.40	4.69	2.56	2.51	8.23	7.54
13-3	2.04	2.41	5.48	2.60	2.55	9.29	15.00
14-1	1.99	2.36	6.67	2.60	2.52	10.70	15.70
14-2	2.22	2.40	4.69	2.56	2.51	8.24	7.34
14-3	2.04	2.41	5.48	2.60	2.55	9.29	15.04
15-1	1.98	2.36	6.67	2.60	2.52	10.66	16.03
15-2	2.23	2.40	4.69	2.56	2.51	8.27	7.04
15-3	2.05	2.41	5.48	2.60	2.55	9.30	14.91

**Table D3. Properties Determined from Extractions and DSR Tests on Core Samples from Section 28040000 in Bradford County (continued).**

Sample No.	G <sub>mb</sub>	G <sub>mm</sub>	P <sub>b</sub> (%)	G <sub>se</sub>	G <sub>sb</sub>	V <sub>be</sub> (%)	% AV
16-1	1.94	2.36	6.67	2.60	2.52	10.41	18.03
16-2	2.21	2.40	4.69	2.56	2.51	8.23	7.52
16-3	2.08	2.41	5.48	2.60	2.55	9.45	13.56

**Gradation**

Property	Layer 1	Layer 2	Layer 3
Retained 3/4	0	0	0
Retained 3/8	0	0.19	0
Retained #4	5.26	25.54	0.51
% #200	5.72	6.58	8.62
Ave. V <sub>be</sub> (%)	10.57	8.20	9.25
Ave. AV (%)	16.7	7.9	15.4

**DSR**

Temp.(°C)	Layer 1			Layer 2			Layer 3		
	Vis.(cP)	G* (Pa)	δ°	Vis.(cP)	G* (Pa)	δ°	Vis.(cP)	G* (Pa)	δ°
52	32,166,700	322,000	57.29	27,400,000	274,500	55.14	30,500,000	305,000	53.60
58	14,700,000	147,000	61.86	14,033,300	140,333	58.52	13,500,000	135,000	59.00
64	6,823,300	68,267	66.19	6,210,000	62,100	63.85	5,810,000	58,133	64.60
70	3,093,300	30,933	70.48	2,756,700	27,567	69.24	2,363,300	23,633	69.82
76	1,460,000	14,600	74.39	1,193,300	11,933	74.13	1,030,000	10,300	74.62
82	647,000	6,473	78.24	439,300	4,393	79.04	435,300	4,353	79.16
88	315,000	3,150	81.25	204,700	2,047	82.42	206,000	2,060	82.14
A-VTS	9.10	-2.97		9.87	-3.25		9.99	-3.29	

**Table D4. Properties Determined from Extractions and DSR Tests on Core Samples from Section 50100000 in Gadsden County.**

Sample No.	G <sub>mb</sub>	G <sub>mm</sub>	P <sub>b</sub> (%)	G <sub>se</sub>	G <sub>sb</sub>	V <sub>be</sub> (%)	% AV
1-1	2.21	2.46	5.71	2.69	2.66	11.59	10.06
1-2	2.24	2.39	6.54	2.63	2.56	11.98	5.98
1-3	2.23	2.46	5.03	2.65	2.65	11.04	9.01
1-4	2.25	2.37	5.75	2.57	2.50	10.05	5.08
2-1	2.23	2.46	5.71	2.69	2.66	11.66	9.49
2-2	2.25	2.39	6.54	2.63	2.56	12.01	5.71
2-3	2.25	2.46	5.03	2.65	2.65	11.14	8.19
2-4	2.17	2.37	5.75	2.57	2.50	9.67	8.60
3-1	2.21	2.46	5.71	2.69	2.66	11.56	10.27
3-2	2.30	2.39	6.54	2.63	2.56	12.27	3.66
3-3	2.31	2.46	5.03	2.65	2.65	11.40	6.07
3-4	2.14	2.37	5.75	2.57	2.50	9.57	9.55
4-1	2.26	2.46	5.71	2.69	2.66	11.83	8.23
4-2	2.30	2.39	6.54	2.63	2.56	12.27	3.69
4-3	2.23	2.46	5.03	2.65	2.65	11.02	9.18
4-4	2.23	2.37	5.75	2.57	2.50	9.95	6.00
5-1	2.23	2.46	5.71	2.69	2.66	11.66	9.54
5-2	2.26	2.39	6.54	2.63	2.56	12.06	5.37
5-3	2.23	2.46	5.03	2.65	2.65	11.01	9.28
5-4	2.26	2.37	5.75	2.57	2.50	10.09	4.69
6-1	2.28	2.46	5.71	2.69	2.66	11.94	7.34
6-2	2.30	2.39	6.54	2.63	2.56	12.30	3.47
6-3	2.29	2.46	5.03	2.65	2.65	11.32	6.72
6-4	2.24	2.37	5.75	2.57	2.50	10.01	5.43
7-1	2.30	2.46	5.71	2.69	2.66	12.03	6.68
7-2	2.30	2.39	6.54	2.63	2.56	12.27	3.73
7-3	2.28	2.46	5.03	2.65	2.65	11.28	7.08
7-4	2.23	2.37	5.75	2.57	2.50	9.97	5.79
8-1	2.28	2.46	5.71	2.69	2.66	11.91	7.59
8-2	2.26	2.39	6.54	2.63	2.56	12.07	5.27
8-3	2.31	2.46	5.03	2.65	2.65	11.42	5.87
8-4	2.20	2.37	5.75	2.57	2.50	9.84	7.05

**Gradation**

Property	Layer 1	Layer 2	Layer 3	Layer 4
Retained 3/4	0	0	0	0.35
Retained 3/8	0.14	5.12	0.46	10.2
Retained #4	45.52	22.77	29.79	28.19
% #200	4.15	8.37	4.93	6.36
Ave. V <sub>be</sub> (%)	11.77	12.15	11.20	9.89
Ave. AV (%)	8.6	4.6	7.7	6.5

**DSR**

Temp.(°C)	Layer 1			Layer 2			Layer 3		
	Vis.(cP)	G* (Pa)	$\delta^\circ$	Vis.(cP)	G* (Pa)	$\delta^\circ$	Vis.(cP)	G* (Pa)	$\delta^\circ$
52	51,400,000	514,000	56.71	3,185,000	31,850	73.63	23,900,000	239,000	54.93
58	23,250,000	232,500	60.60	1,330,000	13,350	77.12	10,900,000	109,000	58.73
64	10,750,000	107,500	63.89	590,000	5,900	80.08	5,695,000	57,050	63.09
70	4,910,000	49,100	66.67	266,500	2,670	82.77	2,890,000	28,900	66.42
76	2,370,000	23,700	69.76	128,000	1,280	85.15	1,310,000	13,100	70.79
82	1,205,000	12,050	71.77	58,200	583	86.88	656,500	6,565	74.52
88	561,000	5,610	75.52	31,800	318	88.56	310,000	3,100	78.39
A-VTS	8.58 -2.78			10.56 -3.52			8.58 -2.79		

Temp.(°C)	Layer 4		
	Vis.(cP)	G* (Pa)	$\delta^\circ$
52	43,762,000	438,700	48.70
58	21,751,000	218,090	54.50
64	10,111,000	101,370	60.20
70	4,571,100	45,832	65.50
76	2,103,100	21,087	70.60
82	967,300	9,699	75.00
88	459,900	4,611	78.70
A-VTS	8.84 -2.87		

**Table D5. Properties Determined from Extractions and DSR Tests on Core Samples from Section 58060000 in Santa Rosa County.**

Sample No.	G <sub>mb</sub>	G <sub>mm</sub>	P <sub>b</sub> (%)	G <sub>se</sub>	G <sub>sb</sub>	V <sub>be</sub> (%)	% AV
1-1	2.15	2.39	7.09	2.66	2.54	11.42	10.05
1-2	2.18	2.42	7.60	2.72	2.64	13.54	10.13
1-3	2.08	2.41	6.61	2.65	2.54	10.12	13.37
1-4	2.39	2.56	5.12	2.78	2.72	10.15	6.56
1-5	2.45	2.49	5.90	2.73	2.69	12.82	1.54
2-1	2.19	2.39	7.09	2.66	2.54	11.62	8.51
2-2	2.18	2.42	7.60	2.72	2.64	13.53	10.23
2-3	2.11	2.41	6.61	2.65	2.54	10.27	12.14
2-4	2.41	2.56	5.12	2.78	2.72	10.23	5.83
2-5	2.43	2.49	5.90	2.73	2.69	12.70	2.45
3-1	2.19	2.39	7.09	2.66	2.54	11.65	8.26
3-2	2.16	2.42	7.60	2.72	2.64	13.40	11.07
3-3	2.06	2.41	6.61	2.65	2.54	9.99	14.55
3-4	2.41	2.56	5.12	2.78	2.72	10.24	5.69
3-5	2.45	2.49	5.90	2.73	2.69	12.82	1.53
4-1	2.21	2.39	7.09	2.66	2.54	11.76	7.39
4-2	2.33	2.42	7.60	2.72	2.64	14.49	3.83
4-3	2.06	2.41	6.61	2.65	2.54	10.02	14.29
4-4	2.42	2.56	5.12	2.78	2.72	10.27	5.38
4-5	2.42	2.49	5.90	2.73	2.69	12.66	2.79
5-1	2.22	2.39	7.09	2.66	2.54	11.77	7.31
5-2	2.31	2.42	7.60	2.72	2.64	14.34	4.83
5-3	2.05	2.41	6.61	2.65	2.54	9.97	14.65
5-4	2.44	2.56	5.12	2.78	2.72	10.35	4.66
5-5	2.45	2.49	5.90	2.73	2.69	12.83	1.52
6-1	2.19	2.39	7.09	2.66	2.54	11.64	8.34
6-2	2.19	2.42	7.60	2.72	2.64	13.61	9.67
6-3	2.06	2.41	6.61	2.65	2.54	10.03	14.20
6-4	2.41	2.56	5.12	2.78	2.72	10.23	5.80
6-5	2.42	2.49	5.90	2.73	2.69	12.68	2.67
7-1	2.18	2.39	7.09	2.66	2.54	11.57	8.90
7-2	2.20	2.42	7.60	2.72	2.64	13.65	9.39
7-3	2.08	2.41	6.61	2.65	2.54	10.09	13.62
7-4	2.44	2.56	5.12	2.78	2.72	10.34	4.73
7-5	2.44	2.49	5.90	2.73	2.69	12.79	1.77
8-1	2.19	2.39	7.09	2.66	2.54	11.63	8.42
8-2	2.16	2.42	7.60	2.72	2.64	13.40	11.07
8-3	2.10	2.41	6.61	2.65	2.54	10.21	12.66
8-4	2.33	2.56	5.12	2.78	2.72	9.90	8.83
8-5	2.37	2.49	5.90	2.73	2.69	12.42	4.66
9-1	2.21	2.39	7.09	2.66	2.54	11.74	7.56
9-2	2.23	2.42	7.60	2.72	2.64	13.85	8.05
9-3	2.12	2.41	6.61	2.65	2.54	10.31	11.73
9-4	2.41	2.56	5.12	2.78	2.72	10.23	5.83
9-5	2.43	2.49	5.90	2.73	2.69	12.70	2.45

### Gradation

Property	Layer 1	Layer 2	Layer 3	Layer 4	Layer 5
Retained 3/4	0	0	0	0	0
Retained 3/8	1.88	0	0.82	1.43	1.87
Retained #4	22.23	4.30	3	30.36	27.75
% #200	6.29	9.83	6.94	4.23	5.38
Ave. $V_{bc}$ (%)	11.65	13.76	10.11	10.22	12.71
Ave. AV (%)	8.3	8.7	13.5	5.9	2.4

### DSR

Temp.(°C)	Layer 1			Layer 2			Layer 3		
	Vis.(cP)	G* (Pa)	$\delta^\circ$	Vis.(cP)	G* (Pa)	$\delta^\circ$	Vis.(cP)	G* (Pa)	$\delta^\circ$
52	36,968,000	370,660	57.50	22,892,000	229,520	57.00	37,222,000	373,200	41.60
58	16,785,000	168,290	62.10	10,281,000	103,080	61.40	18,278,000	183,260	47.70
64	7,628,700	76,488	66.40	4,695,200	47,076	65.50	8,709,300	87,323	53.00
70	3,484,100	34,933	70.20	2,204,800	22,106	69.50	4,171,200	41,822	58.40
76	1,592,100	15,963	73.90	1,057,000	10,598	73.00	2,055,800	20,612	63.40
82	821,900	8,241	76.70	530,800	5,322	76.30	1,048,000	10,508	67.60
88	409,200	4,103	79.40	279,400	2,801	79.20	523,800	5,252	72.50
A-VTS	8.79 -2.86			8.84 -2.88			8.28 -2.67		

Temp.(°C)	Layer 4			Layer 5		
	Vis.(cP)	G* (Pa)	$\delta^\circ$	Vis.(cP)	G* (Pa)	$\delta^\circ$
52	70,700,000	708,000	46.10	7,400,000	74,000	67.22
58	36,066,700	360,667	52.77	2,850,000	28,500	72.06
64	15,266,700	153,333	58.92	1,160,000	11,600	79.51
70	6,070,000	60,700	64.89	501,000	5,010	79.95
76	2,630,000	26,300	69.97	226,000	2,260	82.93
82	1,225,000	12,250	74.19	91,900	919	85.33
88	511,000	5,110	78.56	46,900	469	87.18
A-VTS	9.36 -3.06			11.04 -3.69		

**Table D6. Properties Determined from Extractions and DSR Tests on Core Samples from Section 86190000 in Broward County.**

Sample No.	G <sub>mb</sub>	G <sub>mm</sub>	P <sub>b</sub> (%)	G <sub>se</sub>	G <sub>sb</sub>	V <sub>be</sub> (%)	% AV
1-1	2.10	2.32	5.19	2.49	2.53	11.84	9.28
1-2	2.28	2.36	6.19	2.58	2.51	11.42	3.65
1-3	2.21	2.38	5.77	2.59	2.52	9.93	7.36
2-1	2.13	2.32	5.19	2.49	2.53	12.01	8.01
2-2	2.27	2.36	6.19	2.58	2.51	11.40	3.89
2-3	2.29	2.38	5.77	2.59	2.52	10.28	4.07
3-1	2.12	2.32	5.19	2.49	2.53	11.91	8.76
3-2	2.30	2.36	6.19	2.58	2.51	11.55	2.62
3-3	2.28	2.38	5.77	2.59	2.52	10.24	4.46
4-1	2.10	2.32	5.19	2.49	2.53	11.82	9.49
4-2	2.31	2.36	6.19	2.58	2.51	11.60	2.19
4-3	2.22	2.38	5.77	2.59	2.52	10.00	6.68
5-1	2.12	2.32	5.19	2.49	2.53	11.96	8.42
5-2	2.18	2.36	6.19	2.58	2.51	10.92	7.89
5-3	2.23	2.38	5.77	2.59	2.52	10.04	6.32

**Gradation**

Property	Layer 1	Layer 2	Layer 3
Retained 3/4	0	0	0
Retained 3/8	3.26	8.39	7.69
Retained #4	46.06	27.79	28.91
% #200	7.81	6.21	6.46
Ave. V <sub>be</sub> (%)	11.91	11.38	10.10
Ave. AV (%)	8.8	4.0	5.8

**DSR**

Temp.(°C)	Layer 1			Layer 2			Layer 3		
	Vis.(cP)	G* (Pa)	δ°	Vis.(cP)	G* (Pa)	δ°	Vis.(cP)	G* (Pa)	δ°
52	72,850,000	728,500	69.99	7,136,700	71,367	70.46	12,600,000	126,000	61.58
58	29,900,000	299,000	67.59	2,923,300	29,233	72.74	5,513,300	55,133	66.43
64	13,333,300	133,333	67.49	1,263,300	12,633	79.85	2,433,300	24,333	71.03
70	6,083,300	60,833	68.03	561,700	5,617	79.20	1,100,000	11,000	75.26
76	2,813,300	28,133	71.05	282,300	2,827	82.99	502,000	5,020	79.23
82	2,630,000	26,300	74.51	138,300	1,383	84.28	219,700	2,197	82.57
88	1,196,700	11,967	77.41	64,200	642	86.35	118,000	1,180	84.72
A-VTS	7.54 -2.40			10.07 -3.34			9.82 -3.24		

**Table D7. Properties Determined from Extractions and DSR Tests on Core Samples from Section 93100000 in Palm Beach County.**

Sample No.	G <sub>mb</sub>	G <sub>mm</sub>	P <sub>b</sub> (%)	G <sub>se</sub>	G <sub>sb</sub>	V <sub>be</sub> (%)	% AV
1-1	2.08	2.42	4.97	2.60	2.53	7.70	13.87
1-2	2.29	2.39	5.92	2.60	2.52	10.55	4.17
1-3	2.26	2.36	5.45	2.54	2.49	10.03	4.08
1-4	2.09	2.35	4.89	2.51	2.45	8.15	10.79
2-1	2.06	2.42	4.97	2.60	2.53	7.62	14.75
2-2	2.26	2.39	5.92	2.60	2.52	10.43	5.31
2-3	2.26	2.36	5.45	2.54	2.49	10.03	4.14
2-4	2.23	2.35	4.89	2.51	2.45	8.68	4.95
3-1	2.13	2.42	4.97	2.60	2.53	7.88	11.88
3-2	2.28	2.39	5.92	2.60	2.52	10.54	4.30
3-3	2.25	2.36	5.45	2.54	2.49	10.00	4.45
3-4	2.22	2.35	4.89	2.51	2.45	8.66	5.17
4-1	2.10	2.42	4.97	2.60	2.53	7.75	13.30
4-2	2.28	2.39	5.92	2.60	2.52	10.53	4.35
4-3	2.25	2.36	5.45	2.54	2.49	9.97	4.69
4-4	2.14	2.35	4.89	2.51	2.45	8.33	8.82
5-1	2.09	2.42	4.97	2.60	2.53	7.72	13.59
5-2	2.29	2.39	5.92	2.60	2.52	10.59	3.86
5-3	2.16	2.36	5.45	2.54	2.49	9.59	8.34
5-4	2.27	2.35	4.89	2.51	2.45	8.84	3.29

**Gradation**

Property	Layer 1	Layer 2	Layer 3	Layer 4
Retained 3/4	0	0	0	4.46
Retained 3/8	0.35	1.94	5.84	10.88
Retained #4	43.84	27.78	27.44	20.33
% #200	5.37	6.71	5.95	6.52
Ave. V <sub>be</sub> (%)	7.73	10.53	9.92	8.53
Ave. AV (%)	13.5	4.4	5.1	6.6

**DSR**

Temp.(°C)	Layer 1			Layer 2			Layer 3		
	Vis.(cP)	G* (Pa)	δ°	Vis.(cP)	G* (Pa)	δ°	Vis.(cP)	G* (Pa)	δ°
52	188,480,000	1,889,800	27.97	5,583,300	55,833	68.28	2,626,700	26,300	71.22
58	118,720,000	1,190,400	39.87	2,426,700	24,267	72.36	1,110,000	11,100	75.33
64	61,408,000	615,700	48.41	1,000,000	10,000	76.43	522,300	5,227	78.95
70	30,833,300	308,333	55.21	486,700	4,867	79.57	233,700	2,340	81.95
76	15,400,000	154,000	58.62	231,300	2,313	82.53	122,700	1,227	84.49
82	5,436,700	54,400	66.59	105,000	1,050	85.20	59,200	592	86.06
88	2,680,000	26,800	70.12	57,500	575	86.91	30,400	304	87.82
A-VTS	7.69	-2.45		10.08	-3.34		10.2	-3.40	

Temp.(°C)	Layer 4		
	Vis.(cP)	G* (Pa)	$\Delta^\circ$
52	12,333,300	123,333	64.02
58	5,440,000	54,400	68.50
64	2,420,000	24,200	73.16
70	1,160,000	11,633	76.38
76	514,300	5,143	80.41
82	244,300	2,443	82.81
88	109,700	1,097	85.13
A-VTS	9.78	-3.23	

**Table D8. Properties Determined from Extractions and DSR Tests on Core Samples from Section 93310000 in Palm Beach County.**

Sample No.	G <sub>mb</sub>	G <sub>mm</sub>	P <sub>b</sub> (%)	G <sub>se</sub>	G <sub>sb</sub>	V <sub>be</sub> (%)	% AV
1-1	2.02	2.38	4.72	2.54	2.47	6.86	14.97
1-2	2.18	2.32	5.78	2.51	2.45	10.06	5.92
1-3	2.18	2.34	6.27	2.56	2.50	11.31	6.74
2-1	2.04	2.38	4.72	2.54	2.47	6.92	14.27
2-2	2.17	2.32	5.78	2.51	2.45	10.00	6.51
2-3	2.22	2.34	6.27	2.56	2.50	11.50	5.11
3-1	2.11	2.38	4.72	2.54	2.47	7.14	11.55
3-2	2.18	2.32	5.78	2.51	2.45	10.07	5.83
3-3	2.20	2.34	6.27	2.56	2.50	11.41	5.87
4-1	2.09	2.38	4.72	2.54	2.47	7.08	12.26
4-2	2.18	2.32	5.78	2.51	2.45	10.05	6.04
4-3			6.27		2.50	#VALUE!	

### Gradation

Property	Layer 1	Layer 2	Layer 3
Retained 3/4	0	0	0
Retained 3/8	0.57	0.25	4.7
Retained #4	38.14	28.59	28.9
% #200	6.35	5.71	6.23
Ave. V <sub>be</sub> (%)	7.0	10.05	11.41
Ave. AV (%)	13.3	6.1	5.9

### DSR

Temp.(°C)	Layer 1			Layer 2			Layer 3		
	Vis.(cP)	G* (Pa)	$\Delta^\circ$	Vis.(cP)	G* (Pa)	$\delta^\circ$	Vis.(cP)	G* (Pa)	$\delta^\circ$
52	107,000,000	1,070,000	48.73	13,666,700	136,667	61.81	6,286,700	62,900	66.50
58	50,733,300	507,333	55.43	5,850,000	58,500	66.59	2,666,700	26,667	70.87
64	23,466,700	234,667	60.41	2,646,700	26,467	71.04	1,090,000	10,933	75.16
70	10,700,000	107,000	65.17	1,140,000	11,400	75.06	527,300	5,273	78.63
76	5,003,300	50,033	69.45	529,300	5,293	78.83	243,000	2,430	81.95
82	2,626,700	26,267	72.83	259,300	2,597	81.63	105,000	1,050	84.85
88	1,103,300	11,067	76.89	117,700	1,177	84.23	57,800	579	86.69
A-VTS	8.32	-2.68		9.81	-3.24		10.3	-3.42	

**Table D9. Properties Determined from Extractions and DSR Tests on Core Samples from Section 77040000 in Seminole County.**

Sample No.	G <sub>mb</sub>	G <sub>mm</sub>	P <sub>b</sub> (%)	G <sub>se</sub>	G <sub>sb</sub>	V <sub>be</sub> (%)	% AV
1-1	2.22	2.39	6.38	2.63	2.52	10.20	7.32
1-2	2.34	2.39	5.92	2.61	2.52	10.63	2.17
1-3	2.32	2.38	5.20	2.56	2.50	9.82	2.19
1-4	2.27	2.37	6.07	2.59	2.51	10.89	4.42
1-5			6.32		2.61		
2-1	2.08	2.39	6.38	2.63	2.52	9.56	13.16
2-2	2.16	2.39	5.92	2.61	2.52	9.81	9.71
2-3	2.22	2.38	5.20	2.56	2.50	9.38	6.61
2-4	2.27	2.37	6.07	2.59	2.51	10.91	4.22
2-5	2.06	2.41	6.32	2.64	2.61	11.48	14.46
3-1	2.00	2.39	6.38	2.63	2.52	9.22	16.19
3-2	2.21	2.39	5.92	2.61	2.52	10.04	7.56
3-3	2.24	2.38	5.20	2.56	2.50	9.48	5.64
3-4	2.25	2.37	6.07	2.59	2.51	10.82	5.05
3-5	2.25	2.41	6.32	2.64	2.61	12.54	6.58
4-1	2.09	2.39	6.38	2.63	2.52	9.60	12.79
4-2	2.16	2.39	5.92	2.61	2.52	9.81	9.66
4-3	2.17	2.38	5.20	2.56	2.50	9.16	8.77
4-4	2.06	2.37	6.07	2.59	2.51	9.92	12.92
4-5			6.32		2.61		
5-1	2.10	2.39	6.38	2.63	2.52	9.68	12.05
5-2	2.26	2.39	5.92	2.61	2.52	10.25	5.61
5-3	2.30	2.38	5.20	2.56	2.50	9.73	3.15
5-4			6.07		2.51		
5-5			6.32		2.61		
6-1	1.99	2.39	6.38	2.63	2.52	9.18	16.58
6-2	2.17	2.39	5.92	2.61	2.52	9.87	9.10
6-3	2.25	2.38	5.20	2.56	2.50	9.53	5.11
6-4	2.18	2.37	6.07	2.59	2.51	10.50	7.86
6-5	2.06	2.41	6.32	2.64	2.61	11.46	14.63
7-1	2.15	2.39	6.38	2.63	2.52	9.91	9.97
7-2	2.35	2.39	5.92	2.61	2.52	10.66	1.86
7-3	2.31	2.38	5.20	2.56	2.50	9.75	2.93
7-4	2.06	2.37	6.07	2.59	2.51	9.90	13.14
7-5			6.32		2.61		
8-1	2.04	2.39	6.38	2.63	2.52	9.38	14.79
8-2	2.26	2.39	5.92	2.61	2.52	10.26	5.52
8-3	2.32	2.38	5.20	2.56	2.50	9.80	2.43
8-4	2.17	2.37	6.07	2.59	2.51	10.41	8.66
8-5	2.06	2.41	6.32	2.64	2.61	11.47	14.53
9-1	2.07	2.39	6.38	2.63	2.52	9.51	13.56
9-2	2.35	2.39	5.92	2.61	2.52	10.68	1.68
9-3	2.34	2.38	5.20	2.56	2.50	9.91	1.31
9-4	2.27	2.37	6.07	2.59	2.51	10.93	4.07
9-5	2.03	2.41	6.32	2.64	2.61	11.31	15.70
10-1	2.06	2.39	6.38	2.63	2.52	9.48	13.82
10-2	2.31	2.39	5.92	2.61	2.52	10.49	3.39
10-3	2.34	2.38	5.20	2.56	2.50	9.88	1.67
10-4	2.11	2.37	6.07	2.59	2.51	10.15	10.88
10-5	2.08	2.41	6.32	2.64	2.61	11.61	13.53

**Table D9. Properties Determined from Extractions and DSR Tests on Core Samples from Section 77040000 in Seminole County (continued).**

Sample No.	G <sub>mb</sub>	G <sub>mm</sub>	P <sub>b</sub> (%)	G <sub>se</sub>	G <sub>sb</sub>	V <sub>be</sub> (%)	% AV
11-1	2.05	2.39	6.38	2.63	2.52	9.45	14.10
11-2	2.24	2.39	5.92	2.61	2.52	10.20	6.13
11-3	2.24	2.38	5.20	2.56	2.50	9.46	5.83
11-4	1.92	2.37	6.07	2.59	2.51	9.21	19.19
11-5			6.32		2.61		
12-1	2.08	2.39	6.38	2.63	2.52	9.57	12.99
12-2	2.26	2.39	5.92	2.61	2.52	10.26	5.57
12-3	2.25	2.38	5.20	2.56	2.50	9.50	5.42
12-4	2.11	2.37	6.07	2.59	2.51	10.13	11.10
12-5			6.32		2.61		
13-1	2.06	2.39	6.38	2.63	2.52	9.49	13.77
13-2	2.32	2.39	5.92	2.61	2.52	10.52	3.13
13-3	2.27	2.38	5.20	2.56	2.50	9.58	4.61
13-4	2.07	2.37	6.07	2.59	2.51	9.94	12.75
13-5			6.32		2.61		
14-1	2.20	2.391	6.38	2.63	2.52	10.14	7.86
14-2	2.18	2.391	5.92	2.61	2.52	9.90	8.82
14-3	2.32	2.376	5.2	2.56	2.50	9.81	2.30
14-4	2.29	2.371	6.07	2.59	2.51	10.98	3.60
14-5	2.07	2.408	6.32	2.64	2.61	11.53	14.12

**Gradation**

Property	Layer 1	Layer 2	Layer 3	Layer 4	Layer 5
Retained 3/4	0	0	0	0	0
Retained 3/8	0.45	1.34	5.1	4.35	2.62
Retained #4	7.17	23.1	26.78	19.65	9.2
% #200	6.73	9.03	9.15	8.51	9.56
Ave. V <sub>be</sub> (%)	9.60	10.24	9.63	10.36	11.63
Ave. AV (%)	12.8	5.7	4.1	9.1	13.4

**DSR**

Temp.(°C)	Layer 1			Layer 2			Layer 3		
	Vis.(cP)	G* (Pa)	δ°	Vis.(cP)	G* (Pa)	δ°	Vis.(cP)	G* (Pa)	δ°
52	16,400,000	164,000	58.74	8,193,300	81,933	67.24	6,256,700	62,600	67.74
58	7,290,000	72,900	63.33	3,456,700	34,567	71.48	2,646,700	26,500	71.95
64	3,330,000	33,300	67.74	1,520,000	15,200	75.54	1,190,000	11,900	75.76
70	1,523,300	15,233	72.23	664,700	6,650	79.14	550,000	5,500	79.24
76	733,000	7,330	76.28	326,300	3,263	82.23	258,000	2,580	82.08
82	361,000	3,610	79.38	134,700	1,347	84.91	134,000	1,340	84.39
88	165,000	1,650	82.46	73,700	737	86.68	60,700	607	86.16
A-VTS	9.33 -3.06			10.17 -3.37			9.98 -3.31		

Temp.(°C)	Layer 4			Layer 5		
	Vis.(cP)	G* (Pa)	$\delta^\circ$	Vis.(cP)	G* (Pa)	$\delta^\circ$
52	27,933,300	279,333	57.96	99,900,000	999,000	44.26
58	12,300,000	123,000	62.33	46,833,300	468,333	51.14
64	5,563,300	55,633	66.44	23,800,000	238,333	53.87
70	2,476,700	24,767	70.63	12,100,000	121,000	56.69
76	1,133,300	11,333	74.63	6,070,000	60,733	59.93
82	482,000	4,820	78.36	3,280,000	32,800	62.62
88	245,000	2,450	81.08	1,840,000	18,400	65.75
A-VTS	9.46 -3.10			7.36 -2.33		

**Table D10. Properties Determined from Extractions and DSR Tests on Core Samples from Section 79270000 in Volusia County.**

Sample No.	G <sub>mb</sub>	G <sub>mm</sub>	P <sub>b</sub> (%)	G <sub>se</sub>	G <sub>sb</sub>	V <sub>be</sub> (%)	% AV
1-1	2.06	2.38	6.01	2.59	2.48	8.50	13.20
1-2	2.23	2.39	5.84	2.60	2.49	9.03	6.90
1-3			5.75		2.49		
2-1	2.12	2.38	6.01	2.59	2.48	8.74	10.78
2-2	2.27	2.39	5.84	2.60	2.49	9.19	5.21
2-3	2.27	2.39	5.75	2.60	2.49	9.00	4.95
3-1	2.16	2.38	6.01	2.59	2.48	8.92	8.96
3-2	2.23	2.39	5.84	2.60	2.49	9.04	6.76
3-3	2.22	2.39	5.75	2.60	2.49	8.80	7.10
4-1	2.17	2.38	6.01	2.59	2.48	8.94	8.77
4-2	2.17	2.39	5.84	2.60	2.49	8.80	9.21
4-3	2.27	2.39	5.75	2.60	2.49	9.00	5.00
5-1	2.18	2.38	6.01	2.59	2.48	8.98	8.31
5-2	2.25	2.39	5.84	2.60	2.49	9.11	5.99
5-3	2.23	2.39	5.75	2.60	2.49	8.85	6.62
6-1	2.03	2.38	6.01	2.59	2.48	8.35	14.72
6-2	2.14	2.39	5.84	2.60	2.49	8.66	10.67
6-3	2.20	2.39	5.75	2.60	2.49	8.73	7.79
7-1	2.01	2.38	6.01	2.59	2.48	8.27	15.56
7-2	2.19	2.39	5.84	2.60	2.49	8.89	8.31
7-3	2.23	2.39	5.75	2.60	2.49	8.84	6.70

**Gradation**

Property	Layer 1	Layer 2	Layer 3
Retained 3/4	0	0	0.9
Retained 3/8	3.72	1.99	26.04
Retained #4	24.74	24.33	18.42
% #200	3.75	8.06	6.94
Ave. V <sub>be</sub> (%)	8.67	8.96	8.87
Ave. AV (%)	11.5	7.6	6.4

**DSR**

Temp.(°C)	Layer 1			Layer 2			Layer 3		
	Vis.(cP)	G* (Pa)	$\delta^\circ$	Vis.(cP)	G* (Pa)	$\delta^\circ$	Vis.(cP)	G* (Pa)	$\delta^\circ$
52	25,033,300	250,667	74.05	20,966,700	209,667	61.45	12,133,300	121,333	71.11
58	10,216,700	102,167	72.35	9,136,700	91,367	65.66	5,043,300	50,433	71.40
64	4,436,700	44,367	72.12	3,943,300	39,467	69.83	2,283,300	22,833	73.76
70	1,997,600	19,967	74.36	1,806,700	18,067	73.84	1,050,000	10,500	76.87
76	950,700	9,507	76.30	853,700	8,540	77.62	508,700	5,087	79.84
82	449,000	4,490	80.21	352,300	3,523	81.20	235,300	2,357	82.26
88	208,000	2,080	82.52	167,300	1,673	83.77	109,000	1,090	84.75
A-VTS	9.49 -3.11			9.75 -3.21			9.74 -3.21		

**Table D11. Properties Determined from Extractions and DSR Tests on Core Samples from Section 90060000 in Monroe County.**

Sample No.	G <sub>mb</sub>	G <sub>mm</sub>	P <sub>b</sub> (%)	G <sub>se</sub>	G <sub>sb</sub>	V <sub>be</sub> (%)	% AV
1-1	2.11	2.39	5.44	2.58	2.48	7.85	11.59
1-2	2.16	2.33	6.79	2.56	2.47	11.23	7.08
1-3	2.15	2.31	7.02	2.55	2.45	11.50	7.06
1-4	2.09	2.34	6.77	2.58	2.45	9.76	10.77
2-1	2.05	2.39	5.44	2.58	2.48	7.65	13.84
2-2	2.14	2.33	6.79	2.56	2.47	11.08	8.30
2-3	2.17	2.31	7.02	2.55	2.45	11.60	6.24
2-4			6.77		2.45		
3-1	2.08	2.39	5.44	2.58	2.48	7.75	12.72
3-2	2.18	2.33	6.79	2.56	2.47	11.31	6.40
3-3	2.11	2.31	7.02	2.55	2.45	11.31	8.57
3-4	2.11	2.34	6.77	2.58	2.45	9.86	9.86
4-1	2.07	2.39	5.44	2.58	2.48	7.71	13.20
4-2	2.26	2.33	6.79	2.56	2.47	11.73	2.95
4-3	2.22	2.31	7.02	2.55	2.45	11.88	3.96
4-4	2.10	2.34	6.77	2.58	2.45	9.79	10.55
5-1	2.09	2.39	5.44	2.58	2.48	7.76	12.57
5-2	2.23	2.33	6.79	2.56	2.47	11.56	4.38
5-3	2.22	2.31	7.02	2.55	2.45	11.89	3.87
5-4			6.77		2.45		
6-1	2.14	2.39	5.44	2.58	2.48	7.98	10.08
6-2	2.26	2.33	6.79	2.56	2.47	11.74	2.92
6-3	2.21	2.31	7.02	2.55	2.45	11.80	4.58
6-4			6.77		2.45		
7-1	2.05	2.39	5.44	2.58	2.48	7.63	14.11
7-2	2.17	2.33	6.79	2.56	2.47	11.24	7.04
7-3	2.21	2.31	7.02	2.55	2.45	11.81	4.49
7-4			6.77		2.45		
8-1			5.44		2.48		
8-2	2.24	2.33	6.79	2.56	2.47	11.62	3.84
8-3	2.22	2.31	7.02	2.55	2.45	11.86	4.07
8-4			6.77		2.45		
9-1	2.05	2.39	5.44	2.58	2.48	7.63	14.06
9-2	2.16	2.33	6.79	2.56	2.47	11.23	7.07
9-3	2.16	2.31	7.02	2.55	2.45	11.58	6.40

**Table D11. Properties Determined from Extractions and DSR Tests on Core Samples from Section 90060000 in Monroe County (continued).**

Sample No.	G <sub>mb</sub>	G <sub>mm</sub>	P <sub>b</sub> (%)	G <sub>se</sub>	G <sub>sb</sub>	V <sub>be</sub> (%)	% AV
9-4	2.10	2.34	6.77	2.58	2.45	9.81	10.32
10-1	2.06	2.39	5.44	2.58	2.48	7.67	13.62
10-2	2.15	2.33	6.79	2.56	2.47	11.17	7.58
10-3	2.11	2.31	7.02	2.55	2.45	11.30	8.65
10-4			6.77		2.45		
11-1	2.29	2.39	5.44	2.58	2.48	8.54	3.80
11-2	2.22	2.33	6.79	2.56	2.47	11.54	4.55
11-3	2.18	2.31	7.02	2.55	2.45	11.69	5.49
11-4			6.77		2.45		
12-1	2.17	2.39	5.44	2.58	2.48	8.07	9.07
12-2	2.09	2.33	6.79	2.56	2.47	10.86	10.20
12-3	2.06	2.31	7.02	2.55	2.45	11.02	10.91
12-4			6.77		2.45		

**Gradation**

Property	Layer 1	Layer 2	Layer 3	Layer 4
Retained 3/4	0	0	0	0
Retained 3/8	0.6	4.43	7.55	7.75
Retained #4	42.31	29.44	28.23	28.92
% #200	8.37	6.49	6.06	6.11
Ave. V <sub>be</sub> (%)	7.84	11.36	11.60	7.36
Ave. AV (%)	11.7	6.0	6.2	10.4

**DSR**

Temp.(°C)	Layer 1			Layer 2			Layer 3		
	Vis.(cP)	G* (Pa)	δ°	Vis.(cP)	G* (Pa)	δ°	Vis.(cP)	G* (Pa)	δ°
52	162,666,700	1,626,667	45.60	16,533,300	165,333	64.04	17,900,000	179,000	62.94
58	96,766,700	968,000	49.22	6,716,700	67,167	69.40	7,343,300	73,500	68.50
64	47,533,300	475,333	54.85	3,083,300	30,833	73.97	3,206,700	32,067	72.96
70	18,066,700	180,667	62.85	1,270,000	12,700	77.75	1,380,000	13,833	77.16
76	8,430,000	84,300	67.83	609,300	6,097	81.63	671,700	6,717	80.63
82	3,990,000	39,900	72.03	293,700	2,937	87.10	290,300	2,903	83.84
88	1,750,000	17,500	76.36	144,700	1,447	84.01	138,000	1,380	85.63
A-VTS	8.29 -2.66			9.70 -3.19			9.89 -3.26		

Temp.(°C)	Layer 4		
	Vis.(cP)	G* (Pa)	δ°
52	64,400,000	644,000	58.15
58	27,266,700	272,667	63.04
64	11,833,300	118,667	68.35
70	5,093,300	50,967	73.22
76	2,240,000	22,400	77.48
82	903,700	9,047	81.04
88	459,700	4,600	84.12
A-VTS	9.45 -3.09		

**Table D12. Properties Determined from Extractions and DSR Tests on Core Samples from Section 87060000 in Dade County.**

Sample No.	G <sub>mb</sub>	G <sub>mm</sub>	P <sub>b</sub> (%)	G <sub>se</sub>	G <sub>sb</sub>	V <sub>be</sub> (%)	% AV
1-1	2.06	2.32	6.34	2.53	2.46	10.32	11.04
1-2	2.30	2.36	7.94	2.65	2.45	11.28	2.62
1-3	2.26	2.33	7.07	2.58	2.44	10.97	3.01
1-4	2.23	2.33	7.55	2.59	2.48	12.61	4.26
1-5	2.17	2.32	7.55	2.58	2.55	14.84	6.34
1-6	2.20	2.32	3.98	2.45	2.57	12.55	5.45
2-1	2.04	2.32	6.34	2.53	2.46	10.22	11.90
2-2	2.19	2.36	7.94	2.65	2.45	10.76	7.19
2-3	2.24	2.33	7.07	2.58	2.44	10.87	3.90
2-4	2.27	2.33	7.55	2.59	2.48	12.86	2.37
2-5	2.19	2.32	7.55	2.58	2.55	14.97	5.56
2-6	2.18	2.32	3.98	2.45	2.57	12.48	5.99
3-1	2.12	2.32	6.34	2.53	2.46	10.62	8.43
3-2	2.25	2.36	7.94	2.65	2.45	11.08	4.42
3-3	2.23	2.33	7.07	2.58	2.44	10.81	4.39
3-4	2.27	2.33	7.55	2.59	2.48	12.88	2.21
3-5	2.23	2.32	7.55	2.58	2.55	15.23	3.89
3-6	2.16	2.32	3.98	2.45	2.57	12.34	7.07
4-1	2.13	2.32	6.34	2.53	2.46	10.65	8.17
4-2	2.21	2.36	7.94	2.65	2.45	10.89	6.03
4-3	2.20	2.33	7.07	2.58	2.44	10.68	5.52
4-4	2.26	2.33	7.55	2.59	2.48	12.83	2.61
4-5	2.18	2.32	7.55	2.58	2.55	14.89	6.08
4-6	2.19	2.32	3.98	2.45	2.57	12.54	5.56
5-1	2.12	2.32	6.34	2.53	2.46	10.61	8.55
5-2	2.24	2.36	7.94	2.65	2.45	11.01	5.01
5-3	2.24	2.33	7.07	2.58	2.44	10.85	4.07
5-4	2.27	2.33	7.55	2.59	2.48	12.84	2.51
5-5	2.19	2.32	7.55	2.58	2.55	14.98	5.51
5-6	2.13	2.32	3.98	2.45	2.57	12.19	8.16
6-1	2.24	2.32	6.34	2.53	2.46	11.21	3.31
6-2	2.25	2.36	7.94	2.65	2.45	11.05	4.62
6-3	2.24	2.33	7.07	2.58	2.44	10.86	3.95
6-4	2.29	2.33	7.55	2.59	2.48	12.95	1.66
6-5	2.20	2.32	7.55	2.58	2.55	15.05	5.07
6-6	2.19	2.32	3.98	2.45	2.57	12.53	5.63
7-1	2.12	2.32	6.34	2.53	2.46	10.58	8.76
7-2	2.27	2.36	7.94	2.65	2.45	11.16	3.73
7-3	2.24	2.33	7.07	2.58	2.44	10.89	3.70
7-4	2.23	2.33	7.55	2.59	2.48	12.61	4.24
7-5	2.17	2.32	7.55	2.58	2.55	14.82	6.49
7-6	2.19	2.32	3.98	2.45	2.57	12.50	5.87
8-1	2.06	2.32	6.34	2.53	2.46	10.31	11.12
8-2	2.20	2.36	7.94	2.65	2.45	10.79	6.86
8-3	2.25	2.33	7.07	2.58	2.44	10.93	3.39
8-4	2.23	2.33	7.55	2.59	2.48	12.61	4.26
8-5	2.18	2.32	7.55	2.58	2.55	14.89	6.03
8-6	2.19	2.32	3.98	2.45	2.57	12.49	5.91
9-1	2.09	2.32	6.34	2.53	2.46	10.43	10.09

**Table D12. Properties Determined from Extractions and DSR Tests on Core Samples from Section 87060000 in Dade County (continued).**

Sample No.	G <sub>mb</sub>	G <sub>mm</sub>	P <sub>b</sub> (%)	G <sub>se</sub>	G <sub>sb</sub>	V <sub>be</sub> (%)	% AV
9-2	2.21	2.36	7.94	2.65	2.45	10.86	6.26
9-3	2.27	2.33	7.07	2.58	2.44	11.01	2.60
9-4	2.21	2.33	7.55	2.59	2.48	12.51	5.04
9-5	2.17	2.32	7.55	2.58	2.55	14.82	6.47
9-6	2.18	2.32	3.98	2.45	2.57	12.48	6.01
10-1	2.11	2.32	6.34	2.53	2.46	10.55	9.07
10-2	2.22	2.36	7.94	2.65	2.45	10.91	5.88
10-3	2.29	2.33	7.07	2.58	2.44	11.09	1.93
10-4	2.20	2.33	7.55	2.59	2.48	12.46	5.38
10-5	2.21	2.32	7.55	2.58	2.55	15.07	4.91
10-6	2.13	2.32	3.98	2.45	2.57	12.15	8.45
9-1	2.09	2.32	6.34	2.53	2.46	10.43	10.09
9-2	2.21	2.36	7.94	2.65	2.45	10.86	6.26
9-3	2.27	2.33	7.07	2.58	2.44	11.01	2.60
9-4	2.21	2.33	7.55	2.59	2.48	12.51	5.04
9-5	2.17	2.32	7.55	2.58	2.55	14.82	6.47
9-6	2.18	2.32	3.98	2.45	2.57	12.48	6.01
10-1	2.11	2.32	6.34	2.53	2.46	10.55	9.07
10-2	2.22	2.36	7.94	2.65	2.45	10.91	5.88
10-3	2.29	2.33	7.07	2.58	2.44	11.09	1.93
10-4	2.20	2.33	7.55	2.59	2.48	12.46	5.38
10-5	2.21	2.32	7.55	2.58	2.55	15.07	4.91
10-6	2.13	2.32	3.98	2.45	2.57	12.15	8.45

**Gradation**

Property	Layer 1	Layer 2	Layer 3	Layer 4	Layer Layer 5	Layer 6
Retained 3/4	0	0	0.97	0	0	0
Retained 3/8	0.37	1.36	20.85	10.8	10.8	0.61
Retained #4	42.16	24.29	20.49	21.13	21.13	28.02
% #200	6.18	6.63	7.02	8	8	7.35
Ave. V <sub>be</sub> (%)	10.55	10.98	10.90	12.70	14.94	12.42
Ave. AV (%)	9.0	5.3	3.6	3.5	5.6	6.4

**DSR**

Temp.(°C)	Layer 1			Layer 2			Layer 3		
	Vis.(cP)	G* (Pa)	δ°	Vis.(cP)	G* (Pa)	δ°	Vis.(cP)	G* (Pa)	δ°
52	75,866,700	759,333	50.76	6,780,000	67,833	70.20	3,453,300	34,533	71.49
58	36,200,000	362,000	56.05	2,740,000	27,400	75.16	1,400,000	14,000	75.59
64	16,800,000	168,000	61.71	1,273,300	12,733	79.62	644,000	6,440	79.26
70	7,826,700	78,267	66.79	531,300	5,313	82.74	288,000	2,880	82.18
76	3,596,700	36,033	71.32	258,300	2,583	85.54	141,000	1,410	84.61
82	1,403,300	14,033	76.04	99,900	1,000	86.74	75,500	755	86.44
88	668,000	6,683	79.00	53,500	535	87.63	35,300	353	87.97
A-VTS	8.89	-2.88		10.60	-3.53		10.26	-3.41	

Temp.(°C)	Layer 4			Layer 5			Layer 6		
	Vis.(cP)	G* (Pa)	$\delta^\circ$	Vis.(cP)	G* (Pa)	$\delta^\circ$	Vis.(cP)	G* (Pa)	$\delta^\circ$
52	2,806,700	28,067	74.87	4,726,600	47,300	69.82	5,306,700	53,067	71.29
58	1,163,300	11,633	78.71	1,930,000	19,300	74.29	2,170,000	21,700	76.11
64	565,700	5,660	82.46	878,000	8,780	78.07	943,000	9,430	79.83
70	238,000	2,380	85.19	391,700	3,917	81.27	461,700	4,617	83.20
76	115,000	1,150	86.79	190,700	1,907	83.87	220,300	2,203	86.11
82	51,500	515	88.06	91,400	914	85.73	86,900	869	87.14
88	31,900	319	89.12	47,600	476	88.05	47,000	470	88.13
A-VTS	10.47 -3.49			10.19 -3.38			10.44 -3.47		

**Table D13. Properties Determined from Extractions and DSR Tests on Core Samples from Section 10060000 in Hillsborough County.**

Sample No.	G <sub>mb</sub>	G <sub>mm</sub>	P <sub>b</sub> (%)	G <sub>se</sub>	G <sub>sb</sub>	V <sub>be</sub> (%)	% AV
1-1	2.03	2.38	4.95	2.55	2.46	7.05	14.66
1-2	2.08	2.35	6.67	2.58	2.45	9.38	11.61
1-3	2.29	2.45	4.25	2.60	2.52	6.50	6.32
2-1	2.09	2.38	4.95	2.55	2.46	7.26	12.18
2-2	2.11	2.35	6.67	2.58	2.45	9.53	10.24
2-3	2.25	2.45	4.25	2.60	2.52	6.37	8.06
3-1	2.09	2.38	4.95	2.55	2.46	7.26	12.12
3-2	2.10	2.35	6.67	2.58	2.45	9.51	10.44
3-3	2.31	2.45	4.25	2.60	2.52	6.54	5.61
4-1	2.06	2.38	4.95	2.55	2.46	7.17	13.21
4-2	2.08	2.35	6.67	2.58	2.45	9.40	11.49
4-3	2.19	2.45	4.25	2.60	2.52	6.21	10.36
5-1	2.08	2.38	4.95	2.55	2.46	7.22	12.58
5-2	2.14	2.35	6.67	2.58	2.45	9.66	8.98
5-3	2.15	2.45	4.25	2.60	2.52	6.10	12.09
6-1	2.10	2.38	4.95	2.55	2.46	7.30	11.67
6-2	2.05	2.35	6.67	2.58	2.45	9.26	12.81
6-3	2.21	2.45	4.25	2.60	2.52	6.27	9.58
7-1	2.06	2.38	4.95	2.55	2.46	7.15	13.50
7-2	2.06	2.36	6.67	2.59	2.45	9.05	12.52
7-3	2.34	2.45	4.25	2.60	2.52	6.62	4.46
8-1	2.13	2.38	4.95	2.55	2.46	7.41	10.31
8-2	2.17	2.36	6.67	2.59	2.45	9.52	7.99
8-3	2.12	2.37	4.25	2.51	2.52	8.92	10.27
3-2	2.10	2.35	6.67	2.58	2.45	9.51	10.44
3-3	2.31	2.45	4.25	2.60	2.52	6.54	5.61
4-1	2.06	2.38	4.95	2.55	2.46	7.17	13.21
4-2	2.08	2.35	6.67	2.58	2.45	9.40	11.49
6-6	2.19	2.32	3.98	2.45	2.57	12.53	5.63
7-1	2.12	2.32	6.34	2.53	2.46	10.58	8.76
7-2	2.27	2.36	7.94	2.65	2.45	11.16	3.73

**Gradation**

Property	Layer 1	Layer 2	Layer 3
Retained 3/4	0	3.02	10.54
Retained 3/8	3.39	17.46	12.45
Retained #4	31.16	17.06	21.16
% #200	7.97	8.12	4.81
Ave. V <sub>be</sub> (%)	7.23	9.41	6.69
Ave. AV (%)	12.5	10.8	8.3

**DSR**

Temp.(°C)	Layer 1			Layer 2			Layer 3		
	Vis.(cP)	G* (Pa)	δ°	Vis.(cP)	G* (Pa)	δ°	Vis.(cP)	G* (Pa)	δ°
52	100,866,700	1,008,667	52.12	10,666,700	106,667	66.02	19,666,700	196,667	59.53
58	45,633,300	456,667	58.34	4,443,300	44,467	70.08	8,806,700	88,100	63.53
64	20,400,000	204,000	63.01	1,950,000	19,500	74.06	4,200,000	42,067	67.23
70	9,206,700	92,067	67.22	904,700	9,050	77.52	1,980,000	19,800	71.01
76	4,263,300	42,667	71.29	415,700	4,160	80.77	972,300	9,730	74.79
82	1,783,300	17,867	75.66	181,300	1,813	83.52	498,300	4,983	77.43
88	806,300	8,067	79.06	90,100	902	85.50	242,300	2,423	80.50
A-VTS	8.89 -2.89			10.05 -3.33			8.81 -2.87		

**Table D14. Properties Determined from Extractions and DSR Tests on Core Samples from Section 10160000 in Hillsborough County.**

Sample No.	G <sub>mb</sub>	G <sub>mm</sub>	P <sub>b</sub> (%)	G <sub>sc</sub>	G <sub>sb</sub>	V <sub>be</sub> (%)	% AV
1-1	2.08	2.39	6.84	2.65	2.57	11.69	13.01
1-2	2.24	2.40	6.20	2.63	2.52	9.88	6.77
1-3	2.29	2.39	6.12	2.61	2.52	10.61	4.35
1-4	2.23	2.39	5.18	2.57	2.51	9.23	6.84
2-1	2.07	2.39	6.84	2.65	2.57	11.62	13.54
2-2	2.23	2.40	6.20	2.63	2.52	9.84	7.07
2-3	2.30	2.39	6.12	2.61	2.52	10.67	3.82
2-4	2.36	2.39	5.18	2.57	2.51	9.80	1.06
3-1	2.11	2.39	6.84	2.65	2.57	11.88	11.64
3-2	2.16	2.40	6.20	2.63	2.52	9.55	9.83
3-3	2.14	2.39	6.12	2.61	2.52	9.95	10.27
3-4	2.27	2.39	5.18	2.57	2.51	9.43	4.79
4-1	2.09	2.39	6.84	2.65	2.57	11.76	12.51
4-2	2.17	2.40	6.20	2.63	2.52	9.58	9.55
4-3	2.27	2.39	6.12	2.61	2.52	10.53	5.05
4-4	2.25	2.39	5.18	2.57	2.51	9.33	5.86

**Gradation**

Property	Layer 1	Layer 2	Layer 3	Layer 4
Retained 3/4	0	0.15	0	4.29
Retained 3/8	0.38	22.49	2.75	4.48
Retained #4	11.08	18.44	27.7	20.06
% #200	6.84	7.28	6.39	7.39
Ave. V <sub>be</sub> (%)	11.74	9.71	10.44	9.45
Ave. AV (%)	12.7	8.3	4.4	5.8

**DSR**

Temp.(°C)	Layer 1			Layer 2			Layer 3		
	Vis.(cP)	G* (Pa)	$\delta^\circ$	Vis.(cP)	G* (Pa)	$\delta^\circ$	Vis.(cP)	G* (Pa)	$\delta^\circ$
52	35,366,700	353,667	57.71	5,076,700	50,767	69.66	5,346,700	53,500	69.05
58	15,466,700	154,667	62.54	2,170,000	21,700	74.10	2,230,000	22,300	73.20
64	6,940,000	69,400	66.89	942,300	9,427	78.16	1,040,000	10,400	76.93
70	3,170,000	31,700	71.05	424,700	4,247	81.46	460,700	4,607	80.17
76	1,510,000	15,100	74.97	208,300	2,083	84.20	233,700	2,337	82.94
82	752,000	7,520	78.08	107,700	1,077	86.11	119,300	1,193	85.12
88	341,700	3,417	81.28	58,500	585	87.11	54,000	540	86.72
A-VTS	8.99 -2.93			9.87 -3.27			9.96 -3.30		

Temp.(°C)	Layer 4		
	Vis.(cP)	G* (Pa)	$\delta^\circ$
52	3,120,000	31,200	72.03
58	1,340,000	13,400	75.84
64	603,000	6,030	79.21
70	296,000	2,963	82.09
76	150,700	1,507	84.34
82	65,900	659	84.63
88	34,400	344	87.72
A-VTS	10.47 -3.49		



## APPENDIX E

### BACKCALCULATING ORIGINAL AIR VOIDS

Researchers examined two methods of backcalculating the in-place air voids content at the time of construction (also referred to in this technical memorandum as the initial air voids or original air voids). The first method is based on the air void adjustment model described in the NCHRP Project 1-37A report from Applied Research Associates (2004). This model is a component of the global aging system (GAS) incorporated into the M-E PDG program and relates the air voids content  $VA$  at a given time  $t$  (in months) to the original air voids  $VA_{orig}$ , the mean annual air temperature  $Maat$  in °F, and the original viscosity  $\eta_{orig, 77}$  (in megapoises) at 77 °F. This air void adjustment model is given by the equation:

$$VA = \frac{VA_{orig} + 0.011(t) - 2}{1 + 4.24 \times 10^{-4}(t)(Maat) + 1.169 \times 10^{-3} \left( \frac{t}{\eta_{orig, 77}} \right)} + 2 \quad (E1)$$

The second method is based on an alternative formula given in a supplemental document (Appendix CC-2) to the mechanistic-empirical pavement design guide (Applied Research Associates, 2001). NCHRP researchers used this alternative formula (given in Equation 2 below) to backcalculate the initial air voids on LTPP calibration sections:

$$VA = \frac{VA_{orig} + \exp(-1.0528 * t) - 1}{1 + 0.01406 t + 0.00125 t^{0.2307} Maat - 0.00325 t \eta_{orig, 77}} \quad (E2)$$

NCHRP researchers used Equation 2 to come up with a table of recommended initial air voids content to use for calibrating the distress models in the M-E PDG program. The researchers noted in their report that the recommended values generally came from this equation but that alternative values were recommended based on experience for cases where unrealistic predictions of initial air voids content were obtained.

For the verification reported in this memorandum, TTI researchers used both Equations E1 and E2 to backcalculate the initial or original air voids content of the asphalt concrete mixtures placed on the US27 LTPP sections in Palm Beach County. Table E1 summarizes data on the LTPP sections tested in this Florida DOT implementation project.

**Table E1. Data for Backcalculating Initial Air Voids Content on US27 LTPP Sections.**

Section	AC lift	$VA_{orig}^*$ (percent)	$VA_{aged}^{**}$ (percent)	Time since construction (months)	$Maat$ (°F)	$Pen$ at 77 °F*	Computed $\eta_{orig, 77}$ (MPOise)
120103	Top	4.02	2.0	135	74	54.8	3.85
	Middle	5.84	3.9	135	74	41.7	7.11
	Bottom	4.68	3.3	135	74	40	7.81
120105	Top	4.02	2.7	135	74	54.8	3.85
	Middle	5.84	3.5	135	74	41.7	7.11
	Bottom	4.68	2.8	135	74	40	7.81
120106	Top	4.02	4.7	135	74	54.8	3.85
	Middle	5.84	3.4	135	74	41.7	7.11
	Bottom	4.68	4.8	135	74	40	7.81

\* From LTPP data base

\*\* From laboratory extractions on cores

For the first set of backcalculations, researchers used the following equation to estimate the bitumen viscosity  $\eta$  at the time of construction given the asphalt penetration  $Pen$  at 77 °F from the LTPP data base:

$$\log \eta = 10.5012 - 2.2601 * \log(Pen) + 0.00389 * \log(Pen)^2 \quad (E3)$$

NCHRP researchers also used the above equation to estimate the bitumen viscosity at 77 °F for backcalculating the initial air voids from Equation E2.

Figure E1 shows the comparison of backcalculated original air voids with the corresponding values from the LTPP inventory data. For this figure,  $\eta_{orig, 77}$  was determined using Equation 3 with the asphalt penetration values reported in the LTPP data base and given in Table 1. Researchers then used the computed values of  $\eta_{orig, 77}$  to backcalculate the original air voids from Equations E1 and E2.

To quantify the backcalculation error, researchers' determined the average of the absolute differences between the backcalculated initial air voids and the inventory data. It is observed from Figure E1 that the backcalculated initial or original air voids do not compare well with the inventory data, exhibiting an absolute average absolute difference of about 4 percent from both equations. Researchers consider this error to be quite significant in view of the sensitivity of the performance predictions to the initial air voids content, as will be presented later in this section.

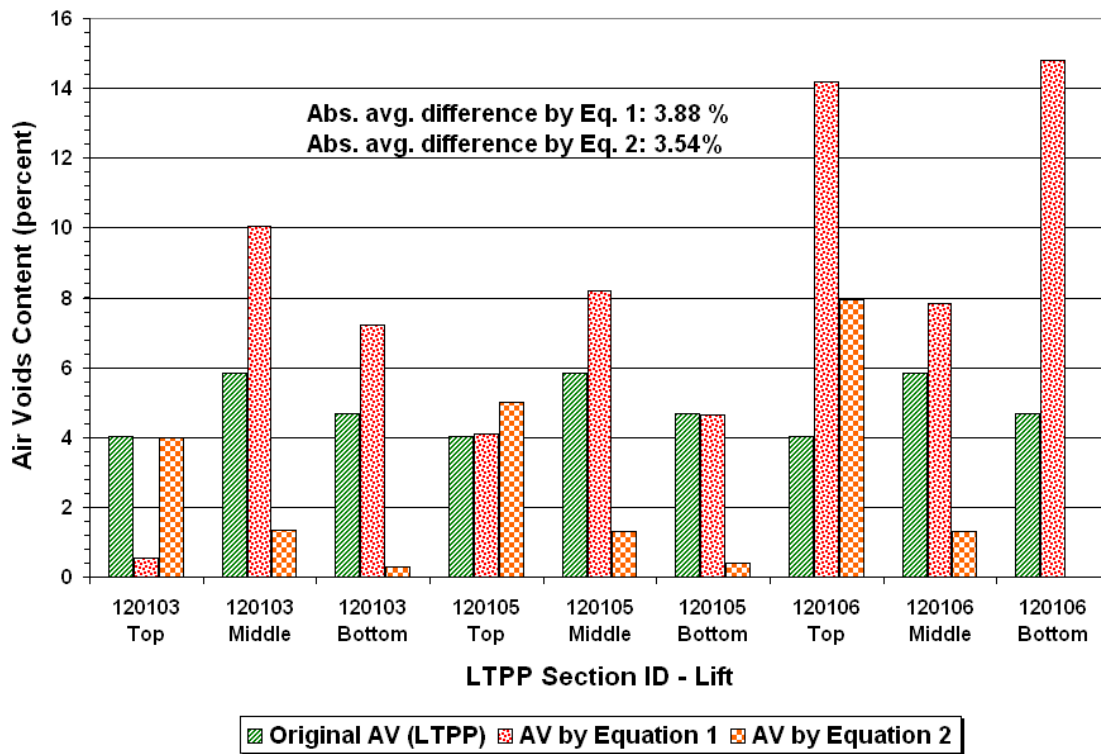


**Figure E1. Comparison of Backcalculated Original Air Voids based on Penetration Data with Corresponding Values from LTPP Inventory Data.**

In addition to estimating the original viscosity from the penetration value reported in the LTPP data base, researchers also used the global aging system in the M-E PDG program to estimate the original viscosity given the DSR test results on the asphalt samples extracted from the cores. Equations 1 and 2 were then used with the predicted viscosities at the time of construction to backcalculate the initial air voids. Below is a step-by-step description of this backcalculation based on the M-E PDG global aging system models:

- Step 1 : Obtain the aged viscosity  $\eta_t$  of the aged material (core sample) at a given temperature from the binder viscosity-temperature relationship determined from DSR tests.
- Step 2 : Calculate the mix laydown viscosity  $\eta_{t=0}$  for the surface lift at the given temperature using the following equations:

$$\log \log(\eta_t) = \alpha = \frac{\log \log(\eta_{t=0}) + A t}{1 + B t} \quad (E4)$$

$$\eta_t = 10^{10^\alpha} \quad (E5)$$

$$D = -14.55 + 10.48 \log(T_R) - 1.88 \log(T_R)^2 \quad (E6)$$

$$C = 10^{274.49 - 193.83 \log(T_R) + 33.94 \log(T_R)^2} \quad (\text{E7})$$

$$B = 0.198 + 0.068 \log C \quad (\text{E8})$$

$$A = -0.004 + 1.412C + C \log Maat + D \log \log \eta_{t=0} \quad (\text{E9})$$

where  $T_R$  is the binder temperature in °R, and  $\eta_{t=0}$  is the mix laydown viscosity (at time of construction).

- Step 3 : Calculate the mix laydown viscosity at different depths ( $\eta_{t=0}$ )<sub>z</sub> for the given temperature using the equations:

$$\eta_{t,z} = \frac{\eta_t (4 + E) - E (\eta_{t=0})_z (1 - 4z)}{4(1 + E z)} \quad (\text{E10})$$

$$E = 23.83 e^{-0.0308 Maat} \quad (\text{E11})$$

where  $\eta_{t,z}$  is the known aged viscosity for the given temperature at time  $t$  (months) and depth  $z$  (inches), and  $\eta_t$  is the aged viscosity of the surface lift for the same temperature and time.

- Step 4 : Estimate the original bitumen viscosity  $\eta_{orig}$  using the calculated value of  $\eta_{t=0}$  for the given temperature in the original to mix laydown model given by the following equations:

$$\log \log (\eta_{t=0}) = a_0 + a_1 \log \log (\eta_{orig}) \quad (\text{E12})$$

$$a_0 = 0.054 + 0.004 \text{code} \quad (\text{E13})$$

$$a_1 = 0.972 + 0.011 \text{code} \quad (\text{E14})$$

where code is the hardening ratio with a recommended value of zero for average hardening resistance. Repeat steps 1 to 4 for the range of temperatures of interest.

- Step 5 : Using the results from the previous steps, determine the original temperature-viscosity relationship for each lift, and compute the original viscosity at 77 °F.
- Step 6 : Calculate the original air voids content for each lift using Equations (E1) and (E2).

The above procedure was used to backcalculate the original air voids for the top lift of each LTPP section along US27. For this analysis, researchers skipped Step 3 of the procedure since the top lift is only 2 inches thick. Figure E2 compares the backcalculated

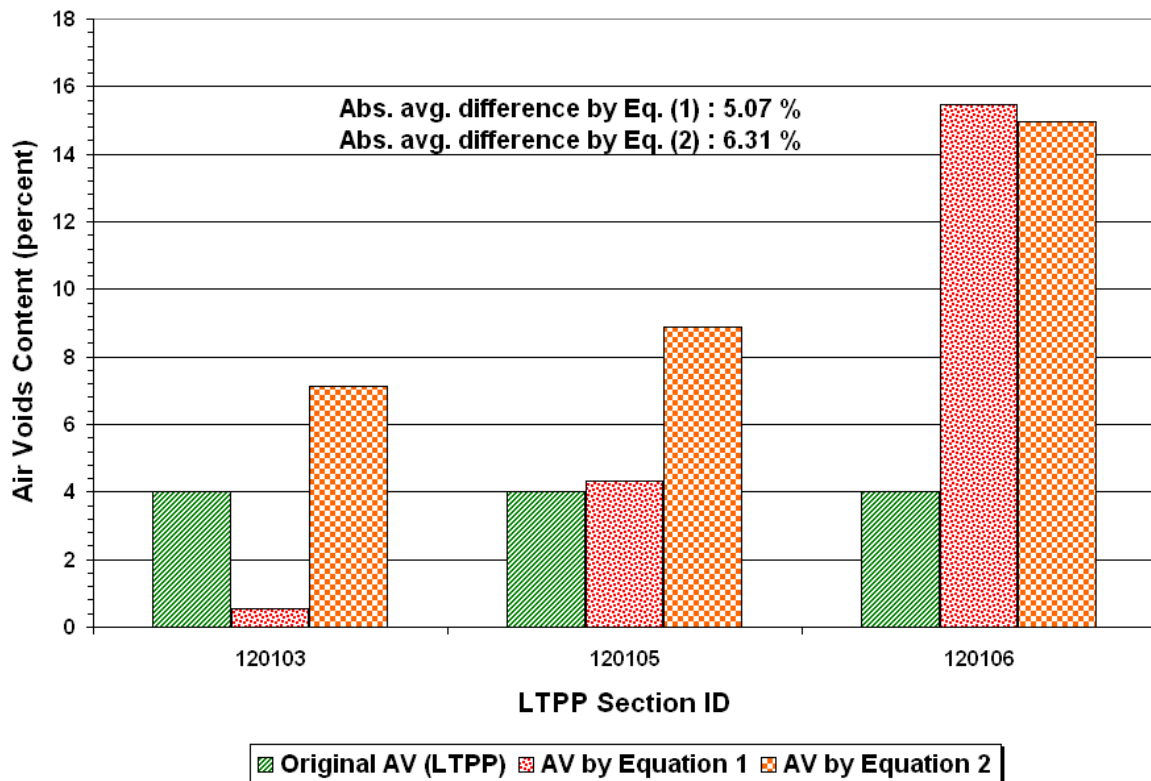


**Figure E2. Comparison of Backcalculated Original Air Voids based on Computed Original Binder Viscosities with Corresponding Values from LTPP Inventory Data.**

original air voids from the above procedure with the corresponding values from the LTPP data base. It is observed that the backcalculated values from Equation E2 are higher than the LTPP inventory data. In terms of the average absolute difference, the predictions using Equation E1 showed less error compared to the predictions from Equation E2. However, are the backcalculation results reasonable?

To answer this question, researchers performed a sensitivity analysis to verify the effect of air voids on the M-E PDG performance predictions. For this analysis, researchers used the M-E PDG program to predict the performance of a PCS segment located along SR37 in Polk County for various specified levels of air voids content. The asphalt concrete layer on this section consists of three lifts, with thicknesses and air voids content given in the second and third columns of Table E2. The air voids content under the third column (C1) were determined from cores taken at the section. Researchers note that the values tabulated under the C1 column do not correspond to initial, as-built conditions, but are taken as the reference values for the purpose of the sensitivity analysis. Researchers varied the air voids content by  $\pm 4$  percent from the reference values and predicted the performance for the 7 cases (C1 to C7) given in Table E2.

**Table E2. Cases Considered in Sensitivity Analysis of Initial Air Voids Content.**

Layer	Thickness (inch)	Air Void (%)						
		C1	C2	C3	C4	C5	C6	C7
1	1.0	13.5	17.5	13.5	13.5	9.5	13.5	13.5
2	1.5	5.5	5.5	9.5	5.5	5.5	1.5	5.5
3	1.5	9.0	9.0	9.0	13.0	9.0	9.0	5.0

Figures E3 to E6 show how the performance predictions varied for the different cases considered in this sensitivity analysis.

It is observed that changes in air voids content of the top lift significantly affected the predicted amount of top-down cracking over the assumed design period (Figure E3). On the other hand, changes in air voids content of the bottom lift significantly affected the predicted level of bottom-up cracking and the progression of roughness as measured by the IRI (Figures E4 and E5). Changes in the air voids content of the middle lift did not show a significant effect on the development of cracking and surface roughness. In addition, Figure E6 shows no effect of air void change on predicted pavement rutting. These results imply that the air voids of the top and bottom lifts need to be accurately determined for the purpose of using the M-E PDG program to predict pavement performance for generating an acceptable flexible pavement design. Given these results, the differences between the backcalculated original air voids and the corresponding values reported in the LTPP data base for the US27 sections raise concerns about the use of backcalculated values for model calibration. In connection with this, researchers note that the NCHRP 1-37A development team made use of the following guidelines with respect to estimating the original air voids for the purpose of calibrating the distress models in that NCHRP project (Applied Research Associates, 2001):

- For layers other than the top layer, if unrealistic values were obtained from the backcalculation, NCHRP researchers considered the original air voids to be close to the aged value (determined from cores), assuming that no significant change occurs in the air voids content over time for asphalt materials below the top layer.
- For the top layer, if unrealistic air voids were backcalculated, researchers estimated the original air voids by adding 3 percent to the design air voids noting that in practice, the construction air voids are typically 3 to 4 percent higher than the design air voids.

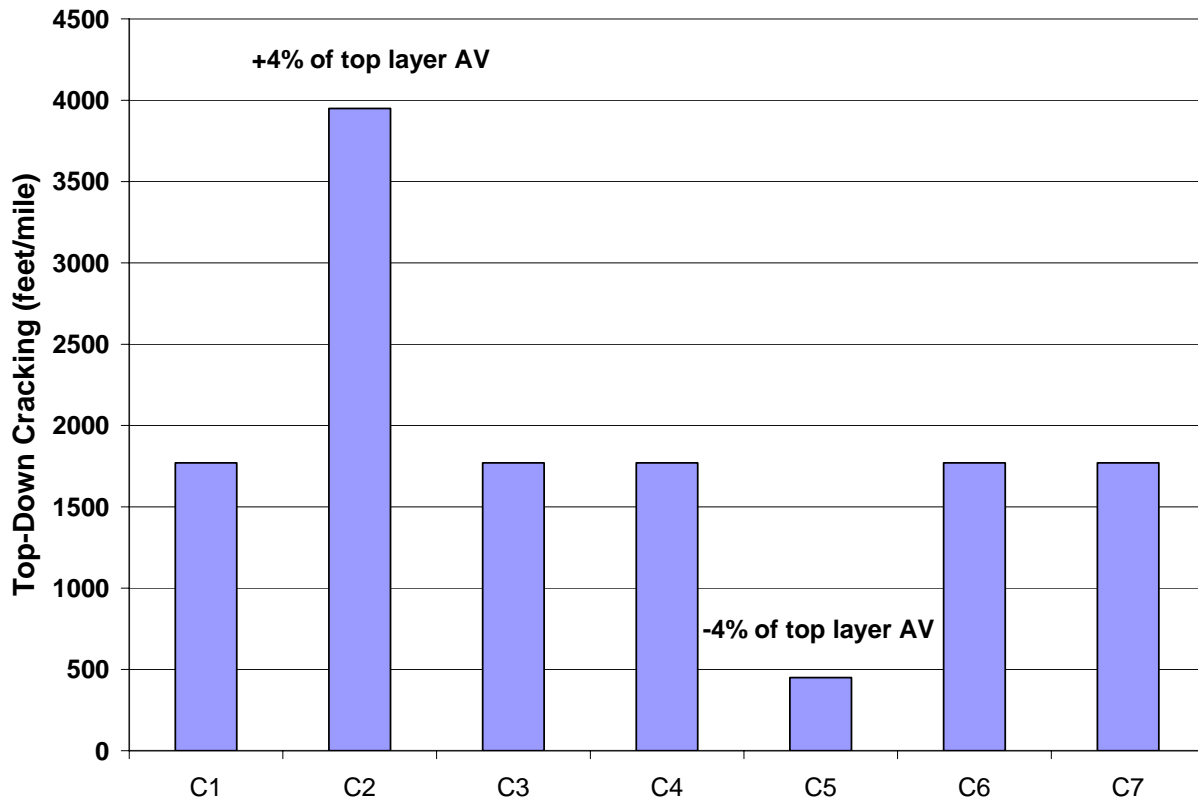


**Figure E3. Top-Down Cracking Sensitivity to the Change of Air Voids.**

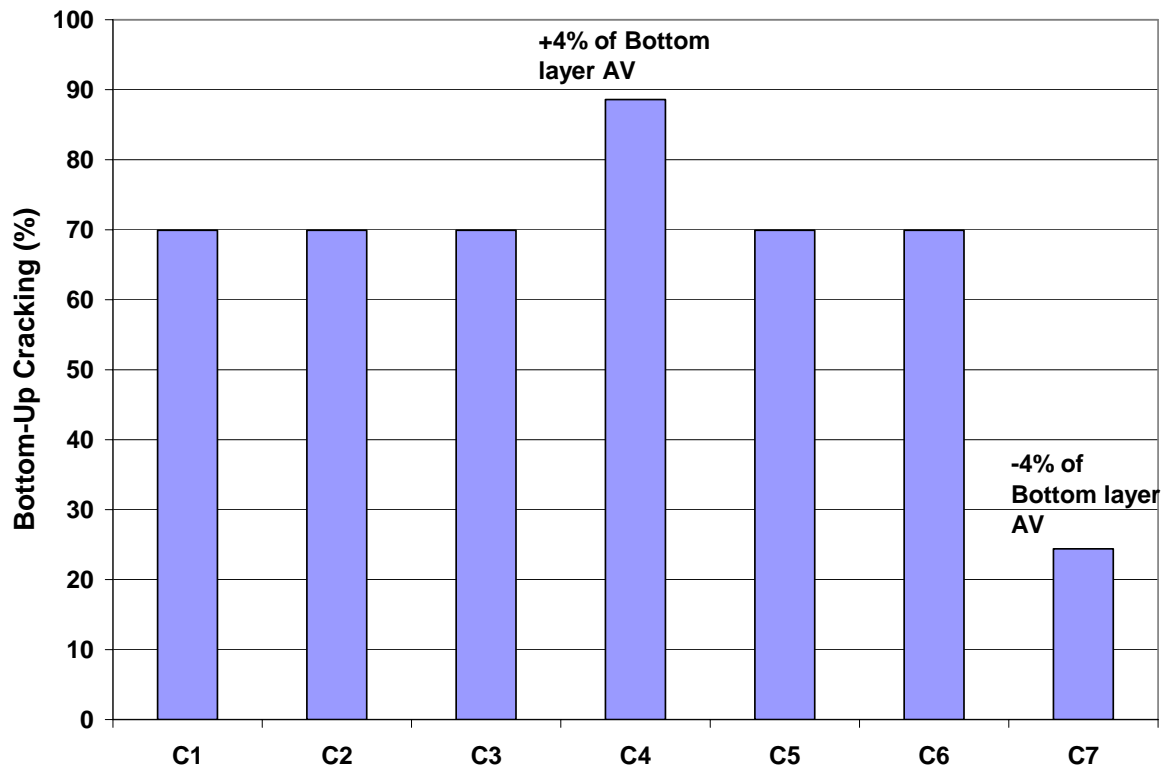


**Figure E4. Bottom-Up Cracking Sensitivity to the Change of Air Voids.**

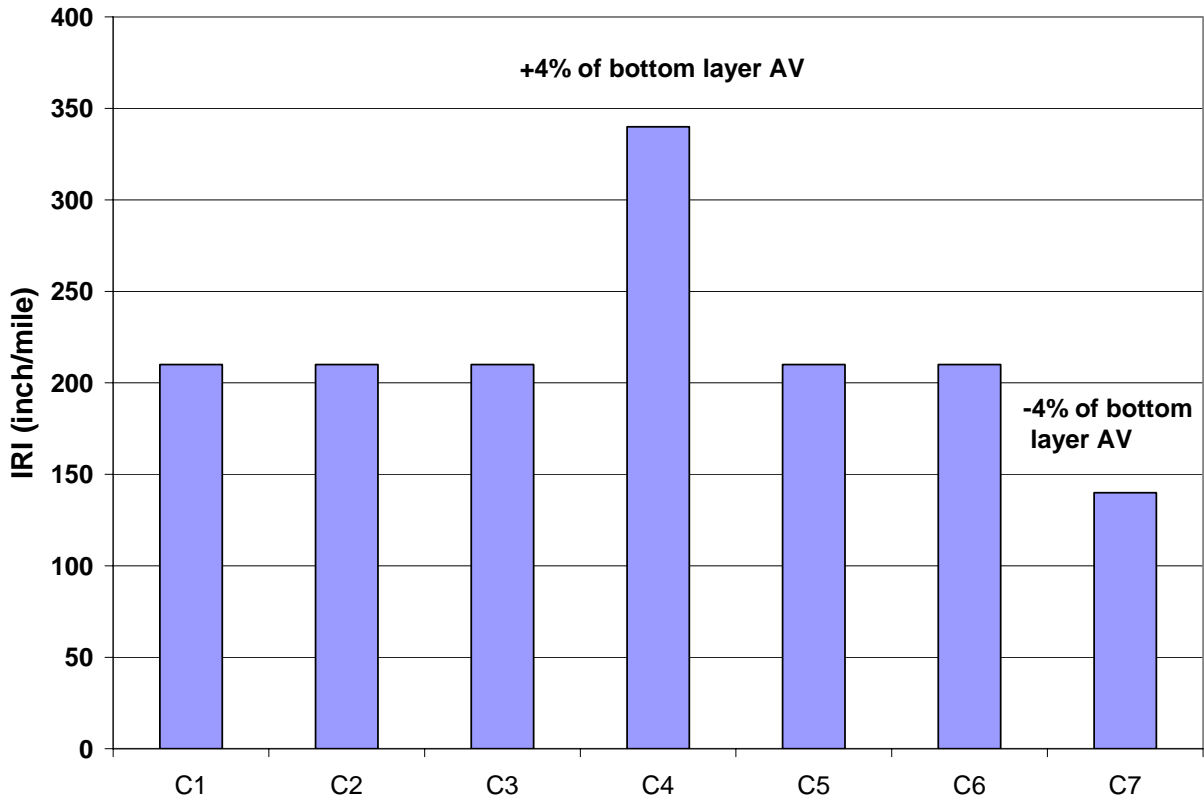


**Figure E5. IRI Sensitivity to the Change of Air Voids.**

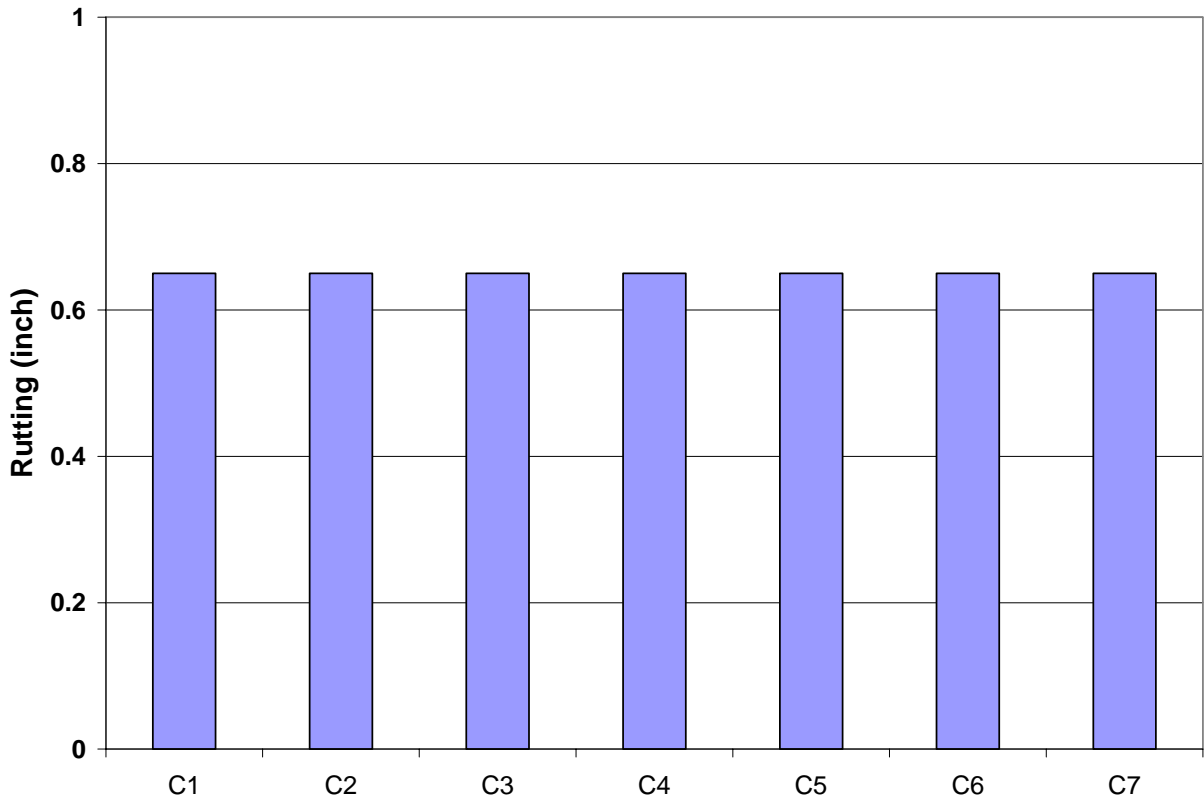


**Figure E6. Rutting Sensitivity to the Change of Air Voids.**

Considering the results from the backcalculations of original air voids presented in this technical memorandum, researchers offer the following recommendations with respect to the use of backcalculated air void content for calibrating the current distress models in the M-E PDG program to Florida conditions:

- For asphalt concrete layers placed before the last resurfacing of a given calibration section, and in the absence of inventory data on air voids content, use the test values for air voids content measured on core samples taken from the section as estimates of the initial air voids for these layers at the time of the last resurfacing. This recommendation is based on the same rationale given in the first guideline noted previously from NCHRP Project 1-37A. Should this recommendation be accepted, implementation of the M-E PDG-based flexible pavement design method would require that the air voids of underlying old asphalt concrete layers be determined from laboratory tests on core samples taken during the pre-construction stage to get the input values needed for pavement design.
- For asphalt concrete layers placed at the time of the last resurfacing, consider the following alternatives:
  - If the construction data are available, use the measured densities and Rice specific gravities from acceptance testing of the in-place pavement to estimate the air voids content of the given asphalt mix for model calibrations.
  - If the construction data are not available, backcalculate the air voids at the time of the last resurfacing using the methods presented in this memorandum. Compare the backcalculated air voids with the design air voids if the data are available. Use the backcalculated value that compares best with the design air voids plus some allowance to consider the difference between design and as-built air voids. For example, the NCHRP guideline used a positive offset of 3 to 4 percent. Consider the air voids measured from core samples of the top layer(s) in evaluating the backcalculated air voids. If the backcalculated air voids from the methods presented in this memorandum are not realistic, estimate the as-built air voids at the time of the last resurfacing as the design air voids plus a reasonable increment established from experience.

Based on the recommendation made above, researchers backcalculated the original air voids using the M-E PDG aging model to check whether the predictions are reasonable based on engineering experience, and to establish the values to use for model calibrations.

Table E3 shows the results of this task. It is observed that most of the predicted original air voids are higher than the values obtained from the cores, reflecting possible densification from traffic loading. With respect to the recommended values for model calibrations, if the difference between the predicted and aged air voids (from the core) is larger than four percent for the top lift, researchers added four percent to the aged air voids to come up with the recommended values shown in Table E3. Otherwise, if the difference is within four percent, the backcalculated original air voids is used. For other than the top lift, if the difference is larger than three percent, the aged air voids from the cores were taken as the recommended values. Otherwise, if the difference is less than three percent and the backcalculated value is larger than the corresponding aged air voids content from the core, the backcalculated original air voids were recommended.

**Table E3. Recommended Original Air Voids for Calibration of M-E PDG Models.**

Section	Layer	Aged air voids from cores (%)	Backcalculated original air voids (%)	Recommended original air voids (%)
16250000	1	12.9	12.9	12.9
	2	7.5	16.5	7.5
	3	5.4	8.5	5.4
	4	12.5	12.6	12.6
	5	9.0	2.6	9.0
16003001	1	13.1	18.4	17.1
	2	5.6	8.1	8.1
	3	8.9	17.5	8.9
26005000	1	15.7	21.8	19.7
	2	8.6	9.4	9.4
	3	8.6	13.7	8.6
	4	9.2	14.5	9.2
28040000	1	16.7	23.8	20.7
	2	7.9	11.0	7.9
	3	15.4	21.5	15.4
50010000	1	8.6	10.7	10.7
	2	4.6	10.6	4.6
	3	7.7	11.5	7.7
	4	6.5	9.9	6.5
58060000	1	8.3	9.8	9.8
	2	8.7	10.3	10.3
	3	13.5	17.0	13.5
	4	5.9	5.4	5.9
	5	2.4	2.8	2.8
86190000	1	8.8	11.2	11.2
	2	4.0	8.1	4.0
	3	5.8	6.0	6.0
93100000	1	13.5	13.5	13.5
	2	4.4	5.7	5.7
	3	5.1	5.9	5.9

**Table E3. Recommended Original Air Voids for Calibration of M-E PDG Models  
(continued).**

93310000	1	13.3	20.6	17.3
	2	6.1	12.7	6.1
	3	5.9	5.7	5.9
77040000	1	12.8	22.4	16.8
	2	5.7	12.0	5.7
	3	4.1	12.6	4.1
	4	9.1	11.5	11.5
	5	13.4	16.5	13.4
79270000	1	11.5	15.4	15.4
	2	7.6	9.2	9.2
	3	6.4	7.3	7.3
90060000	1	11.7	23.2	15.7
	2	6.0	7.0	7.0
	3	6.2	10.4	6.2
	4	10.4	16.7	10.4
87060000	1	9.0	14.7	13.0
	2	5.3	6.6	6.6
	3	3.6	9.6	3.6
	4	3.5	5.1	5.1
	5	5.6	7.7	7.7
	6	6.4	8.6	8.6
10060000	1	12.5	12.4	12.5
	2	10.8	12.3	12.3
	3	8.3	8.8	8.8
10160000	1	12.7	14.1	14.1
	2	8.3	9.3	9.3
	3	4.4	7.6	4.4
	4	5.8	9.7	5.8



**APPENDIX F**

**SUMMARY OF RESILIENT MODULUS DATA OF UNDERLYING  
MATERIALS**



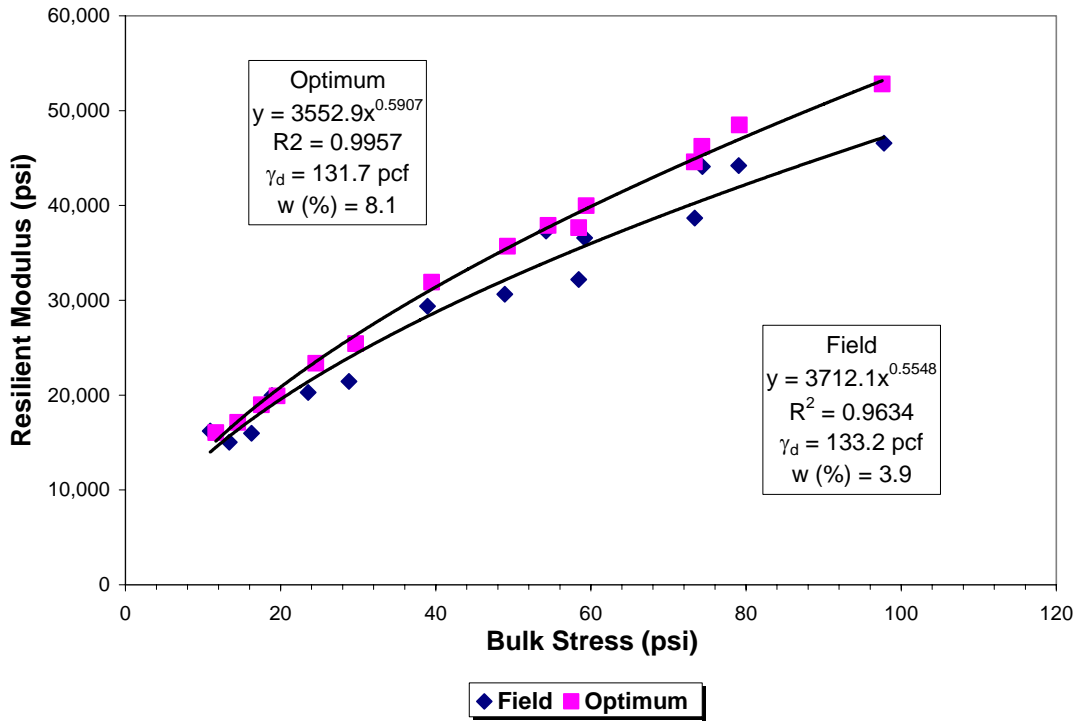


**Figure F1. Resilient Modulus for Base (Section 86190).**

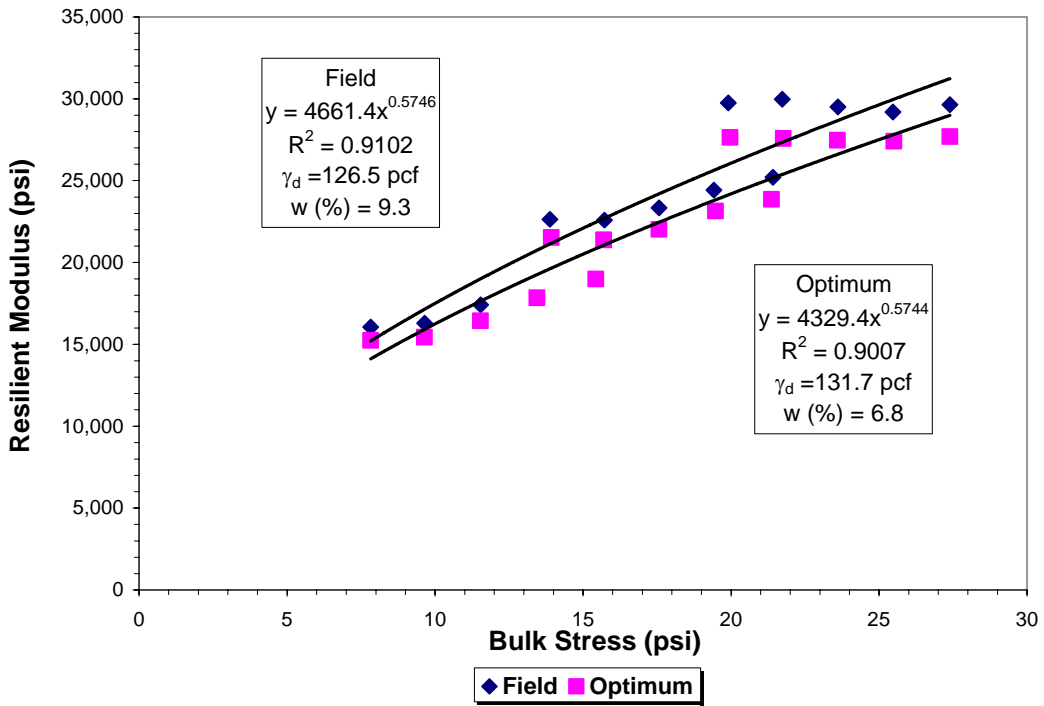


**Figure F2. Resilient Modulus for Subgrade (Section 86190).**

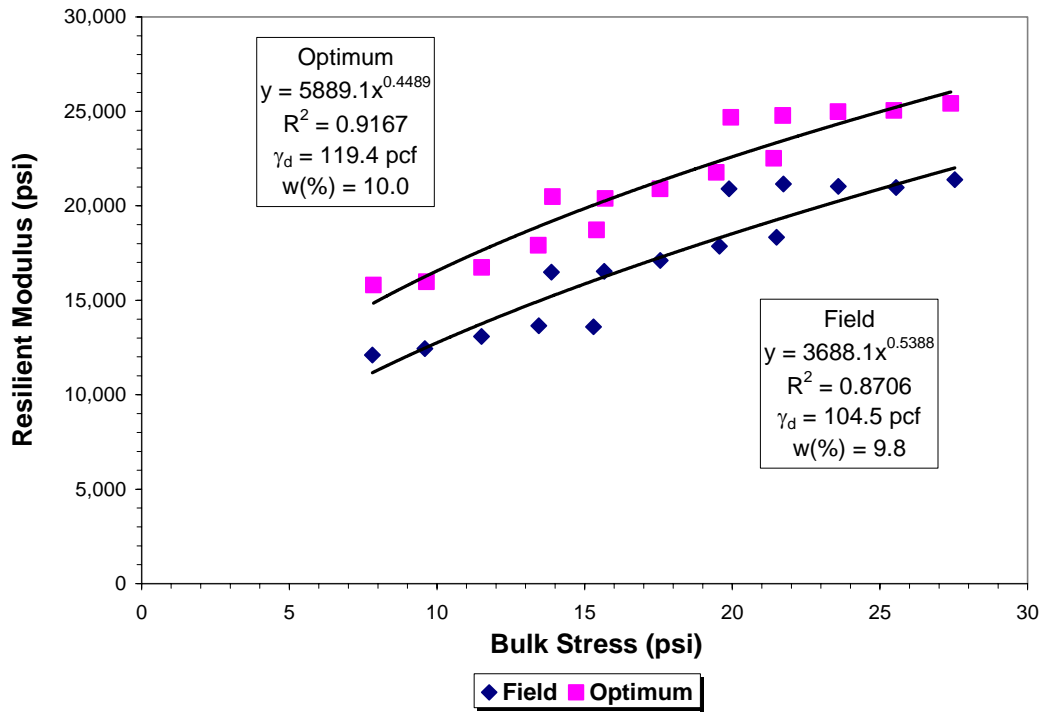


**Figure F3. Resilient Modulus for Embankment (Section 86190).**

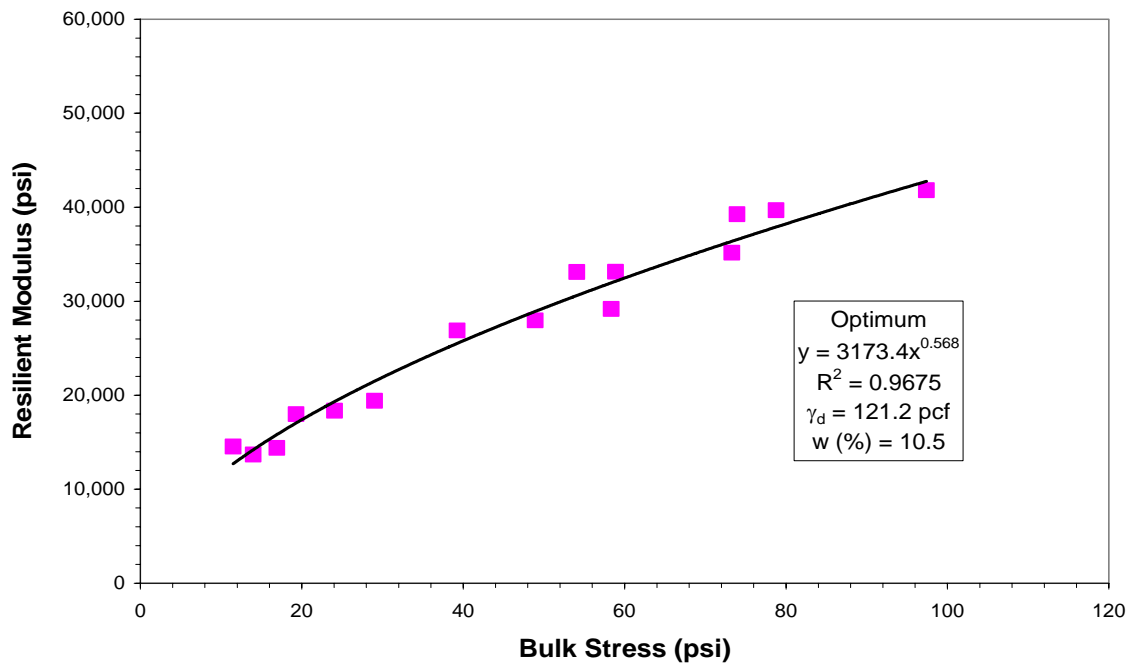


**Figure F4. Resilient Modulus for Base (Section 93100).**

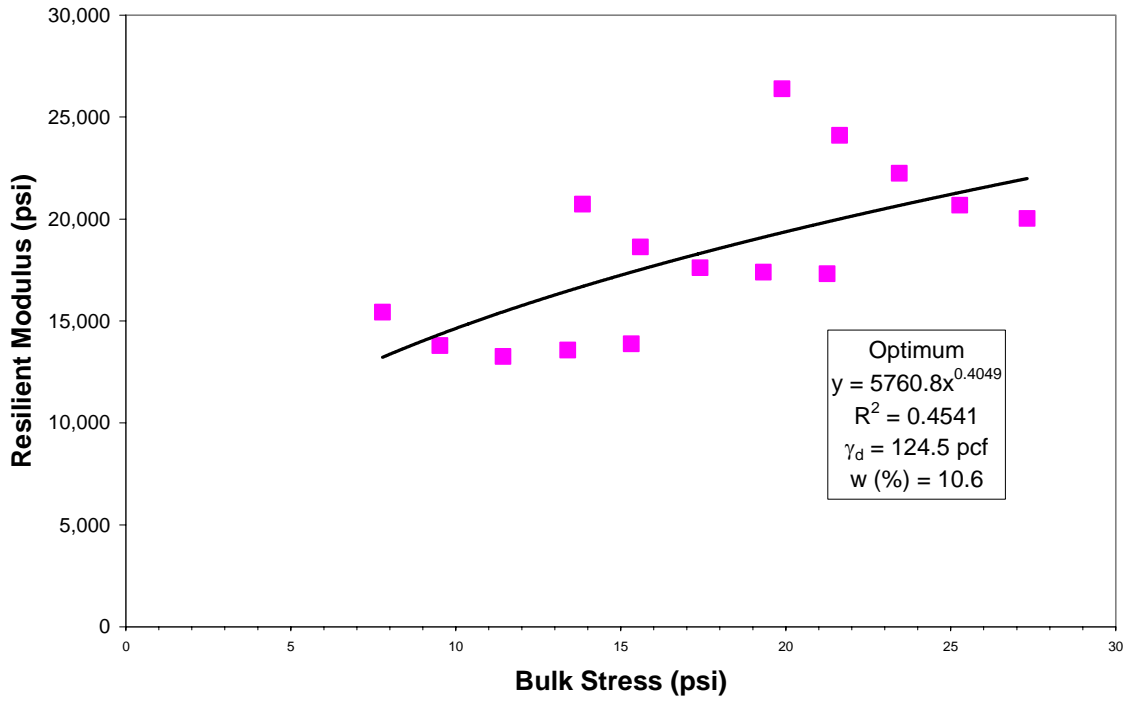


**Figure F5. Resilient Modulus for Subgrade (Section 93100).**

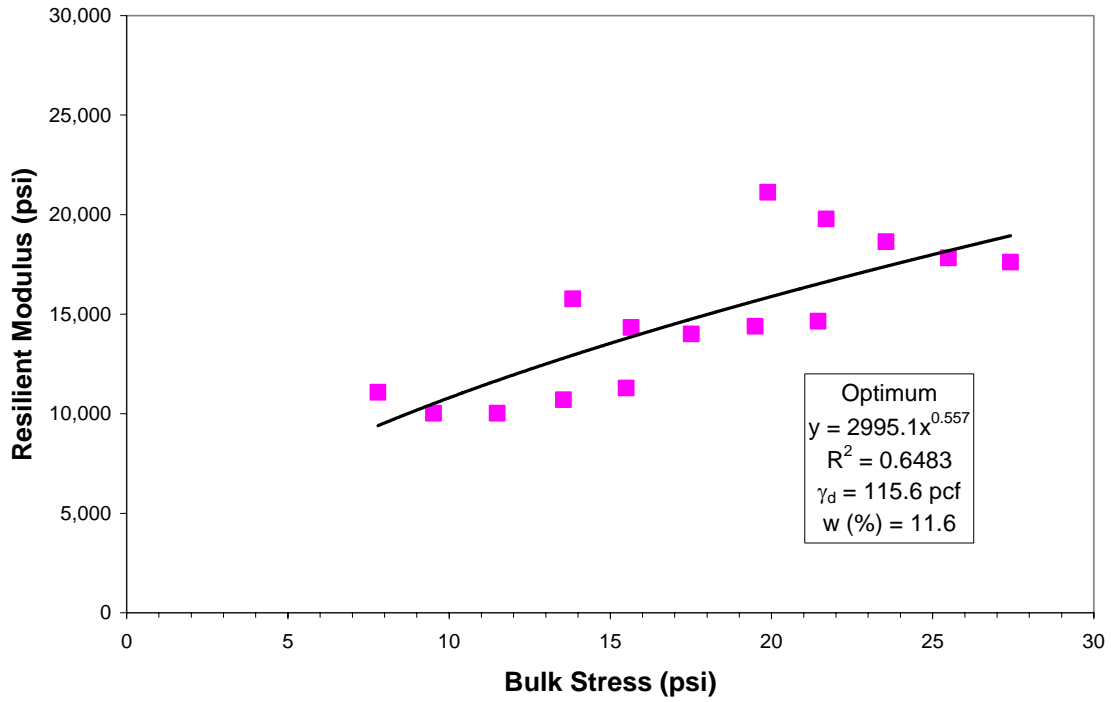


**Figure F6. Resilient Modulus for Embankment (Section 93100).**

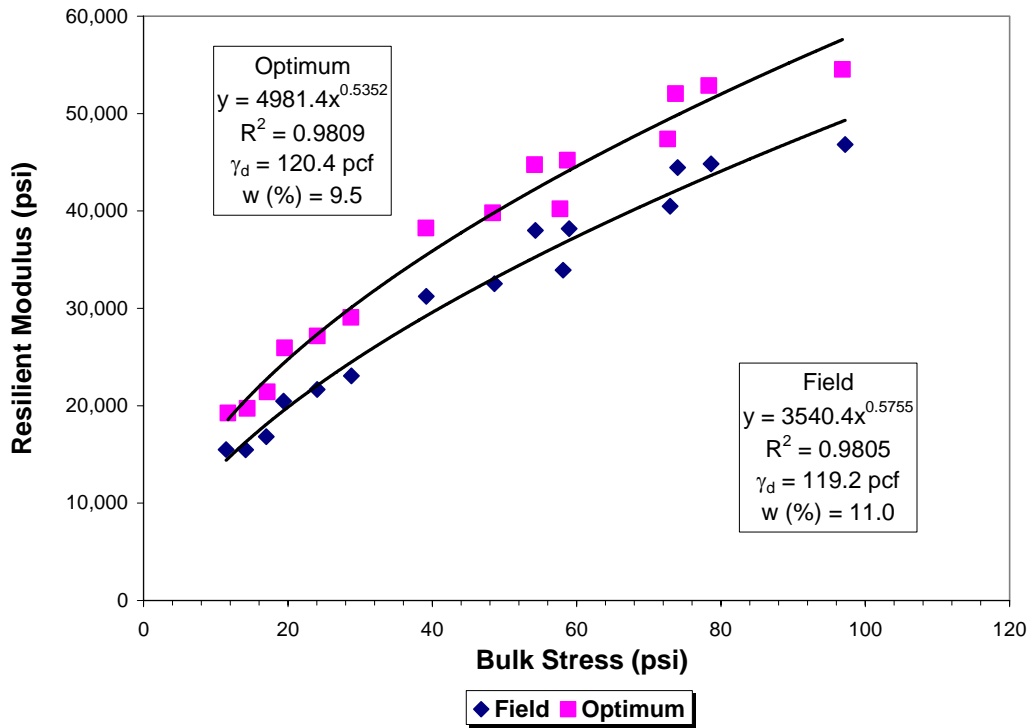


**Figure F7. Resilient Modulus for Base (Section 10060).**

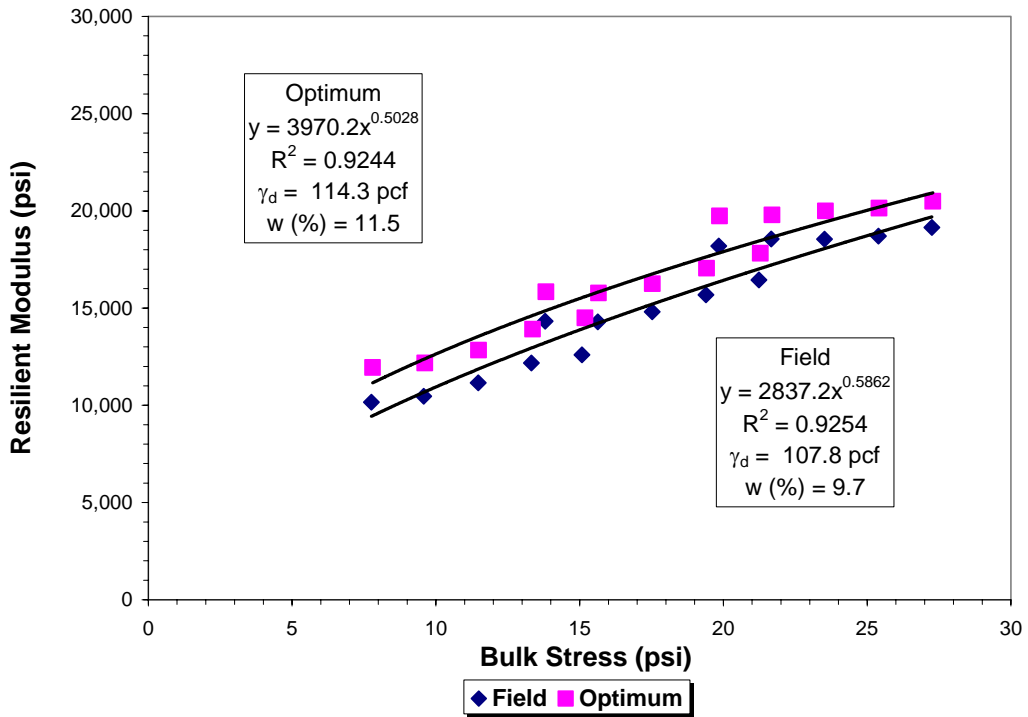


**Figure F8. Resilient Modulus for Subgrade (Section 10060).**

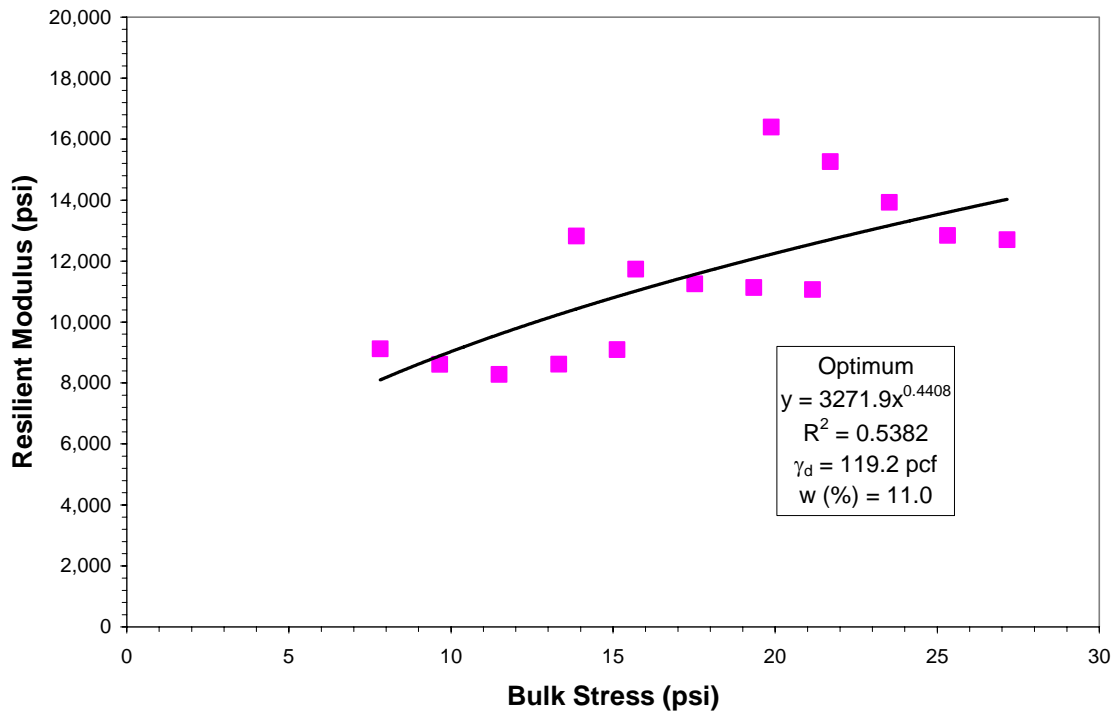


Figure F9. Resilient Modulus for Embankment (Section 10060).

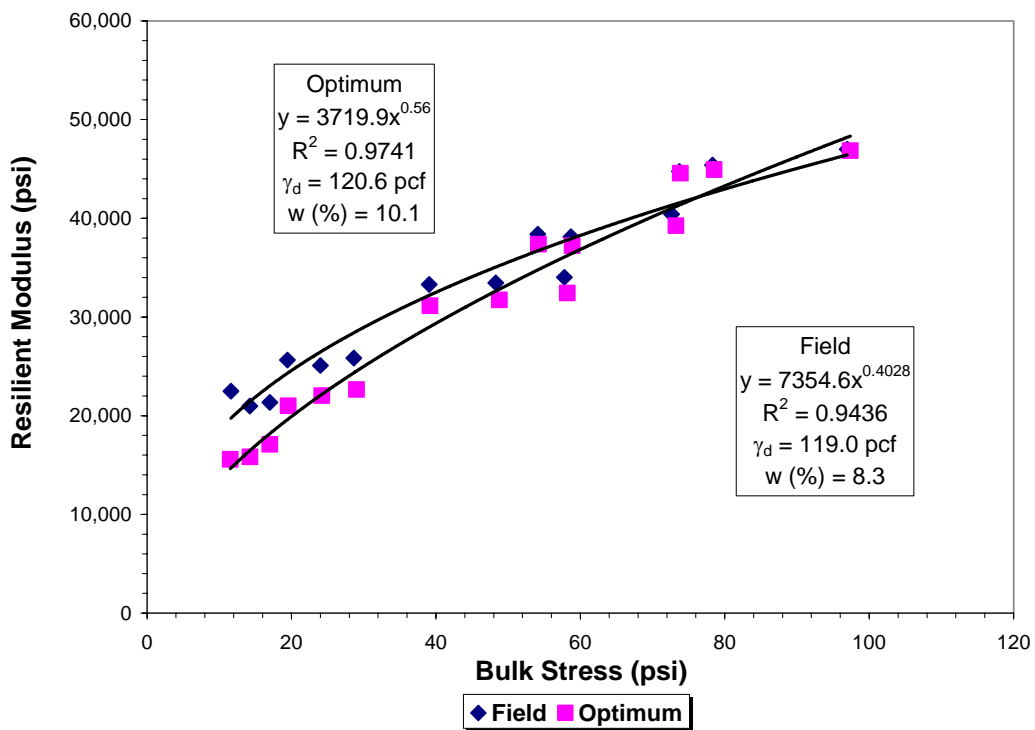
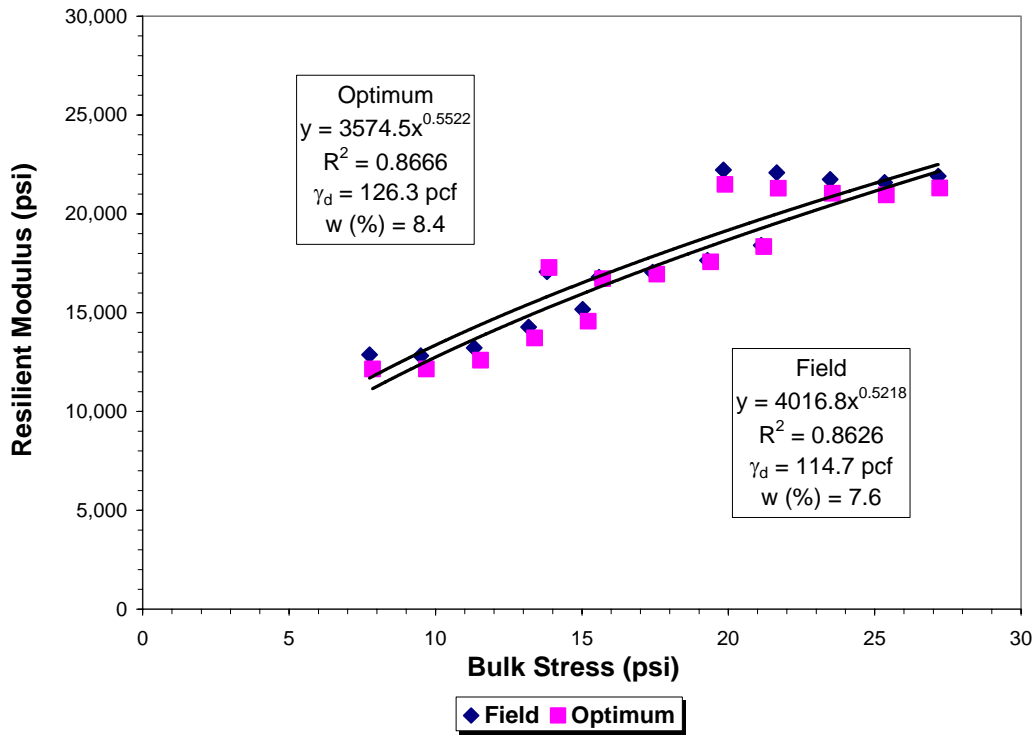
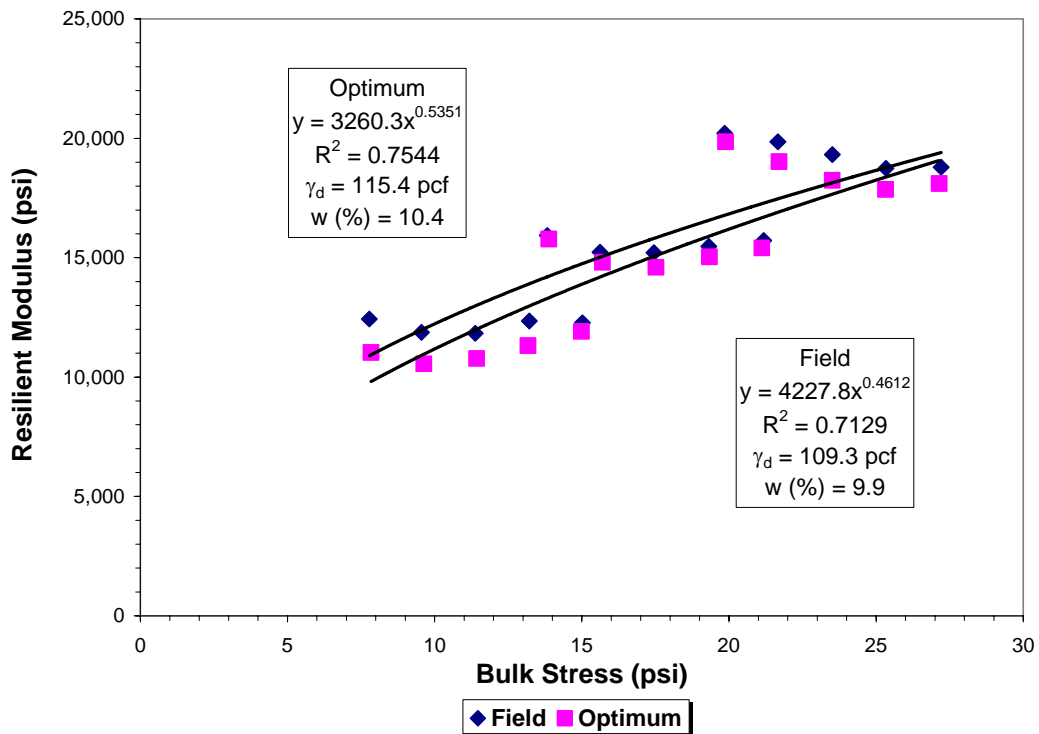


Figure F10. Resilient Modulus for Base (Section 16003).



**Figure F11. Resilient Modulus for Subgrade (Section 16003).**



**Figure F12. Resilient Modulus for Embankment (Section 16003).**

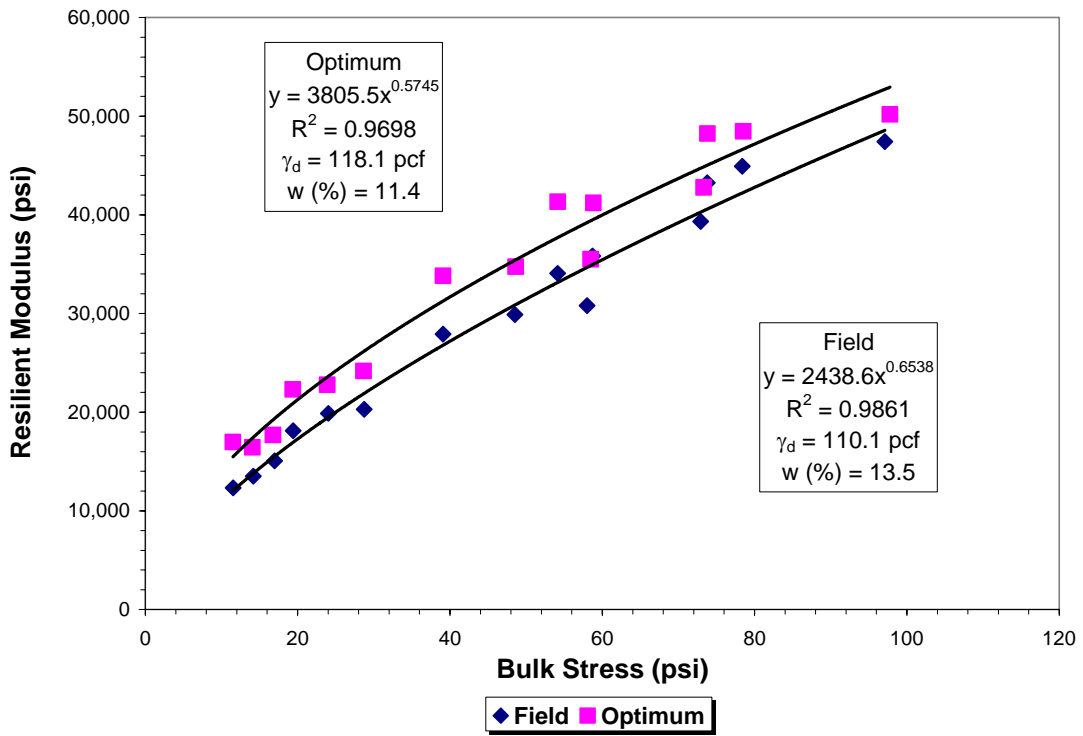


**Figure F13. Resilient Modulus for Base (Section 10160).**

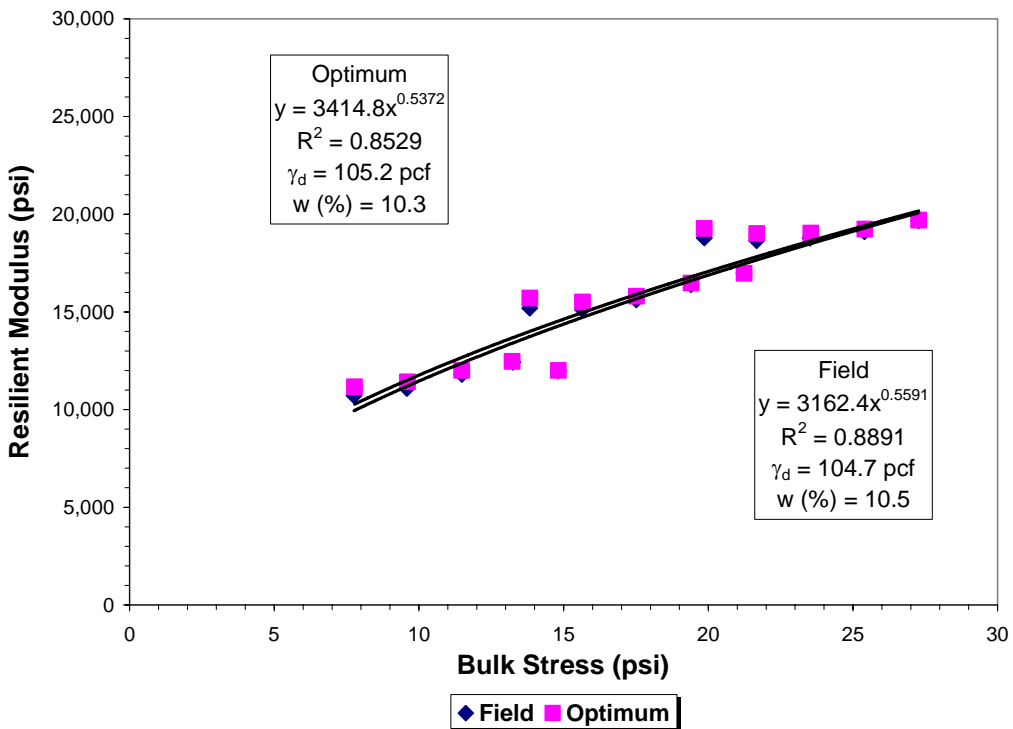


**Figure F14. Resilient Modulus for Subgrade (Section 10160).**

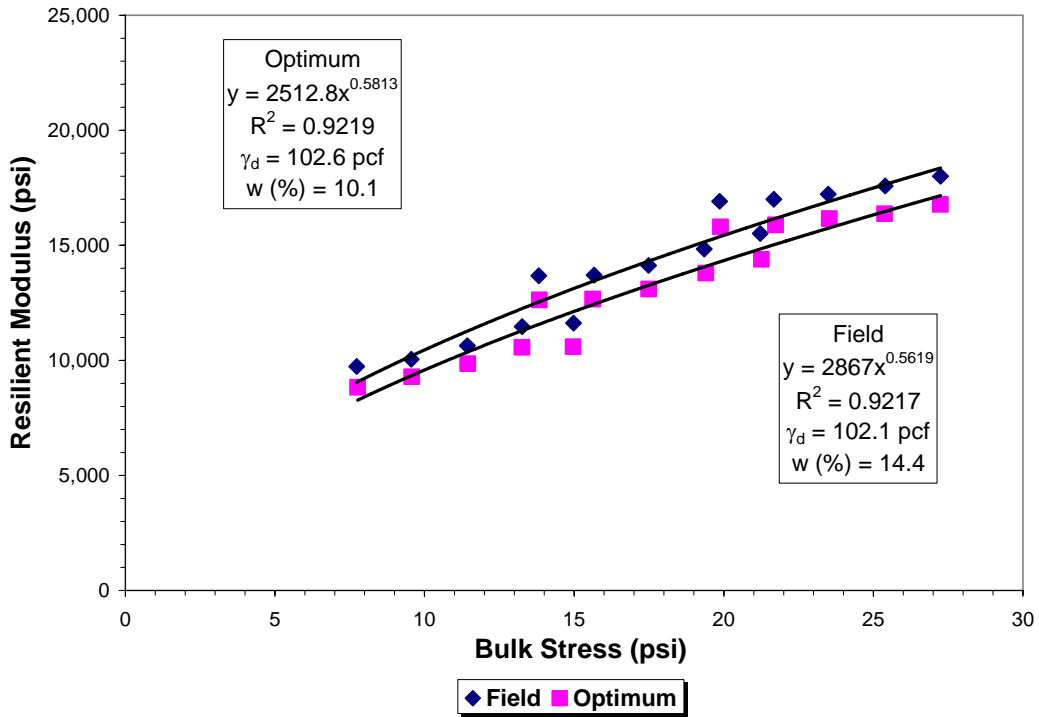


Figure F15. Resilient Modulus for Embankment (Section 10160).

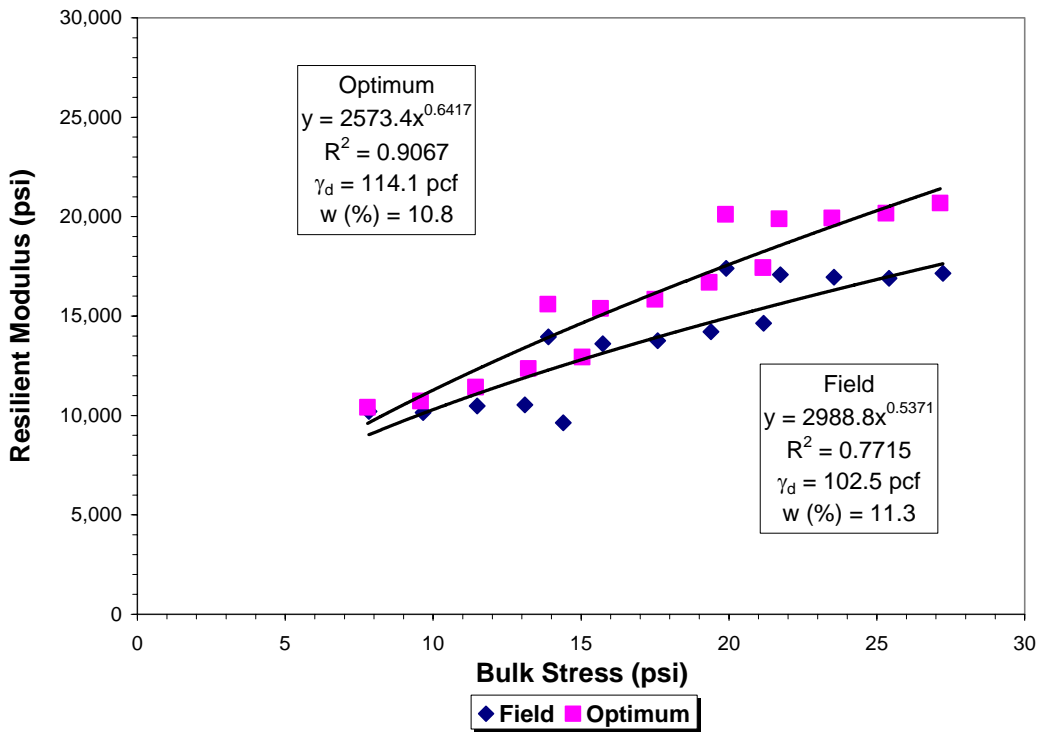
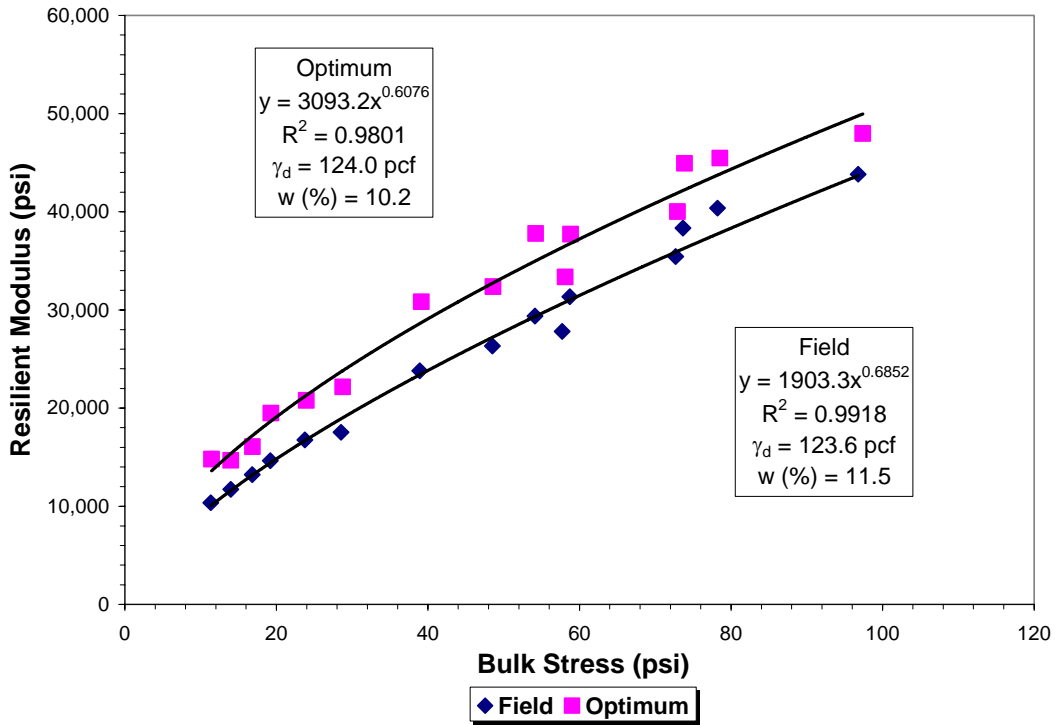
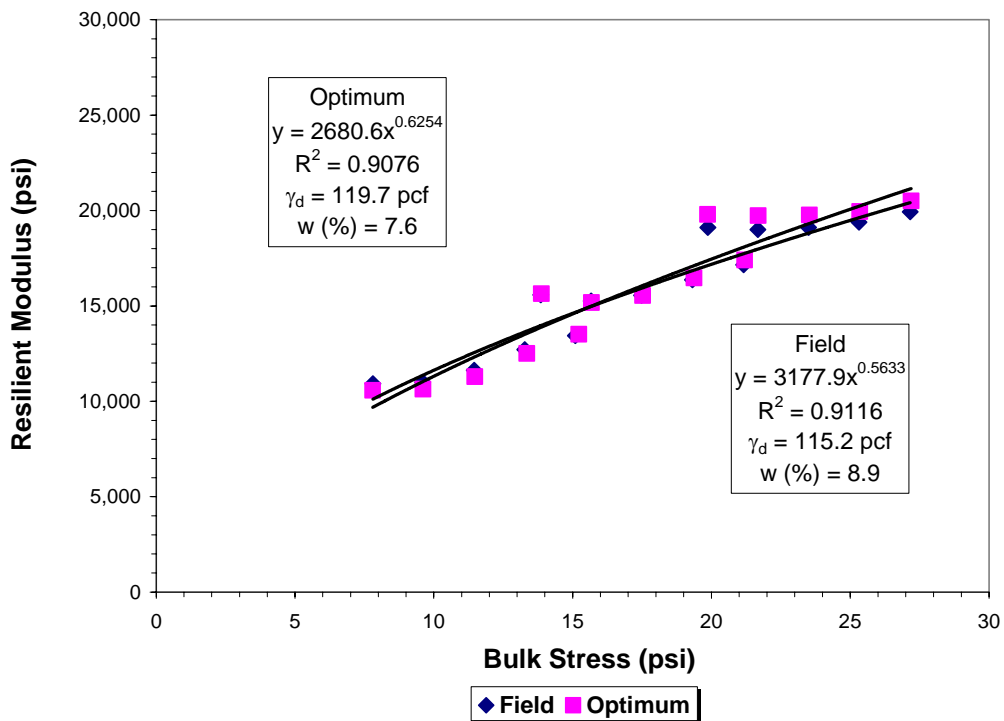


Figure F16. Resilient Modulus for Embankment (Section 16250).



**Figure F17. Resilient Modulus for Base (Section 79270).**



**Figure F18. Resilient Modulus for Subgrade (Section 79270).**

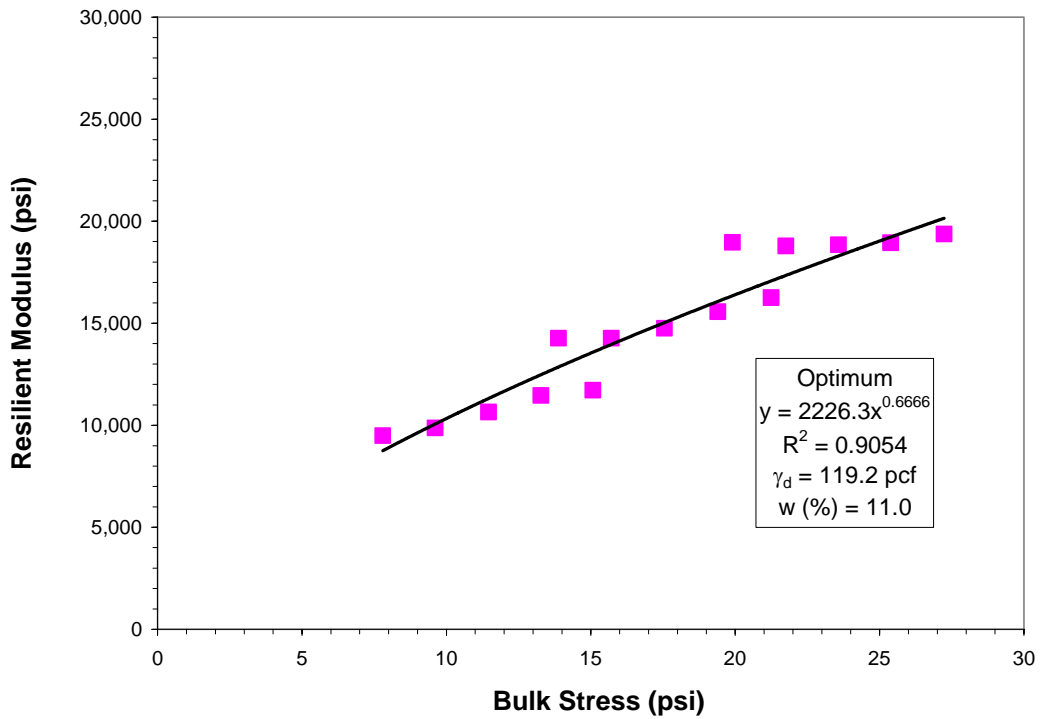


Figure F19. Resilient Modulus for Embankment (Section 79270).

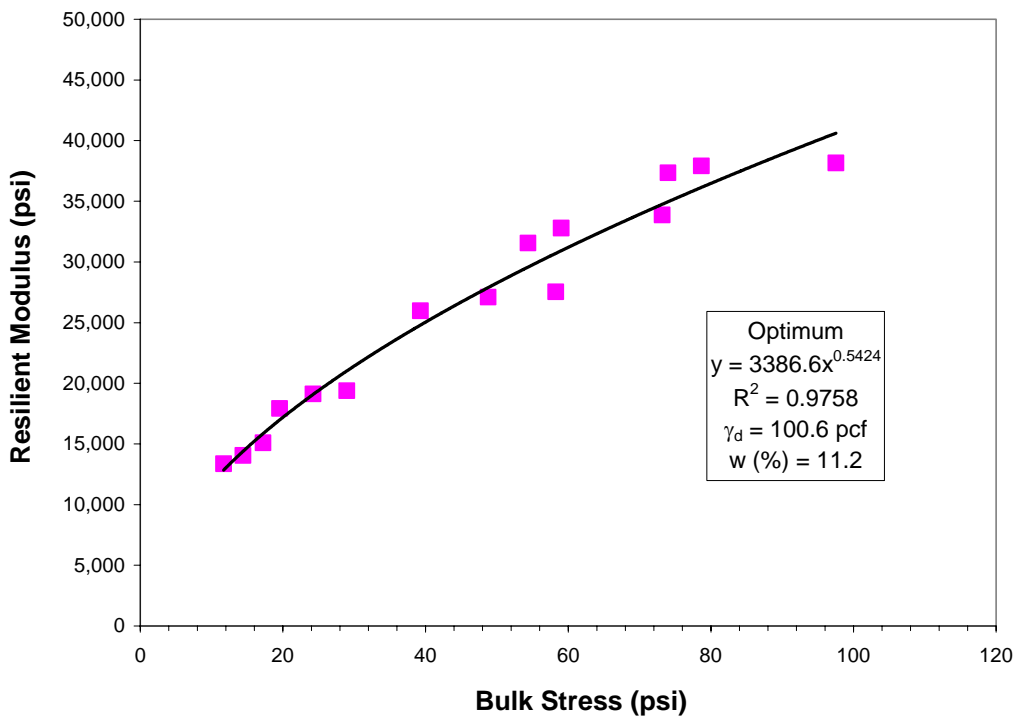
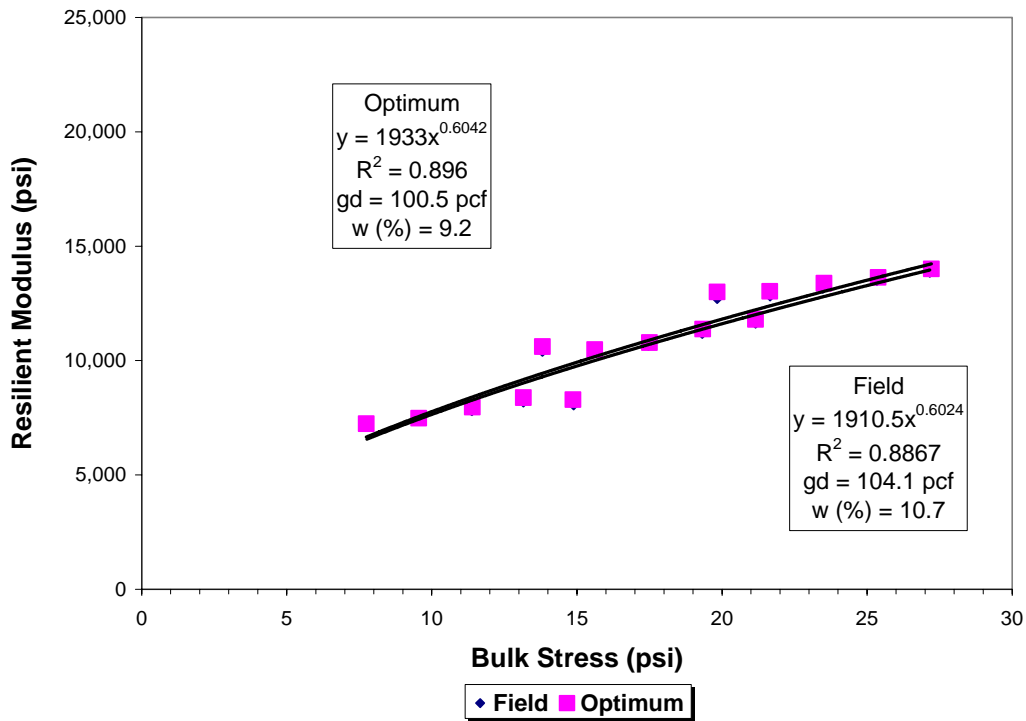
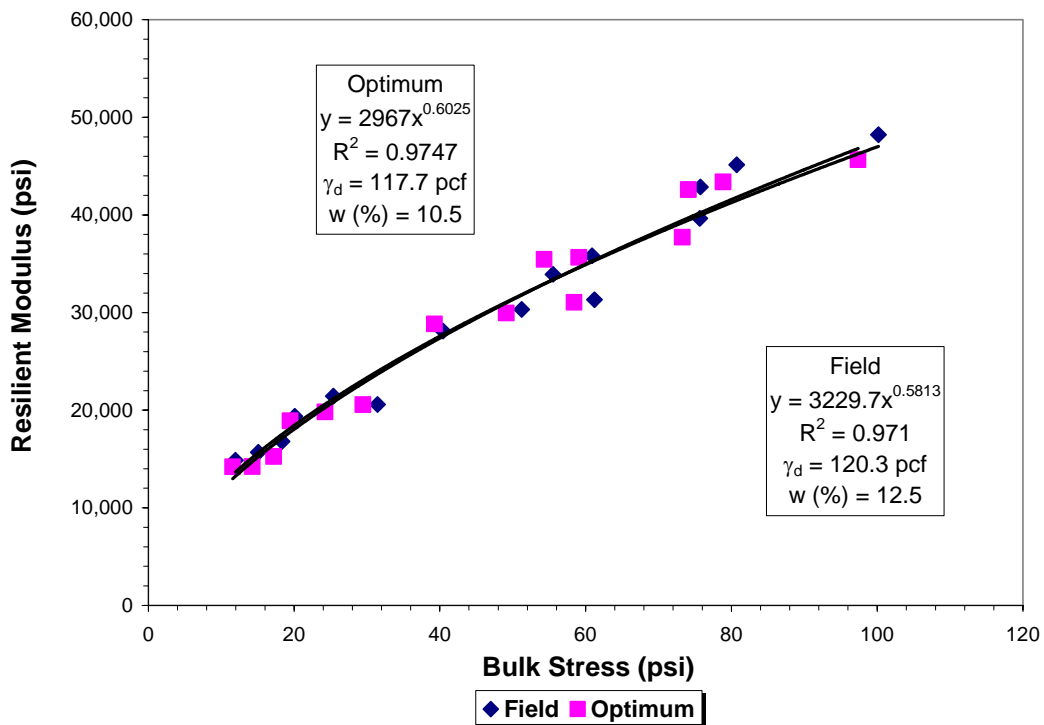


Figure F20. Resilient Modulus for Subgrade (Section 77040).



**Figure F21. Resilient Modulus for Embankment (Section 77040).**



**Figure F22. Resilient Modulus for Base (Section 26005).**

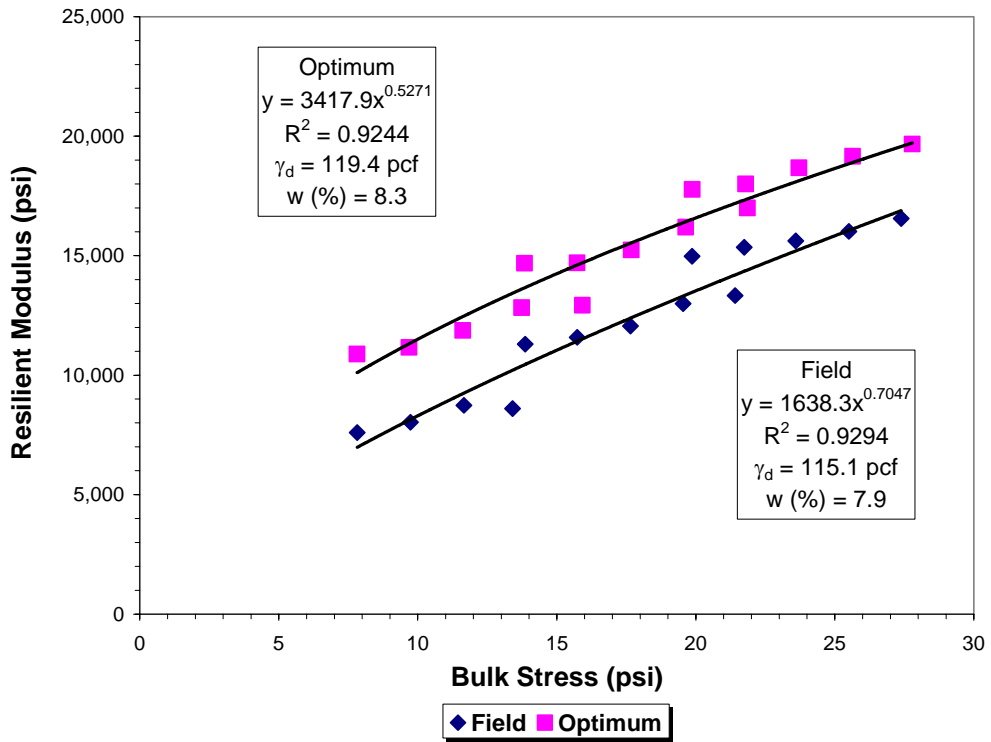


**Figure F23. Resilient Modulus for Subgrade (Section 26005).**

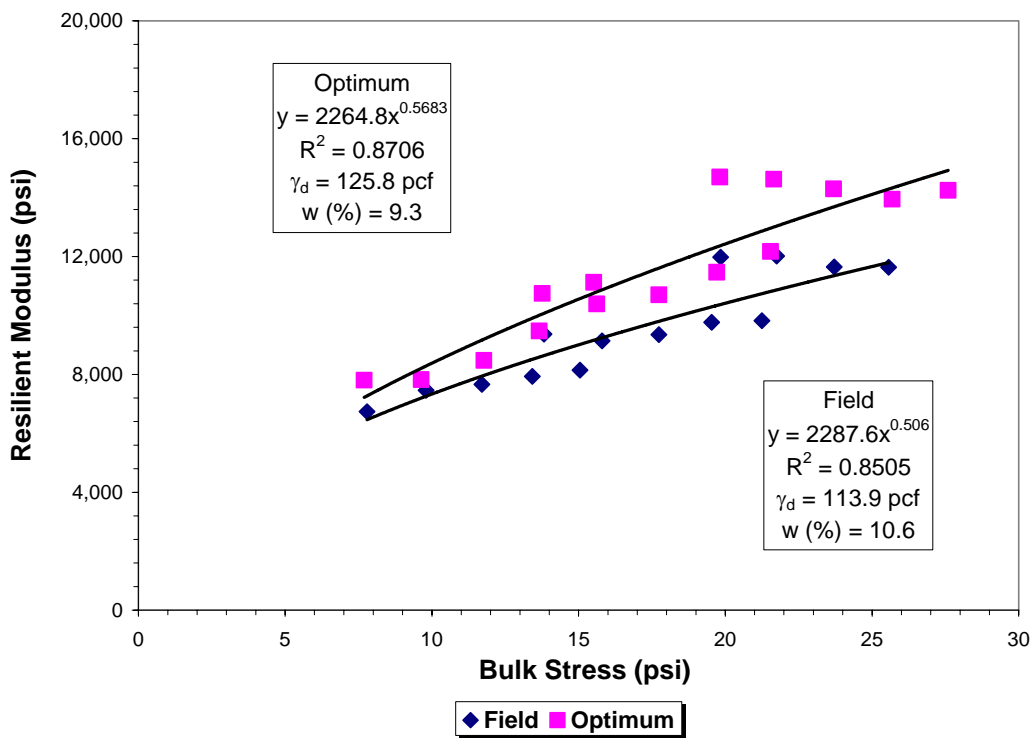


**Figure F24. Resilient Modulus for Embankment (Section 26005).**

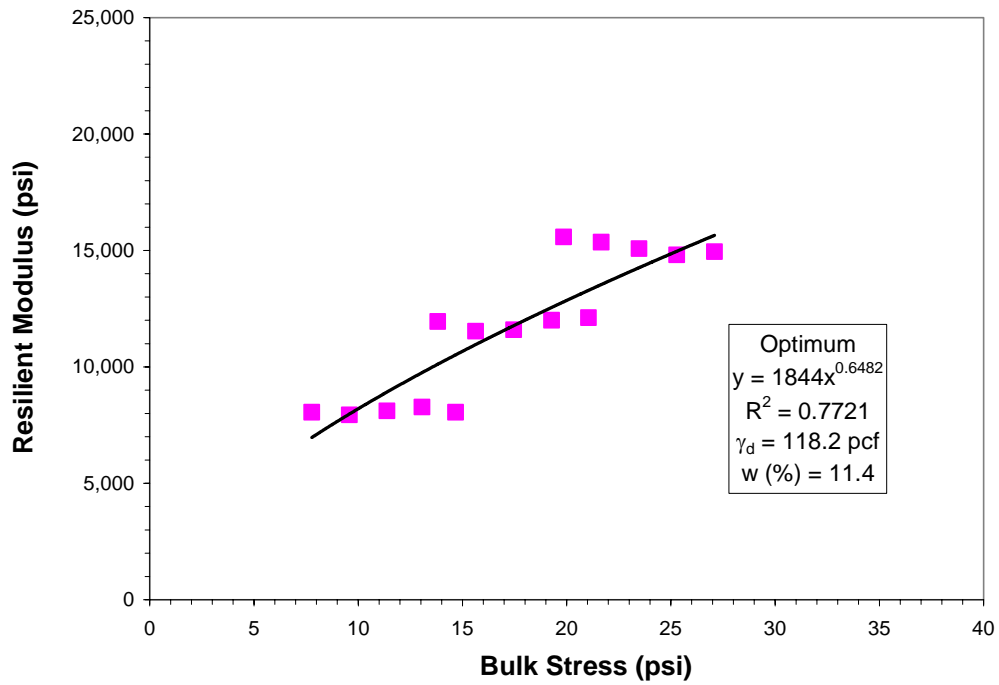


Figure F25. Resilient Modulus for Subgrade (Section 28040).

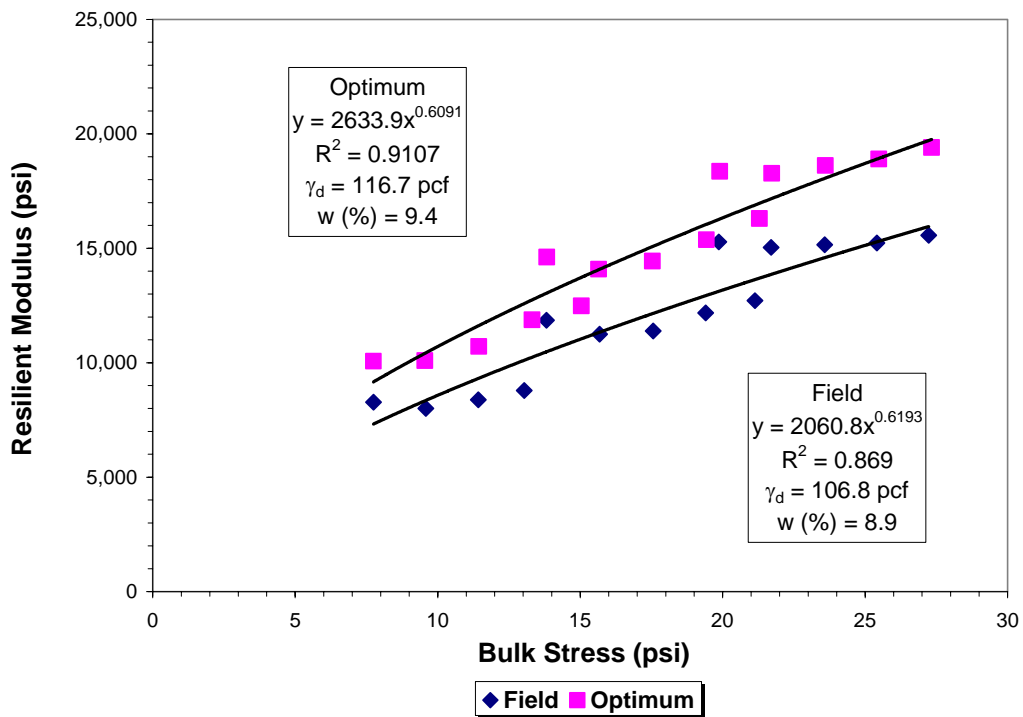


Figure F26. Resilient Modulus for Embankment (Section 28040).

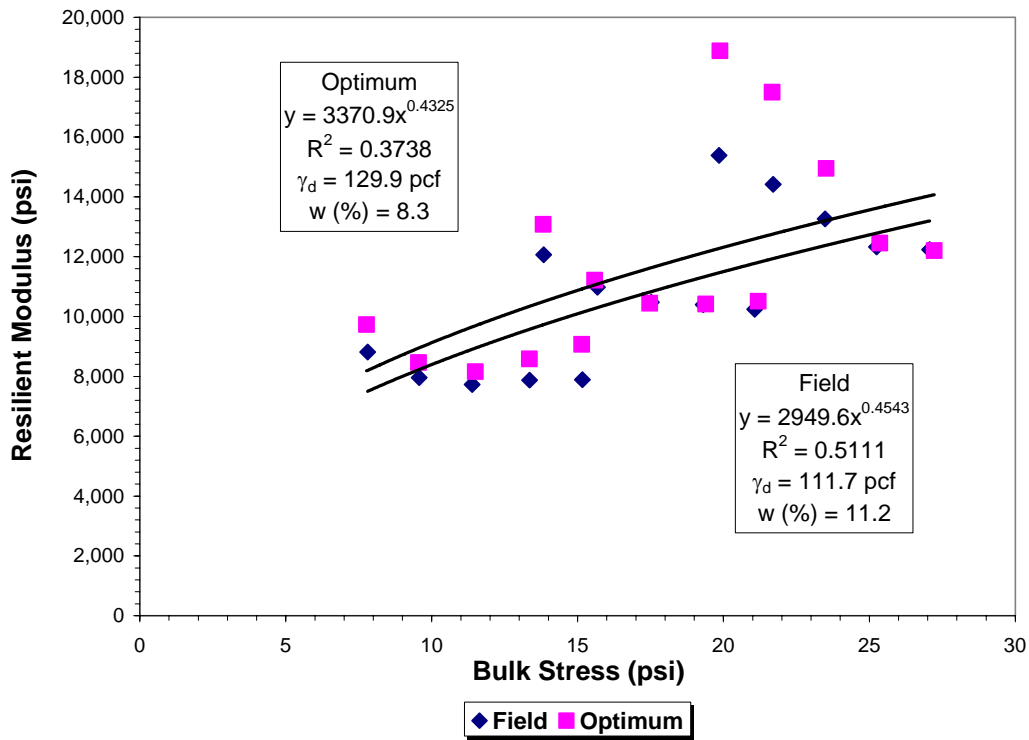


Figure F27. Resilient Modulus for Subgrade (Section 50010).

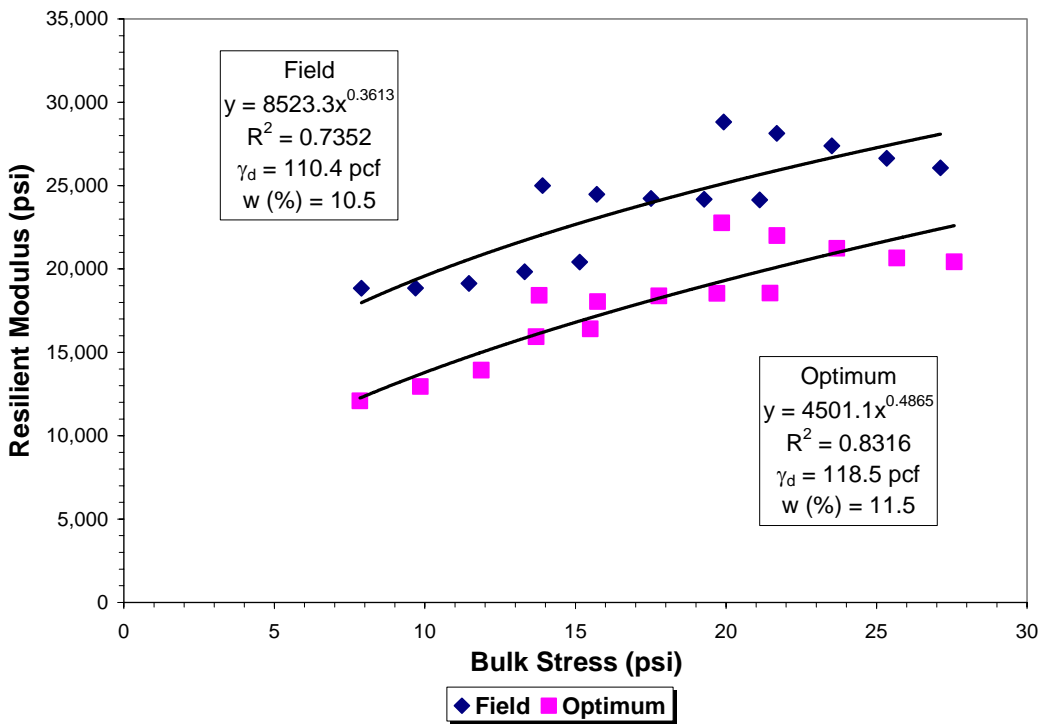
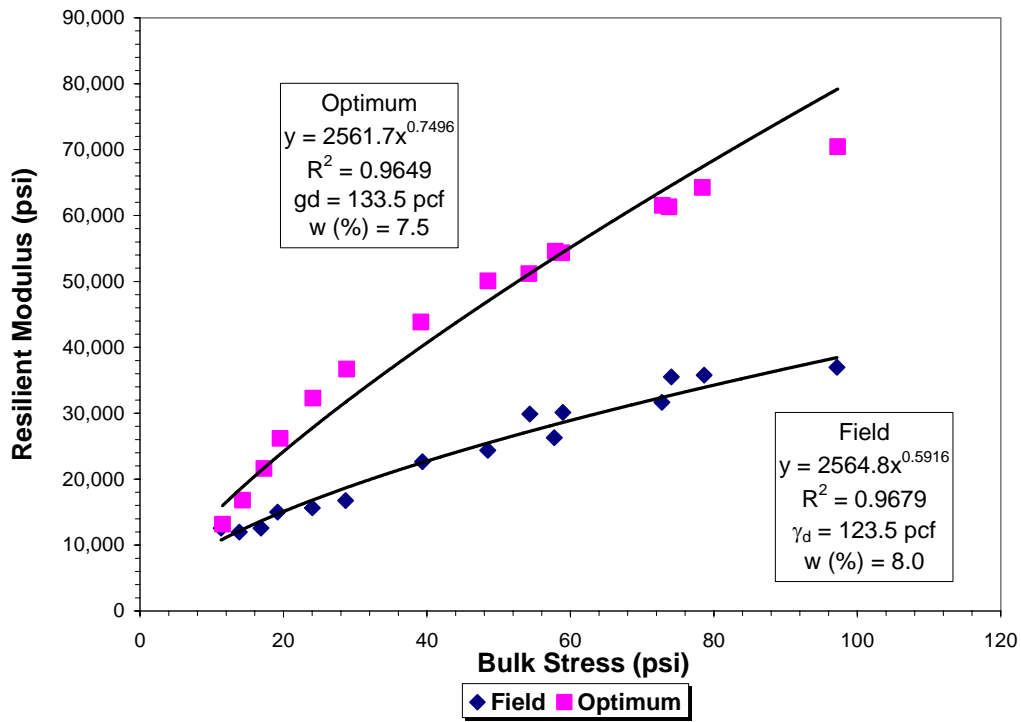
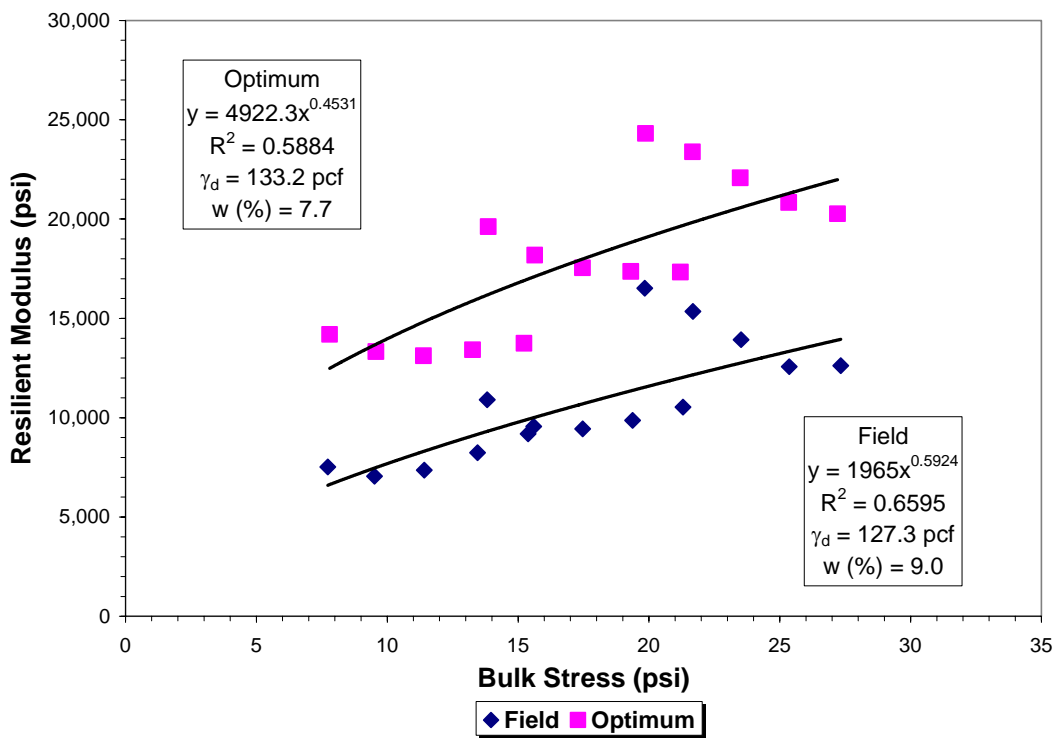


Figure F28. Resilient Modulus for Embankment (Section 50010).



**Figure F29. Resilient Modulus for Base (Section 58060).**



**Figure F30. Resilient Modulus for Subgrade (Section 58060).**

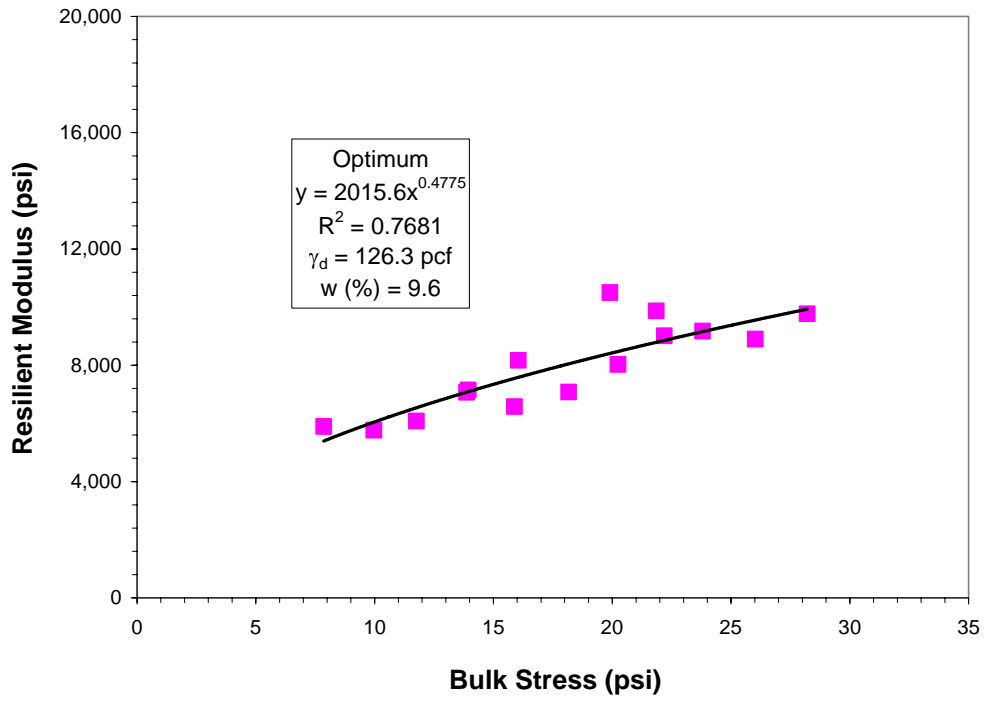


Figure F31. Resilient Modulus for Embankment (Section 58060).

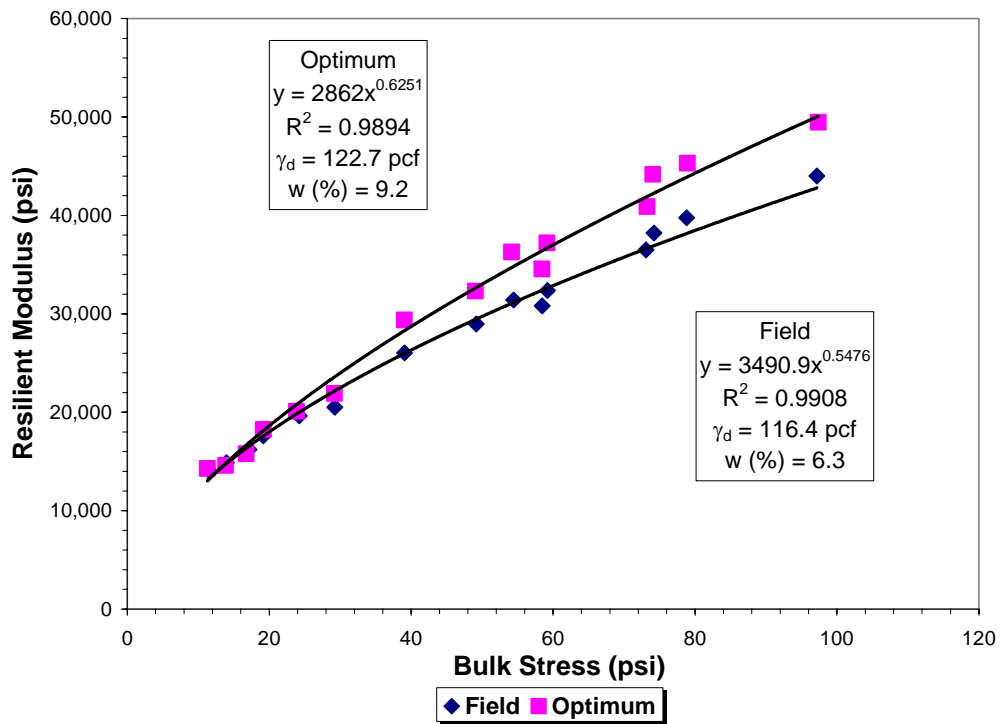
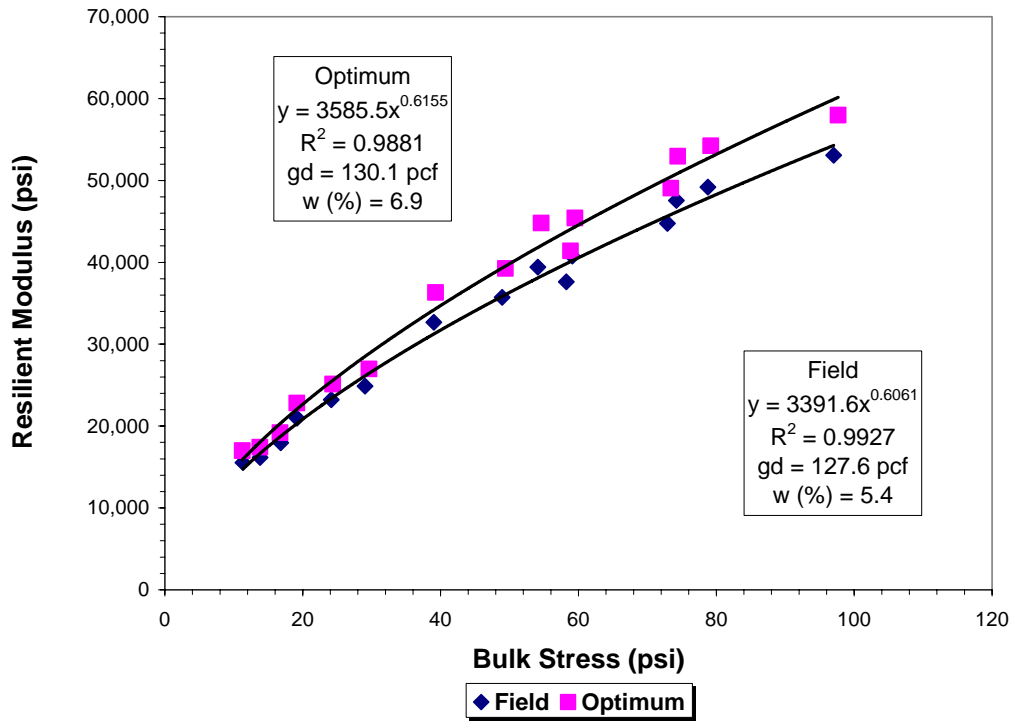
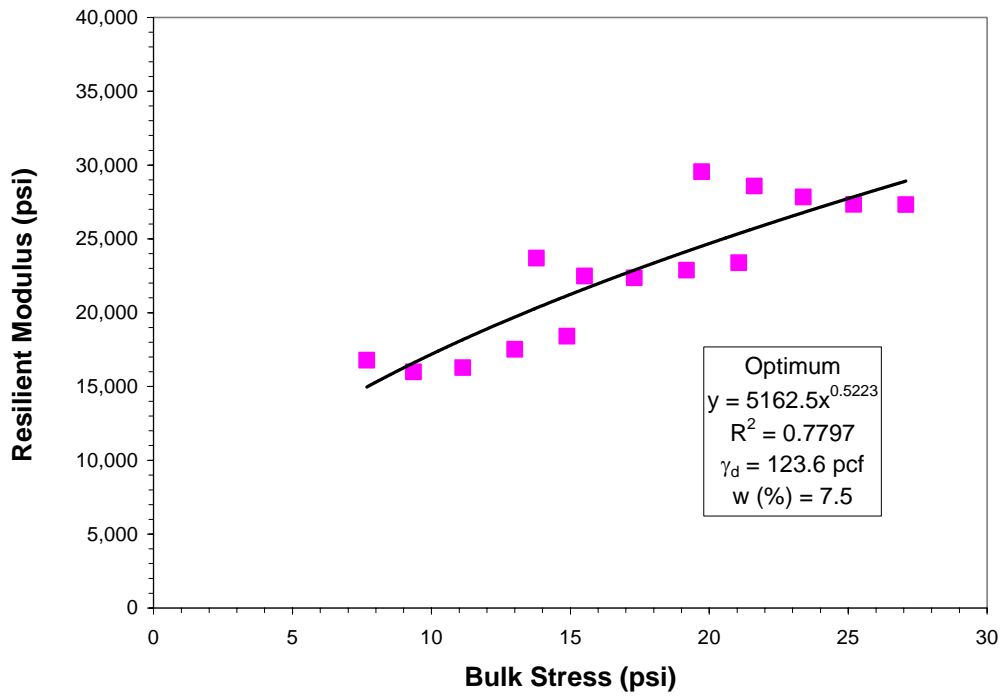


Figure F32. Resilient Modulus for Base (Section 90060).



**Figure F33. Resilient Modulus for Base (Section 87060).**



**Figure F34. Resilient Modulus for Subgrade (Section 87060).**



**APPENDIX G**

**M-E PDG BASED FLEXIBLE PAVEMENT DESIGN TABLES**



**Table G1. Required AC Layer Thickness for New Design with 45 ksi Base Modulus.**

ESALs ( $\times 10^6$ )	Reliability (%)				
	75	80	85	90	95
1	2.0	2.0	2.0	2.0	2.0
2	2.0	2.0	2.0	2.0	2.0
3	2.0	2.0	2.0	2.0	2.0
4	3.0	3.0	3.0	3.0	3.0
5	3.0	3.0	3.0	3.0	3.0
10	3.0	3.0	3.0	3.0	3.0
15	3.0	3.0	3.0	3.0	5.5
20	3.0	3.0	5.0	5.5	6.0
25	5.0	5.5	5.5	6.0	6.5
30	5.5	5.5	6.0	6.0	6.5
35	5.5	6.0	6.0	6.5	7.0
40	5.5	6.0	6.5	6.5	7.0
45	6.0	6.0	6.5	7.0	7.0
50	6.0	6.0	6.5	7.0	7.5
55	6.5	6.5	7.0	7.0	7.5
60	6.5	7.0	7.0	7.5	8.0
65	6.5	7.0	7.5	8.0	8.0
70	7.0	7.5	8.0	8.5	8.5

**Table G2. Required AC Layer Thickness for New Design with 30 ksi Base Modulus.**

ESALs ( $\times 10^6$ )	Reliability (%)				
	75	80	85	90	95
1	2.0	2.0	2.0	2.0	2.0
2	2.0	2.0	2.0	2.0	2.0
3	2.0	2.0	2.0	2.0	2.0
4	3.0	3.0	3.0	3.0	3.0
5	3.0	3.0	3.0	3.0	3.0
10	3.0	5.5	5.5	5.5	5.5
15	5.5	5.5	5.5	5.5	6.0
20	5.5	5.5	6.0	6.0	6.5
25	6.0	6.0	6.0	6.5	7.0
30	6.0	6.0	6.5	6.5	7.0
35	6.0	6.5	6.5	7.0	7.5
40	6.0	6.5	7.0	7.0	7.5
45	6.5	6.5	7.0	7.5	7.5
50	6.5	6.5	7.0	7.5	8.0
55	7.0	7.0	7.5	8.0	8.0
60	7.0	7.5	7.5	8.0	8.5
65	7.0	7.5	8.0	8.5	8.5
70	7.5	8.0	8.5	9.0	9.0

**Table G3. Required AC Overlay Thickness (poor condition, 2-inch existing AC thickness after milling with 30 ksi base modulus).**

ESALs ( $\times 10^6$ )	Reliability (%)				
	75	80	85	90	95
1	1.5	1.5	1.5	1.5	1.5
2	1.5	2.0	2.0	2.0	2.0
3	2.0	2.0	2.5	2.5	3.0
4	2.0	2.0	2.5	3.0	3.0
5	2.5	2.5	3.0	3.0	3.5
10	3.5	3.5	3.5	4.0	4.5
15	4.0	4.0	4.0	4.5	5.0
20	4.0	4.0	4.0	4.5	5.0
25	4.5	4.5	4.5	5.0	5.5
30	4.5	4.5	4.5	5.0	5.5
35	5.0	5.0	5.0	5.5	6.0
40	5.0	5.0	5.0	5.5	6.0
45	5.5	5.5	5.5	6.0	6.5
50	5.5	5.5	5.5	6.0	6.5
55	5.5	5.5	6.0	6.5	7.0
60	5.5	6.0	6.0	6.5	7.0
65	6.0	6.0	6.5	7.0	7.5
70	6.0	6.0	6.5	7.0	7.5

**Table G4. Required AC Overlay Thickness (fair condition, 2-inch existing AC thickness after milling with 30 ksi base modulus).**

ESALs ( $\times 10^6$ )	Reliability (%)				
	75	80	85	90	95
1	1.5	1.5	1.5	1.5	1.5
2	1.5	1.5	1.5	1.5	1.5
3	1.5	1.5	2.0	2.0	2.5
4	2.0	2.0	2.5	2.5	3.0
5	2.0	2.5	2.5	3.0	3.0
10	3.0	3.0	3.5	3.5	4.0
15	3.5	3.5	4.0	4.0	4.5
20	4.0	4.0	4.0	4.5	5.0
25	4.5	4.5	4.5	5.0	5.5
30	4.5	4.5	4.5	5.0	5.5
35	5.0	5.0	5.0	5.5	6.0
40	5.0	5.0	5.0	5.5	6.0
45	5.5	5.5	5.5	6.0	6.5
50	5.5	5.5	5.5	6.0	6.5
55	5.5	5.5	6.0	6.5	6.5
60	5.5	6.0	6.0	6.5	6.5
65	5.5	6.0	6.5	7.0	7.0
70	6.0	6.0	6.5	7.0	7.0

**Table G5. Required AC Overlay Thickness (good condition, 2-inch existing AC thickness after milling with 30 ksi base modulus).**

ESALs ( $\times 10^6$ )	Reliability (%)				
	75	80	85	90	95
<b>1</b>	1.5	1.5	1.5	1.5	1.5
<b>2</b>	1.5	1.5	1.5	1.5	1.5
<b>3</b>	1.5	1.5	2.0	2.0	2.5
<b>4</b>	2.0	2.0	2.5	2.5	3.0
<b>5</b>	2.0	2.5	2.5	3.0	3.0
<b>10</b>	3.0	3.0	3.5	3.5	4.0
<b>15</b>	3.5	3.5	4.0	4.0	4.5
<b>20</b>	3.5	3.5	4.0	4.0	4.5
<b>25</b>	4.0	4.0	4.5	4.5	5.0
<b>30</b>	4.0	4.0	4.5	5.0	5.0
<b>35</b>	4.5	4.5	5.0	5.0	5.5
<b>40</b>	4.5	4.5	5.0	5.5	5.5
<b>45</b>	5.0	5.0	5.5	6.0	6.0
<b>50</b>	5.0	5.0	5.5	6.0	6.0
<b>55</b>	5.0	5.5	6.0	6.0	6.5
<b>60</b>	5.0	5.5	6.0	6.5	6.5
<b>65</b>	5.5	6.0	6.0	6.5	7.0
<b>70</b>	5.5	6.0	6.5	6.5	7.0

**Table G6. Required AC Overlay Thickness (poor condition, 3-inch existing AC thickness after milling with 30 ksi base modulus).**

ESALs ( $\times 10^6$ )	Reliability (%)				
	75	80	85	90	95
<b>1</b>	1.5	1.5	1.5	1.5	1.5
<b>2</b>	1.5	1.5	1.5	1.5	1.5
<b>3</b>	1.5	1.5	1.5	1.5	2.0
<b>4</b>	1.5	1.5	1.5	2.0	2.0
<b>5</b>	1.5	2.0	2.0	2.0	2.5
<b>10</b>	2.0	2.5	3.0	3.5	3.5
<b>15</b>	2.5	3.0	3.5	3.5	4.0
<b>20</b>	2.5	3.0	3.5	4.0	4.5
<b>25</b>	3.0	3.5	4.0	4.5	4.5
<b>30</b>	3.0	4.0	4.0	4.5	5.0
<b>35</b>	3.5	4.0	4.5	5.0	5.0
<b>40</b>	3.5	4.5	4.5	5.0	5.5
<b>45</b>	4.0	5.0	5.0	5.5	5.5
<b>50</b>	4.5	5.0	5.0	5.5	6.0
<b>55</b>	4.5	5.0	5.0	5.5	6.0
<b>60</b>	5.0	5.0	5.0	5.5	6.5
<b>65</b>	5.0	5.5	5.5	6.0	6.5
<b>70</b>	5.0	5.5	6.0	6.5	7.0

**Table G7. Required AC Overlay Thickness (fair condition, 3-inch existing AC thickness after milling with 30 ksi base modulus).**

ESALs ( $\times 10^6$ )	Reliability (%)				
	75	80	85	90	95
<b>1</b>	1.5	1.5	1.5	1.5	1.5
<b>2</b>	1.5	1.5	1.5	1.5	1.5
<b>3</b>	1.5	1.5	1.5	1.5	1.5
<b>4</b>	1.5	1.5	1.5	1.5	1.5
<b>5</b>	1.5	1.5	2.0	2.0	2.0
<b>10</b>	2.0	2.0	2.5	3.0	3.0
<b>15</b>	2.0	2.5	3.0	3.0	3.5
<b>20</b>	2.5	3.0	3.5	3.5	4.5
<b>25</b>	3.0	3.5	4.0	4.0	4.5
<b>30</b>	3.0	4.0	4.0	4.5	5.0
<b>35</b>	3.5	4.0	4.5	4.5	5.0
<b>40</b>	3.5	4.5	4.5	5.0	5.5
<b>45</b>	4.0	4.5	5.0	5.5	5.5
<b>50</b>	4.5	5.0	5.0	5.5	6.0
<b>55</b>	4.5	5.0	5.0	5.5	6.0
<b>60</b>	4.5	5.0	5.0	5.5	6.0
<b>65</b>	4.5	5.0	5.5	5.5	6.0
<b>70</b>	5.0	5.0	5.5	6.0	6.5

**Table G8. Required AC Overlay Thickness (good condition, 3-inch existing AC thickness after milling with 30 ksi base modulus).**

ESALs ( $\times 10^6$ )	Reliability (%)				
	75	80	85	90	95
<b>1</b>	1.5	1.5	1.5	1.5	1.5
<b>2</b>	1.5	1.5	1.5	1.5	1.5
<b>3</b>	1.5	1.5	1.5	1.5	1.5
<b>4</b>	1.5	1.5	1.5	1.5	1.5
<b>5</b>	1.5	1.5	2.0	2.0	2.0
<b>10</b>	2.0	2.0	2.5	2.5	3.0
<b>15</b>	2.0	2.5	3.0	3.0	3.5
<b>20</b>	2.0	3.0	3.0	3.0	4.0
<b>25</b>	2.5	3.0	3.5	3.5	4.0
<b>30</b>	2.5	3.5	4.0	4.0	4.5
<b>35</b>	3.0	3.5	4.0	4.0	5.0
<b>40</b>	3.0	4.0	4.5	4.5	5.0
<b>45</b>	3.5	4.0	5.0	5.0	5.5
<b>50</b>	4.0	4.5	5.0	5.0	5.5
<b>55</b>	4.0	4.5	5.0	5.0	5.5
<b>60</b>	4.5	5.0	5.0	5.5	6.0
<b>65</b>	4.5	5.0	5.0	5.5	6.0
<b>70</b>	4.5	5.0	5.0	6.0	6.0

**Table G9. Required AC Overlay Thickness (poor condition, 4-inch existing AC thickness after milling with 30 ksi base modulus).**

ESALs ( $\times 10^6$ )	Reliability (%)				
	75	80	85	90	95
<b>1</b>	1.5	1.5	1.5	1.5	1.5
<b>2</b>	1.5	1.5	1.5	1.5	1.5
<b>3</b>	1.5	1.5	1.5	1.5	1.5
<b>4</b>	1.5	1.5	1.5	1.5	1.5
<b>5</b>	1.5	1.5	1.5	1.5	1.5
<b>10</b>	1.5	1.5	2.0	2.5	2.5
<b>15</b>	1.5	2.0	2.5	3.0	3.0
<b>20</b>	2.0	2.5	3.0	3.5	3.5
<b>25</b>	2.5	3.0	3.5	3.5	3.5
<b>30</b>	2.5	3.0	3.5	4.0	4.0
<b>35</b>	3.0	3.5	4.0	4.0	4.0
<b>40</b>	3.0	3.5	4.0	4.5	4.5
<b>45</b>	3.5	4.0	4.5	4.5	5.0
<b>50</b>	3.5	4.0	4.5	4.5	5.0
<b>55</b>	3.5	4.0	4.5	4.5	5.0
<b>60</b>	4.0	4.0	4.5	4.5	5.0
<b>65</b>	4.0	4.0	4.5	5.0	5.5
<b>70</b>	4.0	4.5	4.5	5.0	5.5

**Table G10. Required AC Overlay Thickness (fair condition, 4-inch existing AC thickness after milling with 30 ksi base modulus).**

ESALs ( $\times 10^6$ )	Reliability (%)				
	75	80	85	90	95
<b>1</b>	1.5	1.5	1.5	1.5	1.5
<b>2</b>	1.5	1.5	1.5	1.5	1.5
<b>3</b>	1.5	1.5	1.5	1.5	1.5
<b>4</b>	1.5	1.5	1.5	1.5	1.5
<b>5</b>	1.5	1.5	1.5	1.5	1.5
<b>10</b>	1.5	1.5	2.0	2.0	2.0
<b>15</b>	1.5	2.0	2.0	2.5	3.0
<b>20</b>	2.0	2.5	3.0	3.5	3.5
<b>25</b>	2.5	3.0	3.0	3.5	3.5
<b>30</b>	2.5	3.0	3.5	4.0	4.0
<b>35</b>	3.0	3.5	3.5	4.0	4.0
<b>40</b>	3.0	3.5	3.5	4.0	4.5
<b>45</b>	3.5	4.0	4.0	4.5	4.5
<b>50</b>	3.5	4.0	4.0	4.5	4.5
<b>55</b>	3.5	4.0	4.0	4.5	4.5
<b>60</b>	3.5	4.0	4.0	4.5	5.0
<b>65</b>	4.0	4.0	4.0	4.5	5.0
<b>70</b>	4.0	4.0	4.5	4.5	5.0

**Table G11. Required AC Overlay Thickness (good condition, 4-inch existing AC thickness after milling with 30 ksi base modulus).**

ESALs ( $\times 10^6$ )	Reliability (%)				
	75	80	85	90	95
<b>1</b>	1.5	1.5	1.5	1.5	1.5
<b>2</b>	1.5	1.5	1.5	1.5	1.5
<b>3</b>	1.5	1.5	1.5	1.5	1.5
<b>4</b>	1.5	1.5	1.5	1.5	1.5
<b>5</b>	1.5	1.5	1.5	1.5	1.5
<b>10</b>	1.5	1.5	1.5	2.0	2.0
<b>15</b>	1.5	2.0	2.0	2.5	3.0
<b>20</b>	2.0	2.5	2.5	3.0	3.0
<b>25</b>	2.0	2.5	2.5	3.0	3.0
<b>30</b>	2.5	3.0	3.0	3.5	3.5
<b>35</b>	2.5	3.0	3.0	3.5	3.5
<b>40</b>	2.5	3.0	3.0	3.5	4.0
<b>45</b>	3.0	3.5	3.5	4.0	4.5
<b>50</b>	3.0	3.5	3.5	4.0	4.5
<b>55</b>	3.0	3.5	3.5	4.0	4.5
<b>60</b>	3.5	3.5	4.0	4.5	5.0
<b>65</b>	3.5	3.5	4.0	4.5	5.0
<b>70</b>	3.5	4.0	4.0	4.5	5.0

**Table G12. Required AC Overlay Thickness (poor condition, 5-inch existing AC thickness after milling with 30 ksi base modulus).**

ESALs ( $\times 10^6$ )	Reliability (%)				
	75	80	85	90	95
<b>1</b>	1.5	1.5	1.5	1.5	1.5
<b>2</b>	1.5	1.5	1.5	1.5	1.5
<b>3</b>	1.5	1.5	1.5	1.5	1.5
<b>4</b>	1.5	1.5	1.5	1.5	1.5
<b>5</b>	1.5	1.5	1.5	1.5	1.5
<b>10</b>	1.5	1.5	1.5	1.5	1.5
<b>15</b>	1.5	1.5	1.5	2.0	2.0
<b>20</b>	1.5	1.5	2.0	2.5	2.5
<b>25</b>	1.5	2.0	2.0	2.5	2.5
<b>30</b>	1.5	2.0	2.5	3.0	3.0
<b>35</b>	2.0	2.5	2.5	3.0	3.0
<b>40</b>	2.0	2.5	2.5	3.0	3.5
<b>45</b>	2.5	3.0	3.0	3.5	3.5
<b>50</b>	2.5	3.0	3.0	3.5	4.0
<b>55</b>	2.5	3.0	3.0	3.5	4.0
<b>60</b>	3.0	3.0	3.0	3.5	4.0
<b>65</b>	3.0	3.0	3.5	4.0	4.0
<b>70</b>	3.0	3.5	3.5	4.0	4.5

**Table G13. Required AC Overlay Thickness (fair condition, 5-inch existing AC thickness after milling with 30 ksi base modulus).**

ESALs ( $\times 10^6$ )	Reliability (%)				
	75	80	85	90	95
1	1.5	1.5	1.5	1.5	1.5
2	1.5	1.5	1.5	1.5	1.5
3	1.5	1.5	1.5	1.5	1.5
4	1.5	1.5	1.5	1.5	1.5
5	1.5	1.5	1.5	1.5	1.5
10	1.5	1.5	1.5	1.5	1.5
15	1.5	1.5	1.5	1.5	2.0
20	1.5	1.5	2.0	2.5	2.5
25	1.5	2.0	2.0	2.5	2.5
30	1.5	2.0	2.5	3.0	3.0
35	2.0	2.5	2.5	3.0	3.0
40	2.0	2.5	2.5	3.0	3.5
45	2.5	2.5	3.0	3.5	3.5
50	2.5	2.5	3.0	3.5	4.0
55	2.5	2.5	3.0	3.5	4.0
60	2.5	3.0	3.0	3.5	4.0
65	3.0	3.0	3.0	3.5	4.0
70	3.0	3.0	3.5	4.0	4.0

**Table G14. Required AC Overlay Thickness (good condition, 5-inch existing AC thickness after milling with 30 ksi base modulus).**

ESALs ( $\times 10^6$ )	Reliability (%)				
	75	80	85	90	95
1	1.5	1.5	1.5	1.5	1.5
2	1.5	1.5	1.5	1.5	1.5
3	1.5	1.5	1.5	1.5	1.5
4	1.5	1.5	1.5	1.5	1.5
5	1.5	1.5	1.5	1.5	1.5
10	1.5	1.5	1.5	1.5	1.5
15	1.5	1.5	1.5	1.5	2.0
20	1.5	1.5	1.5	2.0	2.0
25	1.5	1.5	1.5	2.0	2.0
30	1.5	2.0	2.0	2.5	2.5
35	1.5	2.0	2.0	2.5	2.5
40	1.5	2.0	2.0	2.5	3.0
45	2.0	2.5	2.5	3.0	3.0
50	2.0	2.5	2.5	3.0	3.5
55	2.0	2.5	2.5	3.0	3.5
60	2.0	2.5	2.5	3.0	3.5
65	2.5	2.5	3.0	3.5	4.0
70	2.5	3.0	3.0	3.5	4.0

**Table G15. Required AC Overlay Thickness (poor condition, 6-inch existing AC thickness after milling with 30 ksi base modulus).**

ESALs ( $\times 10^6$ )	Reliability (%)				
	75	80	85	90	95
1	1.5	1.5	1.5	1.5	1.5
2	1.5	1.5	1.5	1.5	1.5
3	1.5	1.5	1.5	1.5	1.5
4	1.5	1.5	1.5	1.5	1.5
5	1.5	1.5	1.5	1.5	1.5
10	1.5	1.5	1.5	1.5	1.5
15	1.5	1.5	1.5	1.5	1.5
20	1.5	1.5	1.5	1.5	2.0
25	1.5	1.5	1.5	2.0	2.0
30	1.5	1.5	2.0	2.0	2.0
35	1.5	2.0	2.0	2.0	2.5
40	1.5	2.0	2.0	2.0	2.5
45	1.5	2.0	2.0	2.5	2.5
50	1.5	2.0	2.0	2.5	3.0
55	1.5	2.0	2.0	2.5	3.0
60	1.5	2.0	2.0	2.5	3.0
65	2.0	2.0	2.5	2.5	3.0
70	2.0	2.5	2.5	3.0	3.5

**Table G16. Required AC Overlay Thickness (fair condition, 6-inch existing AC thickness after milling with 30 ksi base modulus).**

ESALs ( $\times 10^6$ )	Reliability (%)				
	75	80	85	90	95
1	1.5	1.5	1.5	1.5	1.5
2	1.5	1.5	1.5	1.5	1.5
3	1.5	1.5	1.5	1.5	1.5
4	1.5	1.5	1.5	1.5	1.5
5	1.5	1.5	1.5	1.5	1.5
10	1.5	1.5	1.5	1.5	1.5
15	1.5	1.5	1.5	1.5	1.5
20	1.5	1.5	1.5	1.5	2.0
25	1.5	1.5	1.5	2.0	2.0
30	1.5	1.5	1.5	2.0	2.0
35	1.5	1.5	1.5	2.0	2.5
40	1.5	1.5	1.5	2.0	2.5
45	1.5	1.5	1.5	2.5	2.5
50	1.5	1.5	1.5	2.5	2.5
55	1.5	1.5	2.0	2.5	3.0
60	1.5	1.5	2.0	2.5	3.0
65	1.5	1.5	2.0	2.5	3.0
70	1.5	2.0	2.0	2.5	3.0

**Table G17. Required AC Overlay Thickness (good condition, 6-inch existing AC thickness after milling with 30 ksi base modulus).**

ESALs ( $\times 10^6$ )	Reliability (%)				
	75	80	85	90	95
1	1.5	1.5	1.5	1.5	1.5
2	1.5	1.5	1.5	1.5	1.5
3	1.5	1.5	1.5	1.5	1.5
4	1.5	1.5	1.5	1.5	1.5
5	1.5	1.5	1.5	1.5	1.5
10	1.5	1.5	1.5	1.5	1.5
15	1.5	1.5	1.5	1.5	1.5
20	1.5	1.5	1.5	1.5	1.5
25	1.5	1.5	1.5	1.5	1.5
30	1.5	1.5	1.5	1.5	2.0
35	1.5	1.5	1.5	1.5	2.0
40	1.5	1.5	1.5	1.5	2.0
45	1.5	1.5	1.5	2.0	2.0
50	1.5	1.5	1.5	2.0	2.5
55	1.5	1.5	1.5	2.0	2.5
60	1.5	1.5	1.5	2.0	2.5
65	1.5	1.5	1.5	2.0	3.0
70	1.5	1.5	2.0	2.5	3.0

**Table G18. Required AC Overlay Thickness (poor condition, 2-inch existing AC thickness after milling with 45 ksi base modulus).**

ESALs ( $\times 10^6$ )	Reliability (%)				
	75	80	85	90	95
1	1.5	1.5	1.5	1.5	1.5
2	1.5	1.5	1.5	1.5	1.5
3	1.5	1.5	1.5	1.5	1.5
4	1.5	1.5	1.5	1.5	1.5
5	1.5	1.5	1.5	2.0	2.5
10	2.5	2.5	3.0	3.5	4.0
15	3.0	3.0	3.5	4.0	4.5
20	3.0	3.5	4.0	4.0	4.5
25	3.5	3.5	4.0	4.5	5.0
30	4.0	4.0	4.5	4.5	5.0
35	4.0	4.0	4.5	5.0	5.5
40	4.5	4.5	4.5	5.0	5.5
45	4.5	4.5	5.0	5.5	6.0
50	4.5	5.0	5.0	5.5	6.0
55	5.0	5.0	5.5	5.5	6.0
60	5.0	5.0	5.5	6.0	6.5
65	5.0	5.5	5.5	6.0	6.5
70	5.5	5.5	5.5	6.0	6.5

**Table G19. Required AC Overlay Thickness (fair condition, 2-inch existing AC thickness after milling with 45 ksi base modulus).**

ESALs ( $\times 10^6$ )	Reliability (%)				
	75	80	85	90	95
<b>1</b>	1.5	1.5	1.5	1.5	1.5
<b>2</b>	1.5	1.5	1.5	1.5	1.5
<b>3</b>	1.5	1.5	1.5	1.5	1.5
<b>4</b>	1.5	1.5	1.5	1.5	1.5
<b>5</b>	1.5	1.5	1.5	2.0	2.0
<b>10</b>	2.5	2.5	3.0	3.0	3.5
<b>15</b>	3.0	3.0	3.5	4.0	4.0
<b>20</b>	3.0	3.5	4.0	4.0	4.5
<b>25</b>	3.5	3.5	4.0	4.5	5.0
<b>30</b>	4.0	4.0	4.5	4.5	5.0
<b>35</b>	4.0	4.0	4.5	5.0	5.5
<b>40</b>	4.5	4.5	4.5	5.0	5.5
<b>45</b>	4.5	4.5	5.0	5.5	6.0
<b>50</b>	4.5	5.0	5.0	5.5	6.0
<b>55</b>	4.5	5.0	5.0	5.5	6.0
<b>60</b>	5.0	5.0	5.5	6.0	6.5
<b>65</b>	5.0	5.0	5.5	6.0	6.5
<b>70</b>	5.0	5.5	5.5	6.0	6.5

**Table G20. Required AC Overlay Thickness (good condition, 2-inch existing AC thickness after milling with 45 ksi base modulus).**

ESALs ( $\times 10^6$ )	Reliability (%)				
	75	80	85	90	95
<b>1</b>	1.5	1.5	1.5	1.5	1.5
<b>2</b>	1.5	1.5	1.5	1.5	1.5
<b>3</b>	1.5	1.5	1.5	1.5	1.5
<b>4</b>	1.5	1.5	1.5	1.5	1.5
<b>5</b>	1.5	1.5	1.5	1.5	2.0
<b>10</b>	2.0	2.0	2.5	3.0	3.5
<b>15</b>	2.5	2.5	3.0	3.5	3.5
<b>20</b>	3.0	3.0	3.5	3.5	4.0
<b>25</b>	3.5	3.5	4.0	4.0	4.5
<b>30</b>	3.5	4.0	4.5	4.5	5.0
<b>35</b>	4.0	4.0	4.5	4.5	5.0
<b>40</b>	4.0	4.0	4.5	5.0	5.0
<b>45</b>	4.5	4.5	5.0	5.0	5.5
<b>50</b>	4.5	4.5	5.0	5.5	5.5
<b>55</b>	4.5	4.5	5.0	5.5	5.5
<b>60</b>	4.5	4.5	5.0	5.5	6.0
<b>65</b>	4.5	5.0	5.0	5.5	6.0
<b>70</b>	5.0	5.0	5.5	6.0	6.5

**Table G21. Required AC Overlay Thickness (poor condition, 3-inch existing AC thickness after milling with 45 ksi base modulus).**

ESALs ( $\times 10^6$ )	Reliability (%)				
	75	80	85	90	95
<b>1</b>	1.5	1.5	1.5	1.5	1.5
<b>2</b>	1.5	1.5	1.5	1.5	1.5
<b>3</b>	1.5	1.5	1.5	1.5	1.5
<b>4</b>	1.5	1.5	1.5	1.5	1.5
<b>5</b>	1.5	1.5	1.5	1.5	1.5
<b>10</b>	1.5	1.5	2.0	2.5	3.0
<b>15</b>	2.0	2.5	2.5	3.0	3.5
<b>20</b>	2.5	2.5	3.0	3.5	3.5
<b>25</b>	3.0	3.0	3.0	3.5	4.0
<b>30</b>	3.0	3.0	3.5	4.0	4.0
<b>35</b>	3.0	3.5	3.5	4.0	4.5
<b>40</b>	3.5	3.5	4.0	4.5	4.5
<b>45</b>	3.5	3.5	4.0	4.5	5.0
<b>50</b>	4.0	4.0	4.0	4.5	5.0
<b>55</b>	4.0	4.0	4.5	5.0	5.5
<b>60</b>	4.0	4.0	4.5	5.0	5.5
<b>65</b>	4.0	4.5	5.0	5.0	5.5
<b>70</b>	4.5	4.5	5.0	5.5	6.0

**Table G22. Required AC Overlay Thickness (fair condition, 3-inch existing AC thickness after milling with 45 ksi base modulus).**

ESALs ( $\times 10^6$ )	Reliability (%)				
	75	80	85	90	95
<b>1</b>	1.5	1.5	1.5	1.5	1.5
<b>2</b>	1.5	1.5	1.5	1.5	1.5
<b>3</b>	1.5	1.5	1.5	1.5	1.5
<b>4</b>	1.5	1.5	1.5	1.5	1.5
<b>5</b>	1.5	1.5	1.5	1.5	1.5
<b>10</b>	1.5	1.5	2.0	2.0	2.5
<b>15</b>	2.0	2.5	2.5	2.5	3.0
<b>20</b>	2.5	2.5	3.0	3.0	3.5
<b>25</b>	3.0	3.0	3.0	3.5	4.0
<b>30</b>	3.0	3.0	3.5	4.0	4.0
<b>35</b>	3.0	3.5	3.5	4.0	4.5
<b>40</b>	3.5	3.5	4.0	4.5	4.5
<b>45</b>	3.5	3.5	4.0	4.5	5.0
<b>50</b>	3.5	4.0	4.0	4.5	5.0
<b>55</b>	4.0	4.0	4.5	5.0	5.5
<b>60</b>	4.0	4.0	4.5	5.0	5.5
<b>65</b>	4.0	4.5	5.0	5.0	5.5
<b>70</b>	4.5	4.5	5.0	5.5	6.0

**Table G23. Required AC Overlay Thickness (good condition, 3-inch existing AC thickness after milling with 45 ksi base modulus).**

ESALs ( $\times 10^6$ )	Reliability (%)				
	75	80	85	90	95
1	1.5	1.5	1.5	1.5	1.5
2	1.5	1.5	1.5	1.5	1.5
3	1.5	1.5	1.5	1.5	1.5
4	1.5	1.5	1.5	1.5	1.5
5	1.5	1.5	1.5	1.5	1.5
10	1.5	1.5	2.0	2.0	2.0
15	2.0	2.0	2.0	2.0	2.5
20	2.0	2.0	2.5	3.0	3.0
25	2.5	2.5	3.0	3.5	3.5
30	3.0	3.0	3.0	3.5	4.0
35	3.0	3.0	3.5	3.5	4.0
40	3.0	3.0	3.5	4.0	4.0
45	3.5	3.5	4.0	4.0	4.5
50	3.5	3.5	4.0	4.5	4.5
55	3.5	4.0	4.0	4.5	5.0
60	3.5	4.0	4.0	4.5	5.0
65	3.5	4.0	4.5	5.0	5.5
70	4.0	4.5	4.5	5.0	5.5

**Table G24. Required AC Overlay Thickness (poor condition, 4-inch existing AC thickness after milling with 45 ksi base modulus).**

ESALs ( $\times 10^6$ )	Reliability (%)				
	75	80	85	90	95
1	1.5	1.5	1.5	1.5	1.5
2	1.5	1.5	1.5	1.5	1.5
3	1.5	1.5	1.5	1.5	1.5
4	1.5	1.5	1.5	1.5	1.5
5	1.5	1.5	1.5	1.5	1.5
10	1.5	1.5	1.5	1.5	1.5
15	1.5	1.5	1.5	2.0	2.5
20	2.0	2.0	2.0	2.0	2.5
25	2.0	2.5	2.5	2.5	3.0
30	2.5	2.5	3.0	3.0	3.0
35	2.5	3.0	3.0	3.5	3.5
40	3.0	3.0	3.5	3.5	4.0
45	3.0	3.0	3.5	4.0	4.5
50	3.0	3.5	3.5	4.0	4.5
55	3.0	3.5	3.5	4.0	4.5
60	3.0	3.5	4.0	4.0	5.0
65	3.0	3.5	4.0	4.0	5.0
70	3.5	4.0	4.5	4.5	5.0

**Table G25. Required AC Overlay Thickness (fair condition, 4-inch existing AC thickness after milling with 45 ksi base modulus).**

ESALs ( $\times 10^6$ )	Reliability (%)				
	75	80	85	90	95
<b>1</b>	1.5	1.5	1.5	1.5	1.5
<b>2</b>	1.5	1.5	1.5	1.5	1.5
<b>3</b>	1.5	1.5	1.5	1.5	1.5
<b>4</b>	1.5	1.5	1.5	1.5	1.5
<b>5</b>	1.5	1.5	1.5	1.5	1.5
<b>10</b>	1.5	1.5	1.5	1.5	1.5
<b>15</b>	1.5	1.5	1.5	2.0	2.0
<b>20</b>	2.0	2.0	2.0	2.0	2.5
<b>25</b>	2.0	2.0	2.5	2.5	3.0
<b>30</b>	2.0	2.0	2.5	3.0	3.0
<b>35</b>	2.0	2.5	2.5	3.0	3.5
<b>40</b>	2.5	2.5	3.0	3.5	3.5
<b>45</b>	2.5	3.0	3.0	3.5	4.0
<b>50</b>	2.5	3.0	3.0	3.5	4.0
<b>55</b>	2.5	3.0	3.0	3.5	4.0
<b>60</b>	3.0	3.0	3.5	4.0	4.0
<b>65</b>	3.0	3.0	3.5	4.0	4.5
<b>70</b>	3.0	3.5	4.0	4.0	4.5

**Table G26. Required AC Overlay Thickness (good condition, 4-inch existing AC thickness after milling with 45 ksi base modulus).**

ESALs ( $\times 10^6$ )	Reliability (%)				
	75	80	85	90	95
<b>1</b>	1.5	1.5	1.5	1.5	1.5
<b>2</b>	1.5	1.5	1.5	1.5	1.5
<b>3</b>	1.5	1.5	1.5	1.5	1.5
<b>4</b>	1.5	1.5	1.5	1.5	1.5
<b>5</b>	1.5	1.5	1.5	1.5	1.5
<b>10</b>	1.5	1.5	1.5	1.5	1.5
<b>15</b>	1.5	1.5	1.5	1.5	2.0
<b>20</b>	1.5	1.5	1.5	2.0	2.0
<b>25</b>	1.5	1.5	2.0	2.0	2.5
<b>30</b>	1.5	1.5	2.0	2.5	2.5
<b>35</b>	2.0	2.0	2.5	2.5	3.0
<b>40</b>	2.0	2.0	2.5	3.0	3.0
<b>45</b>	2.5	2.5	3.0	3.0	3.5
<b>50</b>	2.5	2.5	3.0	3.5	3.5
<b>55</b>	2.5	3.0	3.0	3.5	4.0
<b>60</b>	2.5	3.0	3.0	3.5	4.0
<b>65</b>	3.0	3.0	3.5	4.0	4.0
<b>70</b>	3.0	3.5	3.5	4.0	4.5

**Table G27. Required AC Overlay Thickness (poor condition, 5-inch existing AC thickness after milling with 45 ksi base modulus).**

ESALs ( $\times 10^6$ )	Reliability (%)				
	75	80	85	90	95
1	1.5	1.5	1.5	1.5	1.5
2	1.5	1.5	1.5	1.5	1.5
3	1.5	1.5	1.5	1.5	1.5
4	1.5	1.5	1.5	1.5	1.5
5	1.5	1.5	1.5	1.5	1.5
10	1.5	1.5	1.5	1.5	1.5
15	1.5	1.5	1.5	1.5	1.5
20	1.5	1.5	1.5	1.5	1.5
25	1.5	1.5	1.5	2.0	2.0
30	1.5	1.5	2.0	2.0	2.5
35	1.5	2.0	2.0	2.5	2.5
40	1.5	2.0	2.0	2.5	2.5
45	2.0	2.0	2.0	2.5	3.0
50	2.0	2.0	2.5	2.5	3.0
55	2.0	2.0	2.5	2.5	3.0
60	2.0	2.0	2.5	2.5	3.0
65	2.5	2.5	3.0	3.0	3.5
70	2.5	2.5	3.0	3.5	4.0

**Table G28. Required AC Overlay Thickness (fair condition, 5-inch existing AC thickness after milling with 45 ksi base modulus).**

ESALs ( $\times 10^6$ )	Reliability (%)				
	75	80	85	90	95
1	1.5	1.5	1.5	1.5	1.5
2	1.5	1.5	1.5	1.5	1.5
3	1.5	1.5	1.5	1.5	1.5
4	1.5	1.5	1.5	1.5	1.5
5	1.5	1.5	1.5	1.5	1.5
10	1.5	1.5	1.5	1.5	1.5
15	1.5	1.5	1.5	1.5	1.5
20	1.5	1.5	1.5	1.5	1.5
25	1.5	1.5	1.5	2.0	2.0
30	1.5	1.5	2.0	2.0	2.5
35	1.5	2.0	2.0	2.5	2.5
40	1.5	2.0	2.0	2.5	2.5
45	2.0	2.0	2.0	2.5	2.5
50	2.0	2.0	2.5	2.5	3.0
55	2.0	2.0	2.5	2.5	3.0
60	2.0	2.0	2.5	2.5	3.0
65	2.0	2.0	2.5	3.0	3.5
70	2.0	2.5	2.5	3.0	3.5

**Table G29. Required AC Overlay Thickness (good condition, 5-inch existing AC thickness after milling with 45 ksi base modulus).**

ESALs ( $\times 10^6$ )	Reliability (%)				
	75	80	85	90	95
1	1.5	1.5	1.5	1.5	1.5
2	1.5	1.5	1.5	1.5	1.5
3	1.5	1.5	1.5	1.5	1.5
4	1.5	1.5	1.5	1.5	1.5
5	1.5	1.5	1.5	1.5	1.5
10	1.5	1.5	1.5	1.5	1.5
15	1.5	1.5	1.5	1.5	1.5
20	1.5	1.5	1.5	1.5	1.5
25	1.5	1.5	1.5	1.5	2.0
30	1.5	1.5	1.5	1.5	2.0
35	1.5	1.5	1.5	2.0	2.0
40	1.5	1.5	1.5	2.0	2.0
45	1.5	1.5	2.0	2.0	2.0
50	1.5	2.0	2.0	2.0	2.5
55	1.5	2.0	2.0	2.0	2.5
60	1.5	2.0	2.0	2.5	2.5
65	1.5	2.0	2.0	2.5	3.0
70	1.5	2.0	2.5	2.5	3.0

**Table G30. Required AC Overlay Thickness (poor condition, 6-inch existing AC thickness after milling with 45 ksi base modulus).**

ESALs ( $\times 10^6$ )	Reliability (%)				
	75	80	85	90	95
1	1.5	1.5	1.5	1.5	1.5
2	1.5	1.5	1.5	1.5	1.5
3	1.5	1.5	1.5	1.5	1.5
4	1.5	1.5	1.5	1.5	1.5
5	1.5	1.5	1.5	1.5	1.5
10	1.5	1.5	1.5	1.5	1.5
15	1.5	1.5	1.5	1.5	1.5
20	1.5	1.5	1.5	1.5	1.5
25	1.5	1.5	1.5	1.5	1.5
30	1.5	1.5	1.5	1.5	1.5
35	1.5	1.5	1.5	1.5	2.0
40	1.5	1.5	1.5	2.0	2.0
45	1.5	1.5	2.0	2.0	2.0
50	1.5	1.5	2.0	2.0	2.0
55	1.5	1.5	2.0	2.0	2.0
60	1.5	2.0	2.0	2.0	2.5
65	1.5	2.0	2.0	2.5	2.5
70	1.5	2.0	2.5	2.5	2.5

**Table G31. Required AC Overlay Thickness (fair condition, 6-inch existing AC thickness after milling with 45 ksi base modulus).**

ESALs ( $\times 10^6$ )	Reliability (%)				
	75	80	85	90	95
<b>1</b>	1.5	1.5	1.5	1.5	1.5
<b>2</b>	1.5	1.5	1.5	1.5	1.5
<b>3</b>	1.5	1.5	1.5	1.5	1.5
<b>4</b>	1.5	1.5	1.5	1.5	1.5
<b>5</b>	1.5	1.5	1.5	1.5	1.5
<b>10</b>	1.5	1.5	1.5	1.5	1.5
<b>15</b>	1.5	1.5	1.5	1.5	1.5
<b>20</b>	1.5	1.5	1.5	1.5	1.5
<b>25</b>	1.5	1.5	1.5	1.5	1.5
<b>30</b>	1.5	1.5	1.5	1.5	1.5
<b>35</b>	1.5	1.5	1.5	1.5	1.5
<b>40</b>	1.5	1.5	1.5	1.5	1.5
<b>45</b>	1.5	1.5	1.5	1.5	1.5
<b>50</b>	1.5	1.5	1.5	2.0	2.0
<b>55</b>	1.5	1.5	2.0	2.0	2.0
<b>60</b>	1.5	1.5	2.0	2.0	2.0
<b>65</b>	1.5	1.5	2.0	2.0	2.5
<b>70</b>	1.5	1.5	2.0	2.5	2.5

**Table G32. Required AC Overlay Thickness (good condition, 6-inch existing AC thickness after milling with 45 ksi base modulus).**

ESALs ( $\times 10^6$ )	Reliability (%)				
	75	80	85	90	95
<b>1</b>	1.5	1.5	1.5	1.5	1.5
<b>2</b>	1.5	1.5	1.5	1.5	1.5
<b>3</b>	1.5	1.5	1.5	1.5	1.5
<b>4</b>	1.5	1.5	1.5	1.5	1.5
<b>5</b>	1.5	1.5	1.5	1.5	1.5
<b>10</b>	1.5	1.5	1.5	1.5	1.5
<b>15</b>	1.5	1.5	1.5	1.5	1.5
<b>20</b>	1.5	1.5	1.5	1.5	1.5
<b>25</b>	1.5	1.5	1.5	1.5	1.5
<b>30</b>	1.5	1.5	1.5	1.5	1.5
<b>35</b>	1.5	1.5	1.5	1.5	1.5
<b>40</b>	1.5	1.5	1.5	1.5	1.5
<b>45</b>	1.5	1.5	1.5	1.5	1.5
<b>50</b>	1.5	1.5	1.5	1.5	1.5
<b>55</b>	1.5	1.5	1.5	1.5	2.0
<b>60</b>	1.5	1.5	1.5	2.0	2.0
<b>65</b>	1.5	1.5	2.0	2.0	2.0
<b>70</b>	1.5	1.5	2.0	2.0	2.5

**APPENDIX H**

**M-E PDG BASED RIGID PAVEMENT DESIGN TABLES**



**Table H1. Required PCC Slab Thicknesses (Region 1).**

<b>Design I ESALs (<math>\times 10^6</math>)</b>	<b>Reliability (%)</b>				
	<b>75</b>	<b>80</b>	<b>85</b>	<b>90</b>	<b>95</b>
<b>1</b>	8	8	8	8	8
<b>2</b>	8	8	8	8	8
<b>3</b>	8	8	8	8	8.5
<b>4</b>	8	8	8	8.5	9
<b>5</b>	8	8.5	8.5	9	9.5
<b>6</b>	8.5	9	9	9.5	10
<b>7</b>	9	9	9.5	9.5	10
<b>8</b>	9.5	9.5	9.5	10	10.5
<b>9</b>	10	10	10	10	10.5
<b>10</b>	10.5	10	10	10.5	11
<b>15</b>	10.5	10.5	10.5	11	11.5
<b>20</b>	11	11	11	11.5	12
<b>25</b>	11	11.5	11.5	12	12.5
<b>30</b>	11.5	12	12	12	12.5
<b>35</b>	11.5	12	12	12.5	13
<b>40</b>	12	12.5	12.5	12.5	13
<b>45</b>	12	12.5	12.5	13	13.5
<b>50</b>	12	12.5	12.5	13	13.5
<b>60</b>	12.5	13	13	13.5	14
<b>70</b>	13	13.5	13.5	13.5	14
<b>80</b>	13.5	13.5	13.5	13.5	14
<b>90</b>	13.5	13.5	13.5	13.5	14
<b>100</b>	13.5	13.5	13.5	13.5	14.5

**Table H2. Required PCC Slab Thicknesses (Region 2).**

<b>Design I ESALs (<math>\times 10^6</math>)</b>	<b>Reliability (%)</b>				
	<b>75</b>	<b>80</b>	<b>85</b>	<b>90</b>	<b>95</b>
<b>1</b>	8	8	8	8	8
<b>2</b>	8	8	8	8	8
<b>3</b>	8	8	8	8	8.5
<b>4</b>	8	8	8	8.5	9
<b>5</b>	8	8	8.5	9	9.5
<b>6</b>	8.5	8.5	9	9	9.5
<b>7</b>	9	8.5	9	9.5	10
<b>8</b>	9	9	9.5	9.5	10
<b>9</b>	9	9.5	9.5	10	10
<b>10</b>	9.5	9.5	10	10	10.5
<b>15</b>	10	10	10.5	10.5	11
<b>20</b>	10.5	10.5	11	11	11.5
<b>25</b>	11	11	11	11.5	11.5
<b>30</b>	11	11	11.5	11.5	12
<b>35</b>	11	11.5	12	12	12.5
<b>40</b>	11.5	11.5	12	12	12.5
<b>45</b>	11.5	12	12	12.5	13
<b>50</b>	12	12	12	12.5	13
<b>60</b>	12	12	12.5	13	13.5
<b>70</b>	12.5	12.5	13	13	13.5
<b>80</b>	12.5	13	13	13.5	14
<b>90</b>	13	13	13.5	13.5	14
<b>100</b>	13	13	13.5	13.5	14

**Table H3. Required PCC Slab Thicknesses (Region 3).**

<b>Design I ESALs (<math>\times 10^6</math>)</b>	<b>Reliability (%)</b>				
	<b>75</b>	<b>80</b>	<b>85</b>	<b>90</b>	<b>95</b>
<b>1</b>	8	8	8	8	8
<b>2</b>	8	8	8	8	8
<b>3</b>	8	8	8	8	8
<b>4</b>	8	8	8	8	8.5
<b>5</b>	8	8	8	8.5	9
<b>6</b>	8	8	8.5	9	9.5
<b>7</b>	8.5	8.5	8.5	9	9.5
<b>8</b>	8.5	8.5	9	9.5	9.5
<b>9</b>	8.5	9	9	9.5	10
<b>10</b>	9	9	9.5	9.5	10
<b>15</b>	9.5	9.5	10	10	10.5
<b>20</b>	10	10	10.5	10.5	11
<b>25</b>	10.5	10.5	10.5	11	11.5
<b>30</b>	10.5	10.5	11	11	11.5
<b>35</b>	11	11	11	11.5	12
<b>40</b>	11	11	11.5	11.5	12
<b>45</b>	11	11.5	11.5	12	12
<b>50</b>	11.5	11.5	11.5	12	12.5
<b>60</b>	11.5	11.5	12	12	12.5
<b>70</b>	12	12	12	12.5	13
<b>80</b>	12	12	12.5	12.5	13
<b>90</b>	12	12.5	12.5	13	13
<b>100</b>	12.5	12.5	12.5	13	13.5

**Table H4. Required PCC Slab Thicknesses (Region 4).**

<b>Design I ESALs (<math>\times 10^6</math>)</b>	<b>Reliability (%)</b>				
	<b>75</b>	<b>80</b>	<b>85</b>	<b>90</b>	<b>95</b>
<b>1</b>	8	8	8	8	8
<b>2</b>	8	8	8	8	8
<b>3</b>	8	8	8	8	8
<b>4</b>	8	8	8	8	8
<b>5</b>	8	8	8	8	8.5
<b>6</b>	8	8	8	8	8.5
<b>7</b>	8	8	8	8.5	9
<b>8</b>	8	8	8.5	8.5	9
<b>9</b>	8	8.5	8.5	9	9.5
<b>10</b>	8.5	8.5	9	9	9.5
<b>15</b>	9	9.5	9.5	9.5	10
<b>20</b>	9.5	9.5	10	10	10.5
<b>25</b>	10	10	10	10.5	11
<b>30</b>	10	10.5	10.5	10.5	11
<b>35</b>	10.5	10.5	10.5	11	11.5
<b>40</b>	10.5	10.5	11	11	11.5
<b>45</b>	10.5	11	11	11.5	11.5
<b>50</b>	11	11	11	11.5	12
<b>60</b>	11	11.5	11.5	11.5	12
<b>70</b>	11.5	11.5	11.5	12	12
<b>80</b>	11.5	11.5	12	12	12.5
<b>90</b>	11.5	12	12	12	12.5
<b>100</b>	12	12	12	12.5	13

**Table H5. Required PCC Slab Thicknesses (Region 5).**

<b>Design I ESALs (<math>\times 10^6</math>)</b>	<b>Reliability (%)</b>				
	<b>75</b>	<b>80</b>	<b>85</b>	<b>90</b>	<b>95</b>
<b>1</b>	8	8	8	8	8
<b>2</b>	8	8	8	8	8
<b>3</b>	8	8	8	8	8
<b>4</b>	8	8	8	8	8
<b>5</b>	8	8	8	8	8
<b>6</b>	8	8	8	8	8
<b>7</b>	8	8	8	8	8.5
<b>8</b>	8	8	8	8	8.5
<b>9</b>	8	8	8	8.5	9
<b>10</b>	8	8.5	8.5	8.5	9
<b>15</b>	8.5	9	9	9.5	9.5
<b>20</b>	9	9.5	9.5	9.5	10
<b>25</b>	9.5	9.5	9.5	10	10.5
<b>30</b>	9.5	10	10	10.5	10.5
<b>35</b>	10	10	10	10.5	11
<b>40</b>	10	10.5	10.5	10.5	11
<b>45</b>	10.5	10.5	10.5	11	11.5
<b>50</b>	10.5	10.5	10.5	11	11.5
<b>60</b>	10.5	11	11	11	11.5
<b>70</b>	11	11	11	11.5	12
<b>80</b>	11	11	11.5	11.5	12
<b>90</b>	11.5	11.5	11.5	12	12
<b>100</b>	11.5	11.5	11.5	12	12.5

**Table H6. Required PCC Slab Thicknesses (90% reliability).**

<b>Design II ESALs (<math>\times 10^6</math>)</b>	<b>Region</b>				
	1	2	3	4	5
<b>1</b>	8	8	8	8	8
<b>2</b>	8	8	8	8	8
<b>3</b>	8	8	8	8	8
<b>4</b>	8	8	8	8	8
<b>5</b>	8	8	8	8	8
<b>6</b>	8	8	8	8	8
<b>7</b>	8	8	8	8	8
<b>8</b>	8.5	8	8	8	8
<b>9</b>	9	8.5	8	8	8
<b>10</b>	9	8.5	8	8	8
<b>15</b>	9.5	9.5	9	8.5	8.5
<b>20</b>	10	9.5	9.5	9	9
<b>25</b>	10.5	10	10	9.5	9
<b>30</b>	10.5	10.5	10	9.5	9.5
<b>35</b>	11	10.5	10	10	10
<b>40</b>	11	10.5	10	10	10
<b>45</b>	11.5	11	10.5	10	10
<b>50</b>	11.5	11	10.5	10.5	10
<b>60</b>	12	11.5	11	10.5	10.5
<b>70</b>	12	11.5	11	10.5	10.5
<b>80</b>	12	11.5	11	11	10.5
<b>90</b>	12.5	12	11.5	11	11
<b>100</b>	12.5	12	11.5	11	11

**Texas Transportation Institute  
The Texas A&M University System  
College Station, TX 77843-3135  
979-845-1734  
<http://tti.tamu.edu>**